UNIVERSIDADE ESTADUAL PAULISTA

"Julio de Mesquita Filho"

INSTITUTO DE BIOCIÊNCIAS DE BOTUCATU

CULTURA CELULAR DE MIOBLASTOS DE PEIXES COMO UM MODELO PARA ENTENDER A REGULAÇÃO DO DESENVOLVIMENTO E CRESCIMENTO MUSCULAR.

BRUNO OLIVEIRA DA SILVA DURAN

Orientadora MAELI DAL PAI

Coorientador DANIEL GARCIA DE LA SERRANA CASTILLO

Tese apresentada ao Instituto de Biociências, Campus de Botucatu, UNESP, para obtenção do título de Doutor no Programa de Pós-Graduação em Biologia Geral e Aplicada, Área de concentração *Biologia Celular Estrutural e Funcional*.

Maeli Dal Pai

BOTUCATU – SP
2019

FICHA CATALOGRÁFICA ELABORADA PELA SEÇÃO TÉC. AQUIS. TRATAMENTO DA INFORM.
DIVISÃO TÉCNICA DE BIBLIOTECA E DOCUMENTAÇÃO - CÂMPUS DE BOTUCATU - UNESP
BIBLIOTECÁRIA RESPONSÁVEL: LUCIANA PIZZANI-CRB 8/6772

Duran, Bruno Oliveira da Silva.
Cultura celular de mioblastos de peixes como um modelo para entender a regulação do desenvolvimento e crescimento muscular / Bruno Oliveira da Silva Duran. - Botucatu, 2019

Tese (doutorado) - Universidade Estadual Paulista "Júlio de Mesquita Filho", Instituto de Biociências de Botucatu
Orientador: Maeli Dal Pai
Coorientador: Daniel Garcia de la Serrana Castillo
Capes: 20000006

1. Peixe. 2. Músculo esquelético. 3. Desenvolvimento muscular.

Palavras-chave: Crescimento muscular; Cultura celular; Miogênese; Músculo esquelético; Peixe.

Quando ouvi o sábio astrônomo

Quando ouvi o sábio astrônomo,
Quando as provas, as figuras, foram postas em colunas diante de mim,
Quando ele me mostrou os gráficos e diagramas, para somar, dividir e mensurar,
Quando eu, sentado, ouvi o astrônomo a discursar sob aplausos no anfiteatro,
Logo e inexplicavelmente eu me senti doente e cansado
Até me levantar e sair devagar para caminhar sozinho no ar úmido e místico da noite
E de tempos em tempos olhar em perfeito silêncio para as estrelas.

Walt Whitman

Invictus

Sob o manto da noite que me cobre,
Negro como as profundezas de um pólo a outro,
Eu agradeço a todos os deuses
Por minha alma invencível.
Nas garras ferozes das circunstâncias
Eu não me encolhi, nem chorei alto.
Sob os golpes do destino
Minha cabeça sangra, mas não se curva.
Além deste lugar de ódio e lágrimas
Só assoma o horror da sombra.
Mesmo assim, a ameaça dos anos me encontra
E sempre me encontrará sem medo.
Não importa que o portão seja estreito,
E que a lista seja grande em punições,
Eu sou o mestre do meu destino.
Eu sou o capitão da minha alma.

William Ernest Henley

Dedico este trabalho às pessoas que mais me ajudaram nessa jornada e que estiveram presentes em todos os momentos da minha vida, sempre que precisei.

minha mãe, Sueli de Fatima Oliveira
meu pai, Antonio Francisco da Silva Duran
e meu irmão, Lucas Oliveira da Silva Duran

Muito obrigado por tudo.
Amo vocês mais do que tudo nesse mundo.

AGRADECIMENTOS ESPECIAIS

Agradeço primeiramente à Maeli Dal Pai, minha orientadora e segunda mãe, pessoa a qual admiro imensamente e tenho como exemplo de competência e profissionalismo. Obrigado por todos os ensinamentos, apoio, incentivo e confiança durante os últimos dez anos, sem os quais eu não chegaria até aqui. Minha vida profissional e pessoal foi inteiramente moldada pela senhora, e sou muito grato por ter feito parte da história de seu laboratório. Divido o mérito desse trabalho com a senhora.

Agradeço imensamente ao Daniel Garcia de la Serrana Castillo, meu coorientador, com quem aprendi muito sobre músculo esquelético de peixes, pesquisa científica e ambiente de trabalho. Obrigado por permitir minha experiência internacional em um laboratório de ponta e por ter acreditado em mim, me fazendo dar o melhor para a conclusão dessa tese e me incentivando a buscar cada vez mais conhecimento.

Agradeço do fundo do meu coração aos meus pais, Antonio Francisco da Silva Duran e Sueli de Fatima Oliveira, e ao meu irmão, Lucas Oliveira da Silva Duran. Vocês são a base da minha vida, meu local de reconforto, meu ponto de partida e de chegada. Obrigado por todo o amor, carinho, apoio, paciência e força que me deram. Sei que vocês batalharam muito e se esforçaram ao máximo pensando no meu bem. Hoje sou um ser humano íntegro e digno graças a vocês. Toda a minha dedicação e persistência no trabalho e na vida é para um dia poder retribuir tudo o que vocês fizeram por mim. Eu amo vocês mais que tudo.

Agradeço meus avós, Jacy Rosa de Lima Oliveira e Oswaldo Ribeiro da Silva, meus tios, Suzana Dolores Duran Lemos e Lair de Lemos, e meus primos, Adriana Lemos e Marcelo Lemos. Obrigado pelo amparo e por todo o carinho que vocês sempre dedicaram a mim.

Agradeço muito à minha namorada, Cecilia Luvizutti Ferreira da Silva, que foi a pessoa mais especial que surgiu em minha vida nos últimos anos me presenteando com seu amor, amizade, carinho e companheirismo. Sou uma pessoa melhor agora que tenho você comigo, e dedico minha vida a fazer você feliz. Amo muito você e quero viver para sempre ao seu lado. Agradeço também a Orlando Ferreira da Silva e Irene Luvizutti Ferreira da Silva, pessoas

maravilhosas que tive a sorte de conhecer e agora ter em minha família. Obrigado pela confiança e pelo acolhimento. Podem sempre contar comigo.

AGRADECIMENTOS

Agradeço aos membros da banca de qualificação e de defesa, Adalberto Luis Val, Rafael Henrique Nóbrega, Edson Assunção Mareco, Diogo Teruo Hashimoto, Leonardo Susumu Takahashi, Pedro Luiz Pucci Figueiredo de Carvalho e Robson Francisco Carvalho, pela disponibilidade e pelos valorosos conselhos e sugestões para a melhoria dessa tese e elaboração dos artigos.

Agradeço a todos os docentes e funcionários do Departamento de Morfologia, especialmente os professores Dr. Robson Francisco Carvalho, Dr. Sérgio Luis Felisbino, Dr. Luis Antonio Justulin Jr., Dr. Rafael Henrique Nóbrega, Dra. Flávia Karina Delella e Dr. Wellerson Rodrigo Scarano. Obrigado por todo o aprendizado e por terem feito desse espaço minha segunda casa.

Agradeço a todos os amigos, novos e antigos, do Laboratório de Biologia do Músculo Estriado, Bruno Fantinatti, Carlos Alves, Diogo Moraes, Douglas Marques, Edson Mareco, Erika Perez, Fernanda Alves, Flavia Fernandes, Francielle Mosele, Grasieli de Oliveira, Guilherme Alcarás, Isabele Magiore, Ivan Vechetti, Jason Fernandez, Jakeline Oliveira, Jéssica Silvino, Juarez Ferreira, Juliana Giusti, Leonardo de Moraes, Letícia Oliveira, Maria Laura Kuniyoshi, Paula Freire, Paula Souza, Rafaela Nunes, Raquel Bertaglia, Rodrigo Souza, Rondinelle Salomão, Sarah Cury, Tassiana Gutierrez, Vander Santos e Warlen Piedade. Agradeço especialmente à Fernanda Carani e Fernanda Losi, que tiveram a paciência de me ensinar desde o início praticamente tudo que sei hoje, e à Bruna Zanella, que nos últimos anos me ajudou incansavelmente nas pesquisas, experimentos, relatórios e artigos, sempre com um sorriso no rosto (e uma considerável porção de patadas).

Agradeço aos meus amigos do Departamento de Morfologia, Ana Carolina Camargo, André Teves, Alana Rezende, Ariana Musa, Brenda Minatel, Bruno Martinucci, Caroline Barquilha, Caio Cesar, Cristiane Pinho, Elian Ribeiro, Flávia Bessi, Helga Nunes, Isabela Barbosa, Jordana Oliveira, Ketlin Colombelli, Luiz Frediane, Maira Cucielo, Matheus Fioretto,

Nilton Santos, Teng Fwu Shing e Vivian Cypriano. Agradeço especialmente ao Sérgio Alexandre Alcantara dos Santos, praticamente meu irmão e pessoa a qual sou muito grato pela convivência e companheirismo. Sou muito feliz em ter você como meu amigo.

Agradeço aos meus amigos da escola, Amilson Pedroso, Eduardo Sisti, Giovana Secato, Laura Marchi e Maria Fernanda Rodilhano, e aos meus amigos da universidade, Ana Elisa Sales, Bruno Spinetti, Duílio Zerbinato, Helder Rosa, Marco Aurélio Pessotto, Maria Lúcia Iwai, Mariella Lima, Patricia Dalprat e Raisa Mello. Obrigado por estarem sempre do meu lado, me apoiando nos momentos fáceis e difíceis.

Agradeço à Fundação de Amparo à Pesquisa do Estado de São Paulo (FAPESP) e à Coordenação de Aperfeiçoamento de Pessoal de Nível Superior (CAPES) pelas bolsas e auxílios financeiros concedidos: processos nº 2015/03234-8, 2016/01086-4, 2016/19683-9 e 2016/05009-4, Fundação de Amparo à Pesquisa do Estado de São Paulo (FAPESP). Agradeço ao Conselho Nacional de Desenvolvimento Científico e Tecnológico (CNPq) pelos auxílios financeiros concedidos: 447233/2014 e 302656/2015-4.

SUMÁRIO

RESUMO

Os peixes são um grupo de organismos de extrema importância ecológica, ambiental e principalmente econômica, devido à produção de carne destinada à alimentação dos seres humanos. A carne é composta basicamente por músculo esquelético, um tecido biológico altamente especializado que constitui cerca de 60% da massa corporal dos peixes, e está intimamente relacionado à fisiologia desses animais. A miogênese e o crescimento do músculo esquelético são dependentes da proliferação e migração de células denominadas mioblastos, que podem levar ao aumento do número de fibras musculares (hiperplasia) e/ou aumento do tamanho das fibras musculares (hipertrofia). Esse crescimento é regulado por diversos sinais extrínsecos, como temperatura e oxigenação, e intrínsecos, como fatores transcricionais, microRNAs, hormônios e nutrientes. Além da proliferação e diferenciação dos mioblastos, o tamanho das fibras musculares também é influenciado por esses fatores através de um delicado balanço entre as vias de sinalização de síntese e degradação proteica. Em peixes, essas redes moleculares que controlam a homeostase e o crescimento do músculo esquelético tiveram uma expansão em seu número de componentes devido a um evento de duplicação total do genoma, que culminou com o aumento da complexidade desses organismos e, possivelmente, para uma maior diversidade biológica. Uma das maneiras de estudar essas vias sinalizatórias e entender a complexidade da regulação do crescimento muscular é através das culturas celulares primárias de mioblastos de peixes. Durante o desenvolvimento das culturas celulares de mioblastos ocorre a retomada das principais etapas da miogênese, como a proliferação e migração dos mioblastos, a diferenciação e fusão em miotubos, e a maturação das fibras musculares. O ambiente *in vitro* das culturas celulares de mioblastos apresenta menor número de variáveis quando comparadas ao músculo esquelético num nível sistêmico, permitindo as análises sob condições controladas. Dessa forma, o objetivo de nosso trabalho foi utilizar culturas celulares primárias de mioblastos de peixes como ferramentas para investigar diferentes aspectos do crescimento do músculo esquelético. Estudos como o nosso, que fornecem novas informações quanto aos mecanismos moleculares e celulares que regulam o tecido muscular nos peixes, podem contribuir para a obtenção de melhorias na piscicultura intensiva, relacionadas ao aumento de massa muscular e qualidade de carne.

ABSTRACT

Fish are a group of organisms of extreme ecological, environmental and mainly economic importance, due to the meat production intended for humans. Meat is primarily composed of skeletal muscle, a highly specialized biological tissue that constitutes about 60% of fish body mass, and it is closely related to the physiology of these animals. Myogenesis and skeletal muscle growth are dependent on the proliferation and migration of cells called myoblasts, which can promote an increase in muscle fibre number (hyperplasia) and/or increase in muscle fibre size (hypertrophy). This growth is regulated by several extrinsic signals, such as temperature and oxygenation, and intrinsic signals, such as transcriptional factors, microRNAs, hormones and nutrients. In addition to myoblasts proliferation and differentiation, the muscle fibre sizes are also influenced by these factors through a delicate balance between protein synthesis and degradation signaling pathways. In fish, these molecular networks that control homeostasis and skeletal muscle growth had an expansion in their number of components due to an event of whole genome duplication, culminating with increased complexity and, possibly, a higher biological diversity of these animals. One way to study these signaling pathways and understand the complexity of muscle growth regulation is through primary cell cultures of fish myoblasts. During the myoblast cell culture development, the main stages of myogenesis are recapitulated, such as myoblast proliferation and migration, differentiation and fusion into myotubes, and maturation of muscle fibres. The *in vitro* environment of the myoblast cell cultures has fewer number of variables when compared to the skeletal muscle at a systemic level, allowing the analyses under controlled conditions. Thus, the aim of our work was the use of fish myoblast primary cell cultures as tools to investigate different aspects of skeletal muscle growth. Studies such as ours, which provide new information on the molecular and cellular mechanisms that regulate fish muscle tissue, may contribute to improvements in intensive fish farming, related to increased muscle mass and meat quality.

1. INTRODUÇÃO

1.1. Peixes

Por conveniência, o termo "peixes" é utilizado para descrever os vertebrados estudados na Ictiologia, animais que de modo geral apresentam brânquias, membros em forma de nadadeiras e tegumento coberto por escamas de origem dérmica. No entanto, os peixes não constituem uma unidade taxonômica já que não compõem um grupo monofilético, ou seja, não possuem um ancestral comum exclusivo. Para isso, seria necessário incluir o ancestral comum mais recente e todos os seus descendentes, que nesse caso abrange também os tetrápodes (Nelson, 2006). Alguns autores restringem o termo "peixes" somente aos peixes ósseos com mandíbula, enquanto muitos outros também incluem tubarões e raias. Alguns poucos estudiosos também incluem vertebrados sem mandíbula, como as lampréias e os peixes-bruxa. De qualquer forma, os peixes são animais de enorme importância, especialmente ecológica e ambiental, atuando como elementos chave em diversas cadeias alimentares e até mesmo como indicadores de poluição em ambientes aquáticos. É o grupo mais diverso dentre os vertebrados, representando pouco mais que a metade do número total de espécies existentes; 27977 espécies de peixes e 26734 espécies de tetrápodes válidas em 2006 (Nelson, 2006). Além disso, os peixes exibem enorme variabilidade em morfologia, hábitos alimentares, comportamento e habitat, de modo que essa riqueza de informações e diversidade, muitas vezes não exploradas, tem atraído cada vez mais o interesse de pesquisadores e direcionado o foco das pesquisas a esses animais.

Outro aspecto relevante é a extrema importância econômica que os peixes possuem, devido principalmente à produção de carne destinada à alimentação dos seres humanos. Segundo o relatório "O Estado Mundial da Pesca e Aquicultura 2016", elaborado pela Food and Agriculture Organization of the United Nations (FAO), estima-se que a produção aquícola global deve alcançar cerca de 200 milhões de toneladas em 2025, um aumento de quase 20% em comparação ao período compreendido entre os anos de 2013 a 2015 (FAO, 2016). Nesse contexto, os países em desenvolvimento, incluindo o Brasil, contribuirão significativamente para esse expressivo crescimento. O Brasil possui inúmeras vantagens para o desenvolvimento da aquicultura e pesca extrativista marinha, como grande extensão litorânea, 5,5 milhões de hectares de reservatórios de água doce, condições ambientais e climatológicas altamente favoráveis, mão de obra relativamente barata, investimentos no setor e crescente mercado interno (Pinheiro, 2014). Além de uma considerável contribuição para o PIB nacional (aproximadamente R$ 5 bilhões), a atividade aquícola brasileira alavancou rapidamente nas últimas décadas, com uma

transição de quase zero nos anos 80 para mais de meio milhão de toneladas de peixes em 2014 (Saint-Paul, 2017), de modo que o consumo brasileiro de peixe per capita aumentou cerca de 30% no período compreendido entre os anos de 2000 e 2009, bem mais que o registrado para a carne bovina (10%) (Pinheiro, 2014). Por essas razões, a produção de pesca e aquicultura brasileira deve crescer mais de 100% até 2025 (104%), sendo esse aumento o maior estimado na região da América Latina e Caribe, seguido por México (54,2%) e Argentina (53,9%) (FAO, 2016).

O boletim estatístico elaborado pelo Ministério da Pesca e Aquicultura mostra a produção de pescado da aquicultura em 2011, revelando as espécies mais utilizadas na piscicultura brasileira. A maior produção continua sendo da tilápia do Nilo (*Oreochromis niloticus*) (47%) (MPA, 2013), um dos peixes de água doce mais cultivados do mundo. Apesar de ser uma espécie originária da bacia do rio Nilo, na África, a tilápia do Nilo foi introduzida em diversas regiões subtropicais e temperadas do planeta, devido a sua adaptabilidade a uma ampla gama de ambientes e sistemas de cultivo (El-Sayed, 2006). Outras espécies não-nativas com contribuições menores para a produção nacional são a carpa (*Cyprinus carpio*) (7%) e a truta arco-íris (*Oncorhynchus mykiss*) (0,6%) (MPA, 2013). Apesar do baixo impacto da truta arco-íris no cenário brasileiro, os salmonídeos constituem um dos principais grupos de peixes na aquicultura. Ao longo dos anos, as criações de trutas e do salmão do Atlântico (*Salmo salar*) se espalharam por todos os continentes (Berthelot et al., 2014), e atualmente tem marcante produção na Europa e em países como Estados Unidos e Chile (FAO, 2016).

O Brasil possui cerca de 3 mil espécies de peixes nativos, muitas com potencial para uma produção mais significativa na piscicultura, como o dourado (*Salminus brasiliensis*), jaú (*Zungaro zungaro*), piau (*Leporinus* spp.), matrinxã (*Brycon amazonicus*), pintado (*Pseudoplatystoma* spp.), pirarucu (*Arapaima gigas*) e jundiá (*Rhamdia quelen*) (MPA, 2013; Pinheiro, 2014; IBGE, 2016). Se compararmos a países asiáticos, em que 95% da produção baseia-se em peixes nativos daquele continente, a participação das espécies nativas na aquicultura brasileira ainda é baixa. Isso devido à relativa falta de conhecimento sobre a biologia, reprodução, nutrição e domesticação desses animais, enquanto existem muito mais informações básicas para a criação de espécies introduzidas (Saint-Paul, 2017). No entanto, esse panorama está mudando, e o foco da aquicultura nacional, que antes se concentrava exclusivamente em espécies exóticas, vem sendo direcionado para os peixes nativos. Os principais responsáveis por isso são membros da família Characidae popularmente conhecidos como pacu (*Piaractus mesopotamicus*), tambaqui (*Colossoma macropomum*), tambacu (híbrido

entre pacu e tambaqui) e pirapitinga (*Piaractus brachypomus*), que correspondem à maioria dos peixes nativos cultivados e representam quase 40% da produção nacional (MPA, 2013; IBGE, 2016). O pacu é encontrado nas bacias dos rios Paraná, Paraguai e Uruguai, mas sua distribuição está mais concentrada nas planícies alagadas da região Centro-Oeste do Brasil, sendo um dos peixes mais estudados no Sul, Sudeste e Centro-Oeste brasileiros (Urbinati e Gonçalves, 2005). É uma espécie que apresenta diversas características economicamente interessantes, como rusticidade, alta fertilidade, rápido crescimento, adaptação à alimentação artificial e carne saborosa, podendo atingir até 20 kg (Santos et al., 2012).

A mudança da produção de pesca e aquicultura para as espécies nativas é o caminho para o desenvolvimento da atividade aquícola, permitindo uma maior acessibilidade da população, estímulo do mercado interno, ampliar a exportação e aumentar o consumo de pescado (Saint-Paul, 2017). Uma vez que a demanda vem crescendo e esses produtos contribuem com uma grande parcela da alimentação da população mundial, é necessária a implementação cada vez maior de políticas públicas na pesca e aquicultura. Esse cenário revela a importância das pesquisas científicas com peixes, contemplando os mais diversos domínios como toxicologia, imunologia, ecologia, genética, fisiologia e nutrição, buscando aumentar o nível de conhecimento para a criação desses animais. Apesar do zebrafish (*Danio rerio*) e do medaka (*Oryzias latipes*) serem amplamente utilizados como organismos modelo para o entendimento de muitos processos biológicos, existem certas limitações devido ao pequeno tamanho que atingem, como o estudo do músculo esquelético durante o crescimento do animal (Froehlich et al., 2013). Peixes como a tilápia do Nilo, a truta arco-íris e o pacu (Figura 1) são excelentes modelos experimentais para esse tipo de estudo e em outras áreas científicas, tanto pelo grande tamanho corporal que atingem quanto pelo alto valor e interesse econômico que possuem.

Tilápia do Nilo (*Oreochromis niloticus*)

Pacu (*Piaractus mesopotamicus*)

Truta arco-íris (*Oncorhynchus mykiss*)

Figura 1: Exemplares de tilápias do Nilo (*Oreochromis niloticus*), pacu (*Piaractus mesopotamicus*) e truta arco-íris (*Oncorhynchus mykiss*), peixes de grande importância econômica e científica.
(http://ref.data.fao.org/photo?entryId=2cc8a2e8-5aca-4b5e-9ff3-bfe0731ddcda
http://isabelpellizzer.com.br/teodoro-sampaio-sp/
http://www.invasivespeciesinitiative.com/rainbow-trout/).

1.2. Músculo esquelético

O tecido muscular esquelético é considerado um tecido fundamental, assim como o epitelial, conjuntivo e nervoso. A função básica dos músculos é a produção de força e geração de movimento, possíveis através da capacidade de contração e relaxamento de suas células. Isso faz com que o tecido muscular esquelético seja essencial para vários processos fisiológicos de um organismo, como a locomoção, manutenção e mudanças na postura e respiração, além de um importante papel no metabolismo, agindo como fonte energética, e também na produção de calor e manutenção da temperatura corporal (Junqueira e Carneiro, 2013; revisado por Frontera e Ochala, 2015).

As células do tecido muscular esquelético são conhecidas como fibras musculares. São células alongadas, podendo chegar até 30 cm de comprimento, cilíndricas, com um diâmetro que varia de 10 a 100 µm, e multinucleadas (Junqueira e Carneiro, 2013). O citoplasma (sarcoplasma) das fibras é totalmente preenchido por estruturas cilíndricas denominadas

miofibrilas, que são formadas por filamentos de proteínas contráteis. As miofibrilas deslocam os vários núcleos em direção à membrana plasmática (sarcolema), ou seja, para a periferia das células, sendo essa uma característica exclusiva do músculo esquelético (revisado por Frontera e Ochala, 2015). O músculo esquelético está sujeito a variações no diâmetro de suas fibras musculares, que depende de fatores como o próprio músculo considerado, idade e sexo do organismo, estado de nutrição, exercício físico e diversas patologias.

Os músculos são revestidos por uma camada espessa de tecido conjuntivo denominado epimísio, que emite septos para o interior do tecido separando-o em feixes. O tecido conjuntivo que envolve esses feixes de fibras musculares, também conhecidos como fascículos, é conhecido como perimísio. Além do epimísio e perimísio, uma delgada camada de tecido conjuntivo envolve cada uma das fibras musculares, e recebe o nome de endomísio, formado pela lâmina basal em associação com fibras reticulares (revisado por Kjaer, 2004) (Figura 2). O tecido conjuntivo tem grande importância para a fisiologia do tecido muscular, contribuindo para a união das fibras musculares e permitindo que a força de contração gerada por cada fibra seja transmitida não somente ao músculo inteiro, mas também a outras estruturas, como os ossos e tendões. Além disso, o tecido conjuntivo também permite a inserção de vasos sanguíneos, linfáticos e nervos. Em peixes, a distribuição do tecido conjuntivo no músculo esquelético e a concentração de colágeno variam conforme a espécie, a etologia do animal, a atividade muscular realizada durante os movimentos natatórios e o estágio de desenvolvimento (Michelin et al., 2009).

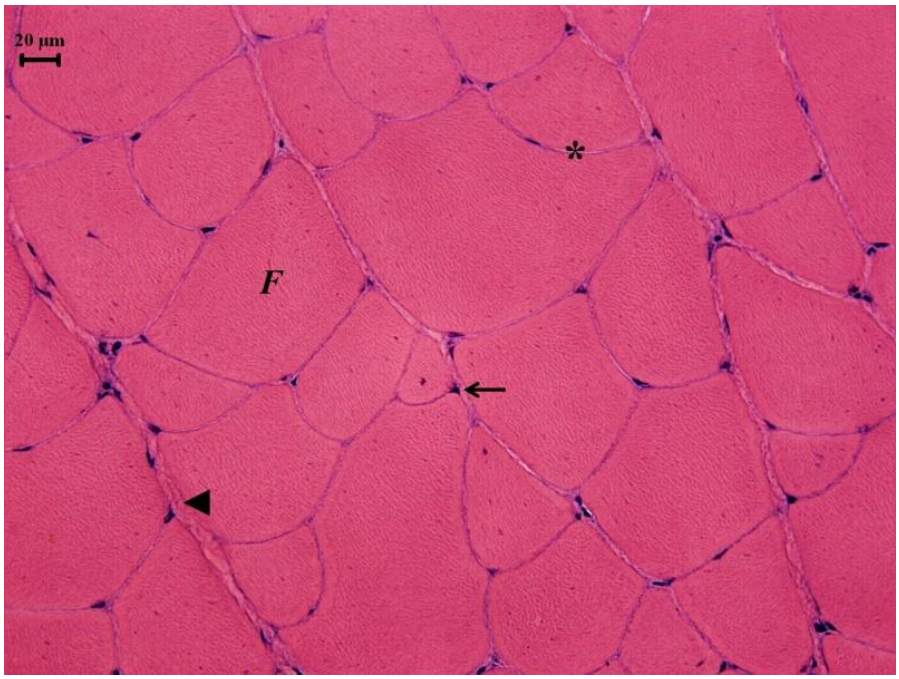

Figura 2: Corte transversal de músculo esquelético de pacu (*Piaractus mesopotamicus*) adulto (imagem de autoria própria). F: fibra muscular; *: endomísio; ◀: perimísio; ←: mionúcleo. Coloração por hematoxilina-eosina (Aumento: 40X; Barra: 20 µm).

As fibras musculares esqueléticas apresentam estriações, devido ao arranjo repetitivo das miofibrilas em unidades conhecidas como sarcômeros (revisado por Frontera e Ochala, 2015). O sarcômero é a unidade funcional básica e contrátil do músculo, e sua repetição ao longo da fibra proporciona uma alternância de faixas escuras (banda A) e claras (banda I), resultando nas estriações transversais características. As miofibrilas são principalmente constituídas de filamentos finos de actina e filamentos grossos de miosina, dispostos longitudinalmente e organizados de maneira simétrica e paralela (Junqueira e Carneiro, 2013). Além disso, existe um conjunto de proteínas regulatórias, como tropomiosina e troponina, e estruturais, como titina, nebulina, alfa actinina, desmina e distrofina. A actina apresenta-se sob a forma de polímeros longos (actina F), constituídos por duas cadeias de monômeros globulares (actina G) torcidas em dupla-hélice. Cada monômero possui um sítio ativo, região na qual ocorre a interação com a miosina. A molécula de miosina é um hexâmero formado por quatro cadeias leves de miosina (MyLC) e duas cadeias pesadas de miosina (MyHC) (revisado por Geeves, 1999; Junqueira e Carneiro, 2013). Apresenta uma dupla hélice, que constitui uma região conhecida como cauda, e uma saliência globular conhecida como cabeça. A cabeça da miosina possui locais específicos para a interação com a actina e para a ligação com a molécula de ATP, que será hidrolisada para a liberação de energia utilizada na contração (revisado por Geeves, 1999). Com relação às proteínas regulatórias, a tropomiosina é composta por duas cadeias em alfa hélice e a troponina apresenta 3 subunidades: TnT, que se liga à tropomiosina; TnC, que tem afinidade pelos íons cálcio; e TnI, que cobre o sítio ativo da actina, local em que ocorre a ligação da actina com a miosina (revisado por Geeves, 1999; Junqueira e Carneiro, 2013).

A contração tem início com a ligação de íons cálcio à subunidade TnC da troponina. Essa ligação promove uma alteração conformacional da troponina que acaba deslocando a tropomiosina. Por sua vez, o deslocamento libera o sítio ativo da actina e permite sua interação com a miosina. A cabeça da miosina apresenta atividade ATPásica, de modo que a hidrólise do ATP em ADP, Pi (fosfato inorgânico) e energia promove uma alteração conformacional que aumenta a curvatura da cabeça (revisado por Geeves, 1999; revisado por Frontera e Ochala, 2015). O movimento da cabeça da miosina empurra o filamento de actina, promovendo o deslizamento dos filamentos contráteis uns sobre os outros. Esse processo se repete várias vezes

durante uma contração, aumentando o tamanho da zona de sobreposição entre os filamentos, o que diminui o tamanho do sarcômero e leva ao encurtamento da fibra muscular (Junqueira e Carneiro, 2013) (Figura 3).

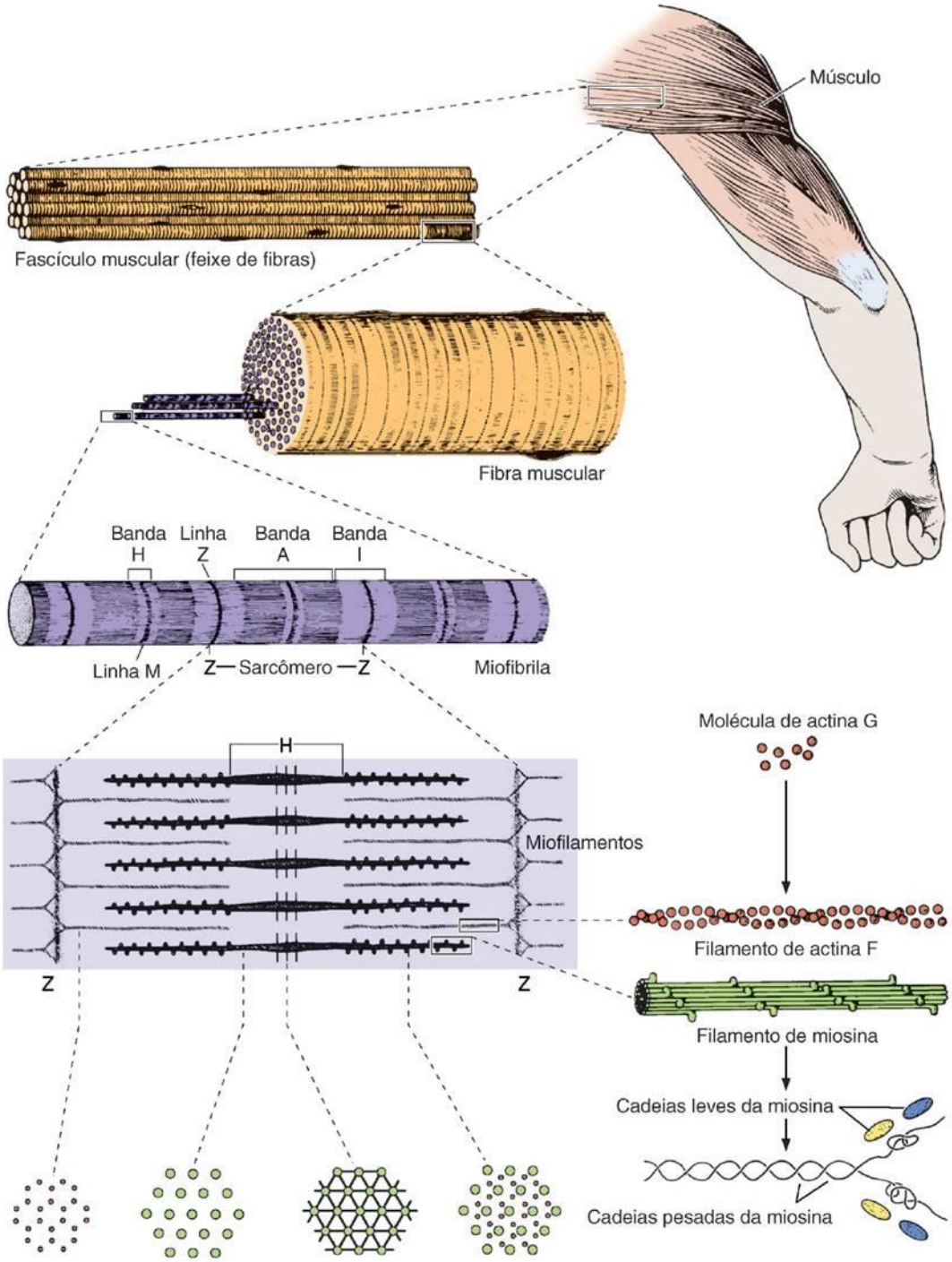

Figura 3: Esquema ilustrando a estrutura do sarcômero. As fibras musculares contêm estruturas denominadas miofibrilas, que são formadas por filamentos de proteínas contráteis organizados

em sarcômeros. Os principais componentes dos sarcômeros são os filamentos de actina e miosina, que interagem e promovem a contração muscular (Junqueira e Carneiro, 2008).

As propriedades do músculo esquelético são determinadas pelo número, tamanho e composição das fibras musculares, e variações na estrutura e função dos componentes das fibras resultam em adaptações a diferentes demandas (plasticidade muscular) (revisado por Blauuw et al., 2013). De modo geral, a classificação dos tipos de fibras musculares é baseada nas características contráteis e metabólicas dessas células. As fibras musculares podem expressar diferentes isoformas de MyHC, que determinam a velocidade de hidrólise do ATP e, consequentemente, a velocidade de contração muscular (revisado por Blauuw et al., 2013). Em mamíferos, as fibras que expressam somente uma isoforma são denominadas puras e são classificadas em tipo 1 (MyHC-β), 2A (MyHC-2A), 2X (MyHC-2X) e 2B (MyHC-2B). Entretanto, uma mesma fibra muscular pode apresentar diferentes isoformas de MyHC, sendo estas denominadas fibras híbridas e classificadas conforme a MyHC predominante, de acordo com o seguinte esquema: 1 ↔ 1/2A ↔ 2A ↔ 2A/2X ↔ 2X ↔ 2X/2B ↔ 2B (Staron et al., 1999). No entanto, esse padrão de expressão das isoformas não é obrigatório; por exemplo, estudos já mostraram fibras musculares co-expressando MyHC do tipo 1 e 2X, mas não a isoforma 2A (Caiozzo et al., 2003). As fibras do tipo 1 apresentam baixa atividade ATPásica, possuindo contração lenta, enquanto as fibras do tipo 2 hidrolisam o ATP mais rapidamente, possuindo contração rápida (revisado por Schiaffino e Reggiani, 2011). Além disso, esses tipos de fibras musculares possuem propriedades metabólicas distintas: as fibras do tipo 1 são caracterizadas por metabolismo aeróbico ou oxidativo, resistência à fadiga e geração reduzida de força mecânica; as fibras do tipo 2B são caracterizadas por metabolismo anaeróbico ou glicolítico, muito suscetíveis à fadiga e geração elevada de força mecânica; e as fibras do tipo 2A e 2X combinam um metabolismo glicolítico e grande geração de força mecânica com a resistência à fadiga (revisado por Blauuw et al., 2013).

Na maioria dos peixes o músculo esquelético constitui cerca de 60% da massa corporal (Johnston, 2001). Essa musculatura está intimamente relacionada à fisiologia desses animais, de modo que possibilita os movimentos natatórios e a adaptação ao meio aquático, representa a principal reserva proteica e compreende a maior porção do filé, a parte mais valiosa do peixe para a indústria da aquicultura (Johnston, 2001; Sänger e Stoiber, 2001). Geralmente, a organização anatômica do músculo esquelético nos peixes se baseia em unidades idênticas chamadas miômeros, estruturas envoltas por camadas de tecido conjuntivo denominadas

miosseptos. Os miômeros se repetem ao longo de todo o comprimento corporal do peixe e possuem um formato em W, que permite um encaixe intrincado dessas unidades e diferentes flexões corporais durante o nado (Van Leeuwen, 1999). O miossepto vertical divide os músculos em antímeros direito e esquerdo e, na região em que se encontra o nervo da linha lateral, um miossepto horizontal (septo transverso) divide a musculatura em epaxial e hipaxial (Currie e Ingham, 2001) (Figura 4).

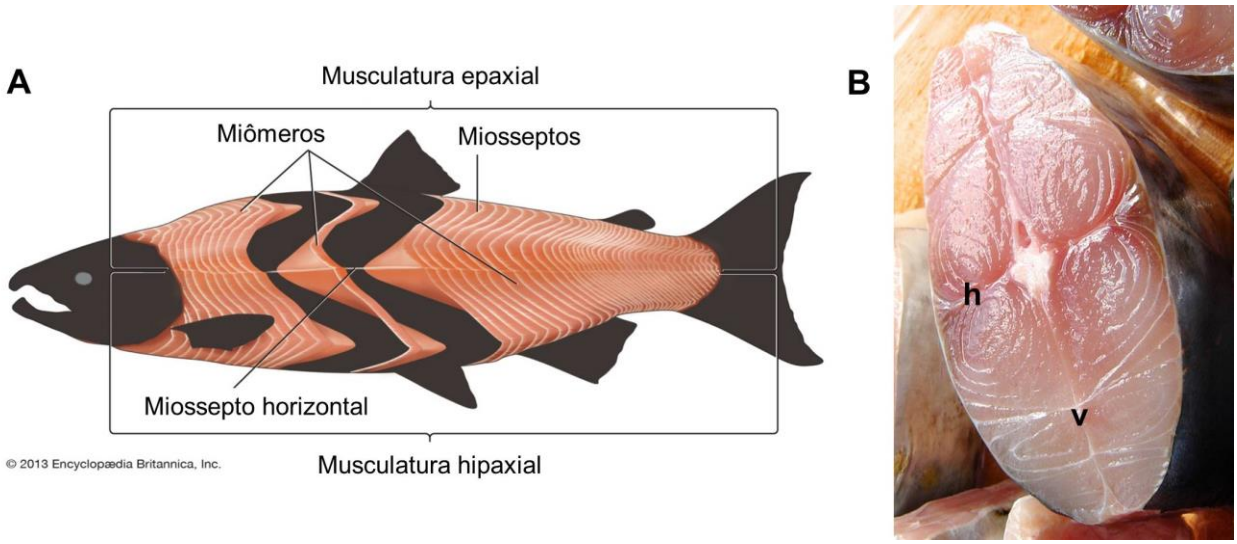

Figura 4: Organização anatômica do músculo esquelético nos peixes. (A) Estrutura dos miômeros e miosspetos e as musculaturas epaxial e hipaxial (adaptado de Encyclopaedia Britannica Online, 2010). (B) Miossepto vertical (v) e miossepto horizontal (h). (https://brunaquaglio.com/2015/12/20/peixes-magro-e-peixes-gordurosos-lista/).

Em peixes, os tipos de fibras musculares encontram-se distribuídos em compartimentos distintos, diferentemente do padrão em mosaico encontrado nos músculos dos mamíferos, em que as diferentes fibras encontram-se entremeadas umas às outras (Barets, 1961; Johnston et al., 1977; Sänger e Stoiber, 2001; Johnston et al., 2004) (Figura 5). Essa é uma das principais diferenças entre os músculos esqueléticos desses animais, tornando os peixes modelos experimentais únicos em pesquisas envolvendo fibras musculares. Três tipos principais de fibras podem ser identificados em peixes: rápidas, lentas e intermediárias. As fibras rápidas (*fast*) compõem cerca de 70% da massa muscular, apresentam diâmetro de 50 a 100 µm e são caracterizadas por velocidade de contração rápida, metabolismo glicolítico e baixas concentrações de mitocôndrias e lipídeos (Sänger e Stoiber, 2001). Além disso, essas fibras possuem pouca mioglobina e menor suprimento sanguíneo, e por isso são também denominadas fibras brancas (músculo esquelético branco). As fibras rápidas são mobilizadas durante os

movimentos bruscos de natação, associados à captura de alimentos e fuga de predadores (Sänger e Stoiber, 2001). As fibras musculares lentas (*slow*) compreendem 10-20% da massa muscular e localizam-se numa região mais superficial do corpo do peixe, com maior espessura em torno da linha lateral. Elas apresentam diâmetro de 25 a 45 µm e são caracterizadas por velocidade de contração lenta, metabolismo oxidativo e elevadas concentrações de mitocôndrias e lipídeos (Sänger e Stoiber, 2001), além de muita mioglobina e alto suprimento sanguíneo, que conferem o aspecto avermelhado ao músculo e a denominação fibras vermelhas (músculo esquelético vermelho). As fibras lentas são utilizadas durante os movimentos lentos e de sustentação, especialmente àqueles exigidos durante a natação migratória (Sänger e Stoiber, 2001). Entre os compartimentos rápido e lento residem as fibras musculares intermediárias que, conforme seu nome, apresentam propriedades contráteis e metabólicas intermediárias entre as fibras rápidas e lentas (Sänger e Stoiber, 2001).

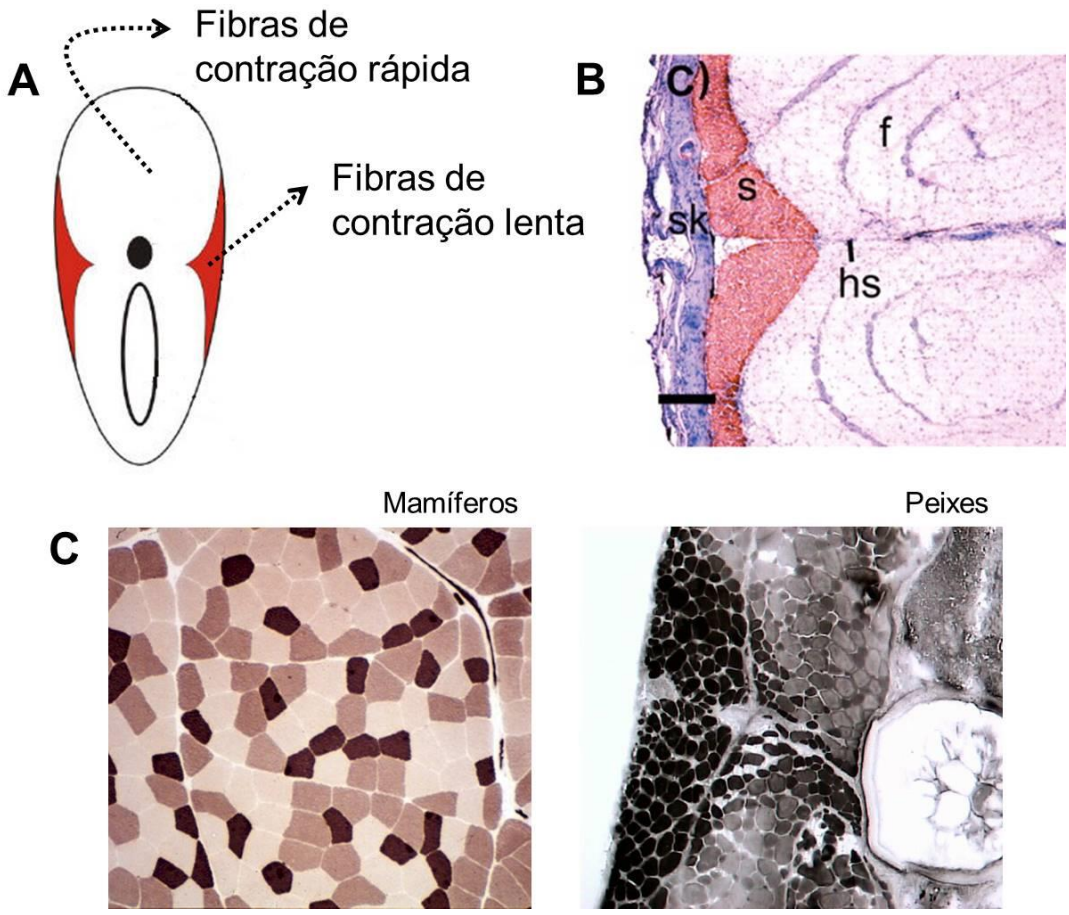

Figura 5: Diferentes tipos de fibras musculares localizados em compartimentos distintos no músculo esquelético de peixes. (A) Esquema indicando a localização das fibras de contração rápida e lenta. (B) Corte transversal do músculo esquelético de juvenil de salvelino ártico

(*Salvelinus alpinus*). As fibras foram marcadas com um anticorpo anti-miosina *slow* (S58 *antibody*) e contra coradas com hematoxilina-eosina. s: fibras musculares de contração lenta (compartimento vermelho); f: fibras musculares de contração rápida (compartimento branco); hs: miossepto horizontal; sk: pele (Johnston et al., 2004). (C) Indicação das diferenças na distribuição dos diferentes tipos de fibras musculares entre mamíferos e peixes. À esquerda um corte transversal do músculo esquelético de rato (*Rattus norvegicus*) (imagem de autoria do grupo de pesquisa), que apresenta padrão em mosaico, e à direita um corte transversal do músculo esquelético de tilápia do Nilo (*Oreochromis niloticus*) (Aguiar et al., 2005), que apresenta compartimentalização. Fibras coradas pela técnica da ATPase ácida (pH=4.6).

1.3. Miogênese

A formação de fibras musculares, ou miogênese, ocorre nas fases iniciais do desenvolvimento embrionário. A mesoderme paraxial, que flanqueia o tubo neural e a notocorda, sofre uma segmentação da região anterior para a posterior, formando estruturas denominadas somitos (revisado por Buckingham e Rigby, 2014). Nos mamíferos, os somitos subdividem-se em uma porção ventral denominada esclerótomo, que originará a coluna vertebral e as costelas, e uma porção dorsal denominada dermomiótomo, responsável pela formação dos músculos do tronco e dos membros, da derme dorsal, de células endoteliais e musculares lisas, e dos vasos sanguíneos (revisado por Buckingham e Rigby, 2014). O dermomiótomo é fonte de populações de células precursoras miogênicas, que delaminam e migram para a formação de uma camada subjacente conhecida como miótomo, cuja porção dorsomedial originará os músculos intrínsecos das costas, enquanto a porção ventrolateral originará os músculos das paredes ventrais e laterais do corpo. Além disso, células do dermomiótomo também migram para locais mais distantes, formando os músculos dos membros, e posteriormente para o interior do miótomo já formado, fornecendo uma população de células progenitoras de reserva que originarão as células satélite no músculo maduro (revisado por Yusuf e Brand-Saberi, 2012).

Nos peixes a classificação de um dermomiótomo ainda é controversa, sendo que a maioria dos trabalhos divide os somitos em esclerótomo e miótomo. Sttelabotte et al. (2007) mostraram que a borda anterior dos somitos fornece uma população de células progenitoras miogênicas equivalentes às células satélite, que serão necessárias para o crescimento muscular do peixe após o nascimento (Sttelabotte et al., 2007). Diferentemente dos mamíferos, o miótomo é relativamente maior que o esclerótomo nos peixes, pois a necessidade de um esqueleto robusto é reduzida devido à flutuabilidade da água e à bexiga natatória, ao passo que a viscosidade do

ambiente aquático exige maior massa muscular para a locomoção (revisado por Stickney et al., 2000).

Durante a somitogênese dos peixes, diferentes tipos celulares formarão e constituirão o miótomo, sendo eles, principalmente, as células adaxiais e as células laterais pré-somíticas (revisado por Stickney et al., 2000). As células adaxiais localizam-se ao redor da notocorda e, sob o estímulo de glicoproteínas secretadas pela notocorda e pelo tubo neural, migram em direção à região superficial do miótomo, formando uma camada única abaixo da epiderme. Nessa região, as células adaxiais fundem-se e originam as fibras musculares lentas, ou seja, a musculatura vermelha do peixe (revisado por Stickney et al., 2000). Um determinado conjunto de células adaxiais não migra para a superfície do miótomo, permanecendo acopladas à notocorda e se diferenciando nas chamadas fibras musculares pioneiras. Essas fibras atravessam toda a extensão do miótomo e orientam a migração das demais células adaxiais à região superficial. Além disso, as fibras musculares pioneiras concentram-se no nível de formação do miossepto horizontal, podendo ter algum papel no desenvolvimento desta estrutura (Halpern et al., 1993). Após migração das células adaxiais, as células laterais pré-somíticas iniciam sua fusão e diferenciação em fibras musculares rápidas, localizadas numa porção mais profunda do miótomo (revisado por Stickney et al., 2000) (Figura 6).

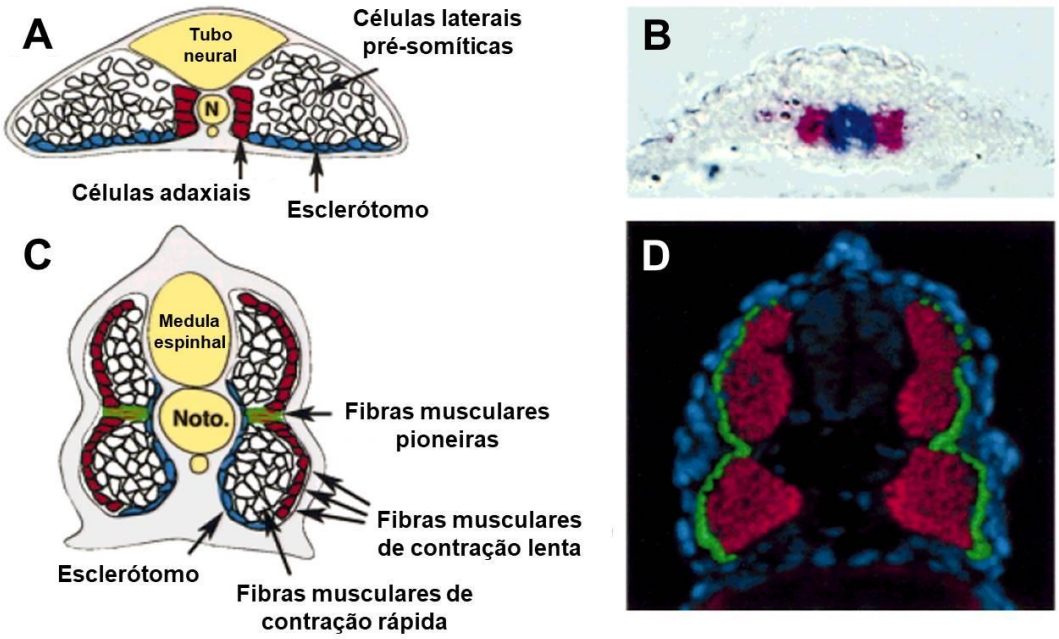

Figura 6: Miogênese embrionária e formação dos tipos de fibras musculares no miótomo de peixes. (A) Esquema de um corte transversal de embrião de zebrafish (*Danio rerio*) com 13 horas, destacando a posição das células adaxiais e células laterais pré-somíticas. (B) As células

adaxiais expressam *myod* (vermelho) enquanto ainda adjacentes à notocorda (azul). (C) Esquema de um corte transversal de embrião de zebrafish (*Danio rerio*) com 24 horas, destacando a posição das fibras musculares de contração lenta, fibras musculares pioneiras e fibras musculares de contração rápida. (D) Fibras musculares de contração lenta (verde - S58 *antibody*) formam uma camada superficial, enquanto as fibras musculares de contração rápida (vermelho - zm4 *antibody*) permanecem numa região mais profunda do miótomo (adaptado de Stickney et al., 2000).

Existe uma "hierarquia genética" (expressão sequencial) de componentes moleculares que regulam o processo miogênico, desde o comprometimento (determinação ou especificação) das células precursoras miogênicas até sua diferenciação em fibras musculares. Os principais deles são os Fatores de Regulação Miogênica (MRFs) (Olson, 1990; revisado por Weintraub, 1993; Johansen e Overturf, 2005), uma família de fatores transcricionais que ativam genes músculo-específicos. A estrutura molecular de um MRF apresenta um domínio altamente conservado, com cerca de 60 aminoácidos, conhecido como *basic helix-loop-helix*. A região *helix-loop-helix* está envolvida com a ligação entre o MRF e outra molécula idêntica, formando um homodímero, ou entre o MRF e os cofatores transcricionais E12 e E47, formando um heterodímero. A região *basic* está envolvida com a ligação do homodímero ou heterodímero a uma sequência específica do DNA (5´-CANNTG-3´), denominada *E-box* (Ma et al., 1994). Essa sequência está presente na região promotora de genes músculo-específicos, que codificam, por exemplo, proteínas contráteis, estruturais e enzimas musculares, de modo que o homodímero ou heterodímero ativam a transcrição desses genes (revisado por Rescan, 2001). Assim, os MRFs controlam o programa miogênico dentro da célula, suprimindo outros possíveis destinos celulares. Dentre os MRFs destacam-se o Myf5 (*myogenic factor 5*), Myod1 (*myogenic differentiation 1*), Myog (*myogenin*) e Mrf4 (*muscle-specific regulatory factor 4*) (Olson, 1990; revisado por Weintraub, 1993). O Myf5 e a Myod1 são conhecidos como MRFs primários, sendo responsáveis principalmente pelo comprometimento das células precursoras à linhagem miogênica e pela proliferação e migração dos mioblastos (célula precursora miogênica já comprometida) no músculo esquelético. A Myog e o Mrf4 são considerados MRFs secundários e estão envolvidos com a diferenciação e fusão dos mioblastos em miotubos, e sua posterior maturação em uma fibra muscular (Johansen e Overturf, 2005; Almeida et al., 2010) (Figura 7).

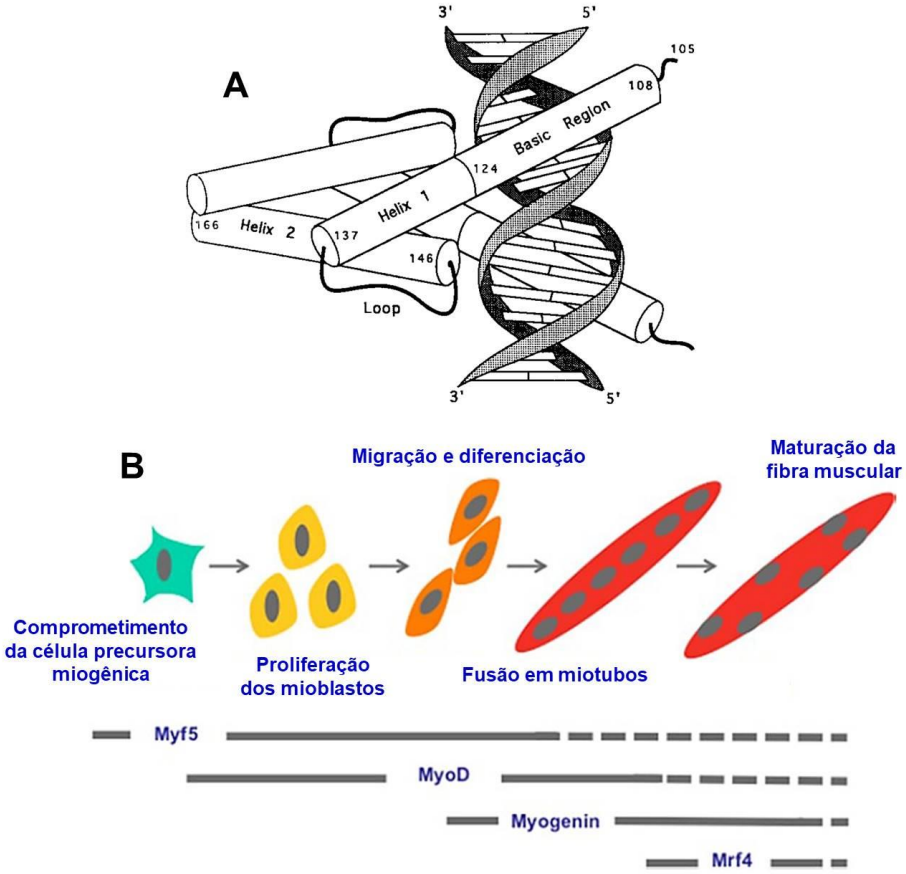

Figura 7: Miogênese e fatores de regulação miogênica (MRFs). (A) Esquema do complexo formado entre um homodímero de Myod e o DNA (Ma et al., 1994). (B) Expressão sequencial e regulação realizada pelos MRFs durante a miogênese do músculo esquelético (adaptado de Zanou e Gailly, 2013).

No entanto, outros fatores expressos anteriormente são necessários para a ativação dos MRFs e direcionamento da célula à miogênese. As células mesodermais são dependentes de moléculas provenientes de tecidos adjacentes para indução da miogênese no somito inicial. Diversas glicoproteínas da família das Wnts, secretadas pelo tubo neural (Wnt1 e Wnt3a) e ectoderme (Wnt6 e Wnt7a), e a molécula sinalizadora Shh (*sonic hedgehog*), secretada pela notocorda, subdividem os somitos em esclerótomo e dermomiótomo, além de induzir a expressão do Myf5 e Myod1 nas células do miótomo (revisado por Hernández-Hernández et al., 2017). Por sua vez, a proteína Bmp4 (*bone morphogenetic protein 4*), secretada pela mesoderme lateral, promove uma regulação negativa desses MRFs (revisado por Hernández-Hernández et al., 2017). Outros componentes importantes da hierarquia miogênica são os fatores transcricionais Pax3 (*paired box 3*) e Pax7 (*paired box 7*). Em mamíferos, o Pax3 é expresso em

todo o dermomiótomo e constitui um marcador de células progenitoras miogênicas migrantes que ainda não ativaram Myf5 e Myod1, ou seja, células que ainda não se comprometeram com a linhagem miogênica (revisado por Buckingham e Rigby, 2014). Altos níveis de Pax3 direcionam as células do dermomiótomo para o destino miogênico, enquanto baixos níveis podem dar origem a células da derme, endoteliais, musculares lisas e adipócitos. Além disso, O Pax3 regula genes envolvidos no equilíbrio que deve ser mantido entre auto-renovação celular e miogênese, como Fgfr4 (*fibroblast growth factor receptor 4*), Spry2 (*sprouty rtk signaling antagonist 2*) e Myf5 (revisado por Buckingham e Rigby, 2014). Progressivamente ocorre uma redução na expressão do Pax3 e um aumento na expressão do Pax7. A expressão do Pax7 fica mais restrita à porção central do dermomiótomo, local em que células Pax3/Pax7-positivas migram e fornecem uma população celular de reserva no miótomo (revisado por Buckingham e Rigby, 2014). Dessa forma, o Pax7 se torna um marcador molecular das células satélite, necessárias para a miogênese pós-natal e regeneração do músculo adulto. Após a expressão de Pax3 e Pax7, as células que definitivamente irão contribuir para a formação de fibras musculares passam a expressar sequencialmente Myf5, Myod1, Myog e Mrf4 (revisado por Buckingham e Rigby, 2014). A hierarquia miogênica prevalece no músculo esquelético dos vertebrados, mas os peixes possuem uma particularidade. Enquanto as células precursoras miogênicas dos mamíferos somente expressam MRFs após migrarem para os locais em que definitivamente irão se diferenciar em fibras musculares maduras, as células adaxiais já são Myf5/MyoD-positivas antes mesmo do início da formação dos somitos, ainda adjacentes à notocorda (Figura 6B) (revisado por Stickney et al., 2000; Stellabotte et al., 2007; revisado por Buckingham e Rigby, 2014). Apesar de as células laterais pré-somíticas somente expressarem esses fatores após a somitogênese, esse comprometimento precoce das células adaxiais demonstra uma identidade miogênica antecipada no músculo esquelético dos peixes (revisado por Stickney et al., 2000).

1.4. Crescimento muscular pós-natal

O crescimento pós-natal do músculo esquelético nos peixes envolve uma população de células precursoras miogênicas que, após estímulos, reativam o programa miogênico embrionário e originam mioblastos capazes de fusão (revisado por Johnston et al., 2011). Essas são as células-tronco do tecido muscular e também são conhecidas como mioblastos indiferenciados ou células satélite, devido à localização na periferia das fibras musculares, entre a lâmina basal e o sarcolema (Mauro, 1961; Koumans et al., 1990) (Figura 8).

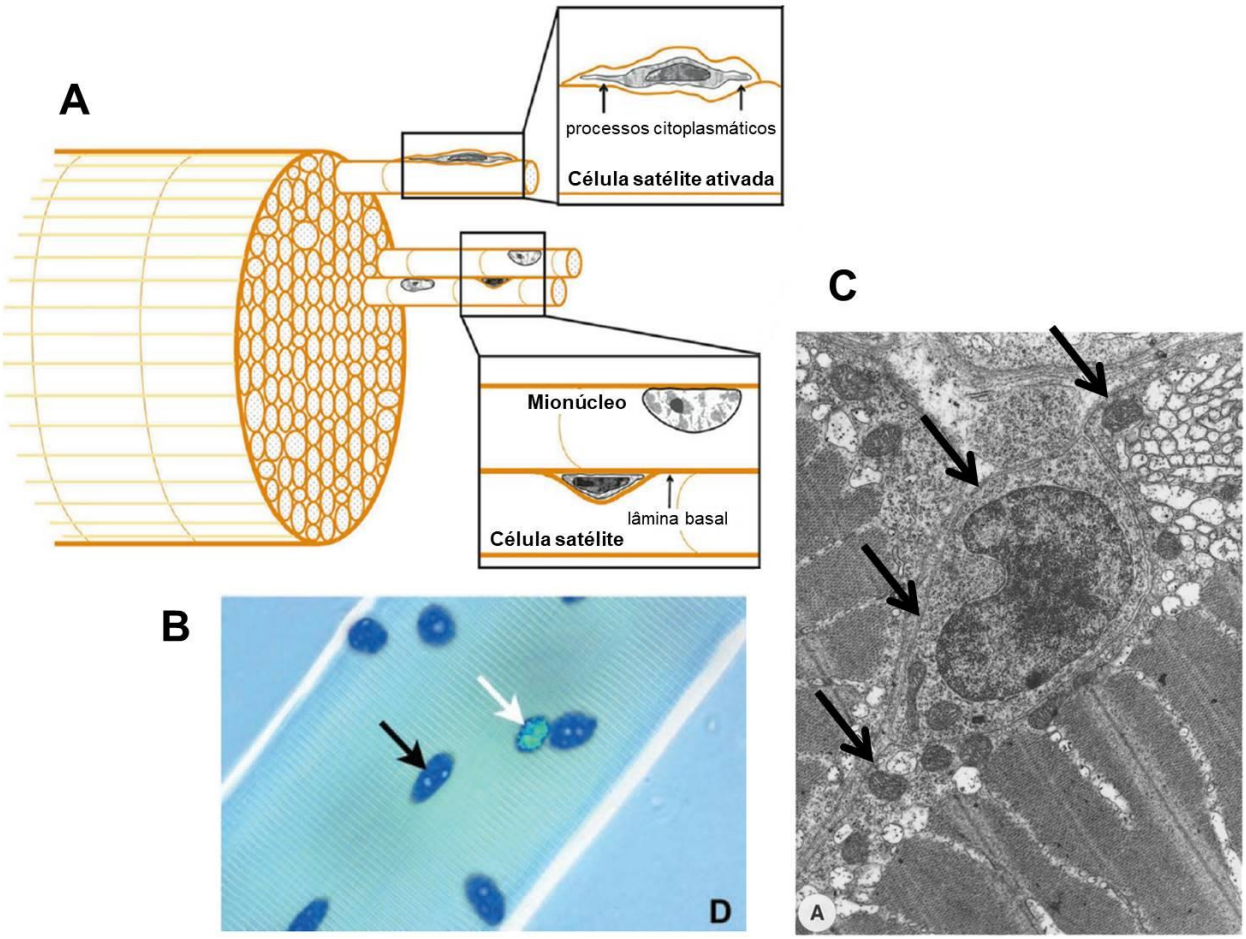

Figura 8: Célula satélite do músculo esquelético. (A) Esquema mostrando a posição da célula satélite, entre a lâmina basal e o sarcolema da fibra muscular (adaptado de Hawke e Garry, 2001). (B) Imunocitoquímica de fibra muscular de mamífero, indicando alta expressão de Pax7 pela célula satélite (flecha branca) em comparação ao mionúcleo (flecha preta). (C) Microscopia eletrônica de transmissão do músculo esquelético de carpa comum (*Cyprinus carpio*). ↘: lâmina basal envolvendo ambas a célula satélite e a fibra muscular (Koumans et al., 1990).

Os núcleos de células satélite constituem de 2 a 7% dos núcleos musculares em indivíduos saudáveis, e são relativamente grandes e com cromatina muito condensada, ou seja, permanecem funcionalmente inativos ou num estado quiescente. Essa quiescência é mantida pelo Pax7, que reprime genes envolvidos com a diferenciação dos mioblastos (revisado por Buckingham e Rigby, 2014). Durante a ativação, as células satélite reduzem a expressão de Pax7 e aumentam a expressão dos MRFs, originando os mioblastos, cuja proliferação e diferenciação são os mecanismos que promovem a hiperplasia (aumento do número de fibras musculares) e hipertrofia (aumento do tamanho das fibras) (Rowlerson e Veggetti, 2001; revisado por Johnston

et al., 2011). Durante o crescimento hiperplásico, os mioblastos proliferam, migram e agregam-se na superfície de fibras musculares pré-existentes, iniciando os processos de diferenciação e fusão e originando os miotubos, que posteriormente formam fibras musculares maduras. No crescimento hipertrófico, após a proliferação, migração e diferenciação, os núcleos dos mioblastos são internalizados nas fibras musculares em crescimento, de modo que promovem uma maior síntese de miofibrilas e, consequentemente, aumentam a área e o diâmetro de fibras pré-existentes (revisado por Johnston et al., 2011) (Figura 9).

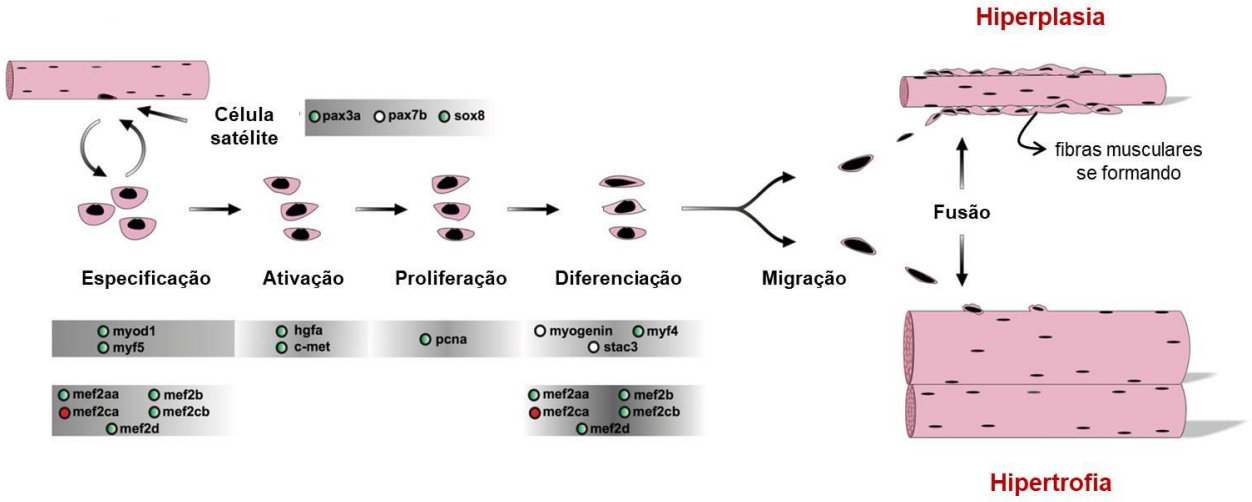

Figura 9: Crescimento pós-natal do músculo esquelético em peixes. Ocorre a retomada dos eventos da miogênese, especialmente proliferação e diferenciação de mioblastos, que irão culminar com os processos de recrutamento ou hiperplasia muscular, aumentando o número de fibras, e hipertrofia muscular, aumentando o tamanho das fibras. Esferas brancas indicam componentes com maior expressão nas fibras musculares de contração rápida; esferas vermelhas indicam componentes com maior expressão nas fibras musculares de contração lenta; esferas verdes indicam componentes que não apresentam diferenças de expressão entre os tipos de fibras musculares (adaptado de Mareco et al., 2015).

A contribuição dos mecanismos de hiperplasia e hipertrofia no crescimento muscular pós-natal tem sido estudada em muitas espécies de peixes. Estudos mostraram que em muitos desses animais existem duas "ondas" de intenso crescimento hiperplásico (Rowlerson e Veggetti, 2001; Johnston et al., 2003). A primeira é conhecida como hiperplasia estratificada, uma continuidade da miogênese embrionária, que promove a formação de novas fibras musculares em camadas. Essa hiperplasia ocorre a partir de zonas germinativas e é responsável pelo espessamento da musculatura nos estágios iniciais do desenvolvimento (Rowlerson e Veggetti, 2001). A segunda

é denominada hiperplasia em mosaico, que promove a formação de novas fibras em toda a musculatura do peixe, a qual também apresenta fibras musculares num estágio de maturação mais avançado (Rowlerson e Veggetti, 2001; Almeida et al., 2010). Dessa forma, o músculo esquelético apresenta fibras musculares com diâmetro pequeno entre fibras de maior diâmetro, como um mosaico, permitindo um maior desenvolvimento da massa muscular (Figura 10). Os peixes que apresentam ambos os tipos de crescimento hiperplásico são denominados peixes de crescimento somático indeterminado, nos quais o grande aumento da massa muscular proporcionado pela hiperplasia em mosaico permite atingirem um grande tamanho corporal e também confere importância econômica à espécie (Rowlerson e Veggetti, 2001). Por outro lado, os peixes que apresentam somente a hiperplasia estratificada são denominados peixes de crescimento somático determinado, que atingem um tamanho fixo uma vez que a hiperplasia cessa nos estágio mais iniciais do desenvolvimento, tornando o crescimento hipertrófico das fibras o principal mecanismo de crescimento muscular pós-natal nessas espécies (Biga e Goetz, 2006; Froehlich et al., 2013).

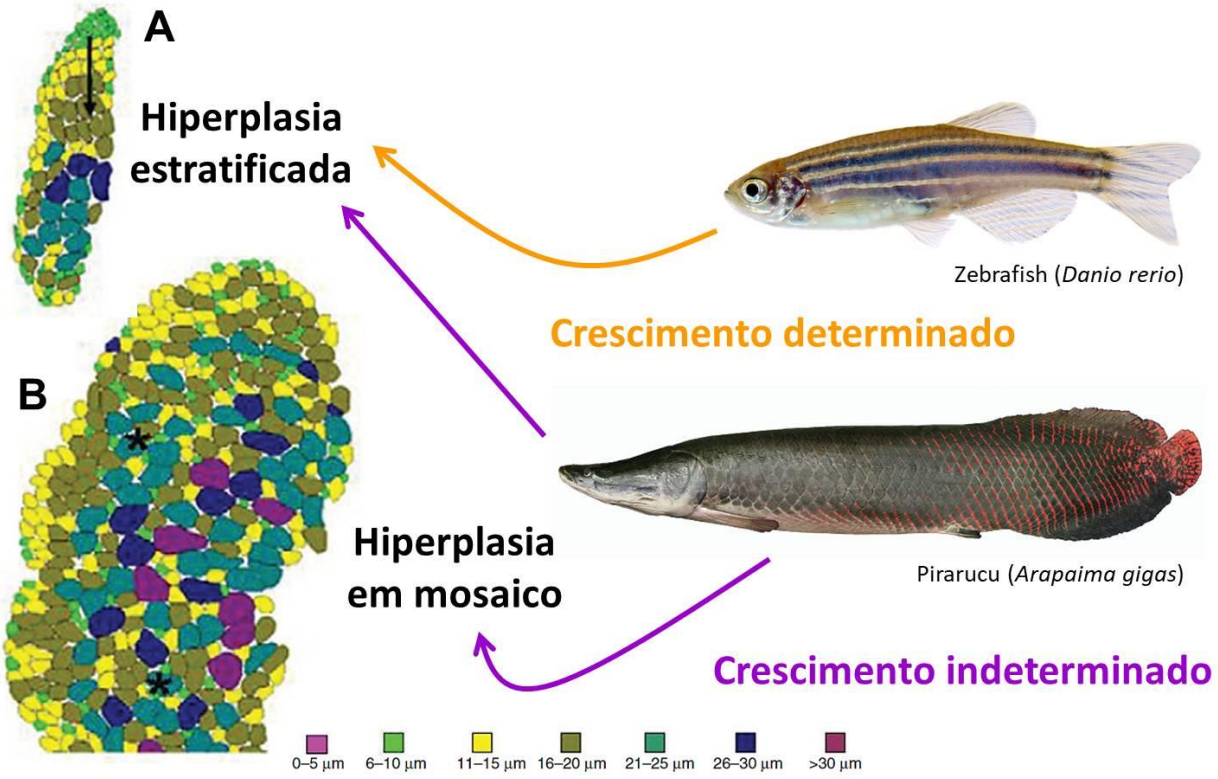

Figura 10: Crescimento hiperplásico do músculo esquelético de peixes. (A) Hiperplasia estratificada, em que a formação das fibras ocorre em camadas. A flecha preta ilustra o sentido do crescimento conforme o diâmetro das fibras musculares. (B) Hiperplasia em mosaico, em que

novas fibras são formadas entre fibras musculares já maduras, de maior tamanho. Os asteriscos ilustram fibras musculares cercadas por fibras "jovens" (adaptado de Johnston et al., 2009). Peixes que apresentam somente a hiperplasia estratificada, como o zebrafish, são denominados peixes de crescimento somático determinado, enquanto peixes que apresentam ambas as hiperplasias estratificada e em mosaico, como o pirarucu, são denominados peixes de crescimento somático indeterminado.

O crescimento muscular é um processo multifatorial que integra sinais extrínsecos e intrínsecos em sua regulação. Dentre os fatores extrínsecos se destacam a temperatura, salinidade, oxigenação, intensidade e duração de luz, pH e fluxo de água (revisado por Johnston, 2006). Com relação aos sinais intrínsecos, além da regulação pelos MRFs e outros fatores transcricionais, nós podemos citar hormônios, citocinas e fatores de crescimento. Esses componentes influenciam diretamente o tamanho da fibra muscular, através de um delicado balanço entre a síntese e a degradação proteica, cujas vias de sinalização se inter-relacionam e modulam uma a outra (Sandri, 2008). Para que ocorra um aumento de massa muscular, o balanço deve ser favorável à síntese proteica, fortemente influenciada pela via Igf/Pi3k/Mtor. Por outro lado, a atrofia muscular (redução no tamanho das fibras musculares) é decorrente de um balanço favorável à degradação de proteínas, mediada principalmente pelo Mafbx e Murf1 (atrogenes) (revisado por Glass, 2005) (Figura 11).

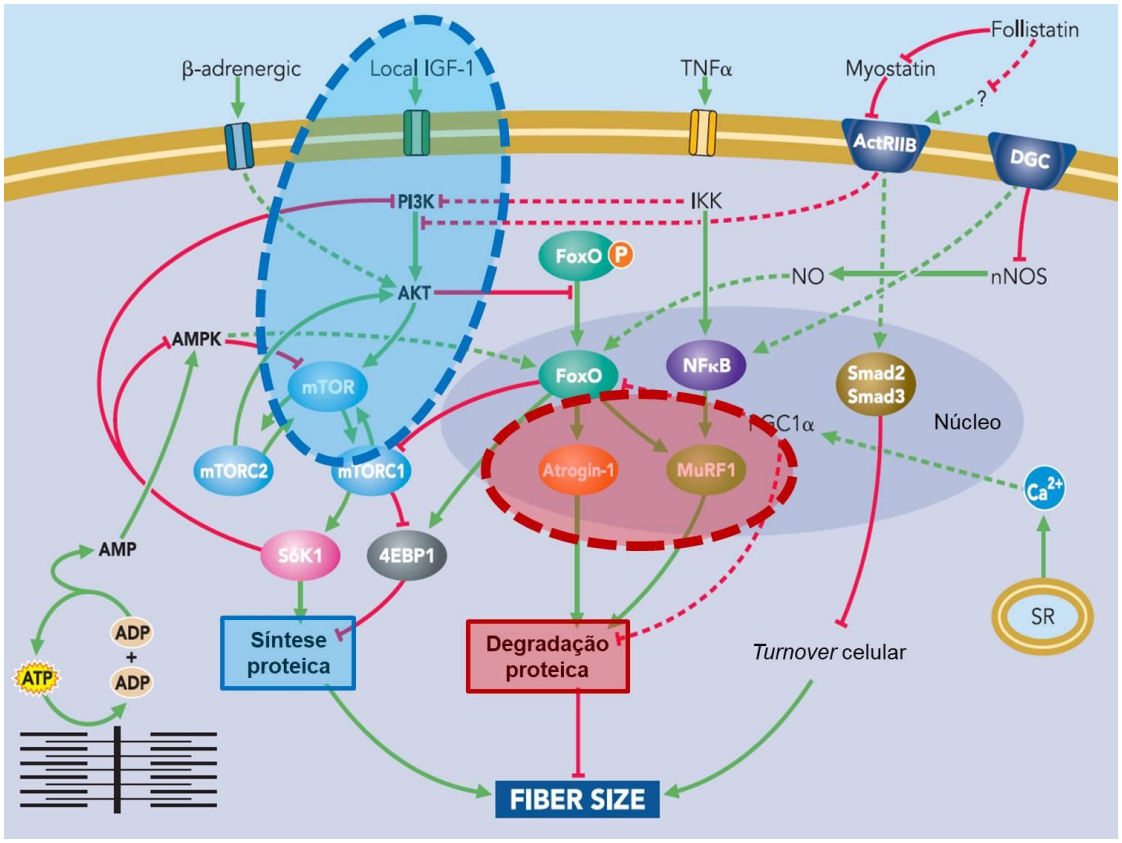

Figura 11: Vias de sinalização da síntese e degradação proteica regulando o crescimento do músculo esquelético de peixes. A síntese proteica tem início com a ligação do Igf1 em seu receptor de membrana, desencadeando uma cascata que ativa o Pi3k e Mtor (círculo azul). A degradação proteica é desencadeada por diversas formas, mas culmina geralmente com a ativação do Mafbx (Atrogin-1) e Murf1 (círculo vermelho), que quebram proteínas sarcoméricas e outros componentes musculares (adaptado de Sandri, 2008).

Os principais fatores que regulam a síntese proteica são o Igf1 e Igf2 (*insulin like growth factor*), juntamente com seus próprios receptores (Igfr - *insulin like growth factor receptor*) e proteínas ligantes (Igfbp - *insulin like growth factor binding protein*) (revisado por Johnston et al., 2011). O Igf1 é um dos mais estudados e caracterizados fatores promotores de crescimento muscular. Em vertebrados o Igf1 é sintetizado principalmente pelo fígado, em resposta a nutrientes e ao hormônio de crescimento (GH - *growth hormone*). O Igf1 produzido no fígado é secretado para o sistema circulatório para gerar um efeito endócrino, mas outros tecidos também apresentam uma produção local de Igf1, incluindo o músculo esquelético, gerando efeitos parácrinos e autócrinos (revisado por Johnston et al., 2011). Quando o Igf1 se liga ao seu

receptor de membrana (Igf1r) desencadeia uma cascata de fosforilação ao promover a ativação do Pi3k (*phosphatidylinositol-3-kinase*), necessário para a produção do *phosphatidylinositol-3,4,5-triphosphate*. Esse componente recruta o Akt (*protein kinase B*), responsável pela ativação do Mtor (*mechanistic target of rapamycin kinase*) (Sandri, 2008). O Mtor processa e integra sinais nutricionais, energéticos e de crescimento, regulando o ciclo celular, transcrição gênica, organização do citoesqueleto e síntese de proteínas. Essa quinase forma dois complexos multiméricos conhecidos como TORC1 e TORC2 (Sandri, 2008). O TORC1 contém a proteína Rptor (*regulatory associated protein of mtor complex 1*) e estimula a síntese proteica pela ativação do Rps6k (*ribosomal protein s6 kinase*) e inibição do Eif4ebp1 (*eukaryotic translation initiation factor 4e-binding protein 1*). O TORC2 contém a proteína Rictor (*rptor independent companion of mtor complex 2*) e estimula a fosforilação e ativação do Akt, gerando um *feedback* positivo (Vélez et al., 2014). Estudos vêm demonstrando que, além da integração de sinais endócrinos, a ativação da síntese proteica também envolve outros caminhos. Alguns trabalhos mostraram efeitos estimulatórios dos aminoácidos, seja pela ativação da via do Mtor (Seiliez et al., 2008; Vélez et al., 2014) ou de membros do sistema de Igfs (Bower e Johnston, 2010b; Garcia de la serrana e Johnston, 2013). Esses estudos suportam a existência de estímulos nutricionais no crescimento do músculo esquelético de peixes e reforçam a necessidade de experimentos com aminoácidos, uma vez que essas moléculas são comumente administradas na dieta desses animais visando atender ou exceder os requisitos dietéticos para um crescimento ideal e eficiente conversão alimentar. Os aminoácidos essenciais, também denominados indispensáveis, representam nutrientes de grande importância para o desenvolvimento e crescimento de peixes, uma vez que esses animais não são capazes de sintetizá-los. Dentre os aminoácidos essenciais mais comumente utilizados em dietas para peixes temos a lisina, metionina, treonina, triptofano e leucina (revisado por Li et al., 2008). Os aminoácidos não-essenciais são também chamados de dispensáveis, ou seja, são sintetizados pelo organismo. Dentre os aminoácidos não-essenciais, destacam-se a alanina e glutamina (revisado por Li et al., 2008). Os aminoácidos possuem inúmeros papéis nos organismos, servindo amplamente como "blocos" para a construção de proteínas e como substratos energéticos, mas também possuem funções que variam dependendo do aminoácido. Cleveland e Radler (2019) mostraram que a leucina e fenilalanina reduzem as taxas de degradação proteica em culturas de células musculares de trutas arco-íris, enquanto a valina e lisina aumentam a proteólise quando em excesso perante outros aminoácidos essenciais (Cleveland e Radler, 2019). Além de inibir a degradação de proteínas, a leucina tem um importante papel como ativador da síntese proteica em mamíferos

(Garlick, 2005; Duan et al., 2016). Recentemente, o mecanismo através do qual os aminoácidos estimulam a síntese de proteínas tem sido descrito em mamíferos, com a identificação dos complexos Rrag GTPases (*ras related gtp binding*) e Lamtor (*late endosomal/lysosomal adaptor, mapk and mtor activator*) como sensores de aminoácidos e promotores da ativação do Mtor (Sancak et al., 2010; Demetriades et al., 2014). Visto o papel do sistema de Igfs e dos aminoácidos no aumento da síntese de proteínas, a aplicação dessas moléculas em peixes apresenta-se como um potencial tratamento para a obtenção de crescimento muscular, com possíveis intervenções na piscicultura.

Além do papel na síntese de proteínas, o Akt previne a expressão de genes relacionados à degradação proteica e atrofia muscular, através da fosforilação do Foxo (*forkhead box o*) (revisado por Bonaldo e Sandri, 2013). A fosforilação do Foxo promove sua translocação do núcleo para o sarcoplasma, impedindo que desempenhe seu papel como fator transcricional. No entanto, a baixa atividade do Akt aumenta os níveis de Foxo nuclear (defosforilado), que promove a ativação do Murf (*muscle-specific ring finger protein*) e Mafbx (*muscle atrophy f-box protein*) (revisado por Bonaldo e Sandri, 2013), também denominados Trim63 (*tripartite motif containing 63*) e Fbxo32 (*f-box protein 32*), respectivamente. O Murf e o Mafbx são enzimas ubiquitina ligases cuja função é a transferência de ubiquitinas a determinado substrato proteico. Esse substrato, uma vez poliubiquitinado, é ancorado ao complexo proteassoma, para que seja realizada sua degradação. Ambos Murf e Mafbx regulam a degradação de diversos componentes presentes no músculo esquelético; o Murf controla a degradação de proteínas sarcoméricas, como a troponina e as cadeias pesadas e leves de miosinas, enquanto o Mafbx promove a degradação da Myod e do Eif3j (*eukaryotic translation initiation factor 3 subunit j*), crucial para a síntese proteica (revisado por Bonaldo e Sandri, 2013). Além da sinalização por Akt-Foxo, outras vias estimulam a degradação de proteínas no músculo esquelético, como a resposta inflamatória mediada principalmente pelo Nfkb (*nuclear factor kappa b*) e a ação da miostatina (Mstn - *myostatin*), que também culminam com a ativação do Murf e Mafbx (revisado por Bonaldo e Sandri, 2013).

Ainda dentro desse contexto, um modelo experimental muito utilizado para o estudo do crescimento muscular em peixes é o de jejum e realimentação (*fasting-refeeding*) (Johnston et al., 2011). Após esses tratamentos o crescimento do animal ocorre com mais rapidez em comparação a peixes que são continuamente alimentados, um fenômeno conhecido por crescimento compensatório (Nikki et al., 2004). Dessa forma, os experimentos de jejum e realimentação são comumente utilizados para manipular a taxa de crescimento dos peixes, um

parâmetro cujas variações são decorrentes, principalmente, de alterações no crescimento e fenótipo do músculo esquelético. O período de jejum está diretamente relacionado a uma maior degradação de proteínas musculares, enquanto que a realimentação desencadeia uma síntese proteica mais exacerbada (Bower et al., 2009).

1.5. Duplicação do genoma

Em peixes, as vias de sinalização que regulam o crescimento do músculo esquelético tiveram uma expansão de seu número de componentes moleculares quando comparada a outros vertebrados, devido a um evento de duplicação total do genoma (WGD - *whole genome duplication*). As WGDs apesar de raras são eventos dramáticos que resultam na duplicação súbita da sequência completa do genoma, que moldaram profundamente a evolução dos vertebrados e representam marcos evolutivos a partir dos quais algumas linhagens se diversificaram (Berthelot et al., 2014; revisado por Glasauer e Neuhauss, 2014). Dessa forma, a WGD tem uma importância crucial para os genomas dos vertebrados, pois fornece matérias-primas nas quais a seleção natural pode agir para promover radiações adaptativas e inovações evolutivas (Taylor et al., 2003). Estima-se que há 333-225 milhões de anos, o genoma ancestral de todos os peixes teleósteos sofreu um evento de WGD específico, denominado *teleost-specific 3rd WGD* (Ts3R), precedido de outros dois eventos de WGD mais antigos comuns a todos vertebrados (Jaillon et al., 2004; Dehal e Boore, 2005). Nesse contexto, os salmonídeos possuem um interesse particular devido a um evento adicional e relativamente recente de WGD, estimado há 100-25 milhões de anos, denominado *salmonid-specific 4th WGD* (Ss4R) (Berthelot et al., 2014) (Figura 12). Vários trabalhos avaliaram os efeitos da Ss4R no músculo esquelético, descrevendo a expansão de diversas famílias de genes (Macqueen et al., 2010; Garcia de la serrana e Johnston, 2013; Macqueen et al., 2013) e como eles são diferencialmente regulados durante o desenvolvimento das células musculares (Bower e Johnston, 2010a; Bower e Johnston, 2010b; Garcia de la serrana e Johnston, 2013; García de la serrana et al., 2014a).

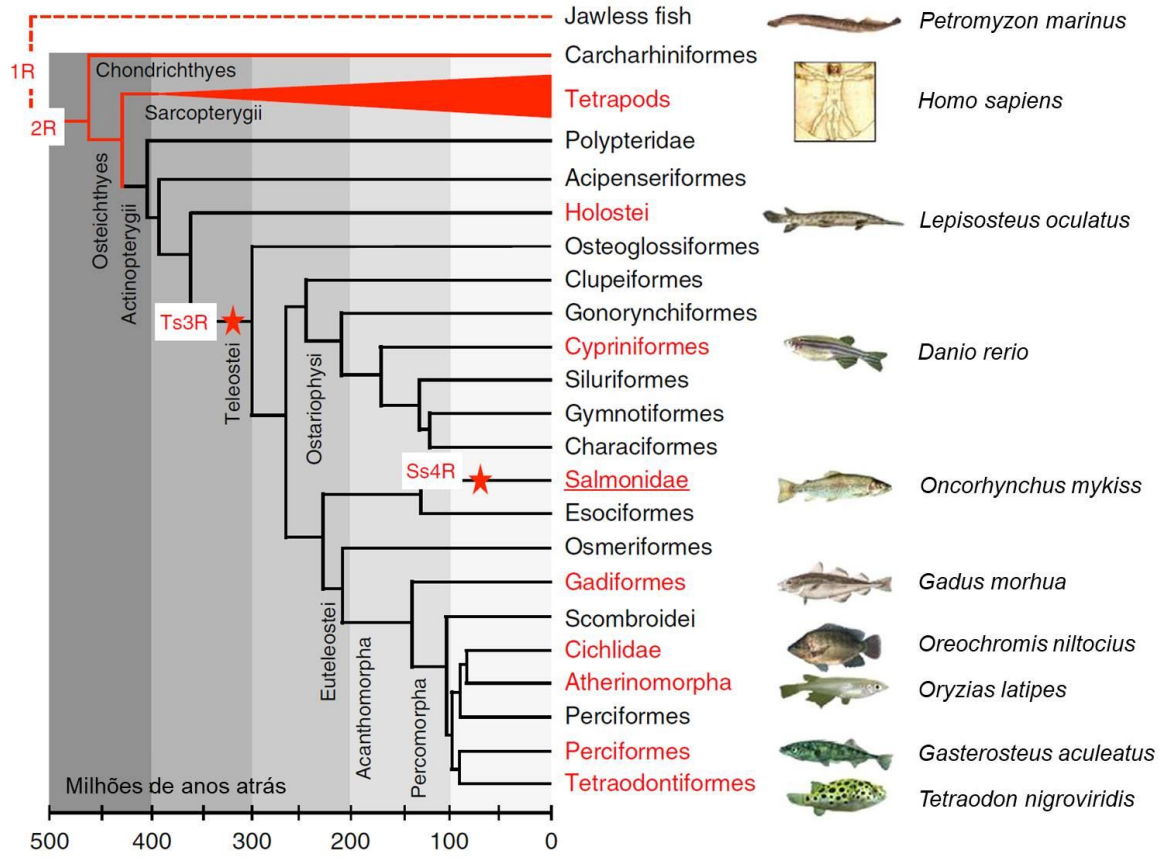

Figura 12: História evolutiva e duplicação total do genoma em peixes. As estrelas vermelhas indicam a posição evolutiva da duplicação do genoma específica de teleósteos (Ts3R) e específica dos salmonídeos (Ss4R), que expandiram o número de componentes moleculares que regulam o crescimento do músculo esquelético (adaptado de Berthelot et al., 2014).

Após a WGD ocorre a perda de muitas cópias de genes redundantes, num processo conhecido como fracionamento gênico. Entretanto, cerca de 15 a 21% dos genes duplicados (genes parálogos) derivados do Ts3R foram retidos através de mecanismos de subfuncionalização e/ou neofuncionalização (Garcia de la serrana et al., 2014b). Durante a subfuncionalização cada gene parálogo adquire parte da função original do gene ancestral, culminando muitas vezes em uma regulação compartilhada de determinado processo biológico. Na neofuncionalização os parálogos adquirem uma função diferente do gene ancestral, o que pode conferir uma vantagem adaptativa (Maere e Van de Peer, 2010) (Figura 13). Essas funções divergentes têm sido investigadas em diversas famílias de proteínas, como Igfbps e Akirins, que sofreram uma expansão após retenção diferencial decorrente da Ts3R e Ss4R (Macqueen et al., 2010; Macqueen et al., 2013). Através dos mecanismos de subfuncionalização e

neofuncionalização, a WGD promove um aumento da complexidade dos organismos, podendo contribuir para uma maior diversidade biológica.

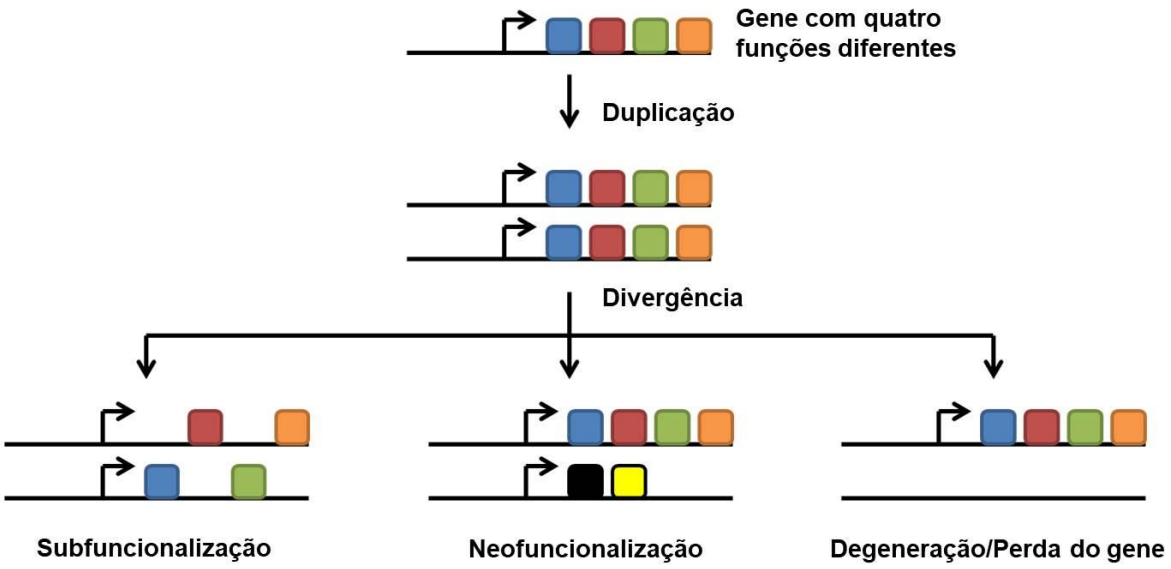

Figura 13: Esquema indicando os mecanismos que sucedem um evento de duplicação do genoma; subfuncionalização (cópias com função compartilhada), neofuncionalização (cópia com nova função) ou perda do gene.
(adaptado de https://en.wikipedia.org/wiki/Gene_redundancy).

Além disso, estudos recentes mostraram diferenças na retenção de genes parálogos entre as superordens de teleósteos Ostariophysi, a qual pertencem o zebrafish e o pacu, e Acanthopterygii, a qual pertence a tilápia do Nilo. Garcia de la serrana et al. (2014b) mostraram que 510 e 418 parálogos, que surgiram após o Ts3R, foram diferencialmente retidos nas superordens Ostariophysi e Acanthopterygii, respectivamente, indicando a existência de parálogos linhagem-específicos (LSPs - *lineage specific paralogues*) (Garcia de la serrana et al., 2014b). Essa retenção diferencial sugere que os LSPs possam ter sofrido diferentes mecanismos de subfuncionalização e/ou neofuncionalização durante o processo evolutivo das superordens. Muitos deles são componentes essenciais nas vias de miogênese, síntese e degradação proteica no músculo esquelético (Garcia de la serrana et al., 2014b), e alguns trabalhos sugerem que esses genes parálogos apresentam diferentes padrões de expressão (Mareco et al., 2015). No entanto, apesar dos avanços realizados na identificação dos LSPs, os seus papéis fisiológicos permanecem desconhecidos na maioria dos casos e muitos pesquisadores não abordam essa temática em suas investigações.

1.6. microRNAs

Atualmente é consenso que a propagação da informação genética é muito mais complexa que aquela definida pelo dogma central da biologia molecular, no qual o DNA promove a síntese do RNA que vai ser traduzido em uma proteína. Existem diversos outros mecanismos envolvidos no controle do metabolismo celular e definição do fenótipo, como a metilação do DNA, a modificação de histonas e a regulação por RNAs não codificantes (Chuang e Jones, 2007). Dentre os RNAs não codificantes destacam-se os microRNAs (miRNAs), uma classe de pequenos RNAs regulatórios que apresentam um importante papel nos mais diversos processos biológicos de um organismo, inclusive no desenvolvimento e crescimento muscular (revisado por Ge e Chen, 2011; revisado por Bizuayehu e Babiak, 2014). A função principal dos miRNAs é a regulação pós-transcricional de genes, promovida pela inibição traducional ou degradação de RNAs mensageiro (mRNAs) (Bartel e Chen, 2004; revisado por Filipowicz et al., 2008; revisado por Ge e Chen, 2011). Na maioria dos casos, essa repressão se dá através de complementaridade de bases entre os nucleotídeos 2 a 7 da região 5' do miRNA, conhecidos como sequência *seed*, e a região 3' não traduzida (3'UTR - 3' untranslated region) dos mRNAs alvo (Williams et al., 2009) (Figura 14).

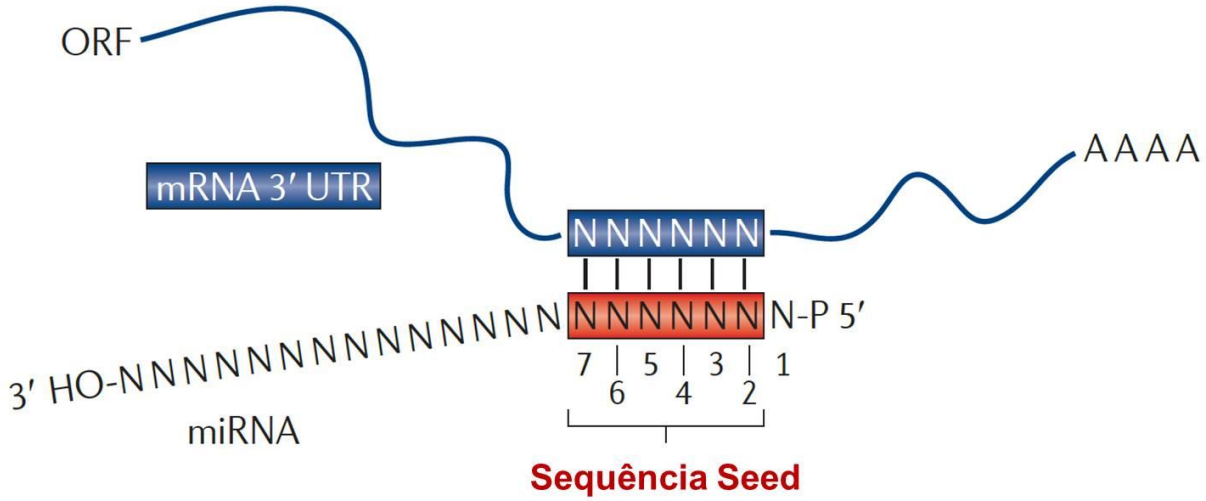

Figura 14: Complementaridade de bases entre miRNA e seu mRNA alvo. A complementaridade geralmente ocorre através da ligação entre os nucleotídeos 2 a 7 da região 5' do miRNA (sequência *seed*) e a região 3'UTR do mRNA alvo. Essa ligação é determinante no reconhecimento do alvo e suficiente para desencadear o silenciamento. ORF: open reading frame; 3'UTR (3' untranslated region) (adaptado de Huntzinger e Izaurralde, 2011).

Com relação à biogênese, os genes de miRNAs são sintetizados no núcleo como longos transcritos primários, denominados pri-miRNAs, principalmente pela ação da RNA polimerase II. Os pri-miRNAs podem codificar um ou mais miRNAs, e são posteriormente processados pela enzima nuclear Drosha (*drosha ribonuclease III*) (Lee et al., 2003) gerando uma estrutura em *hairpin* com sequência de aproximadamente 70 nucleotídeos, conhecida como miRNA precursor (pre-miRNA). Os pre-miRNAs são então transportados ao citoplasma pela Exportin-5, onde serão processados pela enzima Dicer (*dicer ribonuclease III*) em um miRNA dupla-fita (*duplex*) com aproximadamente 22 nucleotídeos (revisado por Winter et al., 2009; revisado por Ge e Chen, 2011). Em seguida, apenas uma única fita do duplex de miRNA é incorporada a proteínas da família Ago (*argonaute, risc catalytic component*) para formar um complexo de silenciamento induzido por RNA (RISC - *RNA-induced silencing complex*), que associa-se com o sítio de complementaridade do mRNA alvo e promove sua repressão (revisado por Winter et al., 2009; revisado por Bizuayehu e Babiak, 2014). A outra fita do *duplex* é degradada ou pode associar-se a um novo RISC para a regulação de outro mRNA alvo (Figura 15).

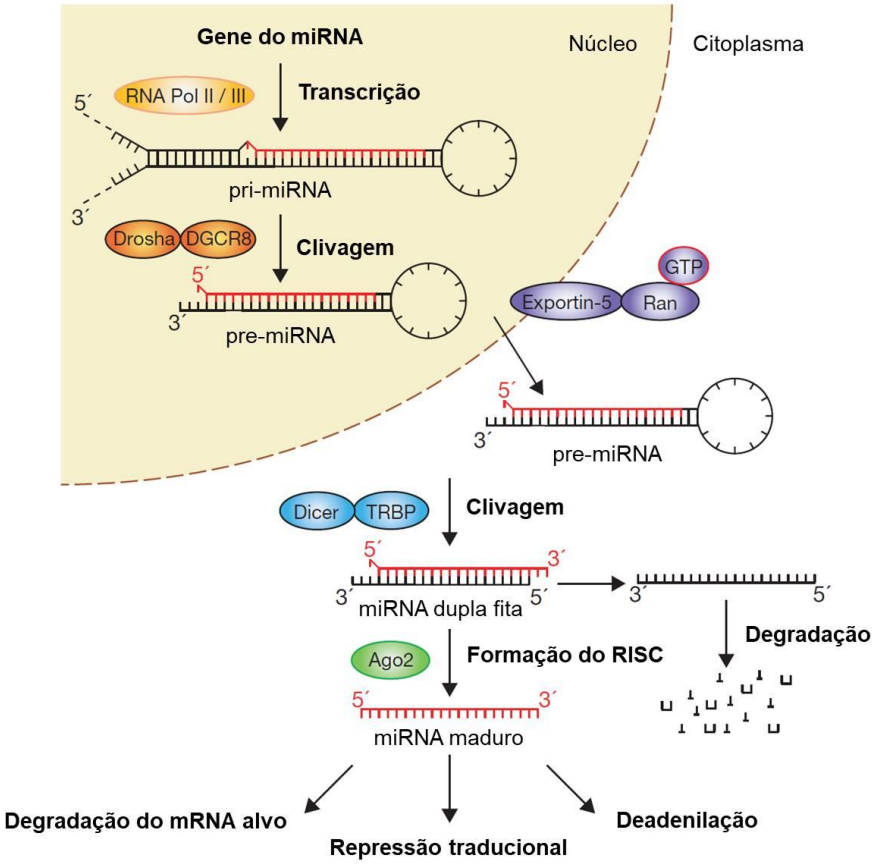

Figura 15: Biogênese dos miRNAs. A via de regulação do miRNA tem início com a transcrição do gene em pri-miRNA e seu processamento em pre-miRNA no interior do núcleo. O pre-

miRNA é transportado ao citoplasma e clivado para produção de um miRNA de dupla fita. A fita funcional é incorporada num complexo de silenciamento, que vai se ligar ao mRNA alvo e promover sua degradação, repressão traducional ou deadenilação (adaptado de Winter et al., 2009).

Os miRNAs exercem os efeitos em seus alvos num padrão combinatório, o que aumenta a complexidade e potencial regulatório da expressão gênica. Um único miRNA pode ter diversos mRNAs alvo e, da mesma forma, mRNAs individuais podem ser regulados por diferentes miRNAs (revisado por van Rooij et al., 2008; Guo et al., 2010). Assim, a maioria dos miRNAs promove uma regulação refinada e orquestrada de vias de sinalização e funções biológicas comuns (revisado por van Rooij et al., 2008; revisado por Goljanek-Whysall et al., 2012).

Análises filogenéticas revelam a existência de uma alta conservação dos miRNAs entre os vertebrados, e sugerem uma correlação positiva entre o número de genes de miRNAs e a complexidade do organismo (Sempere et al., 2006; Lee et al., 2007). Estudos têm mostrado que em mamíferos mais de 60% dos mRNAs tem sítios conservados de ligação a miRNAs (Friedman et al., 2009; Guo et al., 2010) e, baseado nessa conservação de miRNAs em vertebrados, pode-se prever que um conjunto considerável de mRNAs é modulado por miRNAs também em peixes teleósteos (revisado por Bizuayehu e Babiak, 2014). Além disso, a extensão da participação dos miRNAs regulando vias moleculares nos peixes pode ser ainda maior e mais complexa devido a WGD, e Berthelot et al. (2014) mostrou que os genes de miRNAs foram quase todos retidos como cópias duplicadas em contraste com genes codificantes de proteínas (Berthelot et al., 2014).

Os miRNAs em peixes estão envolvidos na embriogênese, desenvolvimento e em diversos processos fisiológicos de diferentes tecidos (Wienholds et al., 2005; Giraldez et al., 2006; Yin et al., 2008; Staton et al., 2011; Biyashev et al., 2012; Flynt et al., 2009; Huang et al., 2012; Yan et al., 2012b; Yin et al., 2012). Tanto a formação quanto o crescimento muscular são profundamente regulados por vários miRNAs, e alguns deles são classificados como músculo-específicos devido à sua expressão específica ou alta nos músculos cardíacos e/ou esqueléticos, especialmente o miR-1, miR-133, miR-206 e miR-499. Esses miRNAs participam em processos como miogênese, proliferação de mioblastos e diferenciação em miotubos, especificação de tipos de fibras e regeneração muscular (Chen et al., 2006; van Rooij et al., 2009; Chen et al., 2010; revisado por Ge e Chen, 2011; McCarthy, 2011), orquestrando o destino e fenótipo das células musculares.

Com relação ao envolvimento de miRNAs no crescimento muscular, ambos miR-1 e miR-133 influenciam os padrões de expressão gênica durante a embriogênese muscular no zebrafish, regulando a organização da actina nos sarcômeros (Mishima et al., 2009). Um possível papel do miR-206 estimulando a diferenciação dos mioblastos foi mostrado por Duran et al. (2015) nos músculos de contração rápida e lenta do pacu, devido à correlação inversa entre os níveis de expressão de miR-206 e *pax7* (Duran et al., 2015), e Yan et al. (2013) mostraram na tilápia do Nilo que o miR-203b regula diretamente a *myod* (Yan et al., 2013). De modo similar, análises moleculares revelaram que os níveis de expressão de miR-1, miR-133 e miR-206 aumentaram conforme o crescimento muscular em diferentes estágios de desenvolvimento do pacu (Duran et al., 2015), carpa (Yan et al., 2012a) e tilápia do Nilo (Yan et al., 2012c; Nachtigall et al., 2015). Em outro estudo, Huang et al. (2012) identificaram diferenças na expressão de miRNAs envolvidos na sinalização por Gh/Igf1 entre o músculo esquelético de tilápias do Nilo com crescimento rápido e normal, com miRNAs *down* e *upregulated* que podem servir como marcadores moleculares em programas de melhoramento de peixes (Huang et al., 2012). Além disso, foram identificados vários miRNAs que regulam as alterações do fenótipo hiperplásico para o hipertrófico no músculo esquelético de zebrafish, fornecendo evidências para o envolvimento de miRNAs nas transições do crescimento muscular (Johnston et al., 2009).

Além do crescimento do músculo, os miRNAs também estão envolvidos com a definição dos tipos de fibras e fenótipo muscular, especialmente o miR-499. Wang et al. (2011) mostraram que o miR-499 é responsável por reprimir a tradução do *sox6* (*sry (sex determining region Y) box 6*) em fibras de contração lenta no zebrafish (Wang et al., 2011), resultados corroborados por análises também em tilápias do Nilo (Nachtigall et al., 2015). O Sox6 é um ativador transcricional que exerce um papel chave na manutenção do fenótipo *fast* nas fibras musculares, reprimindo genes *slow*-específicos como *smyhc1* (*slow myosin heavy chain 1*) e *stnnc* (*slow-specific troponin c*) (von Hofsten et al., 2008). Duran et al. (2015) observaram um aumento na expressão do miR-499 no músculo de contração lenta de juvenis e adultos de pacus, enquanto os transcritos de *sox6* tiveram maior expressão nas fibras de contração rápida, também em ambos os estágios de desenvolvimento. Além disso, o aumento na expressão de *sox6* acompanhou o crescimento do músculo *fast*, como resultado dos menores níveis de miR-499 conforme as fibras se diferenciavam e amadureciam (Duran et al., 2015). Em conjunto, esses estudos indicam o envolvimento do miR-499 na especificação de manutenção do fenótipo *slow* nas fibras musculares, mecanismo conservado entre os vertebrados (Wang et al., 2011).

1.7. Cultura celular primária de mioblastos

A cultura celular é uma técnica *in vitro* que permite a manutenção e estudo de células fora do corpo do organismo original (Junqueira e Carneiro, 2008). As culturas de células permitiram um grande avanço em muitas aplicações médicas, como no desenvolvimento de vacinas, ensaios de drogas e terapias gênicas, e uma expansão muito grande do conhecimento acerca de mecanismos moleculares e vias de sinalização relacionados aos mais diversos processos biológicos (Freshney, 2010). Esses progressos decorrem principalmente da utilização de linhagens celulares, ou seja, células com alterações genéticas ocasionadas por substâncias químicas, vírus ou agentes físicos, cuja proliferação muito acentuada permite que sejam propagadas por longos períodos de tempo (Alves e Guimarães, 2010; Freshney, 2010).

A linhagem celular C2C12 é constituída de mioblastos provenientes de camundongo (*Mus musculus*), sendo amplamente utilizada para a compreensão da regulação do crescimento e desenvolvimento muscular (Yaffe e Saxel, 1977). Para peixes, no entanto, é mais recomendada a utilização de culturas celulares provenientes especificamente de espécies de peixes, devido à grande "distância" evolutiva entre mamíferos e estes animais, apesar da enorme quantidade de conhecimento adquirido a partir das células C2C12. Ainda não foram obtidas linhagens de células musculares provenientes de peixes e, portanto, para estudos relacionados ao músculo esquelético desses animais é necessário o estabelecimento de culturas celulares primárias de mioblastos (revisado por Johnston et al., 2011). As culturas primárias são aquelas preparadas diretamente do tecido de interesse, possuindo as mesmas características celulares, de modo que a cultura primária é o procedimento mais semelhante a estudos *in vivo*. No entanto, os ensaios em culturas celulares primárias devem ser realizados com rapidez, pois as células primárias conseguem manter suas características originais apenas por um curto período de tempo, antes de entrarem em apoptose (Freshney, 2010).

As culturas de mioblastos de peixes recapitulam as principais etapas da miogênese, com uma fase inicial de células precursoras miogênicas quiescentes e comprometimento dos mioblastos, proliferação e migração dos mioblastos, diferenciação e fusão em miotubos, e maturação das fibras musculares (Gabillard et al., 2010b; Vélez et al., 2016) (Figura 16). Além disso, as culturas de mioblastos fornecem um ambiente com um menor número de variáveis daquelas encontradas no músculo esquelético *in vivo*, permitindo as análises de diversas vias de sinalização sob condições controladas. Isso possibilita um estudo mais aprofundado de moléculas regulatórias e a investigação de seus papéis nos diferentes estágios da cultura, especialmente através de ensaio de ganho (superexpressão, miméticos) e perda (*knockout*,

knockdown, antagonistas) de função (revisado por Johnston et al., 2011). Da mesma forma, os meios de cultivo dos mioblastos podem ser modificados para o teste de hipóteses relacionadas ao papel de nutrientes, fatores de crescimento, hormônios, drogas e temperatura na regulação do processo de crescimento muscular (Castillo et al., 2004; Bower and Johnston, 2010b; Gabillard et al., 2010a; Seiliez et al., 2012; Garcia de la serrana and Johnston, 2013; Vélez et al., 2014), assim como muitos outros ensaios manipulativos e farmacológicos.

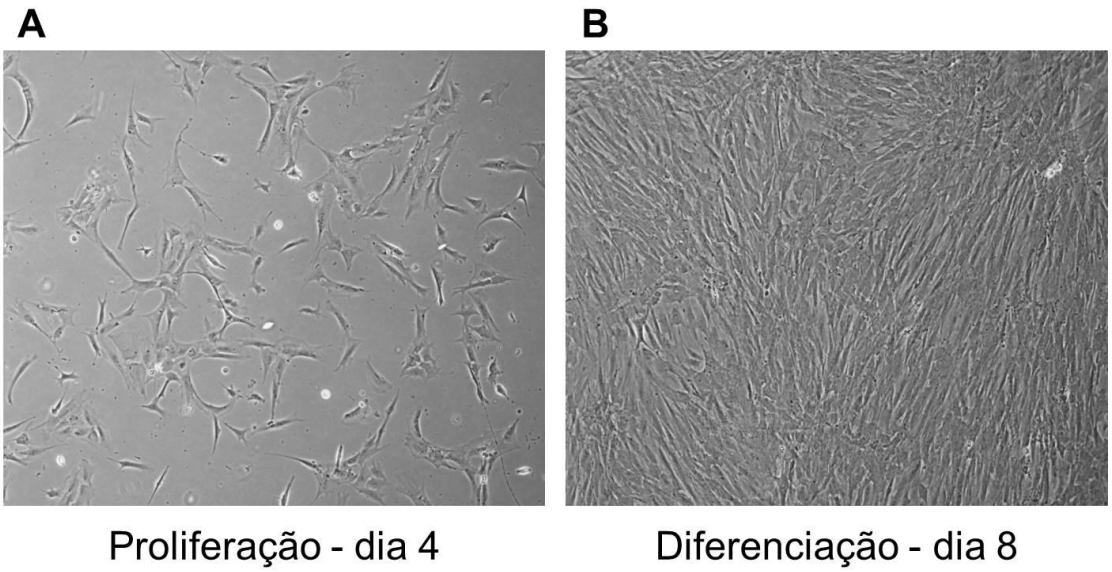

Figura 16: Culturas celulares primárias de mioblastos isolados da musculatura de contração rápida do pacu. (A) Mioblastos no dia 4 de cultura, em período de proliferação. (B) Mioblastos no dia 8 de cultura, em período de diferenciação e fusão em miotubos (imagens de autoria própria).

Froehlich et al. (2013) avaliaram marcadores moleculares da miogênese *in vivo* de peixes em cultura celular de mioblastos de *giant danio* (*Devario aequipinnatus*). Eles observaram que enquanto Pax7 e Myf5 são mais expressos em células precursoras miogênicas recém-ativadas, e Myog é expressa principalmente em miotubos, a expressão de Pax3, Myod e Mstn ocorre em todos os estágios da cultura celular (Froehlich et al., 2013). Células musculares de salmão do Atlântico foram utilizadas para determinar a expressão gênica de parálogos de *myod* durante o desenvolvimento da cultura celular, com *myod1b* e *myod1c* mais relacionadas à proliferação e *myod1a* mais relacionada à diferenciação, comprovando a existência do mecanismo de subfuncionalização da Myod após o WGD (Bower e Johnston, 2010a). Em um experimento interessante, Gabillard et al. (2010a) produziram trutas arco-íris transgênicas que carregavam

green fluorescent protein (GFP) sob o controle do promotor de cadeia leve de miosina *fast*, para monitorar a diferenciação de mioblastos *in vitro* (Gabillard et al., 2010a). Os mioblastos extraídos desses peixes transgênicos expressavam GFP assim que os mioblastos iniciavam os mecanismos de fusão e diferenciação, durante a formação de miotubos, consolidando um sistema *in vitro* de monitoramento em tempo real que permite inúmeras aplicações no crescimento muscular de peixes. Além disso, os autores mostraram que a temperatura, um fator ambiental crucial para o crescimento muscular, diretamente influencia a diferenciação e fusão de células miogênicas (Gabillard et al., 2010a).

Diferentes estudos usaram culturas celulares de mioblastos de peixes para examinar as vias anabólicas relacionadas ao crescimento muscular, especialmente a sinalização por Ins (*insulin*), Igf e Mtor (Castillo et al., 2006; Díaz et al., 2009; Seiliez et al., 2008; Bower and Johnston, 2010b; Cleveland e Weber, 2010; Vélez et al., 2014). Díaz et al. (2009) detectaram um aumento gradual na expressão de *glut4* (*insulin-responsive glucose transporter type 4*) ao longo da diferenciação de células musculares da truta arco-íris, e ambos mioblastos e miotubos tiveram aumento de *glut4* após o tratamento com Ins e Igf1 (Díaz et al., 2009). Além disso, a suplementação de Igf1 e Ins para miócitos de truta promoveu um aumento da síntese proteica (13% para ambos os fatores de crescimento) e diminuição da proteólise (14% e 17%, respectivamente), enquanto a administração de leucina apenas reduziu a degradação proteica (8%) (Cleveland e Weber, 2010). O efeito sinérgico da combinação de tratamentos com fatores de crescimento também é algo sempre avaliado em estudos de cultura celulares de mioblastos de peixes. De fato, a combinação do tratamento com Igf1 e aminoácidos em células musculares "em jejum" de salmão do Atlântico levou a um enorme aumento de transcritos de *igf1*, indicando um possível mecanismo de feedback positivo na produção de Igf1 (Bower e Johnston, 2010b). Além disso, alguns trabalhos anteriores mostraram que a síntese proteica induzida por Igf ocorre apenas se os aminoácidos também estiverem presentes nos meios de cultivo (Bower e Johnston, 2010b; Garcia de la serrana e Johnston, 2013), enquanto os aminoácidos por si só são capazes de estimular as vias de síntese de proteínas em células musculares de peixes (Seiliez et al., 2008; Vélez et al., 2014).

A regulação da miogênese e do crescimento muscular por miRNAs músculo-específicos também foram investigadas usando sistemas *in vitro*. Duran et al. (2015) usaram culturas celulares de mioblastos de pacu para complementar análises *in vivo* da expressão de miR-1, miR-133 e miR-206 em ambos músculos de contração rápida e lenta (Duran et al., 2015). Assim como nas amostras de músculo esquelético, as culturas celulares também mostraram uma correlação

inversa entre os miRNAs e a expressão de seus alvos, corroborando os papéis do miR-1 e miR-206 na diferenciação dos mioblastos. No entanto, as análises *in vitro* forneceram mais informações sobre como o miR-133a e o miR-133b regulam a proliferação e diferenciação de mioblastos, provando seu uso como uma maneira de expandir nosso conhecimento sobre os mecanismos moleculares que regulam o crescimento muscular (Johnston et al., 2011; Duran et al., 2015).

Outro aspecto importante deriva da compartimentalização do músculo esquelético em peixes, que permite o estabelecimento de culturas celulares de mioblastos individuais a partir dos músculos de contração rápida e lenta. Certos processos como o desenvolvimento, metabolismo e determinação dos tipos de fibra são bastante diferentes de acordo com o tipo de músculo, e tais estudos poderiam ser abordados nessas diferentes culturas celulares de mioblastos. Este estudo separado dos tipos musculares é praticamente impossível em mamíferos, devido ao padrão em mosaico do músculo esquelético com fibras rápidas e lentas co-localizadas (revisado por Schiaffino e Reggiani, 2011), tornando os peixes modelos ideais para este tipo de pesquisa. Para isso, é necessário o uso de peixes que apresentem crescimento somático indeterminado e, consequentemente, grande aumento de massa muscular (Rowlerson e Veggetti, 2001), pois em peixes de pequeno tamanho é quase impossível o isolamento de mioblastos suficientes de músculos *fast* e *slow*, restringindo os estudos com culturas celulares de mioblastos (Froehlich et al., 2013). No entanto, os trabalhos publicados até agora apenas desenvolveram culturas celulares de mioblastos de peixes provenientes da musculatura de contração rápida.

2. JUSTIFICATIVA E RELEVÂNCIA DO TEMA

Estudos que visem esclarecer os mecanismos moleculares e celulares envolvidos com a miogênese e o crescimento muscular de peixes permitem o desenvolvimento de um quadro teórico que pode contribuir para a elaboração de novas estratégias de criação e para a obtenção de melhorias na piscicultura intensiva. As culturas celulares primárias de mioblastos são extremamente importantes nesse contexto, pois configuram ferramentas muito úteis para investigar a regulação da miogênese e alterações na celularidade do músculo esquelético, mecanismos diretamente relacionados ao aumento de massa muscular e qualidade de carne, além de fornecerem informações de referência para a pesquisa em outras espécies de peixes.

Além disso, o uso das culturas celulares de mioblastos de peixes possibilita descobertas e uma maior compreensão das particularidades e dos mecanismos que regulam a biologia

molecular, celular e fisiologia do músculo esquelético, gerando conhecimento básico sobre esse tecido biológico tão fundamental para um grupo tão diverso e importante como os peixes.

3. OBJETIVOS

3.1. Objetivo geral

O objetivo de nosso trabalho foi utilizar culturas celulares primárias de mioblastos de peixes para investigar diferentes aspectos do crescimento do músculo esquelético, fornecendo novas informações quanto aos mecanismos moleculares e celulares que regulam o tecido muscular nesses animais.

3.2. Objetivos específicos (separados conforme os capítulos)

Capítulo I: Ascorbic acid stimulates the *in vitro* myoblast proliferation and migration of pacu (*Piaractus mesopotamicus*).

- Estabelecer culturas celulares primárias de mioblastos provenientes do músculo de contração rápida (mioblastos *fast*) de pacus;
- Avaliar os efeitos da suplementação de ácido ascórbico e/ou menadiona (oxidante) na proliferação dos mioblastos;
- Avaliar os efeitos da suplementação de ácido ascórbico e/ou menadiona (oxidante) na migração dos mioblastos;
- Verificar a atividade de enzimas antioxidantes após suplementação de ácido ascórbico nos mioblastos;
- Verificar a expressão gênica de marcadores moleculares de miogênese, síntese e degradação proteica após suplementação de ácido ascórbico nos mioblastos.

Capítulo II: Rainbow trout slow myoblast cell culture as a model to study slow skeletal muscle and the characterization of mir-133 and mir-499 families as a case study.

- Estabelecer e padronizar culturas celulares primárias de mioblastos provenientes do músculo de contração lenta (mioblastos *slow*) de trutas arco-íris;
- Verificar a expressão gênica de marcadores moleculares específicos para confirmação do fenótipo e metabolismo dos mioblastos *slow*;

- Caracterizar as famílias de miRNAs músculo-específicos mir-133 e mir-499 durante o desenvolvimento das culturas celulares de mioblastos *fast* e *slow*;

- Avaliar a expressão de mir-133 e mir-499 em resposta à eletroestimulação aplicada nos mioblastos *slow*.

Capítulo III: Lineage-specific paralogues regulating skeletal muscle growth in Ostariophysi superorder.

- Identificar genes parálogos linhagem-específicos (LSPs) relacionados à miogênese, síntese e degradação proteica no músculo esquelético de pacus e tilápias do Nilo;

- Comparar a expressão dos LSPs no músculo esquelético de pacus e tilápias do Nilo submetidos ao modelo de jejum-realimentação;

- Estabelecer culturas celulares primárias de mioblastos provenientes do músculo de contração rápida (mioblastos *fast*) de pacus;

- Investigar a expressão de LSPs nas culturas celulares de mioblastos submetidas a tratamentos com aminoácidos não-essenciais e leucina.

4. MATERIAL E MÉTODOS

4.1. Criação dos peixes e coleta das amostras

Todos os experimentos e procedimentos foram realizados conforme os princípios éticos na pesquisa animal adotados pelo Colégio Brasileiro de Experimentação Animal (COBEA) e pelo Animals (Scientific Procedures) Act 1986 (Home Office Code of Practice. HMSO: London January 1997). Os protocolos para utilização dos pacus e tilápias do Nilo foram aprovados pela Comissão de Ética no Uso de Animais (CEUA) do Instituto de Biociências, UNESP, Botucatu, São Paulo, Brasil (Protocolo nº 705), e os protocolos para utilização das trutas arco-íris foram aprovados pelo Animal Welfare and Ethics Committee (AWEC) da Universidade de St. Andrews, St. Andrews, Escócia, Reino Unido. Os experimentos foram conduzidos no Laboratório de Biologia do Músculo Estriado (LBME), localizado no Departamento de Morfologia (UNESP, Botucatu, Brasil), e no Scottish Oceans Institute (Universidade de St. Andrews, St. Andrews, Escócia).

Juvenis de pacus e tilápias do Nilo foram cultivados a 28ºC (Saint-Paul, 1989), e juvenis de trutas arco-íris foram cultivadas numa temperatura de 12-15ºC (Raleigh et al., 1984). Os peixes permaneceram sob fotoperíodo natural (12 horas claro e 12 horas escuro) em tanques

dotados de sistemas de recirculação de água e foram alimentados com ração comercial apropriada para seus estágios de desenvolvimento, permanecendo 24 horas em jejum antes dos experimentos. Os animais foram eutanasiados conforme os protocolos descritos pelos comitês de ética.

Amostras de músculo esquelético de contração rápida foram coletadas na região epaxial e amostras do músculo esquelético de contração lenta foram coletadas na região superficial do corpo dos peixes, próximo à linha lateral. Para os experimentos *in vivo* as amostras musculares foram congeladas em nitrogênio líquido e armazenadas a -80°C após a coleta, e para o estabelecimento das culturas celulares as amostras musculares foram imediatamente utilizadas após a coleta.

4.2. Isolamento e cultura celular primária de mioblastos

O protocolo para isolamento e cultura celular de mioblastos foi realizado conforme descrição de Fauconneau e Paboeuf (2000). Inicialmente, os peixes foram imersos em álcool 70% para esterilização das superfícies externas. Amostras de músculo esquelético foram coletadas e colocadas em meio de extração (DMEM, 9 mM $NaHCO_3$, 20 mM HEPES, 15% soro de cavalo e 1% antibióticos; Sigma-Aldrich, USA). Em seguida, os músculos passaram por um processo de dissociação mecânica utilizando-se bisturis e os fragmentos foram lavados 2 vezes em meio de lavagem (DMEM, 9 mM $NaHCO_3$, 20 mM HEPES e 1% antibióticos; Sigma-Aldrich, USA), sendo posteriormente centrifugados (1200 rpm; 5 min; 4°C). Foi realizada a digestão enzimática das amostras pela adição de 0.2% de colagenase tipo I (Sigma-Aldrich, USA) em DMEM, durante 1 hora e 20 minutos à temperatura ambiente e sob agitação. Os fragmentos foram centrifugados (1200 rpm; 20 min; 4°C) e os pellets resultantes foram lavados 2 vezes em meio de lavagem, sendo em seguida centrifugados novamente (1200 rpm; 10 min; 4°C). Para a quebra dos contatos célula-célula foi adicionado 0.1% de tripsina (Sigma-Aldrich, USA) em meio de lavagem, durante 20 min à temperatura ambiente e sob agitação. A suspensão de células foi centrifugada (1200 rpm; 1 min; 4°C) e o sobrenadante foi coletado e misturado ao meio de extração. Os pellets passaram por uma segunda digestão com tripsina, semelhante à primeira. Os sobrenadantes foram centrifugados (1200 rpm; 20 min; 4°C) e o pellet resultante foi ressuspendido em meio completo (DMEM, 9 mM $NaHCO_3$, 20 mM HEPES, 10% soro fetal bovino e 1% antibióticos; Sigma-Aldrich, USA). A suspensão de células foi filtrada em *cell strainers* de 100 e 40 µm (Corning, USA). Após centrifugação (1200 rpm; 20 min; 4°C), as células foram ressuspendidas novamente em meio completo, colocadas em câmara de Neubauer

para a contagem celular e diluídas na concentração de 2×10^6 células/mL. As células suspensas em meio completo foram colocadas em placas previamente tratadas com poli-L-lisina e laminina (Sigma-Aldrich, USA), e foram incubadas em estufa a 28°C (pacus e tilápias do Nilo) ou 18°C (trutas arco-íris) durante, aproximadamente, 12 dias. O meio completo foi trocado todo dia e a morfologia dos mioblastos foi monitorada regularmente em microscópio invertido (Zeiss, Germany).

4.3. Tratamentos realizados nas culturas celulares de mioblastos

Para avaliação do papel do ácido ascórbico na miogênese do músculo esquelético do pacu, foram utilizados 4 grupos experimentais: o grupo Controle (CTR), no qual os mioblastos não foram submetidos a nenhum tratamento, permanecendo em solução salina; o grupo Menadiona (MEN), no qual os mioblastos foram suplementados com o agente oxidante menadiona para indução de estresse oxidativo; o grupo Ácido Ascórbico (AA), no qual os mioblastos foram suplementados com o composto L-ascorbic acid 2-phosphate (Sigma-Aldrich, USA), que é uma forma estável do ácido ascórbico e recomendada para uso em culturas celulares; e o grupo Menadiona e Ácido Ascórbico (MEN+AA), no qual os mioblastos foram suplementados com o L-ascorbic acid 2-phosphate juntamente com a menadiona, para verificação dos efeitos antioxidativos do ácido ascórbico. O L-ascorbic acid 2-phosphate foi adicionado ao meio na concentração de 200 µM e foi continuamente administrado aos mioblastos, e a menadiona foi adicionada ao meio na concentração de 10 µM durante 1 hora.

Para a estimulação com pulsos elétricos (EPS), mioblastos derivados do músculo de contração lenta de trutas arco-íris foram divididos em 3 grupos experimentais: o grupo Controle (CTR), no qual os mioblastos não foram submetidos a nenhum estímulo; o grupo Agudo (A-EPS), no qual os mioblastos foram submetidos a um estímulo agudo e de alta frequência, simulando a inervação da musculatura de contração rápida; e o grupo Crônico (C-EPS), no qual os mioblastos foram submetidos a um estímulo crônico e de baixa frequência, simulando a inervação da musculatura de contração lenta. A partir do dia 4, os mioblastos foram eletroestimulados todo dia através do aparelho *C-Pace EP Cell Culture Stimulator* em conjunto com o *C-Dish Electrode Assemblies* (IonOptix, USA). A estimulação do grupo A-EPS foi aplicada durante 15 minutos e os mioblastos foram submetidos a pulsos de 10 Hz e 30 V por 10 ms, dados a cada 5 segundos. A estimulação do grupo C-EPS foi aplicada durante 2 horas e os mioblastos foram submetidos a pulsos de 1 Hz e 30 V por 2 ms. Os mioblastos foram

eletroestimulados em DMEM e permaneceram 10 minutos em repouso após a aplicação de ambos estímulos.

Para avaliação do tratamento com aminoácidos não-essenciais e leucina na expressão de LSPs no músculo esquelético do pacu, mioblastos após 8 dias de cultura foram incubados por 72 horas em meio livre de aminoácidos, contendo: Earle's balance salt solution 1X, 9 mM NaHCO 3 , 20 mM HEPES, Vitamin Mix 1X, 1% antibióticos e 4 g/L D-glucose (Sigma-Aldrich, USA). Esse meio foi preparado com água deionizada autoclavada e esterilizado através de filtros de 0.22 µm. Os mioblastos foram então cultivados durante 24 horas em meio livre de aminoácidos (-AA), meio suplementado com aminoácidos não-essenciais (NEAA) (Sigma-Aldrich, USA) ou meio suplementado com aminoácidos não-essenciais e L-leucina (NEAA+LEU) (Sigma-Aldrich, USA). Foi adicionado 1% de aminoácidos não-essenciais ao meio livre de aminoácidos, e a L-leucina foi adicionada na concentração de 2.5 mM.

4.4. Imunofluorescência

O ensaio de imunofluorescência foi realizado em culturas celulares de mioblastos em lamínulas de vidro autoclavadas dentro de placas de 6 *wells*. Os mioblastos foram lavados com PBS e posteriormente fixados em 4% paraformaldeído durante 15 minutos. Os mioblastos foram então permeabilizados com 0,1% Triton X-100 (Sigma-Aldrich, USA) por 10 minutos e incubados com solução de bloqueio (1% glicina, 3% albumina sérica bovina (BSA), 8% soro fetal bovino e 0,3% Triton X-100 - Sigma-Aldrich, USA) por 1 hora, para evitar ligações inespecíficas. Os mioblastos foram incubados *overnight* a 4°C com anticorpo primário *rabbit anti-desmin* (Sigma-Aldrich, USA) diluído em solução de bloqueio (1:20). As células foram lavadas e depois incubadas durante 2 horas a 4°C com anticorpo secundário *anti-rabbit FITC* (sc-2090 - Santa Cruz, USA) diluído em solução de bloqueio (1:400). Os núcleos de mioblastos foram marcados com DAPI presente no meio de montagem Vectashield® (Vector Laboratories Inc., USA) e as imagens foram obtidas em microscópio de fluorescência (Olympus, Japan).

4.5. Ensaio de proliferação dos mioblastos

A proliferação dos mioblastos foi avaliada através do ensaio de MTT (*3-(4,5-dimethylthiazol-2-yl)-2,5-diphenyltetrazolium bromide*) e imunomarcação de PCNA (*proliferating cell nuclear antigen*). O ensaio de MTT foi realizado 0, 12, 24, 36, 48 e 72 horas após 1 dia de plaqueamento. O MTT possui coloração amarela e após sua redução por enzimas celulares ocorre a formação de um substrato insolúvel conhecido como formazan, de coloração

roxa ou azulada, cuja intensidade será diretamente proporcional ao aumento da proliferação dos mioblastos. Os mioblastos foram cultivados em placas de 96 *wells* e, após os tratamentos conforme os grupos experimentais, foram incubados com o MTT durante 4 horas a 37°C. Após a remoção do MTT, foram adicionados 200 µL de DMSO (*dimethyl sulfoxide*) em cada *well*, e a leitura da absorbância a 595 nm foi realizada em espectrofotômetro *Asys Expert Plus Microplate Reader* (Biochrom, United Kingdom).

A imunomarcação de PCNA foi realizada 0, 24 e 48 horas após 1 dia de plaqueamento em lamínulas de vidro autoclavadas dentro de placas de 12 *wells*. Os mioblastos foram lavados com PBS e posteriormente fixados em 4% paraformaldeído durante 10 minutos. Os mioblastos foram então pós-fixados em 100% metanol por 10 minutos e incubados com solução de bloqueio (3% albumina sérica bovina (BSA) - Sigma-Aldrich, USA) por 1 hora, para evitar ligações inespecíficas. Os mioblastos foram incubados *overnight* a 4°C com anticorpo primário *mouse anti-PCNA* (sc-56 - Santa Cruz, USA) diluído em 1% BSA (1:500). As células foram lavadas e depois incubadas durante 90 minutos à temperatura ambiente com anticorpo secundário *anti-mouse HRP* (ab6789 - Abcam, USA) diluído em 1% BSA (1:500). Após mais uma etapa de lavagem, os mioblastos foram incubados com solução de DAB (500 µL 3,3'-diaminobenzidina, 4 mL de peróxido de hidrogênio e 4,5 mL de PBS - Sigma-Aldrich, USA), permitindo a identificação de células proliferativas expressando PCNA. Foi utilizada hematoxilina para contracorar os mioblastos, e as lamínulas foram desidratadas numa série graduada de álcool e montadas com Permount. A proliferação foi quantificada como a porcentagem de células PCNA-positivas do número total de núcleos em 10 imagens por lamínula, através do software *ImageJ*® (Schneider et al., 2012). As imagens foram obtidas em microscópio de luz acoplado à câmera digital Leica DMC2900 (Leica, Germany).

4.6. Ensaio de migração dos mioblastos

A migração dos mioblastos foi avaliada através do ensaio de *Wound Healing*. Após confluência de 80-100%. As camadas de mioblastos foram mecanicamente lesadas (riscadas), com o uso de uma ponteira estéril de 200 µL, em formato de cruz no centro de cada *well*. Os restos celulares foram removidos após 2 lavagens em solução salina e os mioblastos foram então incubados com meio completo contendo 2% de soro fetal bovino, para reduzir a taxa proliferativa das células. As áreas lesadas foram avaliadas nos períodos de 0, 6, 12, 18, 24, 30 e 48 horas em microscópio invertido (Zeiss, Germany), e as imagens foram capturadas nesses intervalos de tempo com a utilização de câmera digital acoplada *AxioCam ICc5* (Carl Zeiss

Microscopy, Alemanha). Com a utilização do programa *ImageJ*® (Schneider et al., 2012), foram analisadas a área de fechamento da lesão (redução da área das lesões ao longo do tempo) e a taxa ou velocidade de migração dos mioblastos (variação da área de fechamento das lesões num intervalo de tempo).

4.7. Jejum e realimentação

O modelo de jejum-realimentação, comumente utilizados para manipular a taxa de crescimento dos peixes, foi utilizado para avaliação dos processos de síntese e degradação proteica no músculo esquelético dos pacus e tilápias do Nilo. Os peixes foram submetidos a um período de jejum de 4 dias e, em seguida, foram realimentados com ração comercial padrão por 3 dias. As amostras musculares foram coletadas antes do período de jejum (-4d), diariamente durante o jejum (-3d, -2d, -1d e 0d) e durante a realimentação (6h, 12h, 1d, 2d e 3d).

4.8. Identificação de parálogos linhagem-específicos (LSPs) e miRNAs

Para a seleção dos LSPs relacionados às vias de miogênese, síntese e degradação proteica no músculo esquelético de pacus e tilápias do Nilo, foi necessária a identificação de genes retidos como uma única cópia em Ostariophysi e duas cópias em Acanthopterygii, e genes retidos como duas cópias em Ostariophysi e uma cópia em Acanthopterygii. Inicialmente foi realizado o download das sequências peptídicas das espécies *Danio rerio* e *Astyanax mexicanus*, ambas Ostariophysi, e *Gasteroteus aculeatus* e *Oreochromis niloticus*, ambas Acanthopterygii. Os downloads foram realizados através da ferramenta *BioMart* (http://www.ensembl.org/biomart/martview/a6a738c6a5bb5cfddc3a501898640dfe), disponível na plataforma *Ensembl Genome Browser 89* (http://www.ensembl.org/index.html). Esses arquivos foram visualizados no programa Notepad++, onde as sequências peptídicas dos genes de interesse relativos a cada espécie foram anotadas. Essas sequências foram então comparadas entre si através do programa *BioEdit Sequence Alignment Editor*, que indicou genes retidos de forma diferente entre Ostariophysi e Acanthopterygii. Para que fosse feita a separação do que eram genes parálogos e isoformas de um mesmo gene, foi utilizado o programa de alinhamento *MAFFT version 7* (http://mafft.cbrc.jp/alignment/server/). Após essa primeira seleção, as sequências peptídicas das espécies descritas anteriormente foram também comparadas ao proteoma de *Takifugu rubripes* e *Tetraodon nigroviridis* (Acanthopterygii) no *Ensembl*, e ao transcriptoma de *Ictalurus punctatus* e *Piaractus mesopotamicus* (Ostariophysi) no *BioEdit*. O transcriptoma de *Piaractus mesopotamicus* foi obtido pelo nosso laboratório (Mareco et al.,

2015) e encontra-se disponível no *European Nucleotide Archive* - ENA (número de acesso PRJEB6656).

Para a identificação dos miRNAs mir-133 e mir-499 no músculo esquelético de trutas arco-íris, inicialmente foram obtidas as sequências precursoras dessas moléculas no zebrafish, através da plataforma *Ensembl*. Essas sequências foram comparadas ao genoma de truta arco-íris disponível no *Genoscope* (Berthelot et al., 2014), e as sequências resultantes foram anotadas. Usando o *Ensembl*, as possíveis sequências precursoras do mir-133 e mir-499 da truta arco-íris foram submetidas ao BLAST contra os genomas de outras espécies de teleósteos (*Astyanax mexicanus, Danio rerio, Gasterosteus aculeatus, Oreochromis niloticus, Oryzias latipes, Takifugu rubripes, Tetraodon nigroviridis*) e alguns mamíferos (*Homo sapiens, Mus musculus, Pan troglodytes, Rattus norvegicus*). Além disso, as sequências de miRNAs dos salmonídeos *Salmo salar* e, sempre que possível, *Oncorhynchus kisutch* foram obtidas respectivamente da plataforma *SalmoBase* (Samy et al., 2017) e *NCBI* (http://www.ncbi.nlm.nih.gov).

Foram construídas árvores filogenéticas para as sequências peptídicas dos LSPs através do programa *MEGA7 – Molecular Evolutionary Genetics Analysis* (Kumar et al., 2016) e para as sequências precursoras dos miRNAs mir-133 e mir-499 através do software *BEAST v1.7.4* (Drummond et al., 2012). As árvores filogenéticas foram visualizadas e editadas no software *FigTree v1.4.2* (http://tree.bio.ed.ac.uk/software/figtree/) (Figura 17).

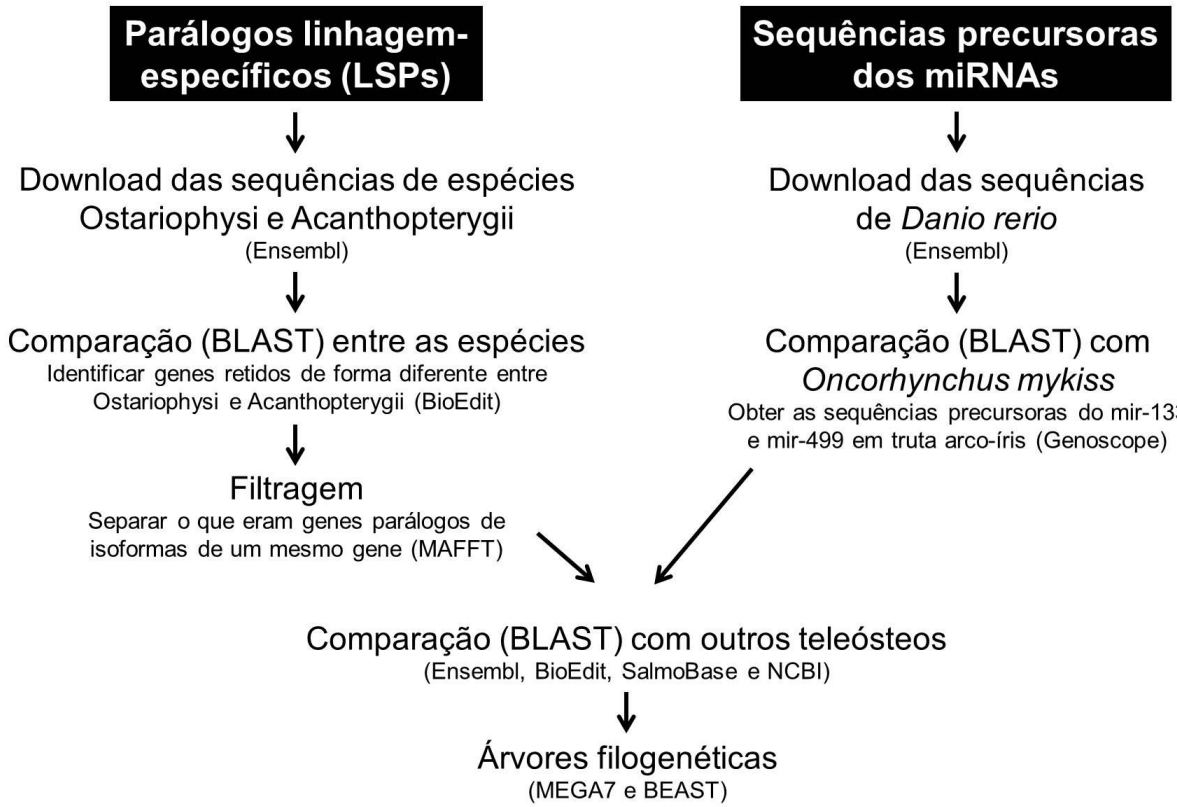

Figura 17: Fluxograma indicando as principais etapas realizadas para a identificação dos parálogos linhagem-específicos (LSPs) entre Ostariophysi e Acanthopterygii, e das sequências precursoras dos miRNAs mir-133 e mir-499 na truta arco-íris.

4.9. Extração, quantificação e análise da integridade de RNA

O RNA total foi extraído tanto das amostras musculares quanto das culturas celulares de mioblastos através do reagente *TRIzol*® (Thermo Fisher Scientific, USA), seguindo as orientações do fabricante. As amostras congeladas foram trituradas com o homogeneizador de tecidos *IKA® T-25 Digital Ultra-Turrax*® (IKA, Germany) em 1 mL de *TRIzol*®/50-100 mg de tecido muscular, e os mioblastos em cultura foram homogeneizados com *cell scrapers* em 1 mL de *TRIzol*®/*well*. O homogeneizado foi transferido para um tubo de 1.5 mL e incubado durante 5 minutos à temperatura ambiente. Foi acrescentado 0.2 mL de clorofórmio e, posteriormente, os tubos foram agitados vigorosamente e incubados por 15 minutos à temperatura ambiente. Em seguida, o material foi centrifugado a 12000 x g por 15 minutos a 4°C. A fase aquosa formada após a centrifugação foi coletada e o RNA foi precipitado através da incubação com 0.5 mL de álcool isopropílico, durante 10 minutos à temperatura ambiente. Em seguida, o material foi novamente centrifugado a 12000 x g por 15 minutos a 4°C, e o pellet de RNA resultante foi lavado com 1 mL de etanol 75%. O material foi centrifugado a 12000 x g por 10 minutos a 4°C e o sobrenadante foi removido cuidadosamente. Após secagem, o pellet de RNA foi dissolvido em *UltraPure™ Distilled Water DNAse, RNAse Free* (Thermo Fisher Scientific, USA) e armazenado a -80°C.

Para a quantificação do RNA foi utilizado o espectrofotômetro *NanoVue™ Plus* (GE Healthcare, USA), que forneceu a medida de absorbância a 260 nm. Também foi realizada a medida de absorbância a 280 nm, que identifica a quantidade de proteínas e permite uma análise da pureza do RNA extraído, garantida pela obtenção de uma razão 260/280 nm superior a 1.8. Nós utilizamos somente amostras com razão igual ou superior a 1.8.

A integridade do RNA total extraído foi avaliada por eletroforese em gel de agarose 1%. A agarose foi dissolvida em tampão TBE 1X (89 mM Tris base, 89 mM ácido bórico, 2 nM EDTA). Uma alíquota de 1 µL do RNA total foi adicionada a 5 µL de uma solução contendo o tampão de corrida OrangeG e o corante *GelRed*® (Biotium, USA). Essa mistura foi aplicada no gel e submetida à corrida eletroforética a 120 V por cerca de 1 hora e 30 minutos. O gel foi fotografado sob luz ultravioleta e a integridade do RNA total extraído foi confirmada pela presença das bandas referentes aos RNAs ribossomais 28S e 18S. Além disso, as amostras foram

submetidas à eletroforese capilar no sistema *2100 Bioanalyzer* (Agilent, USA), que fornece um número de integridade do RNA (RIN) baseado nas bandas do 28S e 18S. A amostra de RNA é classificada num sistema numérico de 1 a 10, sendo 1 o perfil de maior degradação e 10 o perfil de maior integridade. Nós utilizamos somente amostras com um RIN igual ou superior a 7.0.

4.10. Tratamento com DNAse e transcrição reversa

Durante os procedimentos de extração do RNA, pode ser que ocorra contaminação das amostras por DNA genômico. Esse DNA contaminante pode, eventualmente, servir de molde durante a amplificação pela PCR, gerando um produto que não corresponde ao fragmento de interesse. Dessa forma, o RNA total extraído foi submetido ao tratamento com o kit *DNase I, Amplification Grade* (Thermo Fisher Scientific, USA), a fim de eliminar qualquer possível resíduo de DNA genômico contaminante das amostras. Conforme as instruções do protocolo, 1 µL de *10X DNase I Reaction Buffer*, 1 µL de *DNase I Amplification Grade* (1 U/µL) e *UltraPure™ Distilled Water DNAse, RNAse Free* (Thermo Fisher Scientific, USA), na quantidade suficiente para completar 10 µL de solução, foram adicionados a 1 µg do RNA total de cada amostra. Essa solução permaneceu à temperatura ambiente durante 15 minutos e, em seguida, foi acrescida de 1 µL de EDTA (25 mM) e incubada a 65°C por 10 minutos, para a total inativação da enzima *DNase I*.

Foi realizada a transcrição reversa do RNA pelo *High Capacity cDNA archive kit* (Thermo Fisher Scientific, USA), em que 1 µg do RNA total tratado com *DNase I* (11 µL de solução) foram acrescidos de 2 µL de *10X RT Buffer*, 0.8 µL de *25X dNTP Mix* (100mM), 1 µL de *MultiScribe™ Reverse Transcriptase* (50 U/µL), 2 µL de *10X RT Random Primers* e 1 µL de *RNase Inhibitor* (20 U/µL). O volume final da reação foi ajustado para 20 µL com *UltraPure™ Distilled Water DNAse, RNAse Free* (Thermo Fisher Scientific, USA). Cada amostra foi incubada a 25°C por 10 minutos, a 37°C por 120 minutos e a 85°C por 5 minutos. Os produtos da reação de transcrição reversa foram armazenados a -20°C e utilizados nas reações de PCR.

4.11. PCR em tempo real

Primers necessários para amplificação dos genes nas amostras de pacus, tilápias do Nilo ou trutas arco-íris foram desenhados através do software *Primer3 v.0.4.0* (Koressaar e Remm, 2007; Untergasser et al., 2012). Todos os primers foram desenhados para amplificar produtos de 50-200 pares de bases com temperatura de 60ºC. A formação de possíveis estruturas *hairpin* ou dímeros de primers foram avaliadas através do software *NetPrimer* (Premier Biosoft, USA).

Os níveis de expressão dos mRNAs foram detectados por PCR em tempo real, através da plataforma *QuantStudio™ 12K Flex Real-Time PCR System* (Thermo Fisher Scientific, USA). Todas as análises estavam em conformidade com as diretrizes do *Minimum Information for Publication of Quantitative Real-Time PCR experiments* (MIQE) (Bustin et al., 2009). As amostras de cDNA foram amplificadas utilizando-se o *GoTaq® qPCR Master Mix* (Promega, USA) e primers sintetizados pela Invitrogen (USA). Os primers foram diluídos em *UltraPure™ Distilled Water DNAse, RNAse Free* (Thermo Fisher Scientific, USA) e suas concentrações ajustadas para 5 µM. Conforme instruções do fabricante, foram utilizados 8 µL de cDNA diluído (1:20), 1.5 µL de *Primer Forward*, 1.5 µL de *Primer Reverse* e 4 µL de *GoTaq® qPCR Master Mix* (Promega, USA), totalizando um volume final de 15 µL de solução. As reações foram realizadas em duplicata, nas seguintes condições: 95ºC por 10 minutos, seguido por 40 ciclos de desnaturação a 95ºC por 15 segundos e anelamento/extensão a 60ºC por 1 minuto. Foi feita a análise da Curva de Dissociação dos fragmentos ao término de cada reação de PCR, um passo de 20 minutos em que a temperatura da reação aumenta gradualmente de 60 para 95ºC, possibilitando a avaliação da especificidade de amplificação de cada conjunto de primers pela presença de um único pico de fluorescência. A eficiência de reação foi calculada pelo software *LinRegPCR* (Ramakers et al., 2003).

A quantificação relativa da expressão foi realizada pelo método $2^{-\Delta\Delta Ct}$ (Livak e Schmittgen, 2001), utilizando o software *DataAssist™ v3.01* (Thermo Fisher Scientific, USA). As expressões foram normalizadas pelos genes cujos valores de expressão foram constantes entre todas as amostras utilizadas.

5. REFERÊNCIAS GERAIS

Aguiar, D. H., Barros, M. M., Padovani, C. R., Pezzato, L. E. and Dal Pai-Silva, M. (2005). Growth characteristics of skeletal muscle tissue in Oreochromis niloticus larvae fed on a lysine supplemented diet. *J. Fish Biol.* **67**, 1287–1298.

Almeida, F. L. A., Pessotti, N. S., Pinhal, D., Padovani, C. R., Leitão, N. de J., Carvalho, R. F., Martins, C., Portella, M. C. and Dal Pai-Silva, M. (2010). Quantitative expression of myogenic regulatory factors MyoD and myogenin in pacu (Piaractus mesopotamicus) skeletal muscle during growth. *Micron* **41**, 997–1004.

Alves, E. A. and Guimarães, A. C. R. (2010). Cultivo celular. In *Conceitos e métodos para formação de profissionais em laboratórios de saúde* (ed. Molinaro, E.), Caputo, L.), and Amendoeira, R.), p. 254. Rio de Janeiro: Editora da EPSJV - Fiocruz.

Barets, A. (1961). Contributions to the study of "slow" and fast motor systems in the lateral muscle of teleosts. *Arch. Anat. microsc. Morph. Exp.* **50(1)**, 1-187.

Bartel, D. P. and Chen, C.-Z. (2004). Micromanagers of gene expression: the potentially widespread influence of metazoan microRNAs. *Nat. Rev. Genet.* **5**, 396–400.

Berthelot, C., Brunet, F., Chalopin, D., Juanchich, A., Bernard, M., Noël, B., Bento, P., Da Silva, C., Labadie, K., Alberti, A., et al. (2014). The rainbow trout genome provides novel insights into evolution after whole-

genome duplication in vertebrates. *Nat. Commun.* **5**, 3657.

Biga, P. R. and Goetz, F. W. (2006). Zebrafish and giant danio as models for muscle growth: determinate vs. indeterminate growth as determined by morphometric analysis. *Am. J. Physiol. Integr. Comp. Physiol.* **291**, R1327–R1337.

Biyashev, D., Veliceasa, D., Topczewski, J., Topczewska, J. M., Mizgirev, I., Vinokour, E., Reddi, A. L., Licht, J. D., Revskoy, S. Y. and Volpert, O. V. (2012). miR-27b controls venous specification and tip cell fate. *Blood* **119**, 2679–2687.

Bizuayehu, T. T. and Babiak, I. (2014). MicroRNA in Teleost Fish. *Genome Biol. Evol.* **6**, 1911–1937.

Blaauw, B., Schiaffino, S. and Reggiani, C. (2013). Mechanisms Modulating Skeletal Muscle Phenotype. *Compr. Physiol.* **3**, 1645–1687.

Bonaldo, P. and Sandri, M. (2013). Cellular and molecular mechanisms of muscle atrophy. *Dis. Model. Mech.* **6**, 25–39.

Bower, N. I., Taylor, R. G. and Johnston, I. A. (2009). Phasing of muscle gene expression with fasting-induced recovery growth in Atlantic salmon. *Front. Zool.* **6**, 18.

Bower, N. I. and Johnston, I. A. (2010a). Paralogs of Atlantic salmon myoblast determination factor genes are distinctly regulated in proliferating and differentiating myogenic cells. *AJP Regul. Integr. Comp. Physiol.* **298**, R1615–R1626.

Bower, N. I. and Johnston, I. A. (2010b). Transcriptional Regulation of the IGF Signaling Pathway by Amino Acids and Insulin-Like Growth Factors during Myogenesis in Atlantic Salmon. *PLoS One* **5**, e11100.

Buckingham, M. and Rigby, P. W. J. (2014). Gene Regulatory Networks and Transcriptional Mechanisms that Control Myogenesis. *Dev. Cell* **28**, 225–238.

Bustin, S. A., Benes, V., Garson, J. A., Hellemans, J., Huggett, J., Kubista, M., Mueller, R., Nolan, T., Pfaffl, M. W., Shipley, G. L., et al. (2009). The MIQE Guidelines: Minimum Information for Publication of Quantitative Real-Time PCR Experiments. *Clin. Chem.* **55**, 611–622.

Caiozzo, V. J., Baker, M. J., Huang, K., Chou, H., Wu, Y. Z. and Baldwin, K. M. (2003). Single-fiber myosin heavy chain polymorphism: how many patterns and what proportions? *Am. J. Physiol. Integr. Comp. Physiol.* **285**, R570–R580.

Castillo, J., Codina, M., Martínez, M. L., Navarro, I. and Gutiérrez, J. (2004). Metabolic and mitogenic effects of IGF-I and insulin on muscle cells of rainbow trout. *Am. J. Physiol. Integr. Comp. Physiol.* **286**, R935–R941.

Castillo, J., Ammendrup-Johnsen, I., Codina, M., Navarro, I. and Gutiérrez, J. (2006). IGF-I and insulin receptor signal transduction in trout muscle cells. *Am. J. Physiol. Integr. Comp. Physiol.* **290**, R1683–R1690.

Chen, J.-F., Mandel, E. M., Thomson, J. M., Wu, Q., Callis, T. E., Hammond, S. M., Conlon, F. L. and Wang, D.-Z. (2006). The role of microRNA-1 and microRNA-133 in skeletal muscle proliferation and differentiation. *Nat. Genet.* **38**, 228–33.

Chen, J.-F., Tao, Y., Li, J., Deng, Z., Yan, Z., Xiao, X. and Wang, D.-Z. (2010). microRNA-1 and microRNA-206 regulate skeletal muscle satellite cell proliferation and differentiation by repressing Pax7. *J. Cell Biol.* **190**, 867–79.

Chuang, J. C. and Jones, P. A. (2007). Epigenetics and MicroRNAs. *Pediatr. Res.* **61**, 24R–29R.

Cleveland, B. M. and Weber, G. M. (2010). Effects of insulin-like growth factor-I, insulin, and leucine on protein turnover and ubiquitin ligase expression in rainbow trout primary myocytes. *Am. J. Physiol. Integr. Comp. Physiol.* **298**, R341–R350.

Cleveland, B. M. and Radler, L. M. (2019). Essential amino acids exhibit variable effects on protein degradation in rainbow trout (*Oncorhynchus mykiss*) primary myocytes. *Comp. Biochem. Physiol. A Mol. Integr. Physiol.* **229**, 33-39.

Currie, P. and Ingham, P. (2001). Induction and Patterning of Embryonic Skeletal Muscle Cells in the Zebrafish. In *Muscle development and growth* (ed. Johnston, I. A.), pp. 1–17. San Diego: Academic Press.

Dehal, P. and Boore, J. L. (2005). Two Rounds of Whole Genome Duplication in the Ancestral Vertebrate. *PLoS Biol.* **3**, e314.

Demetriades, C., Doumpas, N. and Teleman, A. A. (2014). Regulation of TORC1 in Response to Amino Acid Starvation via Lysosomal Recruitment of TSC2. *Cell* **156**, 786–799.

Díaz, M., Vraskou, Y., Gutiérrez, J. and Planas, J. V. (2009). Expression of rainbow trout glucose transporters GLUT1 and GLUT4 during in vitro muscle cell differentiation and regulation by insulin and IGF-I. *Am. J. Physiol. Integr. Comp. Physiol.* **296**, R794–R800.

Drummond, A. J., Suchard, M. A., Xie, D. and Rambaut, A. (2012). Bayesian Phylogenetics with BEAUti and the BEAST 1.7. *Mol. Biol. Evol.* **29**, 1969–1973.

Duan, Y. H., Li, F. N., Li, Y. H., Tang, Y. L., Kong, X. F., Feng, Z. M., Anthony, T. G., Watford, M., Hou, Y. Q., Wu, G. Y., et al. (2016). The role of leucine and its metabolites in protein and energy metabolism. *Amino Acids*. **48**, 41–51.

Duran, B. O. da S., Fernandez, G. J., Mareco, E. A., Moraes, L. N., Salomão, R. A. S., Gutierrez de Paula, T., Santos, V. B., Carvalho, R. F. and Dal-Pai-Silva, M. (2015). Differential microRNA Expression in Fast- and Slow-Twitch Skeletal Muscle of Piaractus mesopotamicus during Growth. *PLoS One* **10**, e0141967.

El-Sayed, A.-F. M. (2006). *Tilapia culture*. CABI Pub.

FAO (2016). *The State of World Fisheries and Aquaculture 2016*.

Fauconneau, B. and Paboeuf, G. (2000). Effect of fasting and refeeding on in vitro muscle cell proliferation in rainbow trout (Oncorhynchus mykiss). *Cell. Tissue Res.* **301**, 459–63.

Filipowicz, W., Bhattacharyya, S. N. and Sonenberg, N. (2008). Mechanisms of post-transcriptional regulation by microRNAs: are the answers in sight? *Nat. Rev. Genet.* **9**, 102–114.

Flynt, A. S., Thatcher, E. J., Burkewitz, K., Li, N., Liu, Y. and Patton, J. G. (2009). *miR-8* microRNAs regulate the response to osmotic stress in zebrafish embryos. *J. Cell Biol.* **185**, 115–127.

Freshney, R. I. (2010). Culture of animal cells: a manual of basic technique and specialized applications. 6th ed. 732p, Hoboken, NJ, USA: John Wiley & Sons, Inc.

Friedman, R. C., Farh, K. K.-H., Burge, C. B. and Bartel, D. P. (2009). Most mammalian mRNAs are conserved targets of microRNAs. *Genome Res.* **19**, 92–105.

Froehlich, J. M., Galt, N. J., Charging, M. J., Meyer, B. M. and Biga, P. R. (2013). In vitro indeterminate teleost myogenesis appears to be dependent on Pax3. *In Vitro Cell. Dev. Biol. Anim.* **49**, 371–85.

Frontera, W. R. and Ochala, J. (2015). Skeletal muscle: a brief review of structure and function. *Calcif. Tissue Int.* **96**, 183-195.

Gabillard, J.-C., Rallière, C., Sabin, N. and Rescan, P.-Y. (2010a). The production of fluorescent transgenic trout to study in vitro myogenic cell differentiation. *BMC Biotechnol.* **10**, 39.

Gabillard, J. C., Sabin, N. and Paboeuf, G. (2010b). In vitro characterization of proliferation and differentiation of trout satellite cells. *Cell Tissue Res.* **342**, 471–7.

Garcia de la serrana, D. and Johnston, I. A. (2013). Expression of Heat Shock Protein (Hsp90) Paralogues Is Regulated by Amino Acids in Skeletal Muscle of Atlantic Salmon. *PLoS One* **8**, e74295.

García de la serrana, D., Codina, M., Capilla, E., Jiménez-Amilburu, V., Navarro, I., Du, S.-J., Johnston, I. A. and Gutiérrez, J. (2014a). Characterisation and expression of myogenesis regulatory factors during in vitro myoblast development and in vivo fasting in the gilthead sea bream (Sparus aurata). *Comp. Biochem. Physiol. Part A Mol. Integr. Physiol.* **167**, 90–99.

Garcia de la serrana, D., Mareco, E. A. and Johnston, I. A. (2014b). Systematic Variation in the Pattern of Gene Paralog Retention between the Teleost Superorders Ostariophysi and Acanthopterygii. *Genome Biol. Evol.* **6**, 981–987.

Garlick, P. J. (2005). The role of leucine in the regulation of protein metabolism. *J. Nutr.* **135**, 1553s–1556s.

Ge, Y. and Chen, J. (2011). MicroRNAs in skeletal myogenesis. *Cell Cycle* **10**, 441–8.

Geeves, M. A. (1999). Structural mechanism of muscle contraction. *Annu. Rev.Biochem.* **68**, 687-728.

Giraldez, A. J., Mishima, Y., Rihel, J., Grocock, R. J., Van Dongen, S., Inoue, K., Enright, A. J. and Schier, A. F. (2006). Zebrafish MiR-430 Promotes Deadenylation and Clearance of Maternal mRNAs. *Science (80-.).* **312**, 75–79.

Glasauer, S. M. K. and Neuhauss, S. C. F. (2014). Whole-genome duplication in teleost fishes and its evolutionary consequences. *Mol. Genet. Genomics* **289**, 1045–1060.

Glass, D. J. (2005). Skeletal muscle hypertrophy and atrophy signaling pathways. *Int. J. Biochem. Cell Biol.* **37**, 1974–1984.

Goljanek-Whysall, K., Sweetman, D. and Münsterberg, A. E. (2012). microRNAs in skeletal muscle differentiation and disease. *Clin. Sci.* **123**, 611–625.

Guo, H., Ingolia, N. T., Weissman, J. S. and Bartel, D. P. (2010). Mammalian microRNAs predominantly act to decrease target mRNA levels. *Nature* **466**, 835–40.

Halpern, M. E., Ho, R. K., Walker, C. and Kimmel, C. B. (1993). Induction of muscle pioneers and floor plate is distinguished by the zebrafish no tail mutation. *Cell* **75**, 99–111.

Hawke, T. J. and Garry, D. J. (2001). Myogenic satellite cells: physiology to molecular biology. *J. Appl. Physiol.* **91**, 534–551.

Hernández-Hernández, J. M., García-González, E. G., Brun, C. E. and Rudnicki, M. A. (2017). The myogenic regulatory factors, determinants of muscle development, cell identity and regeneration. *Semin. Cell Dev. Biol.* **72**, 10–18.

Huang, C. W., Li, Y. H., Hu, S. Y., Chi, J. R., Lin, G. H., Lin, C. C., Gong, H. Y., Chen, J. Y., Chen, R. H., Chang, S. J., et al. (2012). Differential expression patterns of growth-related microRNAs in the skeletal muscle of Nile tilapia (Oreochromis niloticus)1. *J. Anim. Sci.* **90**, 4266–4279.

Huntzinger, E. and Izaurralde, E. (2011). Gene silencing by microRNAs: contributions of translational repression and mRNA decay. *Nat. Rev. Genet.* **12**, 99–110.

IBGE (2016). *Produção da pecuária municipal*. volume 43. Rio de Janeiro: IBGE.

Jaillon, O., Aury, J.-M., Brunet, F., Petit, J.-L., Stange-Thomann, N., Mauceli, E., Bouneau, L., Fischer, C., Ozouf-Costaz, C., Bernot, A., et al. (2004). Genome duplication in the teleost fish Tetraodon nigroviridis reveals the early vertebrate proto-karyotype. *Nature* **431**, 946–957.

Johansen, K. A. and Overturf, K. (2005). Quantitative expression analysis of genes affecting muscle growth during development of rainbow trout(Oncorhynchus mykiss). *Mar. Biotechnol. (NY).* **7**, 576–87.

Johnston, I. A. (2001). Genetic and Environmental Determinants of Muscle Growth Patterns. In *Muscle development and growth*, pp. 141–186.

Johnston, I. A. (2006). Environment and plasticity of myogenesis in teleost fish. *J. Exp. Biol.* **209**, 2249–2264.

Johnston, I. A., Davison, W. and Goldspink, G. (1977). Energy metabolism of carp swimming muscles. *J. Comp. Physiol.* **114**, 203-16.

Johnston, I. A., Manthri, S., Alderson, R., Smart, A., Campbell, P., Nickell, D., Robertson, B., Paxton, C. G. M. and Burt, M. L. (2003). Freshwater environment affects growth rate and muscle fibre recruitment in seawater stages of Atlantic salmon (Salmo salar L.). *J. Exp. Biol.* **206**, 1337–51.

Johnston, I. A., Abercromby, M., Vieira, V. L. A., Sigursteindóttir, R. J., Kristjánsson, B. K., Sibthorpe, D. and Skúlason, S. (2004). Rapid evolution of muscle fibre number in post-glacial populations of Arctic charr Salvelinus alpinus. *J. Exp. Biol.* **207**, 4343–4360.

Johnston, I. A., Lee, H.-T., Macqueen, D. J., Paranthaman, K., Kawashima, C., Anwar, A., Kinghorn, J. R. and Dalmay, T. (2009). Embryonic temperature affects muscle fibre recruitment in adult zebrafish: genome-wide changes in gene and microRNA expression associated with the transition from hyperplastic to hypertrophic growth phenotypes. *J. Exp. Biol.* **212**, 1781–1793.

Johnston, I. A., Bower, N. I. and Macqueen, D. J. (2011). Growth and the regulation of myotomal muscle mass in teleost fish. *J. Exp. Biol.* **214**, 1617–28.

Junqueira, L. and Carneiro, J. (2008). *Histologia Básica*. 11th ed. (ed. Guanabara Koogan) Rio de Janeiro.

Junqueira, L. and Carneiro, J. (2013). *Histologia Básica, Texto & Atlas*. 12th ed. (ed. Guanabara Koogan) Rio de Janeiro.

Kjaer, M. (2004). Role of Extracellular Matrix in Adaptation of Tendon and Skeletal Muscle to Mechanical Loading. *Physiol. Rev.* **84**, 649–698.

Koressaar, T. and Remm, M. (2007). Enhancements and modifications of primer design program Primer3. *Bioinformatics* **23**, 1289–1291.

Koumans, J. T. M., Akster, H. A., Dulos, G. J. and Osse, J. W. M. (1990). Myosatellite cells of Cyprinus carpio (Teleostei) in vitro: isolation, recognition and differentiation. *Cell Tissue Res.* **261**, 173–181.

Kumar, S., Stecher, G. and Tamura, K. (2016). MEGA7: Molecular Evolutionary Genetics Analysis Version 7.0 for Bigger Datasets. *Mol. Biol. Evol.* **33**, 1870–1874.

Lee, Y., Ahn, C., Han, J., Choi, H., Kim, J., Yim, J., Lee, J., Provost, P., Rådmark, O., Kim, S., et al. (2003). The nuclear RNase III Drosha initiates microRNA processing. *Nature* **425**, 415–419.

Lee, C.-T., Risom, T. and Strauss, W. M. (2007). Evolutionary Conservation of MicroRNA Regulatory Circuits: An Examination of MicroRNA Gene Complexity and Conserved MicroRNA-Target Interactions through Metazoan Phylogeny. *DNA Cell Biol.* **26**, 209–218.

Li, P., Mai, K., Trushenski, J. and Wu, G. (2008). New developments in fish amino acid nutrition: towards functional and environmentally oriented aquafeeds. *Amino Acids*. **37(1)**, 43-53.

Livak, K. J. and Schmittgen, T. D. (2001). Analysis of relative gene expression data using real-time quantitative PCR and the 2(-Delta Delta C(T)) Method. *Methods* **25**, 402–8.

Ma, P. C. M., Rould, M. A., Weintraub, H. and Pabo, C. O. (1994). Crystal structure of MyoD bHLH domain-DNA complex: perspectives on DNA recognition and implications for transcriptional activation. *Cell.* **77**, 451-459.

Macqueen, D. J., Kristjánsson, B. K. and Johnston, I. A. (2010). Salmonid genomes have a remarkably expanded akirin family, coexpressed with genes from conserved pathways governing skeletal muscle growth and catabolism. *Physiol. Genomics* **42**, 134–48.

Macqueen, D. J., Garcia de la serrana, D. and Johnston, I. A. (2013). Evolution of Ancient Functions in the Vertebrate Insulin-Like Growth Factor System Uncovered by Study of Duplicated Salmonid Fish Genomes. *Mol. Biol. Evol.* **30**, 1060–1076.

Maere, S. and Van de Peer, Y. (2010). Duplicate Retention After Small- and Large-Scale Duplications. In *Evolution after Gene Duplication* (ed. Dittmar, K. and Liberles, D.), 329p. Hoboken, NJ, USA: John Wiley & Sons, Inc.

Mareco, E. A., Garcia de la Serrana, D., Johnston, I. A. and Dal-Pai-Silva, M. (2015). Characterization of the transcriptome of fast and slow muscle myotomal fibres in the pacu (Piaractus mesopotamicus). *BMC Genomics* **16**, 182.

Mauro, A. (1961). Satellite cell of skeletal muscle fibers. *J. Biophys. Biochem. Cytol.* **9**, 493-495.

McCarthy, J. J. (2011). The MyomiR network in skeletal muscle plasticity. *Exerc. Sport Sci. Rev.* **39**, 150–4.

Michelin, A. C., Justulin, L. A., Delella, F. K., Padovani, C. R., Felisbino, S. L. and Dal-Pai-Silva, M. (2009). Differential MMP-2 and MMP-9 Activity and Collagen Distribution in Skeletal Muscle from pacu (Piaractus mesopotamicus) During Juvenile and Adult Growth Phases. *Anat. Rec. Adv. Integr. Anat. Evol. Biol.* **292**, 387–395.

Mishima, Y., Abreu-Goodger, C., Staton, A. A., Stahlhut, C., Shou, C., Cheng, C., Gerstein, M., Enright, A. J. and Giraldez, A. J. (2009). Zebrafish miR-1 and miR-133 shape muscle gene expression and regulate sarcomeric actin organization. *Genes Dev.* **23**, 619–632.

MPA (2013). *Boletim estatístico da pesca e aquicultura – Brasil 2011*.

Nachtigall, P. G., Dias, M. C., Carvalho, R. F., Martins, C. and Pinhal, D. (2015). MicroRNA-499 expression distinctively correlates to target genes sox6 and rod1 profiles to resolve the skeletal muscle phenotype in Nile tilapia. *PLoS One* **10**, e0119804.

Nelson, J. S. (2006). *Fishes of the world*. 4th ed. John Wiley.

Nikki, J., Pirhonen, J., Jobling, M. and Karjalainen, J. (2004). Compensatory growth in juvenile rainbow trout, *Oncorhynchus mykiss* (Walbaum), held individually. *Aquaculture*. **235**, 285-296.

Olson, E. N. (1990). MyoD family: a paradigm for development? *Genes Dev.* **4**, 1454-1461.

Pinheiro, A. (2014). Futuro Próspero. In *1º Anuário Brasileiro da Pesca e Aquicultura*, p. 133.

Raleigh, R. F., Hickman, T., Solomon, R. C. and Nelson, P. C. (1984). Habitat suitability information: Rainbow trout. 64p. U.S. Fish Wildl. Serv.

Ramakers, C., Ruijter, J. M., Deprez, R. H. L. and Moorman, A. F. M. (2003). Assumption-free analysis of quantitative real-time polymerase chain reaction (PCR) data. *Neurosci. Lett.* **339**, 62–6.

Rescan, P. Y. (2001). Regulation and functions of myogenic regulatory factors in lower vertebrates. *Comp. Biochem. Physiol. B. Biochem. Mol. Biol.* **130**, 1–12.

Rowlerson, A. and Veggetti, A. (2001). Cellular mechanisms of post-embryonic muscle growth in aquaculture species. In *Muscle development and growth* (ed. Johnston, I. A.), pp. 103–140. San Diego: Academic Press.

Saint-Paul, U. (1989). Aquaculture in latin America. Indigenous species promise increased fields. *NAGA.* 3-5.

Saint-Paul, U. (2017). Native fish species boosting Brazilian's aquaculture development. *Acta Fish. Aquat. Resour.* **5**, 1–9.

Samy, J. K. A., Mulugeta, T. D., Nome, T., Sandve, S. R., Grammes, F., Kent, M. P., Lien, S. and Våge, D. I. (2017). SalmoBase: an integrated molecular data resource for Salmonid species. *BMC Genomics* **18**, 482.

Sancak, Y., Bar-Peled, L., Zoncu, R., Markhard, A. L., Nada, S. and Sabatini, D. M. (2010). Ragulator-Rag Complex Targets mTORC1 to the Lysosomal Surface and Is Necessary for Its Activation by Amino Acids. *Cell* **141**, 290–303.

Sandri, M. (2008). Signaling in Muscle Atrophy and Hypertrophy. *Physiology* **23**, 160–170.

Sänger, A. M. and Stoiber, W. (2001). Muscle fiber diversity and plasticity. In *Muscle development and growth* (ed. Johnston, I. A.), pp. 187–250. San Diego: Academic Press.

Santos, V. B., Santos, R., Salomão, R. and Silva, R. (2012). Reprodução Induzida de Pacu (Piaractus mesopotamicus) com o uso de Diferentes Hormônios Comerciais. *Pesqui. Tecnol. - APTA Reg.* **9**, 1–6.

Schiaffino, S. and Reggiani, C. (2011). Fiber Types in Mammalian Skeletal Muscles. *Physiol. Rev.* **91**, 1447–1531.

Schneider, C. A., Rasband, W. S. and Eliceiri, K. W. (2012). NIH Image to ImageJ: 25 years of image analysis. *Nat. Methods.* **9**, 671–5.

Seiliez, I., Gabillard, J.-C., Skiba-Cassy, S., Garcia-Serrana, D., Gutierrez, J., Kaushik, S., Panserat, S. and Tesseraud, S. (2008). An in vivo and in vitro assessment of TOR signaling cascade in rainbow trout (Oncorhynchus mykiss). *AJP Regul. Integr. Comp. Physiol.* **295**, R329–R335.

Seiliez, I., Sabin, N. and Gabillard, J.-C. (2012). Myostatin inhibits proliferation but not differentiation of trout myoblasts. *Mol. Cell. Endocrinol.* **351**, 220–226.

Sempere, L. F., Cole, C. N., Mcpeek, M. A. and Peterson, K. J. (2006). The phylogenetic distribution of metazoan microRNAs: insights into evolutionary complexity and constraint. *J. Exp. Zool. Part B Mol. Dev. Evol.* **306B**, 575–588.

Staron, R. S., Kraemer, W. J., Hikida, R. S., Fry, A. C., Murray, J. D. and Campos, G. E. R. (1999). Fiber type composition of four hindlimb muscles of adult Fisher 344 rats. *Histochem. Cell Biol.* **111**, 117-123.

Staton, A. A., Knaut, H. and Giraldez, A. J. (2011). miRNA regulation of Sdf1 chemokine signaling provides genetic robustness to germ cell migration. *Nat. Genet.* **43**, 204–211.

Stellabotte, F., Dobbs-McAuliffe, B., Fernandez, D. A., Feng, X. and Devoto, S. H. (2007). Dynamic somite cell rearrangements lead to distinct waves of myotome growth. *Development* **134**, 1253–1257.

Stickney, H. L., Barresi, M. J. F. and Devoto, S. H. (2000). Somite development in zebrafish. *Dev. Dyn.* **219**, 287–303.

Taylor, J. S., Braasch, I., Frickey, T., Meyer, A. and Van de Peer, Y. (2003). Genome Duplication, a Trait Shared by 22,000 Species of Ray-Finned Fish. *Genome Res.* **13**, 382–390.

Untergasser, A., Cutcutache, I., Koressaar, T., Ye, J., Faircloth, B. C., Remm, M. and Rozen, S. G. (2012).

Primer3--new capabilities and interfaces. *Nucleic Acids Res.* **40**, e115.

Urbinati, E. C. and Gonçalves, F. D. (2005). Pacu (Piaractus mesopotamicus). In *Espécies nativas para piscicultura no Brasil* (ed. Baldisserotto, B.) and Gomes, L. de C.), pp. 225–255. Santa Maria: UFSM.

Van Leeuwen, J. L. (1999). A mechanical analysis of myomere shape in fish. *J. Exp. Biol.* **202**, 3405–14.

van Rooij, E., Liu, N. and Olson, E. N. (2008). MicroRNAs flex their muscles. *Trends Genet.* **24**, 159–66.

van Rooij, E., Quiat, D., Johnson, B. A., Sutherland, L. B., Qi, X., Richardson, J. A., Kelm, R. J. and Olson, E. N. (2009). A family of microRNAs encoded by myosin genes governs myosin expression and muscle performance. *Dev. Cell* **17**, 662–73.

Vélez, E. J., Lutfi, E., Jiménez-Amilburu, V., Riera-Codina, M., Capilla, E., Navarro, I. and Gutiérrez, J. (2014). IGF-I and amino acids effects through TOR signaling on proliferation and differentiation of gilthead sea bream cultured myocytes. *Gen. Comp. Endocrinol.* **205**, 296–304.

Vélez, E. J., Lutfi, E., Azizi, S., Montserrat, N., Riera-Codina, M., Capilla, E., Navarro, I. and Gutiérrez, J. (2016). Contribution of in vitro myocytes studies to understanding fish muscle physiology. *Comp. Biochem. Physiol. Part B Biochem. Mol. Biol.* **199**, 67–73.

von Hofsten, J., Elworthy, S., Gilchrist, M. J., Smith, J. C., Wardle, F. C. and Ingham, P. W. (2008). Prdm1- and Sox6-mediated transcriptional repression specifies muscle fibre type in the zebrafish embryo. *EMBO Rep.* **9**, 683–9.

Wang, X., Ono, Y., Tan, S. C., Chai, R. J., Parkin, C. and Ingham, P. W. (2011). Prdm1a and miR-499 act sequentially to restrict Sox6 activity to the fast-twitch muscle lineage in the zebrafish embryo. *Development* **138**, 4399–404.

Weintraub, H. (1993). The myod family and myogenesis: redundancy, networks, and thresholds. *Cell*. **75**, 1241-1244.

Wienholds, E., Kloosterman, W. P., Miska, E., Alvarez-Saavedra, E., Berezikov, E., de Bruijn, E., Horvitz, H. R., Kauppinen, S. and Plasterk, R. H. A. (2005). MicroRNA Expression in Zebrafish Embryonic Development. *Science (80-.).* **309**, 310–311.

Williams, A. H., Liu, N., van Rooij, E. and Olson, E. N. (2009). MicroRNA control of muscle development and disease. *Curr. Opin. Cell Biol.* **21**, 461–469.

Winter, J., Jung, S., Keller, S., Gregory, R. I. and Diederichs, S. (2009). Many roads to maturity: microRNA biogenesis pathways and their regulation. *Nat. Cell Biol.* **11**, 228–234.

Yaffe, D. and Saxel, O. (1977). Serial passaging and differentiation of myogenic cells isolated from dystrophic mouse muscle. *Nature* **270**, 725–7.

Yan, X., Ding, L., Li, Y., Zhang, X., Liang, Y., Sun, X. and Teng, C.-B. (2012a). Identification and profiling of microRNAs from skeletal muscle of the common carp. *PLoS One* **7**, e30925.

Yan, B., Zhao, L.-H., Guo, J.-T. and Zhao, J.-L. (2012b). miR-429 regulation of osmotic stress transcription factor 1 (OSTF1) in tilapia during osmotic stress. *Biochem. Biophys. Res. Commun.* **426**, 294–298.

Yan, B., Guo, J.-T., Zhao, L.-H. and Zhao, J.-L. (2012c). microRNA expression signature in skeletal muscle of Nile tilapia. *Aquaculture* **364-365**, 240–246.

Yan, B., Guo, J.-T., Zhu, C. -d., Zhao, L.-H. and Zhao, J.-L. (2013). miR-203b: a novel regulator of MyoD expression in tilapia skeletal muscle. *J. Exp. Biol.* **216**, 447–451.

Yin, V. P., Thomson, J. M., Thummel, R., Hyde, D. R., Hammond, S. M. and Poss, K. D. (2008). Fgf-dependent depletion of microRNA-133 promotes appendage regeneration in zebrafish. *Genes Dev.* **22**, 728–733.

Yin, V. P., Lepilina, A., Smith, A. and Poss, K. D. (2012). Regulation of zebrafish heart regeneration by miR-133. *Dev. Biol.* **365**, 319–327.

Yusuf, F. and Brand-Saberi, B. (2012). Myogenesis and muscle regeneration. *Histochem. Cell Biol.* **138**, 187–199.

Zanou, N. and Gailly, P. (2013). Skeletal muscle hypertrophy and regeneration: interplay between the myogenic regulatory factors (MRFs) and insulin-like growth factors (IGFs) pathways. *Cell. Mol. Life Sci.* **70**, 4117–4130.

6. CAPÍTULO I

Artigo aceito para publicação na Scientific Reports (fator de impacto: 4.12).

O capítulo I se refere ao trabalho e experimentos desenvolvidos para avaliação do papel do ácido ascórbico na proliferação e migração *in vitro* de mioblastos provenientes do músculo de contração rápida de pacus.

Ascorbic acid stimulates the *in vitro* myoblast proliferation and migration of pacu (*Piaractus mesopotamicus*).

Bruno Oliveira Silva Duran[1], Guilherme Alcarás Góes[1], Bruna Tereza Thomazini Zanella[1], Paula Paccielli Freire[1], Jessica Silvino Valente[1], Rondinelle Artur Simões Salomão[2], Ana Fernandes[3], Edson Assunção Mareco[2], Robson Francisco Carvalho[1] and Maeli Dal-Pai-Silva[1*]

[1]São Paulo State University (UNESP), Institute of Biosciences, Department of Morphology, Botucatu, São Paulo, Brazil
[2]University of West São Paulo (UNOESTE), Presidente Prudente, São Paulo, Brazil
[3]São Paulo State University (UNESP), Institute of Biosciences, Department of Chemistry and Biochemistry, Botucatu, São Paulo, Brazil

* Corresponding author
E-mail: maeli@ibb.unesp.br

ABSTRACT

The postembryonic growth of skeletal muscle in teleost fish involves myoblast proliferation, migration and differentiation, encompassing the main events of embryonic myogenesis. Ascorbic acid plays important cellular and biochemical roles as an antioxidant and contributes to the proper collagen biosynthesis necessary for the structure of connective and bone tissues. However, whether ascorbic acid can directly influence the mechanisms of fish myogenesis and skeletal muscle growth remains unclear. The aim of our work was to evaluate the effects of ascorbic acid supplementation on the *in vitro* myoblast proliferation and migration

of pacu (*Piaractus mesopotamicus*). To provide insight into the potential antioxidant role of ascorbic acid, we also treated myoblasts *in vitro* with menadione, which is a powerful oxidant. Our results show that ascorbic acid-supplemented myoblasts exhibit increased proliferation and migration and are protected against the oxidative stress caused by menadione. In addition, ascorbic acid increased the activity of the antioxidant enzyme superoxide dismutase and the expression of *myog* and *mtor*, which are molecular markers related to skeletal muscle myogenesis and protein synthesis, respectively. This work reveals a direct influence of ascorbic acid on the mechanisms of pacu myogenesis and highlights the potential use of ascorbic acid for stimulating fish skeletal muscle growth.

INTRODUCTION

Piaractus mesopotamicus, which is popularly known as pacu, is a teleost fish with major economic importance and a high market value in Brazilian fisheries and pisciculture. The distribution of pacu is highly concentrated in wetland areas in the Midwest Brazilian region[1] and, along with other members of the Characidae family (*Piaractus mesopotamicus*, *Colossoma macropomum*, *Piaractus brachypomus* and hybrids), pacu represents most native fish farmed, accounting for almost 40% of the national production[2]. In addition to its high economic value, the use of pacu in scientific research has recently increased. Zebrafish (*Danio rerio*) and medaka (*Oryzias latipes*) are teleost fish extensively used for research in many fields, such as genetics, embryology, physiology, toxicology and nutrition, but there are some limitations due to their small sizes, such as the study of myogenesis in cell cultures[3]. Because pacus have a large body size, they have the potential to serve as an excellent model for studies investigating muscle growth in fish.

Skeletal muscle is the most abundant tissue in teleost fish and constitutes approximately 60% of the total body mass. Skeletal muscle allows underwater propulsion, represents the main protein reservoir in fish and forms the bulk of the fillet, which is the main product in the aquaculture industry[4,5]. Postembryonic muscle growth in fish involves a population of resident myogenic precursor cells and encompasses the main events of embryonic myogenesis[6]. Once activated, these cells give rise to myoblasts, whose proliferation, migration and differentiation are the mechanisms that promote hyperplasia (increase in muscle fiber number) and hypertrophy (increase in muscle fiber size)[6,7].

In such a context, fish myoblast cell culture represents a very useful *in vitro* tool to obtain an understanding of the regulation of muscle growth and myogenesis[6,8–10]. By recapitulating key steps, such as cell proliferation and differentiation, myoblast cell culture provides a controlled environment for studying myogenesis regulation[10,11]. Similarly, cell culture media can be modified to evaluate the role of nutrients, growth factors and drugs under precisely controlled conditions[6,9]. Our research group has been successful in standardizing pacu myoblast cell culture, providing a great advance in the understanding of muscle plasticity in this species and generating an important tool for fish muscle growth research[12].

Food intake, composition and availability represent important factors leading to muscle growth[6]. In general, fish exhibit mammal-like nutritional requirements for growth, reproduction and other physiological functions, and in confinement, fish require a nutritionally complete and balanced diet[13]. Several studies have shown that ascorbic acid (vitamin C) plays an important role in the diet of fish. Ascorbic acid-deficient diets, especially fed to larvae fish[14], promote reduced growth, impaired feed conversion, skeletal deformities in the operculum and cartilage of the gills, anemia, delay or decrease in wound healing, reduction in reproductive performance and decrease in hatchability[13,15,16]. Ascorbic acid plays several important cellular and biochemical roles as an antioxidant because of its high reducing potential[17]. Ascorbic acid neutralizes reactive oxygen species (ROS) produced during cellular metabolism or functional activities, which have deleterious effects on several molecules in excessive amounts (oxidative stress)[18]. Oxidative stress can be induced chemically using stressing agents, such as menadione (2-methyl-1,4-naphtoquinone)[19]. Menadione is a polycyclic aromatic ketone that has been widely used as an oxidant and has demonstrated cytotoxic activity via the elevation of superoxide anions and hydrogen peroxide[19–21]. As a cellular reducing agent, ascorbic acid also plays a role in collagen biosynthesis, acting as a cofactor in the hydroxylation of lysine and proline present in procollagen[17]. The formation of a stable collagen matrix is crucial for the structure and maintenance of connective tissue, stimulation of osteogenesis and bone growth[22,23]. Therefore, ascorbic acid directly influences the growth of animals, including fish species, and is necessary for the normal development of their bodies[13]. However, whether ascorbic acid influences fish growth exclusively due to its action on connective and bone tissues or whether it can directly influence the mechanisms of skeletal muscle growth remain unclear.

In skeletal muscle, ascorbic acid is a key factor enhancing carnitine biosynthesis[24], which plays an important role in energy production via beta-oxidation. In addition, this vitamin facilitates glycogen storage[25] and protects cells against exercise-induced ROS generation[26,27].

Muscle tissues contain 40% of the whole-body ascorbic acid content[28]. Some studies have shown that ascorbic acid plays a role in myogenesis *in vitro*, but these studies have focused on myoblast differentiation into myotubes. MacBride (1989) showed the early fusion of chicken embryo myoblasts after the addition of ascorbic acid[29]. Moreover, ascorbic acid could increase the expression of myogenin, which is a differentiation-related myogenic factor, in myoblasts incubated at both 37°C[30] and 30°C[31]. Ikeda et al. (2017) observed that ascorbic acid supplementation in C2C12 myoblasts enhanced myotube formation (differentiation rate); although this ascorbic acid supplementation had no effect on myotube hypertrophy[32]. Compared to myotubes, myoblasts have an increased ability to transport ascorbic acid and exhibit increased DHA (*dehydroascorbic acid*) reductase activity necessary for ascorbic acid metabolic recycling[28]. This same study showed that L6 fast myoblasts[33] are more efficient in ascorbic acid import than C2C12 myoblasts[28]. However, to the best of our knowledge, no study has investigated the role of ascorbic acid in *in vitro* fish myoblast proliferation and migration.

Because fish are highly susceptible to ascorbic acid-deficient diets during the early stages of growth[13,14], we hypothesized that ascorbic acid also has a direct influence on early muscle growth in fish. Thus, the aim of our work was to evaluate myoblast proliferation and migration, which are processes related to the onset of myogenesis, in pacu myoblast cell cultures supplemented with ascorbic acid and its antioxidant role against menadione.

RESULTS

Myoblast cell culture

We successfully isolated and established myoblast cell cultures from the fast-twitch muscle of pacu. The myoblasts showed normal development as reported in a previous work that published results of pacu myoblast cell cultures[12]. However, to increase the amount of RNA and protein for the proposed analyses, we seeded the cells at a high concentration (3×10^6 cells/mL), which reduced the time until the formation of myotubes. We observed an initial stage of round mononucleated cells on days 1-2, their progressive proliferation and elongation between days 3-6, and a final stage of myotubes formation on days 7-10 (Fig 1). We chose to study myoblast proliferation and migration within 4 days after cell plating, since during this time the cells reached 100% confluency and began to fuse and differentiate into myotubes. The myoblasts were separated into the following 4 experimental groups: nontreated myoblasts (CTR group), menadione treated myoblasts (MEN group), ascorbic acid supplemented myoblasts (AA group),

and menadione plus ascorbic acid treated myoblasts (MEN+AA group). In addition to the expression of myogenic regulatory factors (MRFs) already published in our previous work[12], the myogenic cells were identified by staining for desmin, and the nuclei were counterstained with DAPI (4,6-diamidino-2-phenylindole) (Supplementary Fig S1).

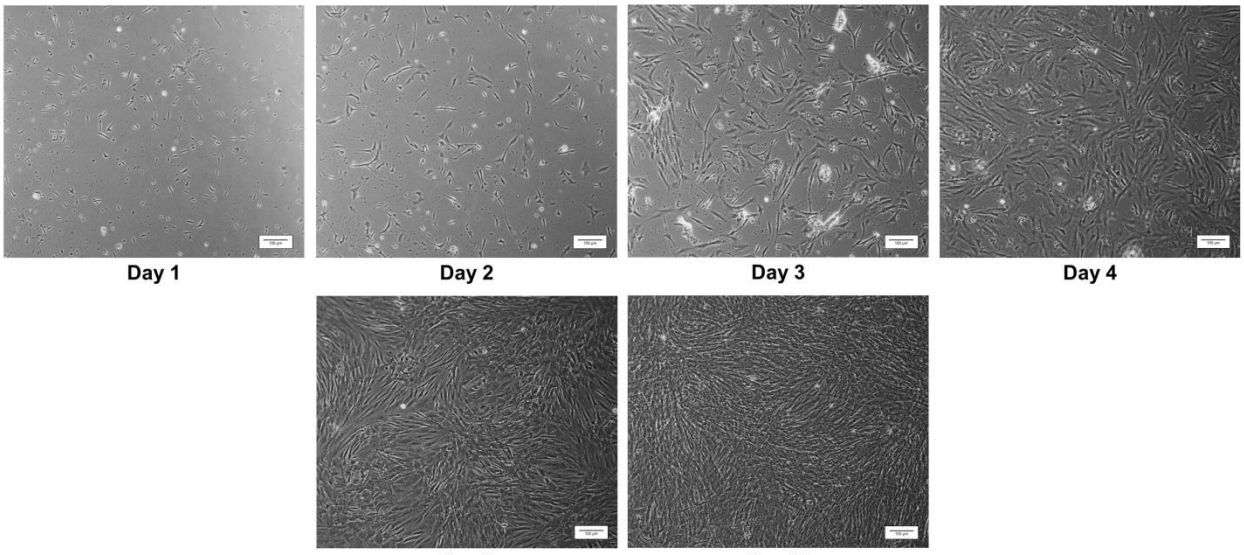

Fig 1. Myoblast cell cultures established using fast-twitch skeletal muscle from juvenile pacus. Myoblasts on days 1 to 4 (during this period, the proliferation and migration mechanisms were studied) and days 7 and 10 (the stages of myotube formation) of cell culture. The images were obtained under an inverted microscope at a 10x magnification (Bars: 100 µm).

We initially performed trypan blue exclusion and MTT (Thiazolyl Blue Tetrazolium Bromide - Sigma-Aldrich, USA) assays to verify the ideal menadione concentration and treatment duration that causes oxidative stress but maintains cell viability (Supplementary Fig S2). The trypan blue exclusion assay showed that menadione treatment for 24 hours drastically reduced myoblast viability, and therefore, this incubation time was quickly discarded from consideration for our studies. Compared with the myoblasts treated only with phosphate buffered saline (PBS), the 1-hour menadione treatment reduced the myoblast viability by 6% (0.1 µM), which was not sufficient to promote oxidative stress, 21% (1 and 10 µM) and 26% (100 µM) (Supplementary Fig S2A). Similarly, the MTT assay showed that the higher menadione concentrations significantly decreased myoblast viability (Supplementary Fig S2B). We chose the 10 µM concentration of menadione and 1-hour duration for the myoblast treatments.

Myoblast proliferation assay

Compared to the CTR and MEN groups, the ascorbic acid supplementation significantly stimulated myoblast proliferation based on both the MTT assay (Fig 2A) and PCNA (*proliferating cell nuclear antigen*) immunostaining (Fig 2B and C). The MTT assay indicated that the proliferation of the ascorbic acid-supplemented myoblasts was increased with significant differences after 12 hours ($p<0.05$). The positive effect of ascorbic acid in the MEN+AA group overcame the menadione oxidative effects, and these myoblasts exhibited a proliferative rate similar to that observed in the AA group at all evaluated time points (Fig 2A). The PCNA immunostaining showed significantly increased proliferation in the AA group on the day following cell plating (0 h) ($p<0.01$) and similar proliferation between the AA and MEN+AA groups at 24 and 48 hours, which was statistically higher that in the CTR and MEN myoblasts ($p<0.05$) (Fig 2C). No significant differences were found between the CTR and MEN groups ($p>0.05$) (Fig 2A and C).

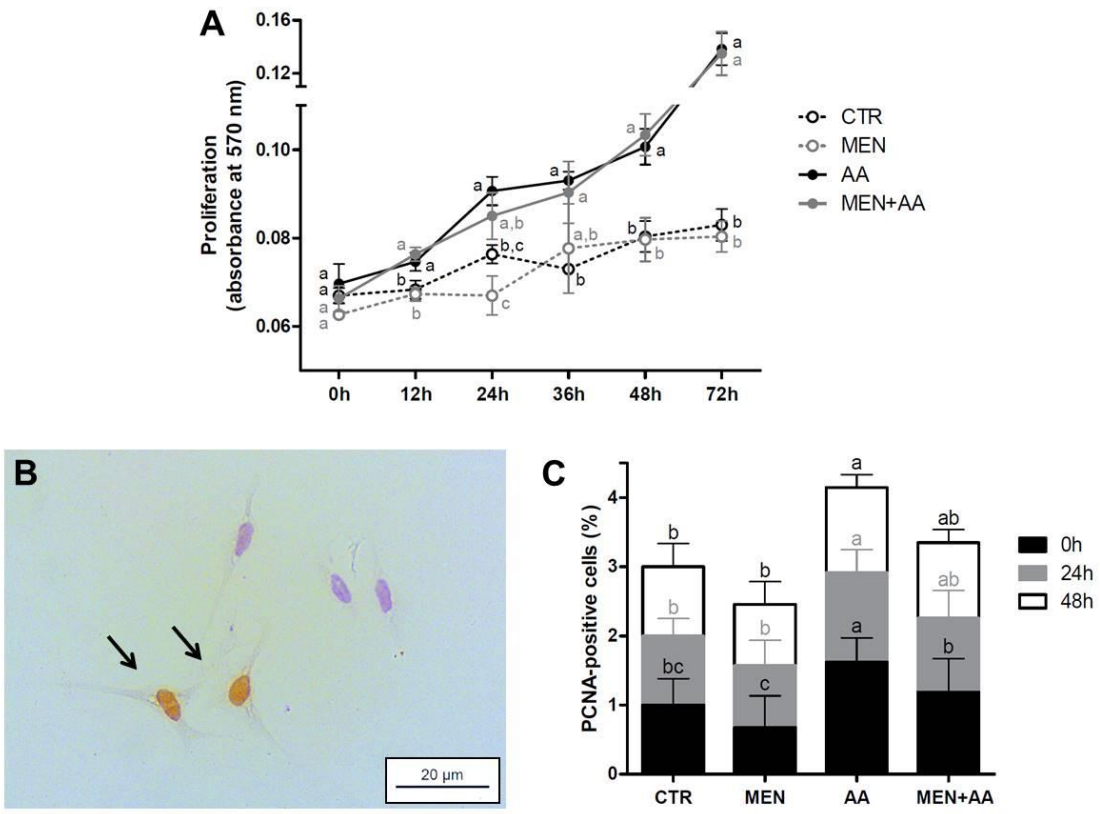

Fig 2. Myoblast proliferation. Cell proliferation was evaluated in myoblasts incubated with menadione (MEN), ascorbic acid (AA), menadione combined with ascorbic acid (MEN+AA) or without treatment (CTR). Ascorbic acid was administered at 200 µM to AA and MEN+AA

myoblasts, and menadione was administered at 10 µM to MEN and MEN+AA myoblasts. (A) MTT assay. Myoblast proliferation was measured considering the absorbance variation 0, 12, 24, 36, 48 and 72 hours after day 1. The data are expressed as the absorbance at 570 nm and presented as the mean ± SD of duplicates from three independent cell cultures. (B) PCNA immunostaining. Representative image of PCNA immunostaining in myoblasts in the CTR group on day 1. Arrows indicate PCNA-positive myoblasts. Image was obtained under a light microscope at a 40x magnification (Bars: 20 µm). (C) Quantification of PCNA-positive cells. Myoblast proliferation was measured considering the percentage of PCNA-stained nuclei 0, 24 and 48 hours after day 1. The data are expressed as the fold change compared with the CTR group and presented as the mean ± SD of duplicates from three independent cell cultures. The different letters indicate significant differences among the groups ($p<0.05$ - One-way ANOVA test, followed by Tukey's multiple comparisons test).

Myoblast migration assay

Considering wound closure, similar myoblasts migration was observed between the AA and MEN+AA groups and between the CTR and MEN groups (Fig 3B). The AA myoblasts showed increased migration compared to those in the CTR and MEN groups at 6, 12, 18 and 24 hours ($p<0.05$). At these initial time points, the MEN myoblasts showed the lowest migration rate, whereas the ascorbic acid-supplemented myoblasts showed the highest migration rate at 12 hours (Fig 3C). The comparison between the MEN and MEN+AA groups, specifically at 6, 12, 18 and 30 hours ($p<0.05$), demonstrated that the ascorbic acid supplementation could reduce menadione's effects and increase migration in the MEN+AA myoblasts. At 48 hours, although no significant differences were observed ($p=0.1453$), the AA myoblasts were able to completely fill the wound area, while some spaces were still visible in the other groups (Fig 3A and B).

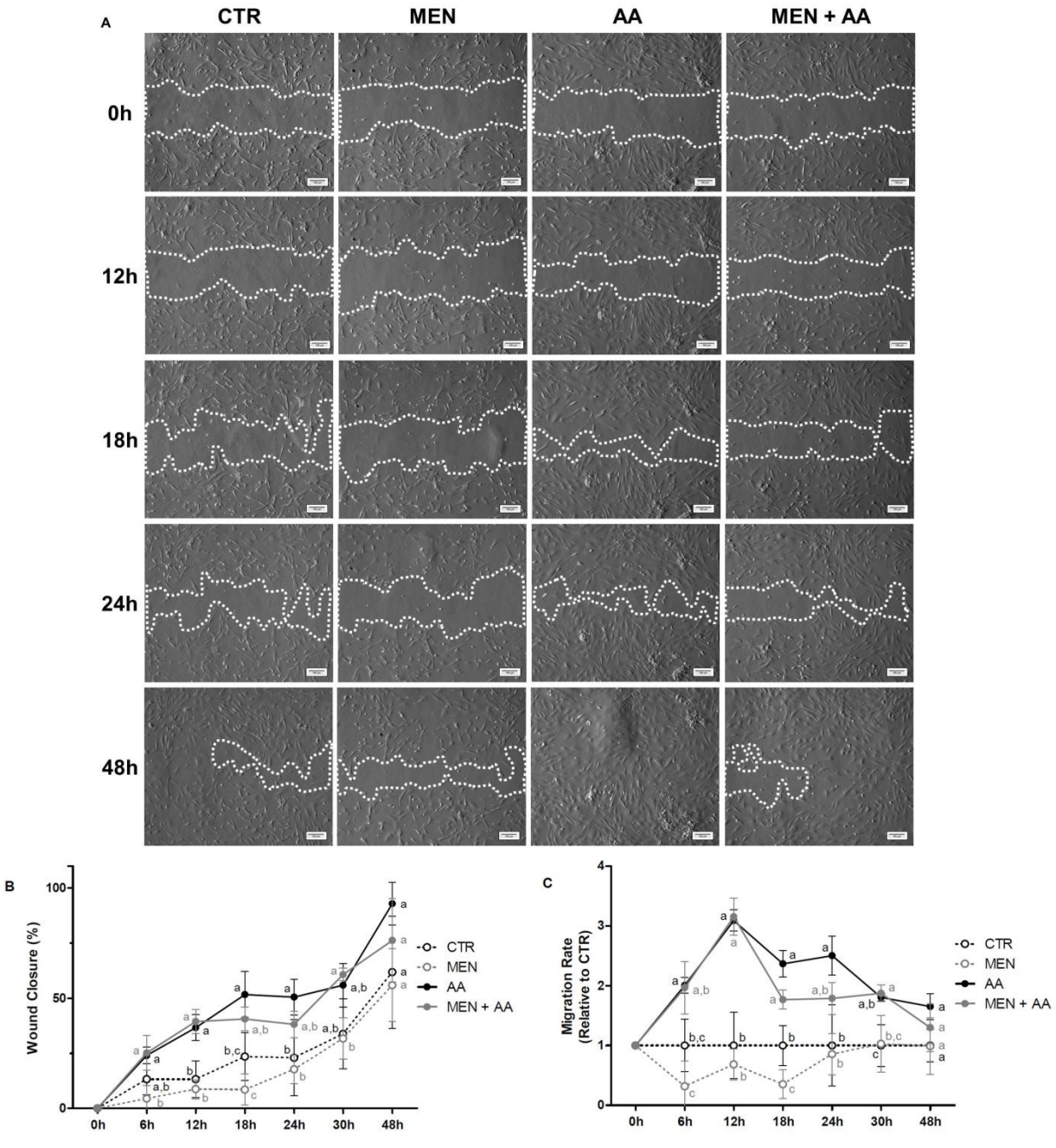

Fig 3. Myoblast migration. Cell migration was evaluated in myoblasts incubated with menadione (MEN), ascorbic acid (AA), menadione combined with ascorbic acid (MEN+AA) or without treatment (CTR). Ascorbic acid was administered at 200 µM to AA and MEN+AA myoblasts, and menadione was administered at 10 µM to MEN and MEN+AA myoblasts. Myoblast migration was measured 0, 6, 12, 18, 24, 30 and 48 hours postwound. (A) Representative images of wound healing assay. The white dashed line delimits the wound area. The images were obtained under an inverted microscope at a 10x magnification (Bars: 100 µm). (B) Wound closure (reduction in wound area sizes over time). The data are expressed as a

percentage and presented as the mean ± SD of duplicates from three independent cell cultures. (C) Migration rate (variation in wound closure over a time interval). The data are expressed as the fold change compared with the CTR group and presented as the mean ± SD of duplicates from three independent cell cultures. The different letters indicate significant differences among the groups ($p<0.05$ - One-way ANOVA test, followed by Tukey's multiple comparisons test).

Superoxide dismutase and catalase activities

The superoxide dismutase (SOD) and catalase (CAT) activities in the MEN group were significantly lower than those in the CTR group ($p<0.001$). Both the AA and MEN+AA groups had increased SOD and CAT activities compared to those in the MEN group ($p<0.01$). Ascorbic acid also resulted in significantly higher SOD activity in the myoblasts in the AA group compared with that in the CTR group ($p<0.01$) (Fig 4).

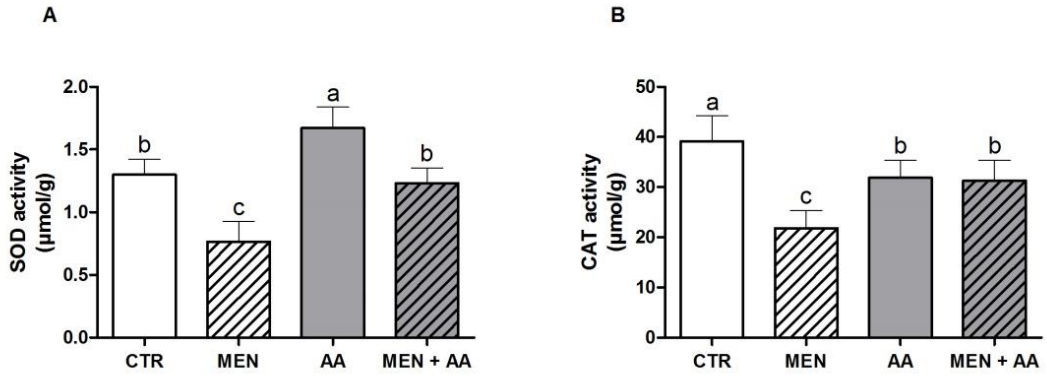

Fig 4. Activities of the antioxidant enzymes superoxide dismutase (SOD) and catalase (CAT). The activities of the SOD (A) and CAT (B) enzymes were evaluated in myoblasts incubated with menadione (MEN), ascorbic acid (AA), menadione combined with ascorbic acid (MEN+AA) or without treatment (CTR). Ascorbic acid was administered at 200 µM to AA and MEN+AA myoblasts, and menadione was administered at 10 µM to MEN and MEN+AA myoblasts. The data are expressed as µmol per g of protein and presented as the mean ± SD of duplicates from three independent cell cultures. The different letters indicate significant differences among the groups ($p<0.05$ - One-way ANOVA test, followed by Tukey's multiple comparisons test).

mRNA expression

Given the high density of the cells seeded on the cell culture plates (3×10^6 cells/mL), we evaluated the expression profile of typical muscle genes throughout development, especially on day 4, when the experiment was performed. On day 4, the myoblasts expressed high levels of all genes evaluated, showing that ascorbic acid experimentation could be properly conducted at this stage of proliferation (Supplementary Fig S3).

The differences in the expression of *myod1* (*myogenic differentiation 1*) among the groups were not statistically significant (p=0.5607), whereas the expression of *myog* (*myogenin*) was slightly upregulated in the AA group compared to that in the CTR, MEN and MEN+AA groups (p<0.05) (Fig 5). Furthermore, the treatment of the myoblasts according to their experimental groups did not promote significant differences in *igf1* (*insulin-like growth factor 1*) expression (p=0.1644), but the *mtor* (*mechanistic target of rapamycin*) levels were significantly upregulated in the AA group (p<0.05). In contrast, the expression levels of *fbxo32* (*f-box protein 32*) were significantly upregulated in the MEN and MEN+AA groups compared to those in the CTR and AA groups (p<0.05) (Fig 6).

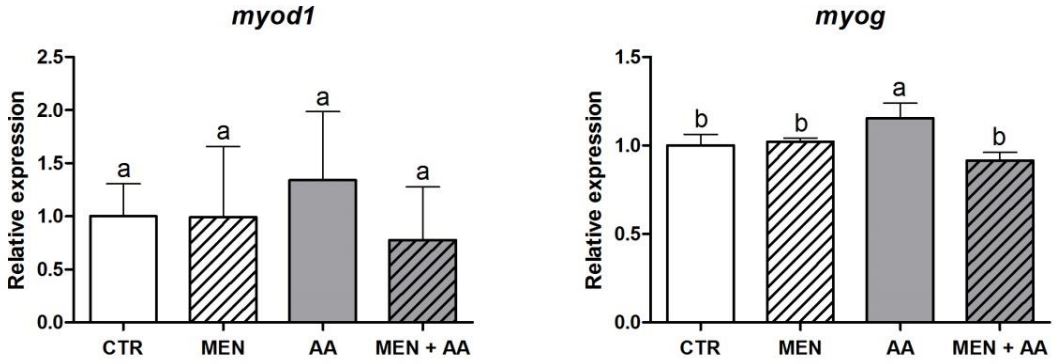

Fig 5. Relative mRNA expression of *myod1* and *myog*. *myod1* and *myog* mRNA expression was assessed by qPCR in myoblasts incubated with menadione (MEN), ascorbic acid (AA), menadione combined with ascorbic acid (MEN+AA) or without treatment (CTR). Ascorbic acid was administered at 200 µM to AA and MEN+AA myoblasts, and menadione was administered at 10 µM to MEN and MEN+AA myoblasts. The data are expressed as the fold change compared with the CTR group and presented as the mean ± SD of duplicates from four independent cell cultures. The different letters indicate significant differences among the groups (p<0.05 - One-way ANOVA test, followed by Tukey's multiple comparisons test).

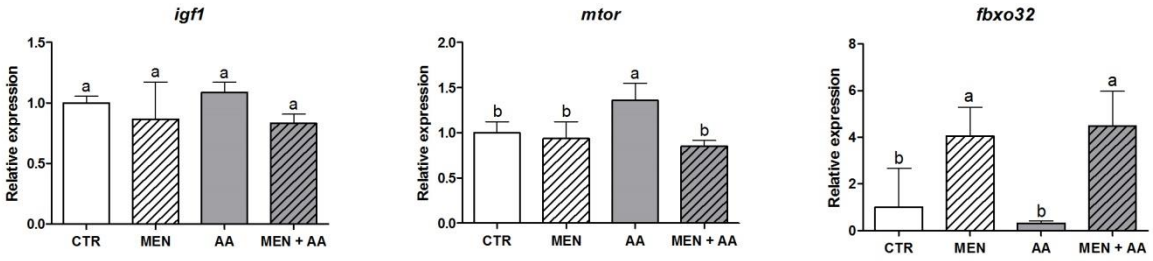

Fig 6. Relative mRNA expression of *igf1*, *mtor* and *fbxo32*. *igf1*, *mtor* and *fbxo32* mRNA expression was assessed by qPCR in myoblasts incubated with menadione (MEN), ascorbic acid (AA), menadione combined with ascorbic acid (MEN+AA) or without treatment (CTR). Ascorbic acid was administered at 200 μM to AA and MEN+AA myoblasts, and menadione was administered at 10 μM to MEN and MEN+AA myoblasts. The data are expressed as the fold change compared with the CTR group and presented as the mean ± SD of duplicates from four independent cell cultures. The different letters indicate significant differences among the groups ($p<0.05$ - One-way ANOVA test, followed by Tukey's multiple comparisons test).

DISCUSSION

Myoblast proliferation and migration

Ascorbic acid supplementation in the fish cell cultures increased myoblast proliferation and migration. Even the myoblasts in the MEN+AA group exhibited an enhancement in these mechanisms, especially compared to the MEN group, highlighting the ability of ascorbic acid to suppress the harmful effects of menadione.

Cell proliferation and migration are essential steps in myogenesis and muscle growth[6]. The increased myoblast proliferation and migration induced by ascorbic acid started early in our experiment and was observed within 1 day of the experiment with a gradual increase in these mechanisms over time. In addition, fish embryos initiate myogenesis during an earlier stage of development than amniotes, which probably reflects the requirement for the generation of swimming propulsion during earlier life stages[6]. This earlier myogenesis and the anticipated action of ascorbic acid help explain the high susceptibility of fish during the early stages of growth to ascorbic acid-deficient diets[13,14], which could lead to impaired myogenesis in addition to connective and bone tissue deformities. We believe that the myoblast proliferation and

migration periods may be crucial for the use of ascorbic acid and other interventions, such as amino acids and endocrine factors, aiming to increase skeletal muscle growth.

In fact, several studies have investigated myogenesis regulation by Igfs, growth hormone (Gh) and amino acids and provided many indications of their proliferative roles. The proliferation of sea bream (*Sparus aurata*) myoblasts was significantly stimulated by Igf1, Igf2 and Gh treatments[34,35]. Moreover, Gh and Igf2 increased the expression of *myf5* (*myogenic factor 5*) and *myod2*[35], which are primary MRFs involved in the initial steps of myogenesis, mainly determination, proliferation and migration[36–38]. Amino acid treatments revealed an interplay with Igfs in Atlantic salmon (*Salmo salar*) myogenic cells, promoting increased expression levels of Igf signaling components[8] and *myod1c*[39] on day 6 of development. This role in proliferation was also observed in a study investigating the impact of amino acid deficiencies on sea bream myoblasts, in which Lysine limitation significantly decreased the mRNA expression of Igf signaling components, *myf5* and *myod2*[40].

In our work, it is possible that ascorbic acid increased myoblast proliferation and migration through its role as an antioxidant agent that could decrease the levels of ROS within the cell. Increased or decreased levels of ROS in the cytoplasm lead to alterations in the redox status of the cell, which is important for controlling the activation of many factors[41,42]. In fact, Barbieri and Sestili (2012) discussed the most relevant signaling pathways triggered and/or affected by ROS in skeletal muscle, with low levels of ROS inducing upregulation of Igf1 and Pgc-1α (*peroxisome proliferator activated receptor gamma coactivator 1 alpha*), and high levels of ROS upregulating FoxO (*forkhead box O*) or Nf-κB (*nuclear factor kappa B*) signaling pathways[43]. In our work, the increased proliferation and migration induced by ascorbic acid were probably due to its direct regulation of the redox status, able to decrease ROS levels/persistence in myoblasts and, consequently, modulate components of the Igf signaling pathway. Moreover, given the crosstalk among signaling pathways controlling muscle growth[44,45], the redox status could also regulate the expression or activity of factors related to myogenesis, such as MRFs. A relatively recent study showed the effects of other antioxidants on primary myogenic cells isolated from skeletal muscle of rainbow trout, testing different doses of anthocyanidins[46]. The anthocyanidins upregulated the expression of *gpx1* (*glutathione peroxidase 1*) and *pax7* (*paired box protein 7*), which contribute to enhancing muscle tissue defense against oxidative stress and delay the progress of myogenic differentiation, respectively[46], maintaining the cells in a quiescent or proliferative state.

Superoxide dismutase and catalase activities

Although no direct measure of ROS were used to confirm the occurrence of menadione-induced oxidative stress and the antioxidant role of ascorbic acid, we evaluated the activities of the antioxidant enzymes SOD and CAT. The myoblasts treated with menadione showed a significant reduction in both SOD and CAT activities, whereas the ascorbic acid supplementation in the AA and MEN+AA groups maintained the high activity of these antioxidant enzymes compared to that in the MEN group. SOD and CAT act sequentially to neutralize oxidative stress. SOD dismutates superoxide anion radicals (O_2^-) generated in the mitochondrial electron transport chain into hydrogen peroxide (H_2O_2), which is converted into H_2O by CAT[47,48]. Due to the high oxidative potential of menadione, we believe that ROS produced following the menadione treatment may have promoted extensive cellular damage and that the antioxidant system could not resist this oxidant-induced injury. However, ascorbic acid, which was continuously supplemented in the cell cultures, may have stimulated the myoblast antioxidant machinery in preparation for the eventual oxidative stress, especially by increasing the activity of SOD, which could act first to avoid exacerbated increases in the ROS levels. In addition, the maintained activities of SOD and CAT by ascorbic acid prevented the drastic oxidative stress caused by menadione in the MEN+AA group.

Similar to our results, Khassaf et al. (2003) showed that the baseline activities of both SOD and CAT were elevated in lymphocytes from ascorbic acid-supplemented individuals[49]. Lü et al. (2010) proposed that antioxidants may act through the enhancement of the activity or expression of antioxidant enzymes, such as SOD, CAT and glutathione peroxidase[18]. In fact, the antioxidant-induced activation of these internal antioxidant enzymes has been studied in different cell line models. Treatment with anthocyanins promoted positive effects on elevating the antioxidant capacity, including increasing the activities of glutathione reductase and peroxidase, in rat hepatocytes[50]. Robb et al. (2008) investigated the long-term exposure of human fibroblasts to resveratrol and observed a dramatic and progressive upregulation of mitochondrial SOD expression and activity[51]. This activation of intracellular antioxidant enzymes by an external antioxidant could explain the high SOD activity in the fish myoblasts supplemented with ascorbic acid in our study. Our results confirm that menadione induced oxidative stress and that ascorbic acid plays an antioxidant role.

mRNA expression

Since skeletal muscle plasticity and individual fiber growth result from a balance between protein synthesis and degradation[42,52], to strengthen our work, we evaluated the mRNA expression of some molecular markers of myogenesis (*myod1* and *myog*), protein synthesis (*igf1* and *mtor*) and protein degradation (*fbxo32*) in pacu myoblasts.

The MRFs Myod1 and Myog control the myogenic program inside the cell and constitute the key factors that determine the progression of myogenesis[53]. In our study, the significant increase in the *myog* levels in the ascorbic acid-supplemented myoblasts represents an enhanced differentiation mechanism. This increase probably occurred due to the increased proliferation and migration of the myoblasts in the AA group as observed in the proliferation and migration assays despite the absence of significant differences in the expression levels of *myod1*. Since proliferation and migration were elevated, the myoblasts could express higher levels of *myog* and initiate fusion and differentiation earlier. Mitsumoto et al. (1994) showed that rat L6 myoblasts expressed higher amount of myogenin at both the mRNA and protein levels after treatment with ascorbic acid[30], and Shima et al. (2011) observed that ascorbic acid increased myogenin expression in mouse C2C12 myoblasts incubated at 30°C, promoting myogenic differentiation at low temperatures[31]. Based on these findings, we can infer that ascorbic acid supplementation is able to accelerate and advance the beginning of myogenesis in fish myoblasts.

Igf1, which is among the most studied and best characterized muscle growth-promoting factors, triggers several downstream cascades that culminate with the activation of Mtor and other components[6,52]. Mtor processes and integrates signals from nutrients, energy status and growth factors, controlling protein synthesis among its other functions[54]. Although *igf1* expression did not significantly differ among the experimental groups, *mtor* was highly expressed in the myoblasts treated exclusively with ascorbic acid, which is indicative of increased protein synthesis in the AA group. These results show possible Mtor activation independent of Igf1. Early studies investigating fish myoblast cell cultures have shown that amino acids independently stimulate protein synthesis[54,55], whereas Igf only stimulates protein synthesis if amino acids are also present in the media[8,9]. These works support the role of nutritional stimulation in skeletal muscle growth in teleost fish, and the activation of *mtor* by our ascorbic acid supplementation could be related to this nutritional pathway, increasing protein synthesis in addition to myoblast proliferation and migration.

Fbxo32, which is also known as Mafbx (*muscle atrophy f-box protein*), regulates the protein degradation in skeletal muscle and presents an usual upregulation during muscle

atrophy[52]. The upregulated expression of *fbxo32* in the MEN and MEN+AA groups indicates increased protein degradation in myoblasts probably due to menadione's action as an oxidant. Similar results were observed by Suzuki et al. (2007), who investigated the involvement of the dystrophin glycoprotein complex (DGC) in the regulation of skeletal muscle atrophy[56]. These authors showed that nNOS (*neuronal nitric oxide synthase*) dissociates from the DGC during atrophy and generates nitric oxide that could induce oxidative stress in skeletal muscle. Nitric oxide increased the levels of Fbxo32/Mafbx and other markers related to the protein degradation pathway[56]. In addition, Eijkelenboom and Burgering (2013) reviewed the function of FoxO, which is a well-known upstream activator of Fbxo32, including its increased transcriptional activity following cellular stress and high generation of ROS[57]. These data corroborate our results, demonstrating that the potent oxidative effect of menadione could increase *fbox32* expression and, consequently, protein degradation. This finding further explains the reduced myoblast proliferation and migration in the MEN group.

CONCLUSIONS

Ascorbic acid supplementation promotes increased myoblast proliferation and migration in cell cultures established using fast-twitch skeletal muscle from pacu. These results may be related to the antioxidant role of ascorbic acid, which protects myoblasts against the harmful effects of menadione, a powerful oxidant.

In addition to the enhanced proliferation and migration, the higher expression of *myog* and *mtor* showed that the ascorbic acid supplementation accelerated the beginning of myogenesis and increased protein synthesis, respectively, indicating that ascorbic acid can directly influence the mechanisms of fish skeletal muscle growth in addition to its action on connective and bone tissue.

Given the beneficial role of ascorbic acid in myogenesis and increased protein synthesis in skeletal muscle, the supplementation of this vitamin in fish is a potential treatment for increasing muscle growth, enabling interventions and improvements in pisciculture of pacu and other fish species.

MATERIALS AND METHODS

Ethics statement and animals

All experiments and procedures were performed in accordance with the Ethical Principles in Animal Research adopted by the Brazilian College of Animal Experimentation (COBEA). The protocol was approved by the Ethics Committee on Animal Use (protocol number 705) of the Institute of Biosciences, São Paulo State University (UNESP), Botucatu, São Paulo, Brazil. Pacus were obtained from the University of West São Paulo (UNOESTE), Presidente Prudente, São Paulo, Brazil. The fish were farmed at 28°C under a natural photoperiod (12 light:12 dark) in 0.5 m^3 storage tanks equipped with a water circulation system. Fast-twitch muscles were collected from juvenile pacus weighing 14.08 ± 5.91 g (mean ± SD; n=10 per cell culture) to establish the primary myoblast cell cultures. The pacus were euthanized with excess benzocaine (Sigma-Aldrich, USA), at a concentration exceeding 250 mg/L, prior to the collection of the muscle samples.

Myoblast cell culture

The myoblasts were isolated and cultured according to the protocol described by Fauconneau and Paboeuf (2000)[58]. Previous work was already published using myoblast cell cultures of pacu[12]. Briefly, the fast-twitch muscles were collected from the epaxial region and mechanically dissociated with scalpels. To release the muscle cells, the fragments were enzymatically digested with 0.2% collagenase type I and 0.1% trypsin (Sigma-Aldrich, USA). The cell suspension was filtered in cell strainers (Corning, USA), allowing for the remove of the debris, centrifuged and the cell pellet was resuspended in DMEM media (Dulbecco's Modified Eagle's Medium, 9 mM $NaHCO_3$ and 20 mM HEPES, pH 7.4 - Sigma-Aldrich, USA) with 1% antibiotics and 10% fetal bovine serum (Sigma-Aldrich, USA). The cells were counted using a hemocytometer (Kasvi, Brazil) and diluted at a concentration of 3×10^6 cells/mL, to increase the amount of RNA and protein for the proposed analyses, especially on day 1 (the next day after cell plating). The amount of cells seeded was 3×10^6 cells/well in 6-well plates (1 mL per well), 1.5×10^6 cells/well in 12-well plates (0.5 mL per well) or 0.187×10^6 cells/well in 96-well plates (0.0625 mL per well). DMEM media with 1% antibiotics and 10% fetal bovine serum were added to each well at the same volume of cell suspension (1 mL/well in 6-well plates, 0.5 mL/well in 12-well plates and 0.0625 mL/well in 96-well plates). The cells were plated in wells previously treated with poly-L-lysine and laminin (Sigma-Aldrich, USA), which have high

affinity for the myoblasts, and incubated at 28°C for 10 days. The media were changed once a day and the myoblasts morphology was regularly monitored in inverted microscope (Zeiss, Germany). The results were achieved from three or four independent cell cultures.

Immunofluorescence

Immunofluorescence was performed in myoblast cell cultures at days 1, 3 and 7 of development in coverslips in 6-well plates. The myoblasts were washed with PBS and then fixed in 4% paraformaldehyde for 15 minutes. The cells were permeabilized with 0.1% Triton X-100 (Sigma-Aldrich, USA) for 10 minutes and incubated in blocking solution (1% glycine, 3% bovine serum albumin (BSA), 8% fetal bovine serum and 0.3% Triton X-100 - Sigma-Aldrich, USA) for 1 hour, to prevent nonspecific binding. The myoblasts were incubated overnight at 4°C with a rabbit anti-desmin primary antibody (Sigma-Aldrich, USA) diluted in blocking solution (1:20). The cells were washed and then incubated for 2 hours at 4°C with an anti-rabbit FITC secondary antibody (sc-2090 - Santa Cruz, USA) diluted in blocking solution (1:400). The myoblasts nuclei were counterstained with DAPI present in Vectashield® mounting medium (Vector Laboratories Inc., USA) and the images were acquired under a fluorescence microscope (Olympus, Japan).

Experimental design and myoblast viability

The following four experimental groups were used to evaluate the role of ascorbic acid in proliferation and migration: the Control group (CTR), in which the myoblasts were not exposed to any treatment; the Menadione group (MEN), in which the myoblasts were treated with menadione (Sigma-Aldrich, USA) to induce oxidative stress; the Ascorbic acid group (AA), in which the myoblasts were supplemented with L-ascorbic acid 2-phosphate (Sigma-Aldrich, USA), which is a stable form of ascorbic acid recommended for use in cell cultures[31,59]; and the Menadione and Ascorbic acid group (MEN+AA), in which the myoblasts were treated with menadione combined with L-ascorbic acid 2-phosphate supplementation to verify the antioxidant effects of ascorbic acid. Based on previous work[31,32,60], L-ascorbic acid 2-phosphate was added to the DMEM media at a concentration of 200 μM in the AA and MEN+AA groups and was continuously administered to the myoblasts (each time the media were changed) since cell plating. Tests were performed to verify the ideal concentration of menadione causing oxidative stress while maintaining cell viability.

The myoblast viability following the treatment with menadione was accessed by trypan blue exclusion and MTT assays. The trypan blue exclusion assay was performed on day 1 in 6-well plates using duplicates from four independent cell cultures. Menadione was solubilized in dimethyl sulfoxide (DMSO) at 1 mg/mL (stock solution) according to the manufacturer's guidelines, and different concentrations were prepared after dilution in PBS (working solution). The myoblasts were treated with 0.1, 1, 10 and 100 µM menadione for 1 and 24 hours. After washing with PBS and harvesting with 0.25% trypsin, the myoblasts were stained with 0.4% trypan blue solution (Sigma-Aldrich, USA). The stained (dead) and unstained (live) myoblasts were counted using a hemocytometer (Kasvi, Brazil), and cell viability was expressed as a percentage of the total number of cells. The MTT assay was performed on day 1 in 96-well plates using duplicates from four independent cell cultures. Metabolically active cells reduce tetrazolium MTT into intracellular purple formazan, whose quantity is directly proportional to the viable and proliferative cells over time[61]. The myoblasts were treated with 10, 100 and 200 µM menadione for 1 hour and then incubated with tetrazolium MTT solution (Sigma-Aldrich, USA) at 37°C for 4 hours. The myoblasts were incubated with 200 µL per well of ≥99.9% DMSO (Sigma-Aldrich, USA) to solubilize the intracellular purple formazan, and the absorbance at 570 nm was measured using an Asys Expert Plus Microplate Reader (Biochrom, United Kingdom). Based on the trypan blue exclusion and MTT assays, the MEN and MEN+AA groups were treated with 10 µM menadione for 1 hour immediately before each experiment. The concentration of 10 µM menadione contained 0.1% DMSO, which is not toxic to cells[62]. To account for the possible effects of DMSO on the menadione treatment, the media in the CTR and AA groups also received the nontoxic concentration of 0.1% DMSO.

Myoblast proliferation assays

Myoblast proliferation was assessed by an MTT assay and PCNA immunostaining. The MTT assay was performed 0, 12, 24, 36, 48 and 72 hours after day 1 in different 96-well plates seeded on the same day using duplicates from three independent cell cultures. Similar to the cell viability test, the myoblasts were incubated with MTT solution (Sigma-Aldrich, USA) at 37°C for 4 hours. After the tetrazolium MTT reduction, the resulting intracellular purple formazan was solubilized by incubating the myoblasts with 200 µL per well of ≥99.9% DMSO (Sigma-Aldrich, USA). The absorbance at 570 nm was quantified using an Asys Expert Plus Microplate Reader (Biochrom, United Kingdom). PCNA immunostaining was performed 0, 24 and 48 hours after day 1 in coverslips on 12-well plates using duplicates from three independent cell cultures.

The myoblasts were washed with PBS and then fixed in 4% paraformaldehyde for 10 minutes. The cells were postfixed in 100% methanol for 10 minutes and incubated in blocking solution (3% BSA – Sigma-Aldrich, USA) for 1 hour to prevent nonspecific binding. The myoblasts were incubated overnight at 4°C with a mouse anti-PCNA primary antibody (sc-56 - Santa Cruz, USA) diluted in 1% BSA (1:500). The cells were washed and then incubated for 90 minutes at room temperature with an anti-mouse HRP secondary antibody (ab6789 - Abcam, USA) diluted in 1% BSA (1:500). After an additional washing step, the myoblasts were incubated with DAB solution (500 µL 3,3'-Diaminobenzidine, 4 mL hydrogen peroxide and 4.5 mL PBS - Sigma-Aldrich, USA) to identify proliferative cells expressing PCNA. Hematoxylin was used to counterstain the myoblasts, and the coverslips were dehydrated in a graded alcohol series and mounted with Permount. Proliferation was quantified as a percentage of PCNA-positive cells of the total number of nuclei in 10 images per coverslip using ImageJ® software[63]. The images were acquired under a light microscope coupled to the digital camera Leica DMC2900 (Leica, Germany).

Myoblast migration assay

Myoblast migration was assessed by a wound healing assay, which was performed after reaching 80-100% confluency (day 4) in 6-well plates using duplicates from three independent cell cultures. Initially, the cell monolayers were mechanically scratched ("wound") in the shape of a cross by a 200 µL sterile tip in the center of each well. The cell debris was removed by two washes with PBS, and the myoblasts were incubated in DMEM media with 1% antibiotics and 2% fetal bovine serum (Sigma-Aldrich, USA) to reduce the cell proliferation rate. The wound areas were evaluated at 0, 6, 12, 18, 24, 30 and 48 hours, and images were captured under an inverted microscope coupled to the digital camera AxioCam ICc5 (Zeiss, Germany). The wound areas corresponding to the area mean of the four lines in the cross-shaped wound were measured using ImageJ® software[63]. The wound areas were used to calculate the reduction in the wound area size over time (wound closure) and the variation in wound closure over the time interval (migration rate or migration speed).

Superoxide dismutase and catalase activity

The assays used to verify the activities of antioxidant enzymes were performed after reaching 80-100% confluency (day 4) in 6-well plates using duplicates from three independent cell cultures. The protein content was extracted from the myoblasts using RIPA buffer and a

protease inhibitor cocktail (Sigma-Aldrich, USA), which is consistent with the manufacturer's recommendations. The extracted protein content was quantified by the Bradford method[64] and used to evaluate the activities of the antioxidant enzymes SOD and CAT. The activity of the SOD enzyme was determined by its ability to inhibit the reduction in nitroblue tetrazolium, causing changes in the color intensity. SOD activity was measured in proper solution (50 mM PBS pH 7.4, 0.1 mM EDTA, 62 µM nitroblue tetrazolium, 98 µM NADH and 3.3 µM phenazine methosulfate - Sigma-Aldrich, USA), and the SOD unit was defined as the amount of enzyme needed to decrease the reference rate to 50% of maximum inhibition[65]. The activity of the CAT enzyme was determined by its ability to decompose hydrogen peroxide (H_2O_2) and was also measured in proper solution (10 mM H_2O_2 and 50 mM sodium and potassium phosphate buffer pH 7.0 - Sigma-Aldrich, USA). The CAT unit was defined as the amount of enzyme necessary for H_2O_2 decomposition at a constant rate of 15 seconds at 240 nm[66]. The enzyme activities were analyzed using the EON microplate reader system with Gen5 2.0 Software (BioTek Instruments, USA).

mRNA expression

The expression analyses were performed after 80-100% confluence (day 4) in 6-well plates using duplicates from four independent cell cultures. The total RNA was extracted from the myoblast cell cultures using TRIzol® Reagent (Thermo Fisher Scientific, USA), according to the manufacturer's recommendations. The RNA was quantified using a NanoVue™ Plus spectrophotometer (GE Healthcare, United Kingdom), and the estimation of the RNA purity was performed by measuring the absorbance at 260 nm (RNA quantity) and 280 nm (protein quantity). The RNA integrity was evaluated through capillary electrophoresis in the 2100 Bioanalyzer (Agilent, USA), which provided a RNA integrity number (RIN) based on the *28S* and *18S ribosomal RNAs*. Only samples with 260/280 ratio ≥ 1.8 and with an RIN ≥ 7.0 were used. To eliminate any possible contaminating genomic DNA from the samples, the extracted RNA was treated with DNase I, Amplification Grade (Thermo Fisher Scientific, USA). The RNA reverse transcription was performed using the High Capacity cDNA Archive Kit (Thermo Fisher Scientific, USA), according to the manufacturer's guidelines.

Primers for the *myod1* (*myogenic differentiation 1*), *myog* (*myogenin*), *igf1* (*insulin like growth factor 1*), *mtor* (*mechanistic target of rapamycin*), *fbxo32* (*f-box protein 32*), *rpl13* (*ribosomal protein L13*), *ppiaa* (*peptidylprolyl isomerase Aa*) and *gapdh* (*glyceraldehyde-3-phosphate dehydrogenase*) mRNAs were designed from *Piaractus mesopotamicus*

transcriptome, obtained by our group[45] and whose raw reads were deposited in the European Nucleotide Archive - ENA (accession number PRJEB6656). These primers were designed using *Primer3 v.0.4.0*[67,68] and *NetPrimer* (Premier Biosoft, USA) softwares (Table 1).

The mRNAs expression levels were detected by quantitative real-time PCR (qPCR) using the QuantStudio™ 12K Flex Real-Time PCR System (Thermo Fisher Scientific, USA). All qPCR performed were compliant with the Minimum Information for Publication of Quantitative Real-Time PCR experiments (MIQE) guidelines[69]. The cDNA samples were amplified using the GoTaq® qPCR Master Mix (Promega, USA) and the respective primers (Table 1), which were synthesized by Invitrogen (USA). The reactions were performed at 95°C for 10 minutes followed by 40 cycles of denaturation at 95°C for 15 seconds and annealing/extension at 60°C for 1 minute. The reaction efficiency was calculated by LinRegPCR software[70,71], and the specificity of each primer set was evaluated by the dissociation curve at the end of each PCR reaction, which confirmed the presence of a single fluorescence peak. The relative quantification of expression was performed by the $2^{-\Delta\Delta Ct}$ method[72] using the DataAssist™ v3.01 software (Thermo Fisher Scientific, USA). The mRNA expression levels were normalized to the *rpl13*, *ppiaa* and *gapdh* mRNAs, whose expressions were constant among all samples.

Statistical analyses

The statistical analyses were performed using the parametric one-way ANOVA test, followed by Tukey's multiple comparisons test. The data are presented as the mean ± SD of duplicates from three or four independent cell cultures. The statistical significance was set at 5% ($p<0.05$) (GraphPad Prism 5 Software, USA).

Data availability statement

All data generated or analysed during this study are included in this published article.

REFERENCES

1. Urbinati, E. C. & Gonçalves, F. D. Pacu (Piaractus mesopotamicus) in *Espécies nativas para piscicultura no Brasil* (eds. Baldisserotto, B. & Gomes, L. C.) 225–255 (UFSM, 2005).
2. IBGE. *Produção da pecuária municipal*. (IBGE, 2016).
3. Froehlich, J. M., Galt, N. J., Charging, M. J., Meyer, B. M. & Biga, P. R. In vitro indeterminate teleost myogenesis appears to be dependent on Pax3. *In Vitro Cell. Dev. Biol. Anim.* **49,** 371–85; 10.1007/s11626-013-9616-2 (2013).
4. Johnston, I. A. Genetic and Environmental Determinants of Muscle Growth Patterns in *Muscle development*

and growth 141–186 (Academic Press, 2001).

5. Sänger, A. M. & Stoiber, W. Muscle fiber diversity and plasticity in *Muscle development and growth* (ed. Johnston, I. A.) **18,** 187–250 (Academic Press, 2001).
6. Johnston, I. A., Bower, N. I. & Macqueen, D. J. Growth and the regulation of myotomal muscle mass in teleost fish. *J. Exp. Biol.* **214,** 1617–28; 10.1242/jeb.038620 (2011).
7. Rowlerson, A. & Veggetti, A. Cellular mechanisms of post-embryonic muscle growth in aquaculture species in *Muscle development and growth* (ed. Johnston, I. A.) **18,** 103–140 (Academic Press, 2001).
8. Bower, N. I. & Johnston, I. A. Transcriptional regulation of the IGF signaling pathway by amino acids and insulin-like growth factors during myogenesis in Atlantic salmon. *PLoS One* **5,** e11100; 10.1371/journal.pone.0011100 (2010).
9. Garcia de la serrana, D. & Johnston, I. A. Expression of Heat Shock Protein (Hsp90) Paralogues Is Regulated by Amino Acids in Skeletal Muscle of Atlantic Salmon. *PLoS One* **8,** e74295; 10.1371/journal.pone.0074295 (2013).
10. Vélez, E. J. *et al.* Contribution of in vitro myocytes studies to understanding fish muscle physiology. *Comp. Biochem. Physiol. Part B Biochem. Mol. Biol.* **199,** 67–73; 10.1016/j.cbpb.2015.12.003 (2016).
11. Gabillard, J. C., Sabin, N. & Paboeuf, G. In vitro characterization of proliferation and differentiation of trout satellite cells. *Cell Tissue Res.* **342,** 471–7; 10.1007/s00441-010-1071-8 (2010).
12. Duran, B. O. da S. *et al.* Differential microRNA Expression in Fast- and Slow-Twitch Skeletal Muscle of Piaractus mesopotamicus during Growth. *PLoS One* **10,** e0141967; 10.1371/journal.pone.0141967 (2015).
13. Rotta, M. A. *Utilização do ácido ascórbico (vitamina C) pelos peixes*. (Embrapa Pantanal, 2003).
14. Dabrowski, K. Ascorbate concentration in fish ontogeny. *J. Fish Biol.* **40,** 273–279; 10.1111/j.1095-8649.1992.tb02572.x (1992).
15. Lovell, T. *Nutrition and Feeding of Fish*. (Springer US, 1989).
16. Tacon, A. G. J. Trastornos nutricionales relacionados con las vitaminas in *Ictiopatología nutricional: signos morfológicos de la carencia y toxicidad de los nutrientes en los peces cultivados* 1–77 (FAO, 1995).
17. Rucker, R. B., Morris, J. & Fascetti, A. J. Vitamins in *Clinical Biochemistry of Domestic Animals* 695–730 (Elsevier, 2008).
18. Lü, J.-M., Lin, P. H., Yao, Q. & Chen, C. Chemical and molecular mechanisms of antioxidants: experimental approaches and model systems. *J. Cell. Mol. Med.* **14,** 840–860; 10.1111/j.1582-4934.2009.00897.x (2010).
19. McKenna, T. Oxidative stress on mammalian cell cultures during recombinant protein expression in *Linköping Studies in Science and Technology Licentiate thesis no. 1425* (Linköpings Universitet, 2009).
20. Gant, T. W., Rao, D. N., Mason, R. P. & Cohen, G. M. Redox cycling and sulphydryl arylation; their relative importance in the mechanism of quinone cytotoxicity to isolated hepatocytes. *Chem. Biol. Interact.* **65,** 157–73 (1988).
21. Monteiro, J. P. *et al.* A biophysical approach to menadione membrane interactions: Relevance for menadione-induced mitochondria dysfunction and related deleterious/therapeutic effects. *Biochim. Biophys. Acta - Biomembr.* **1828,** 1899–1908; 10.1016/j.bbamem.2013.04.006 (2013).
22. Franceschi, R. T., Iyer, B. S. & Cui, Y. Effects of ascorbic acid on collagen matrix formation and osteoblast

differentiation in murine MC3T3-E1 cells. *J. Bone Miner. Res.* **9,** 843–854; 10.1002/jbmr.5650090610 (1994).

23. Lall, S. P. & Lewis-McCrea, L. M. Role of nutrients in skeletal metabolism and pathology in fish — An overview. *Aquaculture* **267,** 3–19; 10.1016/j.aquaculture.2007.02.053 (2007).
24. Rebouche, C. J. Ascorbic acid and carnitine biosynthesis. *Am. J. Clin. Nutr.* **54,** 1147S–1152S; 10.1093/ajcn/54.6.1147s (1991).
25. Russell, P. J., Williams, A. & Austin, T. A. Inhibition of rabbit muscle isozymes by vitamin C. *J. Enzyme Inhib.* **15,** 283–96; 10.3109/14756360009040689 (2000).
26. Sen, C. K. Antioxidants in exercise nutrition. *Sports Med.* **31,** 891–908 (2001).
27. Ashton, T. *et al.* Exercise-induced endotoxemia: the effect of ascorbic acid supplementation. *Free Radic. Biol. Med.* **35,** 284–91; 10.1016/S0891-5849(03)00309-5 (2003).
28. Savini, I. *et al.* Vitamin C homeostasis in skeletal muscle cells. *Free Radic. Biol. Med.* **38,** 898–907; 10.1016/j.freeradbiomed.2004.12.009 (2005).
29. MacBride, R. G. Ascorbic acid facilitates chicken myoblast fusion in vitro. *In Vitro Cell. Dev. Biol.* **25,** 617–20 (1989).
30. Mitsumoto, Y., Liu, Z. & Klip, A. A Long-Lasting Vitamin C Derivative, Ascorbic Acid 2-Phosphate, Increases Myogenin Gene Expression and Promotes Differentiation in L6 Muscle Cells. *Biochem. Biophys. Res. Commun.* **199,** 394–402; 10.1006/bbrc.1994.1242 (1994).
31. Shima, A. *et al.* IGF-I and vitamin C promote myogenic differentiation of mouse and human skeletal muscle cells at low temperatures. *Exp. Cell Res.* **317,** 356–366; 10.1016/j.yexcr.2010.11.001 (2011).
32. Ikeda, K. *et al.* Effects of heat stimulation and l -ascorbic acid 2-phosphate supplementation on myogenic differentiation of artificial skeletal muscle tissue constructs. *J. Tissue Eng. Regen. Med.* **11(5),** 1322–1331; 10.1002/term.2030 (2017).
33. Pin, C. L. & Merrifield, P. A. Developmental Potential of Rat L6 Myoblastsin VivoFollowing Injection into Regenerating Muscles. *Dev. Biol.* **188,** 147–166; 10.1006/dbio.1997.8624 (1997).
34. Rius-Francino, M. *et al.* Differential effects on proliferation of GH and IGFs in sea bream (Sparus aurata) cultured myocytes. *Gen. Comp. Endocrinol.* **172,** 44–49; 10.1016/j.ygcen.2011.03.024 (2011).
35. Jiménez-Amilburu, V. *et al.* Insulin-like growth factors effects on the expression of myogenic regulatory factors in gilthead sea bream muscle cells. *Gen. Comp. Endocrinol.* **188,** 151–158; 10.1016/j.ygcen.2013.02.033 (2013).
36. Bentzinger, C. F., Wang, Y. X. & Rudnicki, M. A. Building Muscle: Molecular Regulation of Myogenesis. *Cold Spring Harb. Perspect. Biol.* **4,** a008342–a008342; 10.1101/cshperspect.a008342 (2012).
37. Almeida, F. L. A. *et al.* Quantitative expression of myogenic regulatory factors MyoD and myogenin in pacu (Piaractus mesopotamicus) skeletal muscle during growth. *Micron* **41,** 997–1004; 10.1016/j.micron.2010.06.012 (2010).
38. Johansen, K. A. & Overturf, K. Quantitative expression analysis of genes affecting muscle growth during development of rainbow trout(Oncorhynchus mykiss). *Mar. Biotechnol. (NY).* **7,** 576–87; 10.1007/s10126-004-5133-3 (2005).
39. Bower, N. I. & Johnston, I. A. Paralogs of Atlantic salmon myoblast determination factor genes are

distinctly regulated in proliferating and differentiating myogenic cells. *Am. J. Physiol. Integr. Comp. Physiol.* **298,** R1615–R1626; 10.1152/ajpregu.00114.2010 (2010).

40. Azizi, S. *et al.* Lysine and Leucine Deficiencies Affect Myocytes Development and IGF Signaling in Gilthead Sea Bream (Sparus aurata). *PLoS One* **11,** e0147618; 10.1371/journal.pone.0147618 (2016).
41. Storz, G. & Polla, B. S. Transcriptional regulators of oxidative stress-inducible genes in prokaryotes and eukaryotes in *Stress-Inducible Cellular Responses* 239–254 (Birkhäuser Basel, 1996).
42. Blaauw, B., Schiaffino, S. & Reggiani, C. Mechanisms Modulating Skeletal Muscle Phenotype. *Comprehensive Physiology* **3(4),** 1645–1687; 10.1002/cphy.c130009 (2013).
43. Barbieri, E. & Sestili, P. Reactive Oxygen Species in Skeletal Muscle Signaling. *J. Signal Transduct.* **2012,** 1–17; 10.1155/2012/982794 (2012).
44. Schiaffino, S., Dyar, K. A., Ciciliot, S., Blaauw, B. & Sandri, M. Mechanisms regulating skeletal muscle growth and atrophy. *FEBS J.* **280,** 4294–4314; 10.1111/febs.12253 (2013).
45. Mareco, E. A., Garcia de la Serrana, D., Johnston, I. A. & Dal-Pai-Silva, M. Characterization of the transcriptome of fast and slow muscle myotomal fibres in the pacu (Piaractus mesopotamicus). *BMC Genomics* **16,** 182; 10.1186/s12864-015-1423-6 (2015).
46. Villasante, A. *et al.* Effect of anthocyanidins on myogenic differentiation in induced and non-induced primary myoblasts from rainbow trout (Oncorhynchus mykiss). *Comp. Biochem. Physiol. Part B Biochem. Mol. Biol.* **196-197,** 102–108; 10.1016/j.cbpb.2016.03.004 (2016).
47. Cadenas, E. & Davies, K. J. Mitochondrial free radical generation, oxidative stress, and aging. *Free Radic. Biol. Med.* **29,** 222–30 (2000).
48. Sommer, D., Fakata, K. L., Swanson, S. A. & Stemmer, P. M. Modulation of the phosphatase activity of calcineurin by oxidants and antioxidants in vitro. *Eur. J. Biochem.* **267,** 2312–22; 10.1046/j.1432-1327.2000.01240.x (2000).
49. Khassaf, M. *et al.* Effect of Vitamin C Supplements on Antioxidant Defence and Stress Proteins in Human Lymphocytes and Skeletal Muscle. *J. Physiol.* **549,** 645–652; 10.1113/jphysiol.2003.040303 (2003).
50. Shih, P.-H., Yeh, C.-T. & Yen, G.-C. Anthocyanins Induce the Activation of Phase II Enzymes through the Antioxidant Response Element Pathway against Oxidative Stress-Induced Apoptosis. *J. Agric. Food Chem.* **55,** 9427–9435; 10.1021/jf071933i (2007).
51. Robb, E. L., Page, M. M., Wiens, B. E. & Stuart, J. A. Molecular mechanisms of oxidative stress resistance induced by resveratrol: Specific and progressive induction of MnSOD. *Biochem. Biophys. Res. Commun.* **367,** 406–412; 10.1016/j.bbrc.2007.12.138 (2008).
52. Sandri, M. Signaling in Muscle Atrophy and Hypertrophy. *Physiology* **23,** 160–170; 10.1152/physiol.00041.2007 (2008).
53. Zanou, N. & Gailly, P. Skeletal muscle hypertrophy and regeneration: interplay between the myogenic regulatory factors (MRFs) and insulin-like growth factors (IGFs) pathways. *Cell. Mol. Life Sci.* **70,** 4117–4130; 10.1007/s00018-013-1330-4 (2013).
54. Vélez, E. J. *et al.* IGF-I and amino acids effects through TOR signaling on proliferation and differentiation of gilthead sea bream cultured myocytes. *Gen. Comp. Endocrinol.* **205,** 296–304; 10.1016/j.ygcen.2014.05.024 (2014).

55. Seiliez, I. *et al.* An in vivo and in vitro assessment of TOR signaling cascade in rainbow trout (Oncorhynchus mykiss). *AJP Regul. Integr. Comp. Physiol.* **295,** R329–R335; 10.1152/ajpregu.00146.2008 (2008).
56. Suzuki, N. *et al.* NO production results in suspension-induced muscle atrophy through dislocation of neuronal NOS. *J. Clin. Invest.* **117,** 2468–2476; 10.1172/JCI30654 (2007).
57. Eijkelenboom, A. & Burgering, B. M. T. FOXOs: signalling integrators for homeostasis maintenance. *Nat. Rev. Mol. Cell Biol.* **14,** 83–97; 10.1038/nrm3507 (2013).
58. Fauconneau, B. & Paboeuf, G. Effect of fasting and refeeding on in vitro muscle cell proliferation in rainbow trout (Oncorhynchus mykiss). *Cell Tissue Res.* **301,** 459–63; 10.1007/s004419900168 (2000).
59. Hata, R.-I. & Senoo, H. L-ascorbic acid 2-phosphate stimulates collagen accumulation, cell proliferation, and formation of a three-dimensional tissuelike substance by skin fibroblasts. *J. Cell. Physiol.* **138,** 8–16; 10.1002/jcp.1041380103 (1989).
60. Lu, A. *et al.* Rapid depletion of muscle progenitor cells in dystrophic mdx/utrophin-/- mice. *Hum. Mol. Genet.* **23,** 4786–4800; 10.1093/hmg/ddu194 (2014).
61. Mosmann, T. Rapid colorimetric assay for cellular growth and survival: application to proliferation and cytotoxicity assays. *J. Immunol. Methods* **65,** 55–63 (1983).
62. Nishimura, M., Nikawa, T., Kawano, Y., Nakayama, M. & Ikeda, M. Effects of dimethyl sulfoxide and dexamethasone on mRNA expression of housekeeping genes in cultures of C2C12 myotubes. *Biochem. Biophys. Res. Commun.* **367,** 603–608; 10.1016/j.bbrc.2008.01.006 (2008).
63. Schneider, C. A., Rasband, W. S. & Eliceiri, K. W. NIH Image to ImageJ: 25 years of image analysis. *Nat. Methods* **9,** 671–5; 10.1038/nmeth.2089 (2012).
64. Bradford, M. M. A rapid and sensitive method for the quantitation of microgram quantities of protein utilizing the principle of protein-dye binding. *Anal. Biochem.* **72,** 248–54 (1976).
65. Ewing, J. F. & Janero, D. R. Microplate Superoxide Dismutase Assay Employing a Nonenzymatic Superoxide Generator. *Anal. Biochem.* **232,** 243–248; 10.1006/abio.1995.0014 (1995).
66. Aebi, H. Catalase in *Methods of Enzymatic Analysis* (ed. Bergmeyer, H. U.) 673–684 (Academic Press, 1974).
67. Koressaar, T. & Remm, M. Enhancements and modifications of primer design program Primer3. *Bioinformatics* **23,** 1289–1291; 10.1093/bioinformatics/btm091 (2007).
68. Untergasser, A. *et al.* Primer3--new capabilities and interfaces. *Nucleic Acids Res.* **40,** e115; 10.1093/nar/gks596 (2012).
69. Bustin, S. A. *et al.* The MIQE Guidelines: Minimum Information for Publication of Quantitative Real-Time PCR Experiments. *Clin. Chem.* **55,** 611–622; 10.1373/clinchem.2008.112797 (2009).
70. Ramakers, C., Ruijter, J. M., Deprez, R. H. L. & Moorman, A. F. M. Assumption-free analysis of quantitative real-time polymerase chain reaction (PCR) data. *Neurosci. Lett.* **339,** 62–6; 10.1016/S0304-3940(02)01423-4 (2003).
71. Ruijter, J. M. *et al.* Amplification efficiency: linking baseline and bias in the analysis of quantitative PCR data. *Nucleic Acids Res.* **37,** e45; 10.1093/nar/gkp045 (2009).
72. Livak, K. J. & Schmittgen, T. D. Analysis of relative gene expression data using real-time quantitative PCR

and the 2(-Delta Delta C(T)) Method. *Methods* **25,** 402–8; 10.1006/meth.2001.1262 (2001).

ACKNOWLEDGEMENTS

We thank Dr. Daniel Garcia de la Serrana Castillo for his help in the establishment of the pacu myoblast cell cultures and valuable discussions. This study was financed by the funding agencies Coordination for the Improvement of Higher Education Personnel (CAPES); National Council for Scientific and Technological Development (CNPq), with grants 447233/2014 and 302656/2015-4; and São Paulo Research Foundation (FAPESP), with grants #2015/03234-8, #2016/01086-4 and #2016/05009-4.

AUTHOR CONTRIBUTIONS

Conceived and designed the experiments: BOSD GAG EAM RFC MDPS. Performed the experiments: BOSD GAG BTTZ PPF JSV RASS. Analyzed the data: BOSD GAG BTTZ PPF JSV EAM AF RFC MDPS. Contributed with reagents/materials/analysis tools: BOSD EAM RASS AF RFC MDPS. Wrote and reviewed the manuscript: BOSD GAG BTTZ RFC MDPS.

SUPPLEMENTARY INFORMATION

Table 1. Primers used for *myod1*, *myog*, *igf1*, *mtor*, *fbxo32*, *rpl13*, *ppiaa* and *gapdh* mRNA amplification by qPCR.

Gene	Accession code	Primer (5'-3')	Amplicon size (bp)
myod1	comp144727_c1_seq4	F: GTTCGTCGTCTTCCTCTTGC R: ACCCGTGCTTTAACACCAAC	191
myog	comp137034_c4_seq6	F: CAGACCAGAGGTTTTATGAA R: TAGATGTTGGGGATGGCTTG	171
igf1	comp134662_c2_seq2	F: ATTCAGCAAGCCAACAGGT R: CGCACAATACATCTCAAGTCG	116
mtor	comp141640_c0_seq15	F: TTGGGAGAGACGTACTGC R: CACAGGACTGGTGTAGGAA	145
fbxo32	comp145335_c1_seq5	F: TCTTTGGTGCTCCCCTTGTG R: TAAAACCGAGGACGGCTGG	231
rpl13	comp141862_c0_seq1	F: ATCAACAGGAAAGTAGCCC R: AGGATGAGTTTGGAGCGGTA	122
ppiaa	comp145566_c0_seq1	F: ATTGTGGTTCGTGAAGTCGC	168

		R: CCGCTGGGCAGAGTGATTAT	
gapdh	comp140533_c0_seq1	F: ACACACGACGACAAGACCAA R: GTCCCTCTCGCTGAAAACTG	267

F, forward; R, reverse. Gene are as follow: *myod1* (*myogenic differentiation 1*), *myog* (*myogenin*), *igf1* (*insulin like growth factor 1*), *mtor* (*mechanistic target of rapamycin*), *fbxo32* (*f-box protein 32*), *rpl13* (*ribosomal protein L13*), *ppiaa* (*peptidylprolyl isomerase Aa*) and *gapdh* (*glyceraldehyde-3-phosphate dehydrogenase*)

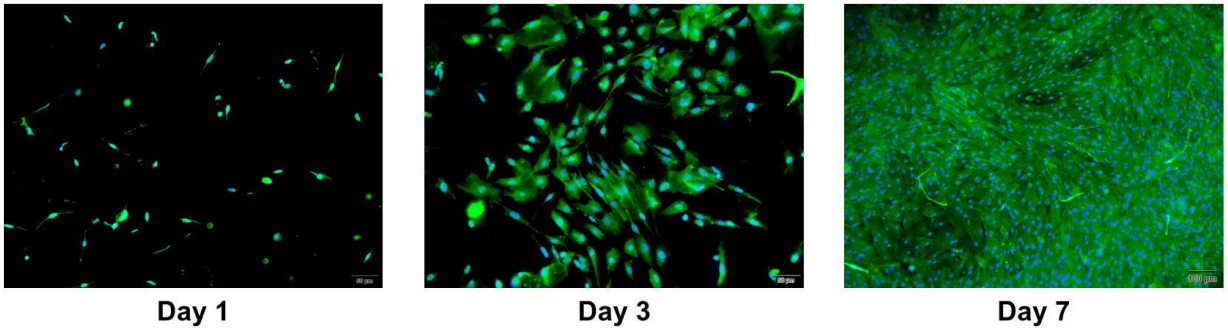

Supplementary Fig S1. Immunofluorescence of myoblast cell cultures established using fast-twitch skeletal muscle from juvenile pacus. The myogenic cells were identified by immunostaining for desmin (green) and the cells nuclei were counterstained with DAPI (blue) on days 1, 3 and 7 of cell culture. The images were obtained under a fluorescence microscope (days 1 and 3 - 20x magnification; Bars: 50 µm; day 7 - 10x magnification; Bar: 100 µm).

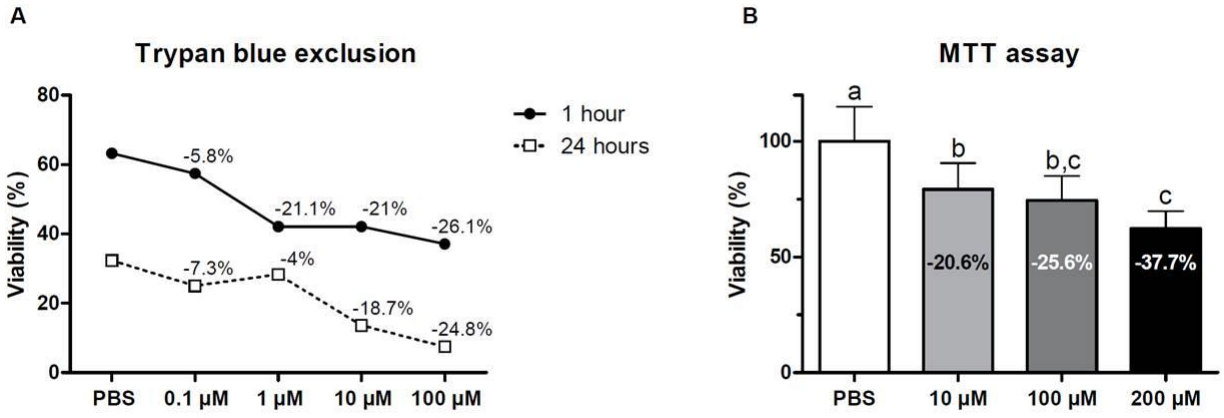

Supplementary Fig S2. The effect of menadione treatment on myoblast viability. (A) Trypan blue exclusion assay. Myoblasts were incubated with PBS or menadione at 0.1, 1, 10 and 100 µM for 1 and 24 hours. The stained (dead) and unstained (live) myoblasts were counted and cell

viability expressed as a percentage of the total number of cells. (B) MTT assay. Myoblasts were incubated with PBS or menadione at 10, 100 and 200 µM for 1 hour. The data are expressed as a percentage and presented as the mean ± SD of duplicates from four independent cell cultures. The different letters indicate significant differences among the groups ($p<0.05$ - One-way ANOVA test, followed by Tukey's multiple comparisons test).

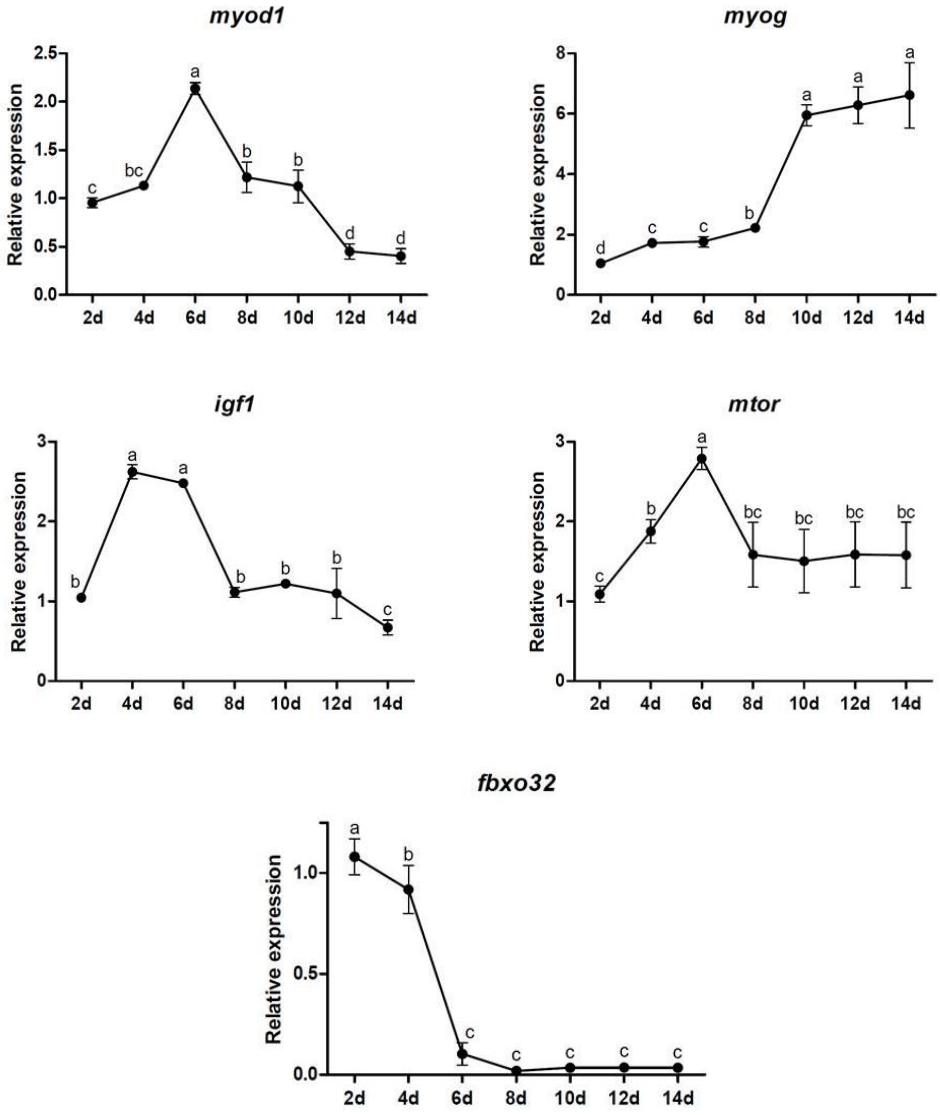

Supplementary Fig S3. Relative mRNA expression of *myod1*, *myog*, *igf1*, *mtor* and *fbxo32* through cell culture development. *myod1*, *myog*, *igf1*, *mtor* and *fbxo32* mRNA expression was assessed by qPCR in myoblast cell cultures on days 2, 4, 6, 8, 10, 12 and 14 of cell culture (d=days). The data are expressed as the fold change compared with 2d and presented as the mean ± SD of duplicates from three independent cell cultures. The different letters indicate significant differences among the groups ($p<0.05$ - One-way ANOVA test, followed by Tukey's multiple comparisons test).

7. CAPÍTULO II

Artigo em fase de revisão após submissão para a Scientific Reports (fator de impacto: 4.12).

O capítulo II se refere ao trabalho e experimentos desenvolvidos para o estabelecimento e padronização da cultura celular primária de mioblastos provenientes do músculo de contração lenta de trutas arco-íris, e também para a caracterização das famílias de microRNAs mir-133 e mir-499 utilizando este modelo *in vitro*.

Rainbow trout slow myoblast cell culture as a model to study slow skeletal muscle and the characterization of mir-133 and mir-499 families as a case study.

Bruno Oliveira da Silva Duran[1], Maeli Dal-Pai-Silva[1*], Daniel Garcia de la serrana[2,3]

[1]Department of Morphology, Institute of Biosciences, São Paulo State University (UNESP), Botucatu, São Paulo, Brazil.
[2]Scottish Oceans Institute, School of Biology, University of St Andrews, St. Andrews, Fife, Scotland, United Kingdom.
[3]Cell Biology, Physiology and Immunology Department, School of Biology, University of Barcelona, Barcelona, Spain.

* Corresponding author
E-mail: maeli@ibb.unesp.br

ABSTRACT

Skeletal muscle is the most abundant tissue in teleost fish, representing up to 60% of the total body mass for some species. Based on their contractile and metabolic properties, skeletal muscle fibres are broadly classified as fast (fast-twitch), slow (slow-twitch) and intermediate. The fish fast skeletal muscle myoblast cell culture *in vitro* model has proved to be a very useful tool to study muscle growth and development, but equivalent models for slow muscle have not been developed. Thanks to the compartmentalization of the two types of skeletal muscle in fish we were able to develop a slow skeletal muscle myoblast cell culture for rainbow trout

(*Oncorhynchus mykiss*) to study its development. Slow myoblast showed equivalent developmental stages than those described for fast myoblast, but with a higher expression of slow muscle markers such as *slow myosin heavy chain* (*smyhc*) and *peroxisome proliferator-activated receptor gamma coactivator 1-alpha* (*pgc-1α*) during differentiation. We also characterized the rainbow trout mir-133 and mir-499 microRNA families in slow and fast myoblasts as a case study to test the utility of the slow myoblast model during normal development and in response to electrical pulse stimulation (EPS) on slow muscle cell cultures. Rainbow trout mir-499 paralogues had a higher transcription in slow myoblast cell culture, whereas mir-133 copies had similar levels in both phenotypes. The slow myoblasts showed significant differences in expression for some of the mir-133 and mir-499 paralogues analysed after chronic stimulation at days 6 and 8 of development. We have successfully established a primary slow myoblast cell culture, which opens the doors to future comparative studies on muscle growth, development and metabolism in fish. We have also characterized the members of the mir-133 and mir-499 families in rainbow trout and their expression profiles during myogenesis, confirming the role of mir-499 on slow muscle phenotype determination and casting doubts about mir-133 role during differentiation. In addition, we have found signs of subfunctionalization of mir-499 paralogues in response to electrostimulation.

KEYWORDS

Slow skeletal muscle; Cell culture; Myoblasts; miRNA; Electrostimulation.

INTRODUCTION

Skeletal muscle is the most abundant tissue in teleost fish and represents up to 60% of total body mass in some species [1]. Skeletal muscle is key for fish underwater propulsion, represents the main protein reservoir and is the main product of the aquaculture industry [1,2].

Muscle fibre types are classified based on muscle fibre contractile and metabolic properties in fast, intermediate and slow [3]. Fast fibres comprise up to 80-90% of the skeletal muscle and are characterized by fast-twitch, predominant anaerobic metabolism, and low concentrations of myoglobin, mitochondria content, lipids and blood irrigation. The fast fibres are recruited during fast swimming activity, associated to food capture and escape behaviour [2]. Slow fibres comprise 5-20% of muscle mass and are superficially located along the fish body, with a thicker region on the lateral line. These fibres are characterized for having slow-twitch, predominant aerobic metabolism, and high levels of myoglobin, mitochondria content, lipids and

blood irrigation [2]. Despite their relative low abundance, the slow muscle plays a critical role in the fish biology, being the main tissue involved in sustained swimming and critical for middle and long-distance migratory fish. The intermediate fibres, in accordance to their name, have intermediate contractile and metabolic properties between fast and slow fibres and lie between these two compartments [2].

Postembryonic skeletal muscle growth occurs through the activation of myogenic precursor cells (MPCs), located between the basal lamina and the sarcolemma of the muscle fibres in a quiescent state (then known as satellite cells) [4–6]. Satellite cells re-enter the cell cycle in response to different stimuli, such as growth factors, hormones, cytokines, injury, exercise and nutrition, becoming activated myoblasts, which proliferate and fuse each other to form new fibres (hyperplasia) or to be incorporated by pre-existent fibres (hypertrophy) [7,8]. The establishment of the fish fast myoblast cell culture model has helped to characterize the molecular networks involved on the control of myogenesis and to better understand the regulation of muscle growth and development [8–10]. The *in vitro* model recapitulates the different stages of the myogenesis with initial quiescent cells, followed by proliferative myoblasts and final myotube formation stages [11,12]. The myoblast cell culture provides a controlled environment that facilitates the study of the molecular networks involved in muscle formation in response to specific inputs, such as growth factors and nutrition, without the background noise of the whole organism [8,10,13,14]. The compartmentalization of skeletal muscle in fish makes possible to isolate myoblast from fast and slow muscle. Similar studies in mammalian systems are very difficult due to the mosaic pattern of the muscle fibres, with fast and slow fibres mixed [15]. Until now, the myoblast cell culture had been only developed for fast skeletal myoblast, while a similar model for slow muscle remained to be established.

Teleost lineage has undergone a specific whole genome duplication (WGD) around 450-320 million years ago (Mya) [16]. As a result of this, several signalling pathways and molecular networks have some of their components expanded with multiple paralogue copies. It has been estimated that after the teleost specific WGD around 15-21% of the duplicated paralogues originated have been retained [17]. In addition to that, the salmonid lineage went through an additional WGD around 75 Mya and with an estimated 50% paralogues retained [18–20]. Several studies have shown that paralogue genes can be differently regulated at transcription level, what might be an indication of subfunctionalization (each paralogue acquires part of the original function of the ancestral gene) or neofunctionalization (paralogue acquires a different function from the ancestral gene) [10,17,21–23].

There is also evidence of microRNA (miRNA) families expanded after the teleost WGD [24]. The primary function of these type of small noncoding RNAs (ncRNA) is the post-transcriptional regulation of gene expression, promoted by translational inhibition and decay of target messenger RNAs (mRNAs) [25]. MiRNAs orchestrate the regulation of their targets to control signalling pathways and common biological functions [26,27]. Based on the high conservation observed in miRNAs among vertebrates, it can be anticipated that a considerable set of mRNAs are under the modulation by miRNAs in teleosts [28]. Some miRNAs such as mir-1, mir-133, mir-206 and mir-499 are specifically or highly expressed in cardiac and/or skeletal muscles, controlling myogenesis, myoblast proliferation, differentiation, fibre type specification and muscle regeneration [25,29,30]. Previous studies in *Piaractus mesopotamicus* showed that fast and slow muscles may have different miRNA expression pattern, as was the case of miR-499 that exhibited significant increase in slow muscle [14], suggesting its involvement in the specification and maintenance of slow-twitch phenotype as previously observed in mammals [30,31]. The innervation pattern has been suggested to be essential for the embryos' muscle fibre type specification; a tonic and low-frequency neural stimulation induces the slow phenotype, whereas a phasic and high-frequency neural stimulation promotes the fast phenotype [32,33]. In the past years, studies have shown that muscle fibre neural activation can be recreated by electrical pulse stimulation (EPS) of cultured skeletal muscle cells [34–36]. EPS models are useful to investigate adaptive responses of skeletal muscle cells to different patterns of contractile activity, for instance the study of molecular and cellular mechanisms during simulation of resistance training or endurance training [37–40].

In the present work we established a slow muscle myoblast cell culture from rainbow trout (*Oncorhynchus mykiss*) [11,41–43] and used it to characterize the mir-133 and mir-499 families during slow and fast myoblasts development and in response to EPS applied on slow muscle cell cultures.

MATERIAL AND METHODS

Ethics statement and animals

All experiments and procedures were approved by the Animal Welfare and Ethics Committee (AWEC) of the University of St Andrews, and were performed in accordance with relevant guidelines and regulations. Rainbow trout (*Oncorhynchus mykiss*) juveniles (10-15 g) were obtained from Frandy Farm (Gleneagles, Scotland) and transported to the Scottish Oceans Institute aquarium facilities (University of St Andrews). Animals were evenly distributed in

duplicated 200 L fibreglass tanks, maintained in a freshwater re-circulatory system at temperature between 12-15^{o}C and fed *ad libitum* daily with commercial diet. Animals were humanely killed by a blow in the head followed by the destruction of the brain with a scalpel according to Schedule 1 protocols as described in the Animals (Scientific Procedures) Act 1986 (Home Office Code of Practice. HMSO: London January 1997).

Myoblast cell culture

A total of 4 myoblasts cell cultures were performed as previously described [44]. Briefly, fast muscle samples were collected from the epaxial region and slow muscle samples were collected near the lateral line of the same animals (n=14-16 fish per culture until a total of 20g per tissue). Muscle was mechanically dissociated with scalpels and enzymatically digested with 0.2% collagenase type I (Sigma-Aldrich, USA) and 0.1% trypsin (Sigma-Aldrich, USA) until obtain two separate suspensions of fast and slow myoblasts. The cell suspensions were filtered through 40 and 100µm cell strainers (Thermo Fischer Scientific, USA) to remove debris. After several washes, cells were resuspended in DMEM media (Dulbecco's Modified Eagle's Medium, 9 mM $NaHCO_3$, 20 mM HEPES, pH 7.4 - Sigma-Aldrich, USA) with 10% fetal bovine serum and 1% antibiotics (Sigma-Aldrich, USA). After cell counting in a Neubauer chamber, cells were diluted to a final concentration of 2×10^6 cells/mL and seeded in poly-L-lysine and laminin pre-treated 6-wells plates. Slow and fast myoblasts were maintained at 18ºC for a total period of 12 days. Culture media was changed every day and the morphology of myoblasts was regularly monitored using a Leica DM IL Inverted Microscope coupled with the Leica DFC320 Digital Camera system (Leica, Germany). Total RNA was extracted from cells at days 2, 4, 6, 8, 10 and/or 12 for expression analysis.

Electrical pulse stimulation (EPS)

Electrostimulation was performed using a C-Pace EP Cell Culture Stimulator in conjunction with the C-Dish Electrode Assemblies (IonOptix, USA). Day 4 developed myoblasts were electrostimulated every day until day 11 following three different protocols: non-treated cells or control plate (CTR), acute treatment (A-EPS; 15 minutes, 10Hz, 30V for 10ms every 5th second) and chronic treatment (C-EPS; 2 hours, 1Hz, 30V for 2ms). The myoblasts were electrostimulated in serum-free DMEM media and remained 10 minutes in rest after application of both stimuli. Morphology was daily monitored to detect any difference in development and RNA extractions for days 6, 8 and 10 of cell culture were performed 2 hours after the EPS.

miRNA phylogenetic analysis

Initially, the precursor sequences of miRNAs mir-133, mir-499 and mir-206 (a miRNA highly expressed in muscle [25,45] were obtained from zebrafish (*Danio rerio*) genome using the Ensembl Genome Browser 89 (http://www.ensembl.org/index.html), used as query against the available rainbow trout genome (https://www.genoscope.cns.fr/trout/) [24] and initially named as *omy-mir-133*, *omy-mir-499* and *omy-mir-206*. Orthologues for mir-133 and mir-499 precursor sequences (pre-miRNA) were retrieved from different teleost species (*Astyanax mexicanus*, *Danio rerio*, *Gasterosteus aculeatus*, *Oreochromis niloticus*, *Oryzias latipes*, *Takifugu rubripes*, *Tetraodon nigroviridis*) and mammals (*Homo sapiens*, *Mus musculus*, *Pan troglodytes*, *Rattus norvegicus*) from the Ensembl database. In addition, orthologues pre-miRNA sequences of salmonids *Salmo salar* and *Oncorhynchus kisutch* were also obtained respectively from SalmoBase (https://salmobase.org/) [46] and NCBI (http://www.ncbi.nlm.nih.gov) when possible. The pre-miRNA sequences were aligned using MAFFT version 7 (http://mafft.cbrc.jp/alignment/server/), while MEGA7 software [47] was used to estimate the best evolutionary model. Bayesian phylogenetic trees were constructed using BEAST v1.7.4 software [48] with 10,000,000 seeds and summarize using TreeAnnotator v.1.7 with a Burning of 1000. The phylogenetic trees were visualized and edited using FigTree v.1.4.2 software (http://tree.bio.ed.ac.uk/software/figtree/).

RNA extraction and reverse transcription

Total RNA was extracted using TRIsure™ (Bioline Reagents, United Kingdom), according to the manufacturer's recommendations, and stored at -80°C for further analysis. Total RNA was quantified by spectrophotometry using a Nanodrop (ND1000) (Thermo Scientific, USA) while integrity was evaluated by 1% ethidium bromide agarose gel electrophoresis. All samples had 280/260nm and 230/260nm ratios above 1.8, indicating high quality RNA. A total of 224 ng of total RNA per sample were reverse transcribed using the miScript II RT Kit and QuantiTec Reverse Transcription Kit (Qiagen, Germany), following the manufacturer's guidelines. The resulting cDNA was used for quantitative PCR (qPCR).

Primer design

Primers for rainbow trout *slow myosin heavy chain* (*smyhc*), *fast myosin heavy chain* (*fmyhc*), *sry sex determining region Y-box 6* (*sox6*) , *six homeobox 1* (*six1*), *insulin-responsive glucose transporter type 4* (*glut4*), *late endosomal/lysosomal adaptor, mapk and mtor activator 3*

(*lamtor3*), *ras related GTP binding D* (*ragd*), *regulatory associated protein of mtor complex 1* (*rptor*), *muscle atrophy f-box protein* (*mafbx/fbxo32*), *peroxisome proliferator-activated receptor gamma coactivator 1 alpha (pgc-1α), creatine kinase, m-type a* (*ckma*), *creatine kinase, m-type b* (*ckmb*), *ribosomal protein L13* (*rpl13*), *ribosomal protein L19* (*rpl19*), paralogues of *omy-mir-133* (133a-1a, 133a-1b and 133a-2) and *omy-mir-499* (499aa, 499ab, 499ba, 499bb), *omy-mir-206-1* and *U6 snRNA* (*U6 small nuclear RNA*) were designed using Primer3 v.0.4.0 [49,50] (Supplementary Table S1). The precursor sequences from each rainbow trout miRNA were used to design the forward and reverse primers in regions with low similarity in order to distinguish expression between copies (primers for *omy-mir-499aa* amplified both 499aa and 499ab copies, resulting in a global *omy-mir-499a* expression (aa+ab)). All primers were designed to amplify 50-200 bp products with annealing temperature of 60ºC. Any possible hairpin or self-dimer structures formed by the primer pairs were estimated using NetPrimer software (Premier Biosoft, USA).

Quantitative real time PCR (qPCR)

All qPCR performed were compliant with the Minimum Information for Publication of Quantitative Real Time PCR experiments (MIQE) guidelines [51]. Each qPCR reaction contained 6 µL of diluted cDNA (1:40), 7.5 µL of SensiFAST™ SYBR® master mix (Bioline Reagents, United Kingdom) and 1.5 µL of 500 nM forward/reverse primer mix. The reactions were performed in duplicates under the following conditions: 95ºC during 2 minutes, 40 cycles of denaturation at 95ºC during 5 seconds and annealing/extension at 65ºC during 20 seconds in a Stratagene MX3005P Real Time PCR Machine (Stratagene, USA). The specificity of each primer set was confirmed by the presence of a single-peak dissociation curve. Relative expression of each gene was estimated using the $2^{-\Delta\Delta Ct}$ method [52]. Different housekeeping candidates were tested (*rpl13*, *rpl19*, *omy-mir-206-1* and *U6 snRNA*) and NormFinder software [53] was used to identify the optimal normalization genes according to their expression stability among all samples. The most suitable and stable genes for normalization were *rpl13*, used for mRNA expression, and *omy-mir-206-1*, used for miRNA expression.

Statistical analysis

Statistical analyses were performed using RStudio v1.0.136 [54] and statistical significance was set at 5% ($p<0.05$). Expression data was analysed using the two-way ANOVA test followed by post hoc Tukey's honestly significant difference (HSD) test, with tissue of origin (*tissue*) and

day of development (*development*) as factors for the analyses. In addition, miRNA expression data from slow and fast myoblasts comparison were analysed using the unpaired t-test with *tissue* as factor, and miRNA expression data from EPS treatments were analysed using the one-way ANOVA test followed by post hoc Dunn's test, with *treatment* as factor for the analysis. Pearson's correlation was used to access interesting relationships between evaluated genes. All graphs were constructed using ggplot2 R package [55].

RESULTS

Myoblast cell culture

Fish myoblast cell culture protocols commonly use small juveniles in order to maximize the number of myoblast extracted per gram of muscle sampled [10,56–58]. However, it is difficult to extract slow muscle without having significant cross-contamination from fast muscle in juvenile animals. As fish grows, it is easier to discriminate and obtain slow muscle minimizing contamination from fast muscle, however the older the animal the less myoblasts it yields per gram of fast muscle. We found that rainbow trout around 15 g yield enough fast and slow myoblasts from individual animals to perform the experiment reported in the present study (Fig 1A).

Slow muscle needed a harder mechanical dissociation compared to fast muscle in order to have small enough fragments to facilitate enzymatic digestion. In addition, while fast muscle sectioning turned DMEM media orange, no similar change was observed in slow muscle. That was a reflect of their essential metabolic differences, with acid lactic from fast skeletal muscle turning phenol red to orange, an early indication of successful extraction of fast and slow muscle. After mechanical sectioning a top thick layer of lipids appear in the slow muscle extraction tubes that, if not removed, persist in the following steps affecting extraction efficiency (Fig 1B). It is interesting to highlight that slow skeletal muscle consistently yielded more myoblasts per gram of tissue than fast skeletal muscle (data not show), suggesting a higher satellite cell density.

Slow and fast myoblasts cell culture had a very similar development, with an initial stage of round mononucleated cells at days 1 and 2, an active proliferative phase between days 3-7 and distinctive myotubes between days 8-12 (Fig 1C).

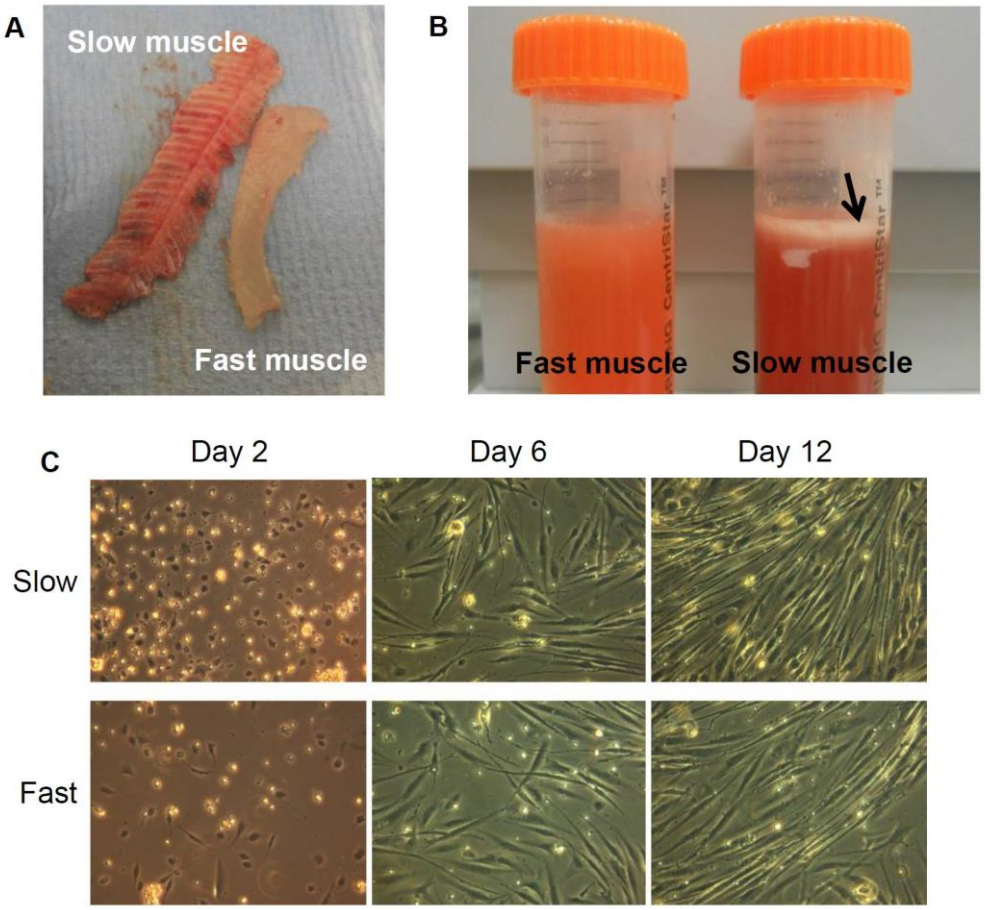

Fig 1. Rainbow trout fast and slow myoblast cell culture establishment. (A) Slow muscle strips were carefully extracted from the surroundings of the lateral line and any remain of fast muscle was removed to avoid cross-contamination. Fast muscle samples were collected from the epaxial region after slow muscle removal. (B) Fast muscle extraction tube showing the DMEM media slightly orange due to pH reduction by lactic acid, and slow muscle extraction tube with a top layer of lipids (black arrow). (C) Rainbow trout fast and slow myoblasts at days 2, 6 and 12 of development (20x magnification).

Characterizaton of slow muscle-derived myoblast cell culture

In order to confirm the phenotype of the slow-derived myoblast cultures, the expression of skeletal muscle gene markers such as *smyhc*, *fmyhc*, *six1* and *sox6* was analysed at days 2, 4, 6, 8, 10 and 12 of culture (Fig 2).

Expression of *fmyhc* and *smhyc* was significantly different between cell cultures and day of development (*tissue* P=0.00 and *development* P=0.00) confirming the slow and fast phenotype (Fig 2A-B). The *fmyhc* was 2.5-fold higher in fast-myoblast than slow-myoblast between days 8

and 12 (Fig 2B) while *smyhc* showed a >12-fold increase in slow-myoblasts compared to fast-myoblasts between days 8 to 12 (Fig 2A), concomitant with the myotube formation (Fig 1C).

The *six1* and *sox6* transcription factors expression levels were higher in fast than slow myoblast cell culture (*tissue* P=0.00 for both *six1* and *sox6*) (Fig 2C-D). Both transcription factors changed their relative expression during cell development of the culture with maximal expression found between days 6 to 10 (*development* P=0.00 for both genes) (Fig 2C-D).

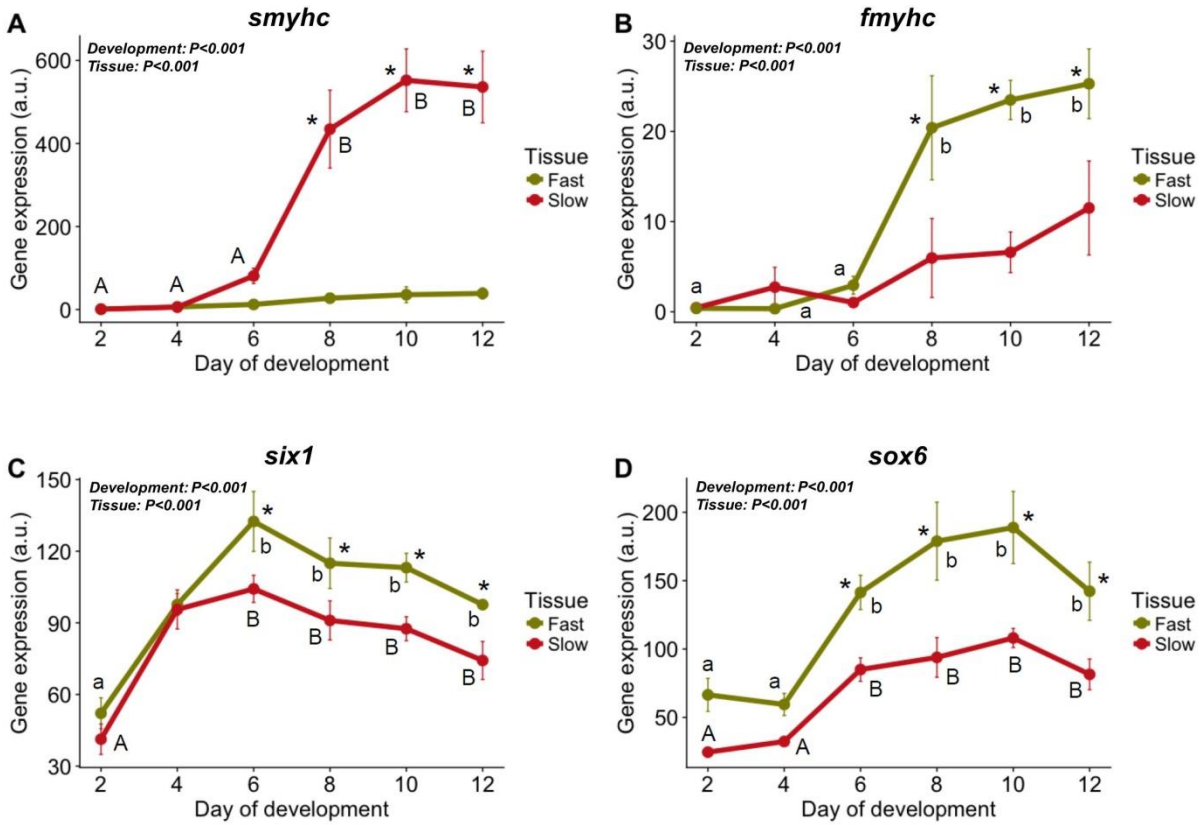

Fig 2. Rainbow trout fast and slow myoblast cell culture characterization. Gene expression in slow and fast myoblast cell culture at days 2, 4, 6, 8, 10 and 12 of development for *slow myosin heavy chain* (*slow myhc*) (A), *fast myosin heavy chain* (*fast myhc*) (B), *six homeobox 1* (*six1*) (C) and *SRY (sex determining region Y) box 6* (*sox6*) (D). Values represent mean ± SE (n=4 independent cell cultures; a.u.= arbitrary units). Significant differences by the tissue of origin (*tissue*) and the day of development (*development*) are shown in the left corner of each graph. Asterisks indicate significant differences between means of slow myoblasts and fast myoblasts cell cultures, and different letters (upper case for slow and lower case for fast) indicate significant differences between means of days of development (P<0.05).

In order to understand the fundamental differences at metabolic level between the two tissues, we determine the expression of genes related to protein synthesis and degradation (*lamtor3*, *ragd*, *rptor* and *mafbx*), glucose uptake (*glut4*) and markers of energy metabolism (*pgc1α*, *ckma* and *ckmb*) during cell culture development (Fig 3).

Despite not being significant, *glut4*, *lamtor3* and *ragd* (*tissue* P=0.58, P=0.22 and P=0.63 respectively) (Fig 3A-C) expression levels were slightly higher in slow than fast myoblasts and decreased between days 8 to 12 in slow myoblasts (*development* P=0.007 for *glut4* and P=0.02 for *ragd*) (Fig 3A and C). Both *rptor* and *mafbx* showed similar transcription profile between slow and fast muscle cells (*tissue* P=0.53 for *rptor* and P=0.05 for *mafbx*) (Fig 3D-E). The *mafbx* expression decreased suddenly after day 2 (*development* P=0.00) and remained low during the rest of the cell culture (Fig 3E). In contrast, *pgc1α* expression did not show statistical differences with the progress of cell cultures (*development* P=0.59), but it was considerably higher in slow-myoblasts compared to fast muscle cell culture (*tissue* P=0.00) (Fig 3F). The expression pattern of *ckma* and *ckmb* paralogues were very similar between slow and fast muscle cells (*tissue* P=0.28 for *ckma* and P=0.36 for *ckmb*), with maximal expression during myotube formation (days 8 to 12) (*development* P=0.00 for both genes) (Fig 3G-H).

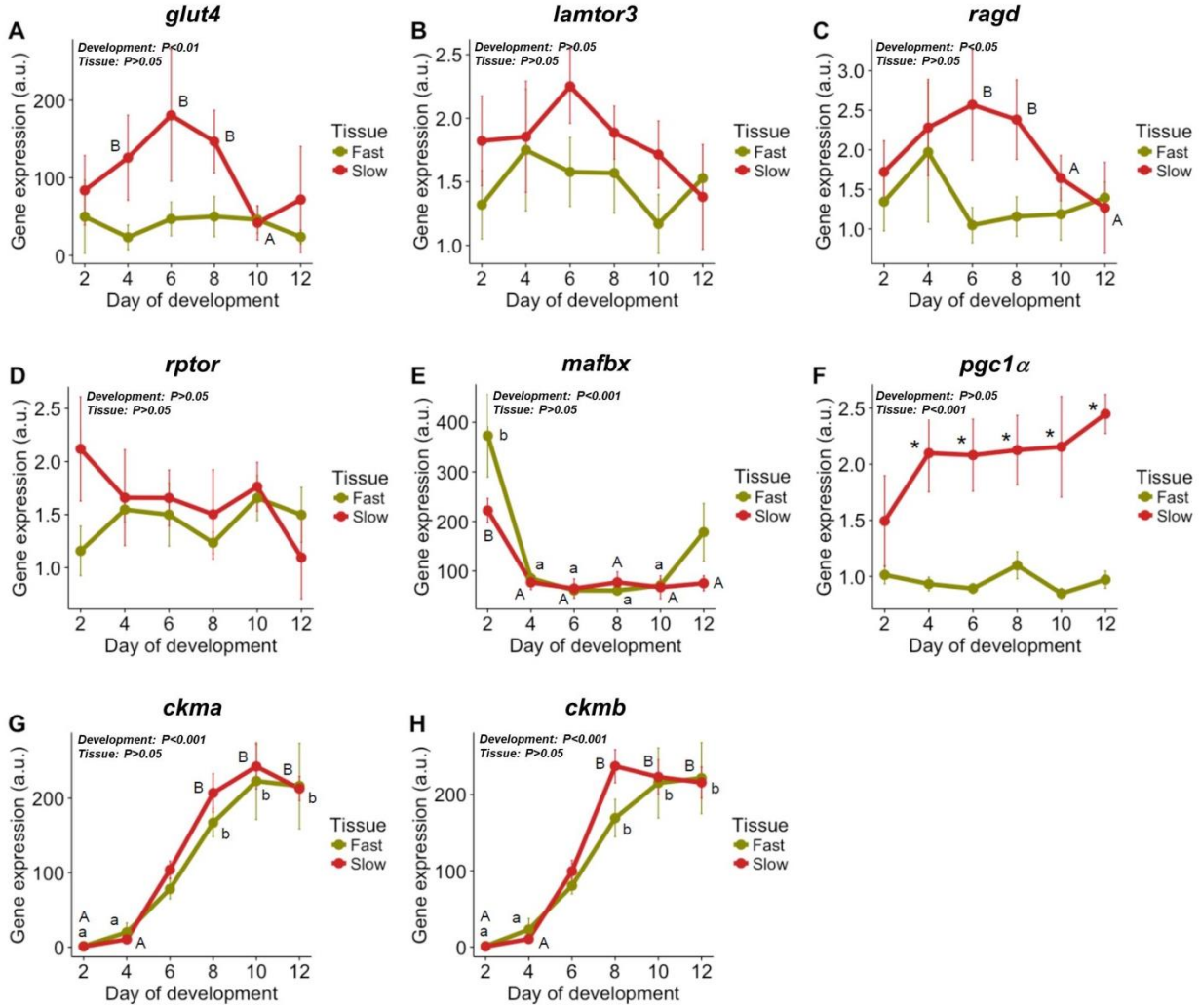

Fig 3. Muscle regulatory signalling components in rainbow trout fast and slow myoblast cell culture. Gene expression in slow and fast myoblast cell culture at days 2, 4, 6, 8, 10 and 12 of development for *insulin-responsive glucose transporter type 4* (*glut4*) (A), *late endosomal/lysosomal adaptor, mapk and mtor activator 3* (*lamtor3*) (B), *ras related GTP binding D* (*ragd*) (C), *regulatory associated protein of mtor complex 1* (*rptor*) (D), *muscle atrophy f-box protein* (*mafbx*) (E), *peroxisome proliferator-activated receptor gamma coactivator 1 alpha* (*pgc1α*) (F), *creatine kinase, m-type a* (*ckma*) (G) and *creatine kinase, m-type b* (*ckmb*) (H). Values represent mean ± SE (n=4 independent cell cultures; a.u.= arbitrary units). Significant differences by the tissue of origin (*tissue*) and the day of development (*development*) are shown in the left corner of each graph. Asterisks indicate significant differences between means of slow myoblasts and fast myoblasts cell cultures, and different letters (upper case for slow and lower case for fast) indicate significant differences between means of days of development (P<0.05).

miRNA identification

Several potential paralogues from the mir-133 and mir-499 families were identified from salmonid genomes. We used phylogenetic analysis to establish their evolutionary relationship and name them accordingly based on the existent zebrafish and salmonid nomenclature.

Phylogenetic analysis confirmed the existence of three copies of mir-133 (Fig 4) and four of mir-499 (Fig 5) in rainbow trout. According to their position relative to zebrafish and Atlantic salmon orthologues, rainbow trout paralogues were named as *omy-mir-133a-1a*, *omy-mir-133a-1b*, *omy-mir-133a-2*, *omy-mir-499aa*, *omy-mir-499ab*, *omy-mir-499ba* and *omy-mir-499bb* (Fig 4 and 5; Supplementary Table S2). The identity of the sequences was over 92% in all cases, with striking 97% for *omy-mir-133a-1a* vs *omy-mir-133a-1b* and *omy-mir-499ba* vs *omy-mir-499bb* (Supplementary Table S3). However, due to a high degree of similarity (Supplementary Fig S1), the primers designed for *omy-mir-499aa* also amplified the *omy-mir-499ab* copy (the expression of both was named *omy-mir-499aa+ab*). We also constructed Bayesian phylogenetic tree for the muscle-specific miRNA mir-206 (Supplementary Fig S2).

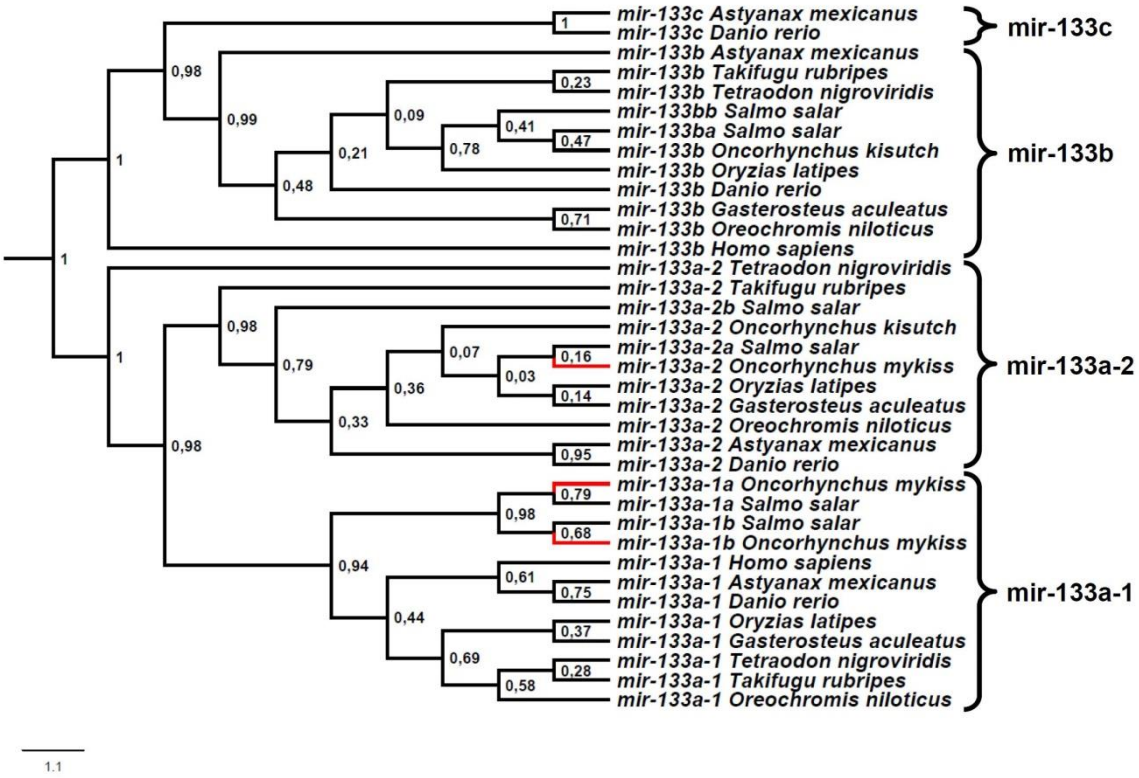

Fig 4. Teleost fish mir-133 phylogenetic analysis. Phylogenetic reconstruction of the mir-133 family using Bayesian methods. The tree was constructed from a highly confidence alignment of 36 nucleotide sequences and used Hasegawa-Kishino-Yano with Gamma distribution (HKY+G)

as best fitted substitution model. Bootstrap-posterior are indicated on the node of each branch. Branches in red indicate the mir-133 copies identified for rainbow trout.

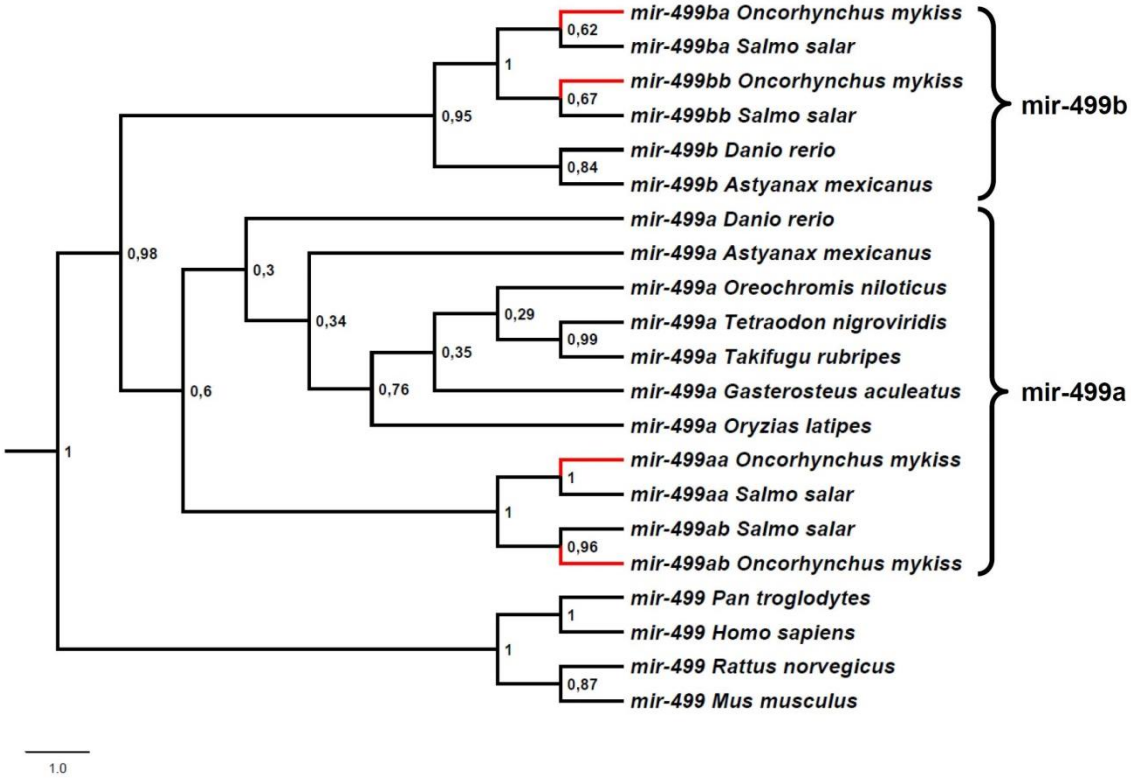

Fig 5. Teleost fish mir-499 phylogenetic analysis. Phylogenetic reconstruction of the mir-499 family using Bayesian methods. The tree was constructed from a highly confidence alignment of 21 nucleotide sequences and used Hasegawa-Kishino-Yano with Gamma distribution (HKY+G) as best fitted substitution model. Bootstrap-posterior values are indicated on the node of each branch. Branches in red indicate the mir-499 copies identified for rainbow trout.

miRNA expression during fast and slow myoblast culture development

Expression of mir-133 and mir-499 paralogues was estimated in slow and fast-derived myoblast cell cultures at days 6, 8 and 10 of development (Fig 6).

No significant differences in expression were found for any of the *omy-mir-133* paralogues between slow and fast myoblasts cell cultures, with stable levels of transcription for all copies during culture development (Fig 6A-C).

Some of the rainbow trout mir-499 paralogues showed significant differences in expression between slow/fast cultures. At day 8, global *omy-mir-499a* expression (*aa*+*ab*) in fast myoblasts was 0.5-fold lower compared to slow myoblasts (*tissue* P=0.01), and expression levels

of *omy-mir-499ab* in fast myoblasts was 0.6-fold lower between days 6 to 8 (*tissue* P=0.01) compared to fast derived myoblasts (Fig 6D-E). The expression of *omy-mir-499ba* were not statistically different between slow and fast myoblasts, whereas *omy-mir-499bb* expression was 0.5-fold lower in fast myoblasts at day 6 (*tissue* P=0.01) (Fig 6F-G). Expression levels of omy-mir-499 copies did not show statistical differences with the progress of cell cultures (*development* P=0.62 for *omy-mir-499aa+ab*, P=0.88 for *omy-mir-499ab*, P=0.86 for *omy-mir-499ba* and P=0.94 for *omy-mir-499bb*) (Fig 6D-G).

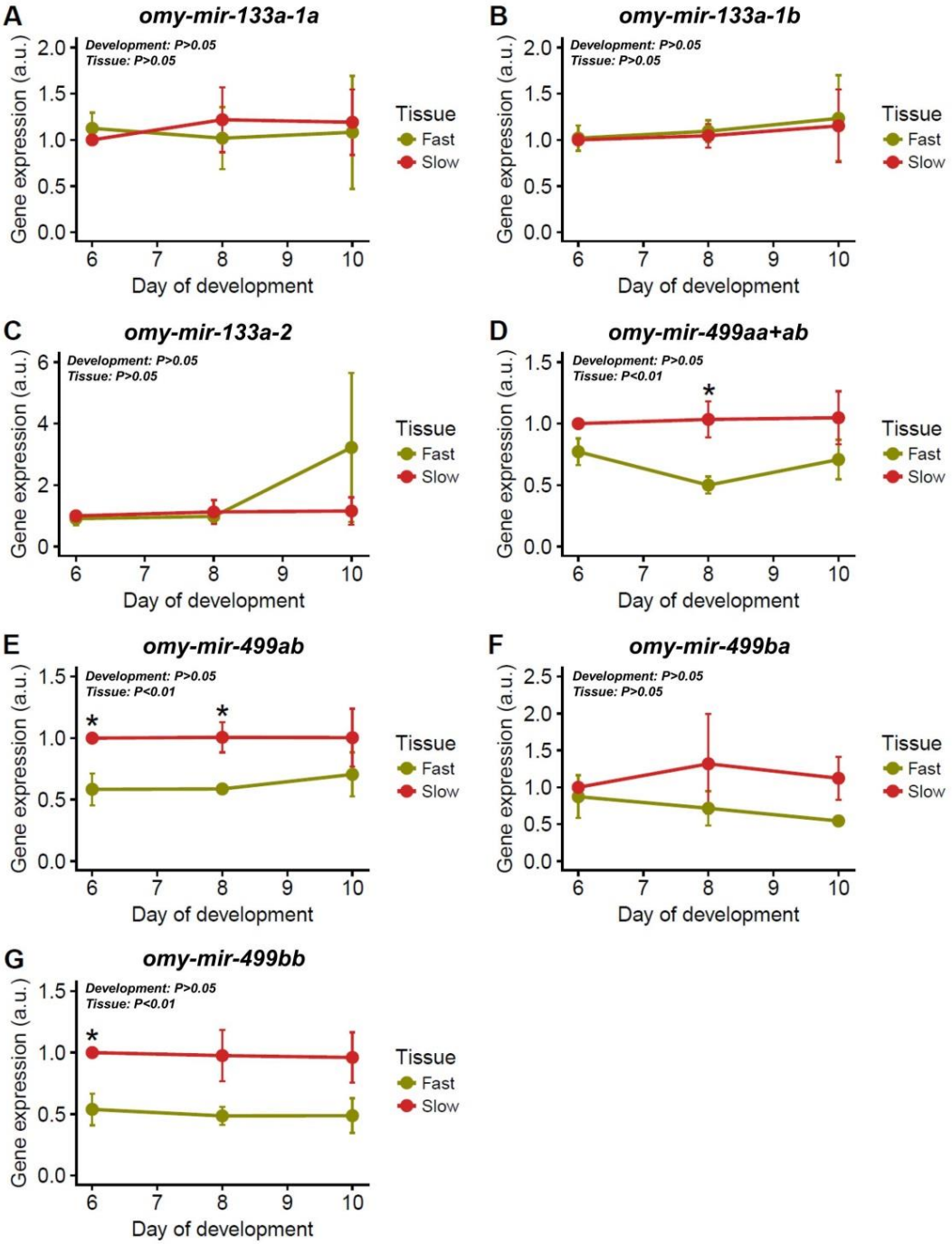

Fig 6. miR-133 and miR-499 paralogue expression in rainbow trout fast and slow myoblast cell culture. Gene expression in slow and fast myoblast cell culture at days 6, 8 and 10 of development for *omy-mir-133a-1a* (A), *omy-mir-133a-1b* (B), *omy-mir-133a-2* (C), *omy-mir-499aa+ab* (D), *omy-mir-499ab* (E), *omy-mir-499ba* (F) and *omy-mir-499bb* (G). Values represent mean ± SE (n=4 independent cell cultures; a.u.= arbitrary units). Significant differences by the tissue of origin (*tissue*) and the day of development (*development*) are shown in the left corner of each graph. Asterisks indicate significant differences between means of slow myoblasts and fast myoblasts cell cultures ($P<0.05$).

In addition to slow and fast cell culture comparison, we also investigated expression of rainbow trout *omy-mir-133* and *omy-mir-499* paralogues in response to EPS applied on slow muscle cell cultures (Fig 7).

All *omy-mir-133* showed minor changes in expression in response to EPS treatments. *Omy-mir-133a-2* abundance increased by 2-fold at day 6 of chronic stimulation (C-EPS group) (*treatment* P=0.04). However, we did not find significant differences on *omy-mir-133a-1a* and *omy-mir-133a-1b* expression in response to EPS protocols due to a high degree of variability between cell cultures (*treatment* P=0.85 for *omy-mir-133a-1a* and P=0.48 for *omy-mir-133a-1b*) (Fig 7A-C).

Expression of *omy-mir-499ab* in C-EPS myoblasts was 0.5-fold lower compared to CTR group at day 6 (*treatment* P=0.02), whereas no significant differences were observed in *omy-mir-499aa+ab* expression between groups (*treatment* P=0.42) (Fig 7D-E). Expression levels of *omy-mir-499ba* in C-EPS myoblasts was 7-fold higher at day 6 (*treatment* P=0.00) and 4-fold higher at day 8 (*treatment* P=0.03) compared to CTR group (Fig 7F). The chronic stimulation also increased expression of *omy-mir-499bb* paralogue, by 2.5-fold at day 6 (*treatment* P=0.00) and by 2-fold at day 8 (*treatment* P=0.02) compared to CTR group. Besides, *omy-mir-499bb* expression at day 6 was 2.3-fold higher in acute-stimulated myoblasts (A-EPS group) compared to CTR group (*treatment* P=0.01) (Fig 7G).

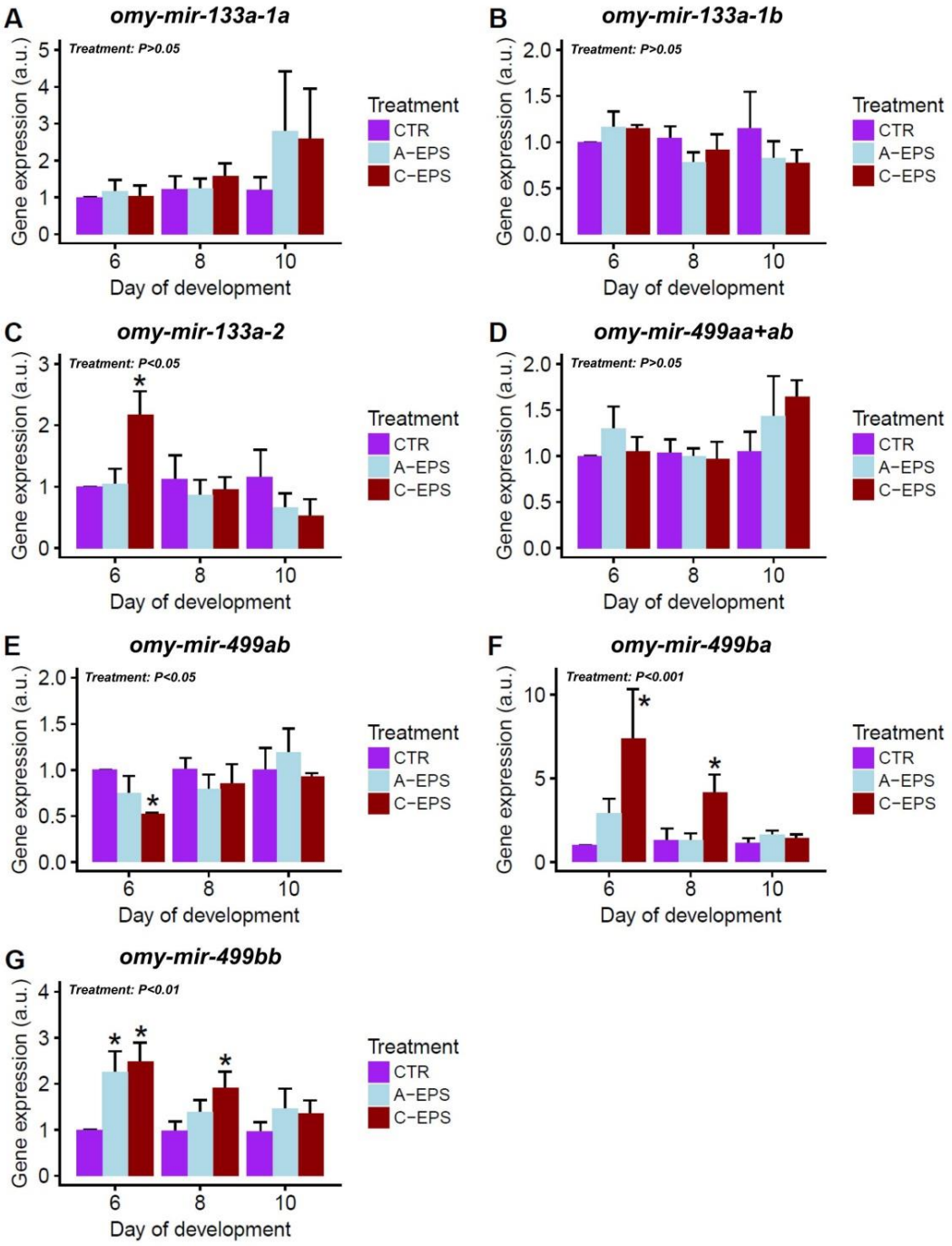

Fig 7. miR-133 and miR-499 paralogue expression in rainbow trout slow myoblast cell culture treated with electrical pulse stimulation (EPS). Gene expression in slow myoblast cell culture at days 6, 8 and 10 of development for *omy-mir-133a-1a* (A), *omy-mir-133a-1b* (B), *omy-mir-133a-2* (C), *omy-mir-499aa+ab* (D), *omy-mir-499ab* (E), *omy-mir-499ba* (F) and *omy-mir-499bb* (G). The treatments are as follow: non-treated myoblasts (CTR, purple bar); myoblasts submitted to acute and high-frequency stimulation (A-EPS, blue bar); and myoblasts submitted to chronic and low-frequency stimulation (C-EPS, red bar). Values represent mean ±

SE (n=4 independent cell cultures; a.u.= arbitrary units). Significant differences by the EPS treatment (*treatment*) are shown in the left corner of each graph. Asterisks indicate significant differences between means of EPS treatments compared to CTR (P<0.05).

To complement our results and provide further insight of miRNA paralogue roles, we performed Pearson's correlation analyses between expression of *omy-mir-133*, *omy-mir-499*, *smyhc*, *fmyhc* and *sox6*, with some noteworthy results, especially the negative correlation between *omy-mir-499* paralogues and *sox6* (Supplementary Fig S3).

DISCUSSION

In the present study we established a viable slow muscle derived myoblast cell culture. In addition to harder mechanical dissociation of slow muscle, other aspects have to be taken in consideration when developing the slow myoblast cell culture: 1) even after enzymatic digestion the slow muscle fragments are much firmer than fast muscle and very easy to lose during washes; 2) after enzymatic digestion slow muscle is specially rich in tissue debris compared to fast muscle, what can make cell counting very difficult if the cells are not very well washed and carefully filtered through a 40 µm and 100 µm cell strainers and 3) for an equivalent amount of tissue the number of myoblasts obtained from slow skeletal muscle is higher than fast skeletal muscle (43% based on Neubauer chamber counting, data not show), therefore, unless the used protocol require samples from the same animals, we recommend to use smaller animals to extract fast myoblast and bigger animals for slow myoblast extraction in order to have enough cells to test all the conditions needed. The difference in the number of myoblasts extracted from slow and fast skeletal muscle is in agreement with previous studies that observed a higher proportion of satellite cells in slow fibres [59]. Slow myoblasts have equivalent development stages compared to fast muscle myoblasts: initial phase of round mononucleated cells that progressively become elongated to finally fuse into myotubes with no morphologically differences between them (Fig 1) [21,57,60].

Despite the morphological similarities between the slow and fast extracted myoblasts they were different at molecular level depending of their tissue of origin, as demonstrated by the expression of *six1*, *sox6* and *smyhc*. Six1 and Sox6 are transcription factors related to the determination of the muscle phenotype. Sox6 repress slow fibres formation [61], while Six1 is required for the determination of the fast fibres [62]. Our results show that *six1* and *sox6* expression from day 4 was significantly lower in slow muscle myoblasts, indicating that slow fibre program

was not repressed (Fig 2). Accordingly, slow derived myoblast had a much higher expression of *slow-twich myosin heavy chains* (*smyhc*), while fast derived myoblast had a higher expression of *fast-twich myosin heavy chain* (*fmyhc*) (Fig 2). Besides confirm the myogenic nature of the cells extracted, the increase of myosin heavy chain expression also confirmed the differentiation into myotubes during the cell culture progression [21]. Our results suggest that myoblasts from slow and fast muscle trend to differentiate to the fibre type of the tissue they were extracted from. This seems in agreement with previous studies on birds where myoblasts extracted from pectoralis major (PM) and anterior latissimus dorsi (ALD) formed myotubes in similar proportions of fast and slow phenotypes as found in the muscle of origin [63].

Surprisingly, slow muscle cell culture showed a higher *fmyhc* expression than expected (Fig 2), which could indicate that slow myoblasts might assumed an intermediate phenotype when cultured, what raises questions about the possibility of some degree of phenotypic plasticity in response to signals such as exercise and/or electrostimulation. However, phenotypic differences between culture systems are maintained, since fast muscle cells had very low levels of *smyhc* expression (Fig 2). Fish myoblasts phenotype plasticity is a field that needs a more detailed research in future studies.

We analysed the expression of genes involved on different metabolic processes in order to get a preliminary idea of the metabolic differences or similarities between slow and fast derived myoblasts. Several of the genes analysed had higher expression in slow muscle cells (*glut4*, *lamtor3*, *ragd* and *pgc1α*), despite only *pgc1α* showed statistical differences (Fig 3). This increased *pgc1α* expression in slow cell cultures is consistent with their phenotype. Pgc1α acts as co-factor of mitochondrial biogenesis, crucial for the oxidative metabolism characteristic of slow muscle [64]. Moreover, slow fibres are significantly more insulin-responsive than fast fibres, due to higher levels of Glut4 protein [65], in agreement with the relatively higher *glut4* transcription on slow muscle cells found in our study. Myoblast proliferation and differentiation into myotubes are regulated by nutritional and endocrine stimuli, especially Igf signalling pathway and amino acids [12,42], necessary to increase synthesis of proteins. Early studies showed that amino acids stimulates protein synthesis by themselves [13,42] suggesting at the same time that Igf stimulates protein synthesis only if amino acids are also present in the media [9,10]. Recently, the Lamtor/Rrag GTPases complex has been identified to act as amino acid sensor and promote Mtor activation, representing an important mechanism through amino acids stimulate protein synthesis by themselves [66,67]. Despite the similar expression pattern of *rptor* throughout cell cultures development, *lamtor3* and *ragd* had higher transcription at day 6 for slow myoblasts and day 4

for fast myoblasts (Fig 3), showing the contribution of Lamtor/Rrag GTPases complex to protein synthesis at the early steps of myogenesis. These data are supported by the low *mafbx* expression on most days of cell culture, in both tissues (Fig 3), which is an E3 ubiquitin ligase that regulates protein degradation and loss of components in skeletal muscle [68]. Also, both slow and fast cell cultures had *ckma* and *ckmb* paralogues expression higher at days 8-12 (Fig 3), what agrees with the role of Ckm on transferring phosphate between phosphocreatine and ATP, replenishing local ATP to myotubes [69].

We also used the slow and fast muscle cell cultures to investigate the effect of WGD on mir-133 and mir-499 families and characterize them during differentiation and in response to electrostimulation. The miRNA mature sequence is highly conserved among orthologues from different vertebrate species and identical between paralogues of the same family [28], but the precursor sequence, including both pri- and pre-miRNA, has some distinct nucleotides that allow to design specific primers to distinguish between orthologues and paralogues. Phylogenetic analysis confirmed the identity of the sequences found for mir-133 and mir-499 in rainbow trout, which were named accordingly to their phylogenetic relationships. We identified three rainbow trout paralogues for mir-133 (*omy-mir-133a-1a*, *omy-mir-133a-1b* and *omy-mir-133a-2*) (Fig 4) and four paralogue copies for mir-499 (*omy-mir-499aa*, *omy-mir-499ab*, *omy-mir-499ba* and *omy-mir-499bb*) (Fig 5). It is also interesting to notice that rainbow trout seems to lack *mir-133b* and *-133c*, indicating a species specific lost.

The *omy-mir-133* paralogues had similar levels of expression between fast and slow myoblast cell cultures with very little variation during the culture development (Fig 6). The mir-133 has been described to be involve in muscle development, preventing myoblast differentiation and enhancing myoblast proliferation [29,70] what seem to be in disagreement with the lack of significant differences on mir-133 expression during cell culture development. It might be possible that mir-133 might have a different role in fish than suggested in mammals, however, due to the miRNA expression analysis was limited from day 6 of development forward while early days were not studied, this hypothesis would need further confirmation on early stages. Similarly, electrostimulation only modified *omy-mir-133a-2* expression, which increased in response to chronic stimulation at day 6, while *omy-mir-133a-1a* and *omy-mir-133a-1b* remained stable (Fig 7). It is possible that EPS treatments could promote more dramatic changes before the evaluated days of cell culture, due to the less established myoblast phenotype before the day 4, as shown by the absence of differences in *six1* and *sox6* levels between fast and slow myoblasts during this period (Fig 2). However, myoblasts at these initial days were more vulnerable to

electrostimulation and did not yield enough RNA for the analyses, requiring further research in future studies. The Pearson's correlation results revealed positive relationships between *omy-mir-133a-1b* and *omy-mir-133a-2*, confirming the close association of these molecules in terms of gene expression suggesting co-regulatory mechanisms. Interestingly, *omy-mir-133a-1b* paralogue correlated positively with *fmyhc* and *sox6* (Supplementary Fig S3). Li et al. (2010) [71] showed that treatment with miR-133a promoted decreased mRNA and protein expression of NFATc4 in C2C12 cells. The NFAT family of transcription factors has been shown to be involved with the regulation of fibre type specification, inducing a slow gene program and inhibiting a fast program once dephosphorylated by calcineurin [72,73]. It is possible that *omy-mir-133a-1b* might regulate *fmyhc* and *sox6* expression through a similar mechanism, but more studies are needed to further explore this hypothesis.

In zebrafish [74], Nile tilapia [75] and pacu [14], miR-499 mediates the translational repression of *sox6*, which is involved in the maintenance of the fast-twitch phenotype in muscle fibres through repression of slow-twitch-specific genes, such as *slow myosin heavy chain 1* and *slow-specific troponin c* [76]. Our results show a negative correlation between several *omy-mir-499* paralogues and *sox6*, suggesting that a similar mechanism might be in place in slow myoblasts cell culture. These data are corroborated by the positive correlation between *omy-mir-499ab* and *slow myhc*, and the negative correlation observed between *omy-mir-499bb* and *fast myhc*. In addition, positive relationships were observed between mir-499 copies (*omy-mir-499aa+ab* vs *omy-mir-499ab*; *omy-mir-499aa+ab* vs *omy-mir-499bb*; *omy-mir-499ab* vs *omy-mir-499bb*; *omy-mir-499ba* vs *omy-mir-499bb*), also suggesting mechanisms of co-regulation and possibly subfunctionalization (Supplementary Fig S3).

The *omy-mir-499* paralogues appeared to have a more complex behaviour than mir-133 components with a general trend to have higher expression in slow myoblasts (Fig 6), that is in agreement with research in mammals suggesting that miR-499 promotes slow fibre type phenotype [30]. In EPS experiment, *mir-499a* copies (*omy-mir-499aa* and *omy-mir-499ab*) showed few significant differences after treatments, but both *mir-499b* copies (*omy-mir-499ba* and *omy-mir-499bb*) had higher expression levels in C-EPS group at days 6 and 8 compared to CTR group (Fig 7). These results show that *mir-499b* copies could be more susceptible to stimuli that might modify fibre phenotype, and could have more active role in fibre type specification. However, considering the decreased expression of *omy-mir-499ab* at day 6 and a tendency of increased expression of *omy-mir-499aa+ab* at day 10 in C-EPS myoblasts (Fig 7), another possibility could be that *omy-mir-499b* paralogues have an early role in slow phenotype

determination, at days 6 and 8, while *omy-mir-499a* copies may act in the late stage of myotube formation, at days 10 to 12. Given the increased expression of *mir-499b* copies in C-EPS group, we believe that our chronic and slow-frequency stimulation protocol enhanced the slow phenotype in cell culture and could be used in skeletal muscle fibre type studies.

CONCLUSIONS

We have successfully established a slow myoblast cell culture. The extraction of slow myoblasts opens the doors to future comparative studies between slow and fast muscle development, regulation and to study the physiology of the slow muscle. We have also characterized the members of the mir-133 and mir-499 family in rainbow trout and their expression profiles during myogenesis, confirming the role of mir-499 on slow muscle phenotype determination and casting doubts about mir-133 role during differentiation. In addition, we have found signs of subfunctionalization of mir-499 paralogues in response to electrostimulation.

DATA AVAILABILITY STATEMENT

All data generated during this study are included in this published article. The datasets analysed during the current study are available in the Ensembl Genome Browser 89 (http://www.ensembl.org/index.html), rainbow trout genome (https://www.genoscope.cns.fr/trout/) [24], SalmoBase (https://salmobase.org/) [46] and NCBI (http://www.ncbi.nlm.nih.gov).

REFERENCES

1. Johnston, I. A. Genetic and Environmental Determinants of Muscle Growth Patterns in *Muscle development and growth* (ed. Johnston, I. A.) **18,** 141–186 (2001).
2. Sänger, A. M. & Stoiber, W. Muscle fiber diversity and plasticity in *Muscle development and growth* (ed. Johnston, I. A.) **18,** 187–250 (Academic Press, 2001).
3. Johnston, I. A. *et al.* Rapid evolution of muscle fibre number in post-glacial populations of Arctic charr Salvelinus alpinus. *J. Exp. Biol.* **207,** 4343–4360 (2004); 10.1242/jeb.01292.
4. Hollway, G. E. *et al.* Whole-Somite Rotation Generates Muscle Progenitor Cell Compartments in the Developing Zebrafish Embryo. *Dev. Cell* **12,** 207–219 (2007); 10.1016/j.devcel.2007.01.001.
5. Seger, C. *et al.* Analysis of Pax7 expressing myogenic cells in zebrafish muscle development, injury, and models of disease. *Dev. Dyn.* **240,** 2440–2451 (2011); 10.1002/dvdy.22745.
6. Rossi, G. & Messina, G. Comparative myogenesis in teleosts and mammals. *Cell. Mol. Life Sci.* **71,** 3081–3099 (2014); 10.1007/s00018-014-1604-5.

7. Johnston, I. A. Environment and plasticity of myogenesis in teleost fish. *J. Exp. Biol.* **209,** 2249–2264 (2006); 10.1242/jeb.02153.
8. Johnston, I. A., Bower, N. I. & Macqueen, D. J. Growth and the regulation of myotomal muscle mass in teleost fish. *J. Exp. Biol.* **214,** 1617–28 (2011); 10.1242/jeb.038620.
9. Bower, N. I. & Johnston, I. A. Transcriptional regulation of the IGF signaling pathway by amino acids and insulin-like growth factors during myogenesis in Atlantic salmon. *PLoS One* **5,** e11100 (2010); 10.1371/journal.pone.0011100.
10. Garcia de la serrana, D. & Johnston, I. A. Expression of Heat Shock Protein (Hsp90) Paralogues Is Regulated by Amino Acids in Skeletal Muscle of Atlantic Salmon. *PLoS One* **8,** e74295 (2013); 10.1371/journal.pone.0074295.
11. Gabillard, J. C., Sabin, N. & Paboeuf, G. In vitro characterization of proliferation and differentiation of trout satellite cells. *Cell Tissue Res.* **342,** 471–7 (2010); 10.1007/s00441-010-1071-8.
12. Vélez, E. J. *et al.* Contribution of in vitro myocytes studies to understanding fish muscle physiology. *Comp. Biochem. Physiol. Part B Biochem. Mol. Biol.* **199,** 67–73 (2016); 10.1016/j.cbpb.2015.12.003.
13. Vélez, E. J. *et al.* IGF-I and amino acids effects through TOR signaling on proliferation and differentiation of gilthead sea bream cultured myocytes. *Gen. Comp. Endocrinol.* **205,** 296–304 (2014); 10.1016/j.ygcen.2014.05.024.
14. Duran, B. O. da S. *et al.* Differential microRNA Expression in Fast- and Slow-Twitch Skeletal Muscle of Piaractus mesopotamicus during Growth. *PLoS One* **10,** e0141967 (2015); 10(11):e0141967.
15. Schiaffino, S. & Reggiani, C. Fiber Types in Mammalian Skeletal Muscles. *Physiol. Rev.* **91,** 1447–1531 (2011); 10.1152/physrev.00031.2010.
16. Jaillon, O. *et al.* Genome duplication in the teleost fish Tetraodon nigroviridis reveals the early vertebrate proto-karyotype. *Nature* **431,** 946–957 (2004); 10.1038/nature03025.
17. Garcia de la serrana, D., Mareco, E. A. & Johnston, I. A. Systematic Variation in the Pattern of Gene Paralog Retention between the Teleost Superorders Ostariophysi and Acanthopterygii. *Genome Biol. Evol.* **6,** 981–987 (2014); 10.1093/gbe/evu074.
18. Macqueen, D. J., Kristjánsson, B. K. & Johnston, I. A. Salmonid genomes have a remarkably expanded akirin family, coexpressed with genes from conserved pathways governing skeletal muscle growth and catabolism. *Physiol. Genomics* **42,** 134–48 (2010); 10.1152/physiolgenomics.00045.2010.
19. Macqueen, D. J., Garcia de la serrana, D. & Johnston, I. A. Evolution of Ancient Functions in the Vertebrate Insulin-Like Growth Factor System Uncovered by Study of Duplicated Salmonid Fish Genomes. *Mol. Biol. Evol.* **30,** 1060–1076 (2013); 10.1093/molbev/mst017.
20. Macqueen, D. J. & Johnston, I. A. A well-constrained estimate for the timing of the salmonid whole genome duplication reveals major decoupling from species diversification. *Proceedings. Biol. Sci.* **281,** 20132881 (2014); 10.1098/rspb.2013.2881.
21. Bower, N. I. & Johnston, I. A. Paralogs of Atlantic salmon myoblast determination factor genes are distinctly regulated in proliferating and differentiating myogenic cells. *AJP Regul. Integr. Comp. Physiol.* **298,** R1615–R1626 (2010); 10.1152/ajpregu.00114.2010.
22. Garcia de la serrana, D., Fuentes, E. N., Martin, S. A. M., Johnston, I. A. & Macqueen, D. J. Divergent

regulation of insulin-like growth factor binding protein genes in cultured Atlantic salmon myotubes under different models of catabolism and anabolism. *Gen. Comp. Endocrinol.* **247,** 53–65 (2017); 10.1016/j.ygcen.2017.01.017.

23. Maere, S. & Van de Peer, Y. Duplicate Retention After Small- and Large-Scale Duplications in *Evolution after Gene Duplication* (eds. Dittmar, K. & Liberles, D.) 329 (John Wiley & Sons, Inc., 2010).
24. Berthelot, C. *et al.* The rainbow trout genome provides novel insights into evolution after whole-genome duplication in vertebrates. *Nat. Commun.* **5,** 3657 (2014); 10.1038/ncomms4657.
25. Ge, Y. & Chen, J. MicroRNAs in skeletal myogenesis. *Cell Cycle* **10,** 441–448 (2011); 10.4161/cc.10.3.14710.
26. van Rooij, E., Liu, N. & Olson, E. N. MicroRNAs flex their muscles. *Trends Genet.* **24,** 159–66 (2008); 10.1016/j.tig.2008.01.007.
27. Goljanek-Whysall, K., Sweetman, D. & Münsterberg, A. E. microRNAs in skeletal muscle differentiation and disease. *Clin. Sci.* **123,** 611–625 (2012); 10.1042/CS20110634.
28. Bizuayehu, T. T. & Babiak, I. MicroRNA in Teleost Fish. *Genome Biol. Evol.* **6,** 1911–1937 (2014); 10.1093/gbe/evu151.
29. Chen, J.-F. *et al.* The role of microRNA-1 and microRNA-133 in skeletal muscle proliferation and differentiation. *Nat. Genet.* **38,** 228–33 (2006); 10.1038/ng1725.
30. van Rooij, E. *et al.* A family of microRNAs encoded by myosin genes governs myosin expression and muscle performance. *Dev. Cell* **17,** 662–73 (2009); 10.1016/j.devcel.2009.10.013.
31. McCarthy, J. J. The MyomiR network in skeletal muscle plasticity. *Exerc. Sport Sci. Rev.* **39,** 150–4 (2011); 10.1097/JES.0b013e31821c01e1.
32. Chin, E. R. *et al.* A calcineurin-dependent transcriptional pathway controls skeletal muscle fiber type. *Genes Dev.* **12,** 2499–509 (1998); 10.1101/gad.12.16.2499.
33. Olson, E. N. & Williams, R. S. Calcineurin Signaling and Muscle Remodeling. *Cell* **101,** 689–692 (2000); 10.1016/S0092-8674(00)80880-6.
34. Thelen, M. H., Simonides, W. S. & van Hardeveld, C. Electrical stimulation of C2C12 myotubes induces contractions and represses thyroid-hormone-dependent transcription of the fast-type sarcoplasmic-reticulum Ca2+-ATPase gene. *Biochem. J.* **321 (Pt 3),** 845–8 (1997).
35. Marotta, M., Bragós, R. & Gómez-Foix, A. M. Design and performance of an electrical stimulator for long-term contraction of cultured muscle cells. *Biotechniques* **36,** 68–73 (2004); 10.2144/04361ST01.
36. Fujita, H., Nedachi, T. & Kanzaki, M. Accelerated de novo sarcomere assembly by electric pulse stimulation in C2C12 myotubes. *Exp. Cell Res.* **313,** 1853–1865 (2007); 10.1016/j.yexcr.2007.03.002.
37. Silveira, L. R., Pilegaard, H., Kusuhara, K., Curi, R. & Hellsten, Y. The contraction induced increase in gene expression of peroxisome proliferator-activated receptor (PPAR)-γ coactivator 1α (PGC-1α), mitochondrial uncoupling protein 3 (UCP3) and hexokinase II (HKII) in primary rat skeletal muscle cells is dependent on reactive oxygen species. *Biochim. Biophys. Acta - Mol. Cell Res.* **1763,** 969–976 (2006); 10.1016/j.bbamcr.2006.06.010.
38. Nedachi, T., Fujita, H. & Kanzaki, M. Contractile C_2C_{12} myotube model for studying exercise-inducible responses in skeletal muscle. *Am. J. Physiol. Metab.* **295,** E1191–E1204 (2008);

3008 10.1152/ajpendo.90280.2008.
3009 39. Burch, N. *et al.* Electric Pulse Stimulation of Cultured Murine Muscle Cells Reproduces Gene Expression
3010 Changes of Trained Mouse Muscle. *PLoS One* **5,** e10970 (2010); 10.1371/journal.pone.0010970.
3011 40. Nikolić, N. *et al.* Electrical Pulse Stimulation of Cultured Human Skeletal Muscle Cells as an In Vitro
3012 Model of Exercise. *PLoS One* **7,** e33203 (2012); 10.1371/journal.pone.0033203.
3013 41. Montserrat, N., Gabillard, J. C., Capilla, E., Navarro, M. I. & Gutiérrez, J. Role of insulin, insulin-like
3014 growth factors, and muscle regulatory factors in the compensatory growth of the trout (Oncorhynchus
3015 mykiss). *Gen. Comp. Endocrinol.* **150,** 462–472 (2007); 10.1016/j.ygcen.2006.11.009.
3016 42. Seiliez, I. *et al.* An in vivo and in vitro assessment of TOR signaling cascade in rainbow trout
3017 (Oncorhynchus mykiss). *AJP Regul. Integr. Comp. Physiol.* **295,** R329–R335 (2008);
3018 10.1152/ajpregu.00146.2008.
3019 43. Cleveland, B. M. & Weber, G. M. Effects of insulin-like growth factor-I, insulin, and leucine on protein
3020 turnover and ubiquitin ligase expression in rainbow trout primary myocytes. *Am. J. Physiol. Integr. Comp.*
3021 *Physiol.* **298,** R341–R350 (2010); 10.1152/ajpregu.00516.2009.
3022 44. Fauconneau, B. & Paboeuf, G. Effect of fasting and refeeding on in vitro muscle cell proliferation in
3023 rainbow trout (Oncorhynchus mykiss). *Cell Tissue Res.* **301,** 459–63 (2000); 10.1007/s004419900168.
3024 45. Ma, G. *et al.* MiR-206, a key modulator of skeletal muscle development and disease. *Int. J. Biol. Sci.* **11,**
3025 345–52 (2015); 10.7150/ijbs.10921.
3026 46. Samy, J. K. A. *et al.* SalmoBase: an integrated molecular data resource for Salmonid species. *BMC*
3027 *Genomics* **18,** 482 (2017); 10.1186/s12864-017-3877-1.
3028 47. Kumar, S., Stecher, G. & Tamura, K. MEGA7: Molecular Evolutionary Genetics Analysis Version 7.0 for
3029 Bigger Datasets. *Mol. Biol. Evol.* **33,** 1870–1874 (2016); 10.1093/molbev/msw054.
3030 48. Drummond, A. J., Suchard, M. A., Xie, D. & Rambaut, A. Bayesian Phylogenetics with BEAUti and the
3031 BEAST 1.7. *Mol. Biol. Evol.* **29,** 1969–1973 (2012); 10.1093/molbev/mss075.
3032 49. Koressaar, T. & Remm, M. Enhancements and modifications of primer design program Primer3.
3033 *Bioinformatics* **23,** 1289–1291 (2007); 10.1093/bioinformatics/btm091.
3034 50. Untergasser, A. *et al.* Primer3--new capabilities and interfaces. *Nucleic Acids Res.* **40,** e115 (2012);
3035 10.1093/nar/gks596.
3036 51. Bustin, S. A. *et al.* The MIQE Guidelines: Minimum Information for Publication of Quantitative Real-Time
3037 PCR Experiments. *Clin. Chem.* **55,** 611–622 (2009); 10.1373/clinchem.2008.112797.
3038 52. Livak, K. J. & Schmittgen, T. D. Analysis of relative gene expression data using real-time quantitative PCR
3039 and the 2(-Delta Delta C(T)) Method. *Methods* **25,** 402–8 (2001); 10.1006/meth.2001.1262.
3040 53. Andersen, C. L., Jensen, J. L. & Ørntoft, T. F. Normalization of Real-Time Quantitative Reverse
3041 Transcription-PCR Data: A Model-Based Variance Estimation Approach to Identify Genes Suited for
3042 Normalization, Applied to Bladder and Colon Cancer Data Sets. *Cancer Res.* **64,** 5245–5250 (2004);
3043 10.1158/0008-5472.CAN-04-0496.
3044 54. RStudio Team. RStudio: Integrated Development for R. *RStudio, Inc., Boston, MA* (2015).
3045 http://www.rstudio.com/.
3046 55. Wickham, H. *Ggplot2 : elegrant graphics for data analysis*. (2016).

56. Castillo, J. *et al.* IGF-I binding in primary culture of muscle cells of rainbow trout: changes during in vitro development. *Am. J. Physiol. Integr. Comp. Physiol.* **283,** R647–R652 (2002); 10.1152/ajpregu.00121.2002.
57. Castillo, J., Ammendrup-Johnsen, I., Codina, M., Navarro, I. & Gutiérrez, J. IGF-I and insulin receptor signal transduction in trout muscle cells. *Am. J. Physiol. Integr. Comp. Physiol.* **290,** R1683–R1690 (2006); 10.1152/ajpregu.00294.2005.
58. Montserrat, N., Sánchez-Gurmaches, J., García de la Serrana, D., Navarro, M. I. & Gutiérrez, J. IGF-I binding and receptor signal transduction in primary cell culture of muscle cells of gilthead sea bream: changes throughout in vitro development. *Cell Tissue Res.* **330,** 503–513 (2007); 10.1007/s00441-007-0507-2.
59. Gibson, M. C. & Schultz, E. The distribution of satellite cells and their relationship to specific fiber types in soleus and extensor digitorum longus muscles. *Anat. Rec.* **202,** 329–337 (1982); 10.1002/ar.1092020305.
60. García de la serrana, D. *et al.* Characterisation and expression of myogenesis regulatory factors during in vitro myoblast development and in vivo fasting in the gilthead sea bream (Sparus aurata). *Comp. Biochem. Physiol. Part A Mol. Integr. Physiol.* **167,** 90–99 (2014); 10.1016/j.cbpa.2013.10.020.
61. Hagiwara, N., Yeh, M. & Liu, A. Sox6 is required for normal fiber type differentiation of fetal skeletal muscle in mice. *Dev. Dyn.* **236,** 2062–2076 (2007); 10.1002/dvdy.21223.
62. Bessarab, D. A., Chong, S.-W., Srinivas, B. P. & Korzh, V. Six1a is required for the onset of fast muscle differentiation in zebrafish. *Dev. Biol.* **323,** 216–228 (2008); 10.1016/J.YDBIO.2008.08.015.
63. Feldman, J. L. & Stockdale, F. E. Skeletal muscle satellite cell diversity: satellite cells form fibers of different types in cell culture. *Dev. Biol.* **143,** 320–34 (1991).
64. Chan, M. C. & Arany, Z. The many roles of PGC-1α in muscle--recent developments. *Metabolism.* **63,** 441–51 (2014); 10.1016/j.metabol.2014.01.006.
65. Kern, M. *et al.* Insulin responsiveness in skeletal muscle is determined by glucose transporter (Glut4) protein level. *Biochem. J.* **270,** 397–400 (1990).
66. Sancak, Y. *et al.* Ragulator-Rag Complex Targets mTORC1 to the Lysosomal Surface and Is Necessary for Its Activation by Amino Acids. *Cell* **141,** 290–303 (2010); 10.1016/j.cell.2010.02.024.
67. Demetriades, C., Doumpas, N. & Teleman, A. A. Regulation of TORC1 in Response to Amino Acid Starvation via Lysosomal Recruitment of TSC2. *Cell* **156,** 786–799 (2014); 10.1016/j.cell.2014.01.024.
68. Sandri, M. Signaling in Muscle Atrophy and Hypertrophy. *Physiology* **23,** 160–170 (2008); 10.1152/physiol.00041.2007.
69. Wyss, M. & Kaddurah-Daouk, R. Creatine and Creatinine Metabolism. *Physiol. Rev.* **80,** 1107–1213 (2000); 10.1152/physrev.2000.80.3.1107.
70. Yu, H., Lu, Y., Li, Z. & Wang, Q. microRNA-133: expression, function and therapeutic potential in muscle diseases and cancer. *Curr. Drug Targets* **15,** 817–28 (2014); 10.2174/1389450115666140627104151.
71. Li, Q., Lin, X., Yang, X. & Chang, J. NFATc4 is negatively regulated in miR-133a-mediated cardiomyocyte hypertrophic repression. *Am. J. Physiol. Circ. Physiol.* **298,** H1340–H1347 (2010); 10.1152/ajpheart.00592.2009.
72. Blaauw, B., Schiaffino, S. & Reggiani, C. Mechanisms Modulating Skeletal Muscle Phenotype. *Compr. Physiol.* **3,** 1645–1687 (2013); 10.1002/cphy.c130009.

73. Schiaffino, S. Fibre types in skeletal muscle: a personal account. *Acta Physiol.* **199,** 451–463 (2010); 10.1111/j.1748-1716.2010.02130.x.

74. Wang, X. *et al.* Prdm1a and miR-499 act sequentially to restrict Sox6 activity to the fast-twitch muscle lineage in the zebrafish embryo. *Development* **138,** 4399–404 (2011); 10.1242/dev.070516.

75. Nachtigall, P. G., Dias, M. C., Carvalho, R. F., Martins, C. & Pinhal, D. MicroRNA-499 expression distinctively correlates to target genes sox6 and rod1 profiles to resolve the skeletal muscle phenotype in Nile tilapia. *PLoS One* **10,** e0119804 (2015); 10.1371/journal.pone.0119804

76. von Hofsten, J. *et al.* Prdm1- and Sox6-mediated transcriptional repression specifies muscle fibre type in the zebrafish embryo. *EMBO Rep.* **9,** 683–9 (2008); 10.1038/embor.2008.73.

ACKNOWLEDGEMENTS

We will like to thank Professor Ian Alistair Johnston from the Scottish Oceans Institute (University of St Andrews) to host the present research in his laboratory facilities. We also thank Dr. Robson Francisco Carvalho and Dr. Edson Assunção Mareco for their valuable discussions.

This work received funding from the MASTS pooling initiative (The Marine Alliance for Science and Technology for Scotland) and their support is gratefully acknowledged. MASTS is funded by the Scottish Funding Council (grant reference HR09011) and contributing institutions. Funding was also provided by the Coordination for the Improvement of Higher Education Personnel (CAPES), National Council for Scientific and Technological Development (CNPq), with grants 447233/2014 and 302656/2015-4, and São Paulo Research Foundation (FAPESP), with grants #2015/03234-8, #2016/19683-9 and #2016/05009-4. The funding agencies did not have roles in design of study, analysis of data or writing of manuscript, providing only the financial resources. DGDLS is a Serra Húnter Fellow of the University of Barcelona.

AUTHOR CONTRIBUTIONS

BOSD, MDPS and DGDLS conceived and designed the experiments. BOSD and DGDLS performed the experiments. BOSD, MDPS and DGDLS analyzed the data. MDPS and DGDLS contributed with reagents/materials/analysis tools. BOSD and DGDLS wrote the paper. All authors read and approved the final manuscript.

SUPPLEMENTARY INFORMATION

Supplementary Table S1: Quantitative PCR primer sequences. Genes are as follow: *slow myhc* (*slow myosin heavy chain*); *fast myhc* (*fast myosin heavy chain*); *sox6* ((*sex determining*

region Y)-box 6); *six1* (*six homeobox 1*); *glut4* (*insulin-responsive glucose transporter type 4*); *lamtor3* (*late endosomal/lysosomal adaptor, mapk and mtor activator 3*); *ragd* (*ras related GTP binding D*); *rptor* (*regulatory associated protein of mtor complex 1*); *mafbx* (*muscle atrophy f-box protein*); *pgc1α* (*peroxisome proliferator-activated receptor gamma coactivator 1 alpha*); *ckma* (*creatine kinase, m-type a*); *ckmb* (*creatine kinase, m-type b*); *rpl13* (*ribosomal protein L13*); *rpl19* (*ribosomal protein L19*); *omy-mir-133a-1a*, *omy-mir-133a-1b*, *omy-mir-133a-2* (precursor sequences of rainbow trout mir-133 paralogues); *omy-mir-499aa+ab*, *omy-mir-499ab*, *omy-mir-499ba*, *omy-mir-499bb* (precursor sequences of rainbow trout mir-499 paralogues); *omy-mir-206-1* (precursor sequence of rainbow trout mir-206); and *U6 snRNA* (*U6 small nuclear RNA*). Accession code based on rainbow trout genome [24] or NCBI (http://www.ncbi.nlm.nih.gov) database.

Gene	Forward primer (5' to 3')	Reverse primer (5' to 3')
slow myhc	AGTTCCGCAAGATTCAGCAT	GCCGACATCACAACTCTTGA
fast myhc	GGCCAAGAAGGCTATCACTG	GCCAGATTCTCAGCCTCATC
sox6	TGGGAGAGGATGATGGAAAG	CCCAGGATCTTGCTGATGTT
six1	TCCCTCTGGATATCGGCGTT	AGAAAACGACCGAGCCTCTC
glut4	GTGCCAGGCTTATTGTCCATATTC	TAGAGAAGATGGCTACCGACAG
lamtor3	TCACCATGGACTGGGGGTTA	TGCGTTATCATTTGCCACTTTG
ragd	AGGGGGTTTCGAAGTACACC	TGAAACCACCTCCGTCTTCG
rptor	CCATCGACAAGATGAGACGA	CCTGGGGAGACAGAGACAGA
mafbx	CAGGAGCCCGAGTGACTTTT	ATCAAATGCACCATCACCCCT
pgc1α	AACCTGAGAGATGACGGGGA	GTGTGTCCGTTTTCAAGGGC
ckma	GTGGGTGGAGTGTTCGACAT	TCCACCATGAGCTTGACACC
ckmb	AGCACACACCCCAAGTTTGA	CAGAAGATCCCAGACGGTCA
rpl13	CACCATTGGCATCTCTGTTG	AGTGCTGTCTCCCTTCTTGG
rpl19	GAGAAGACGACGCAGGATTC	CAAGTGAAGGCACACAGGAA
omy-mir-133a-1a	AGTGAACCCCCAATGCTTT	GGGACCAAATCCATTCAAGA
omy-mir-133a-1b	GACAAACACCTAATGCCTTG	GGGACCAAATCCATTCAAGA
omy-mir-133a-2	TTCACACCAAAAATGCTTT	GGGACCAAATCCATTGAACA
omy-mir-499aa+ab	CTGAGAAGGAGACAGTTAAGACTTG	AGAGTGGAGCCAGCAGAGAC
omy-mir-499ab	AGGAGACAGTTAAGACTTGC	TGAGAATGGAGCCAGCAC
omy-mir-499ba	GAGGGAAGTAGTTAAGACTTG	CTTAAAGTGATGTTCATGAGT
omy-mir-499bb	GAGGGAAGTAGTTAAGACTTA	CTTAAAGTGATGTTCATGAGC

omy-mir-206-1	TCGTTGCCTCCTGTGAAGAC	CTCCATTCCCCTTGTAACCA
U6 snRNA	GGCTTCGGCAGCACATATAC	AACGCTTCACGATTTTGC

Supplementary Table S2: Rainbow trout miRNAs nomenclature. Adopted nomenclature of rainbow trout mir-133, mir-499 and mir-206 precursor sequences based on the Bayesian phylogenetic trees.

Accession code in Genoscope	Precursor sequence nomenclature
Oncorhynchus mykiss scaffold_1560	*omy-mir-133a-1a*
Oncorhynchus mykiss scaffold_79929	*omy-mir-133a-1b*
Oncorhynchus mykiss scaffold_1154	*omy-mir-133a-2*
Oncorhynchus mykiss scaffold_984	*omy-mir-499aa*
Oncorhynchus mykiss scaffold_116	*omy-mir-499ab*
Oncorhynchus mykiss scaffold_347	*omy-mir-499ba*
Oncorhynchus mykiss scaffold_1915	*omy-mir-499bb*
Oncorhynchus mykiss scaffold_13810	*omy-mir-206-1*

Supplementary Table S3: Rainbow trout miRNAs similarity. Percentage of similarity between miRNAs paralogues identified in rainbow trout.

Paralogue	Nucleotide similarity
omy-mir-133a-1a vs *omy-mir-133a-1b*	97%
omy-mir-133a-1a vs *omy-mir-133a-2*	93%
omy-mir-133a-1b vs *omy-mir-133a-2*	92%
omy-mir-499aa vs *omy-mir-499ab*	96%
omy-mir-499ba vs *omy-mir-499bb*	97%

```
>omy-mir-133a-1a AGTGAACCCCCAATGCTTTGCTAAAGCTGGTAAAAAGGAACCAAATCACCTCTTGAATGGATTTGGTCCCCTTCAACCAGCTGTAGCTATGCTTTGATG
>omy-mir-133a-1b GACAAACACCTAATGCCTTGCTAAAGCTGGTAAAAAGGAACCAAATCACCTCTTGAATGGATTTGGTCCCCTTCAACCAGCTGTAGCTATGCTTTGATG
>omy-mir-133a-2  TTCACACCAAAAATGCTTTGCTAAAGCTGGTAAAATGGAACCAAATCAACTGTTCAATGGATTTGGTCCCCTTCAACCAGCTGTAGCTGTGCATTGATC

>omy-mir-499aa+ab  GCTGAGAAGGAGACAGTTAAGACTTGTAGTGATGTTTAGGGAAATTATCACATGAACATCACTTTAAGTCTCTGCTGGCTCCACTCTCATA
>omy-mir-499ab     GCTGAGAAGGAGACAGTTAAGACTTGCAGTGATGTTTAGGGAAATGATCACATGAACATCACTTTAAGTCTGTGCTGGCTCCATTCTCATA

>omy-mir-499ba GTTGAGAGGGAAGTAGTTAAGACTTGCAGTGATGTTTAGGTAACTCAACTCATGAACATCACTTTAAGTCTGTGCTACCTCCACTCTTTCAT
>omy-mir-499bb GTTGAGAGGGAAGTAGTTAAGACTTACAGTGATGTTTCGGTAACTCAGCTCATGAACATCACTTTAAGTCTGTGCTACCTCCACTCTTTCAT

>omy-mir-206-1 TGTCGTTGCCTCCTGTGAAGACATGCTTCCTTATATCCCCATATGAATACTGCCGTTATGGAATGTAAGGAAGTGTGTGGTTACAAGGGGAATGGAGCT
```

Supplementary Fig S1: Rainbow trout mir-133, mir-499 and mir-206 precursor sequences. The yellow boxes show nucleotides that differ between copies. Forward primers are indicated in red and reverse primers are indicated in blue. The underlined sequences correspond to the miRNA mature sequences.

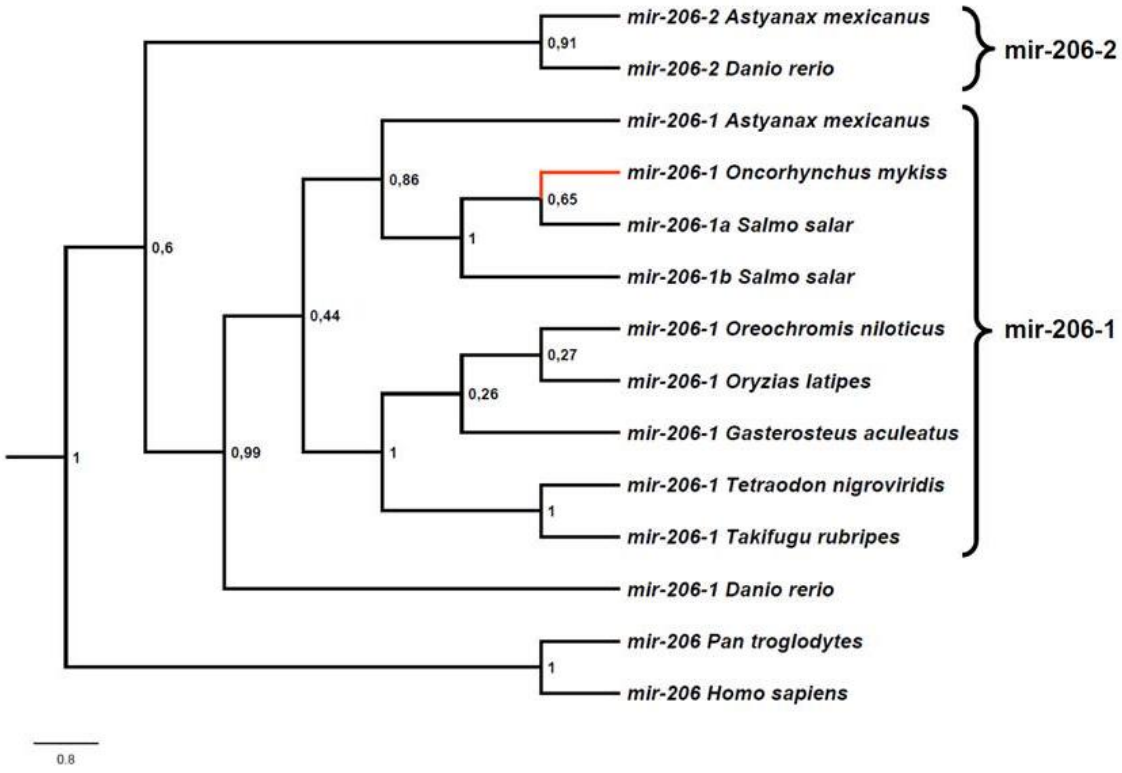

Supplementary Fig S2: Teleost fish mir-206 phylogenetic analysis. Phylogenetic reconstruction of the mir-206 family using Bayesian methods. The tree was constructed from a highly confidence alignment of 14 nucleotide sequences and used Tamura-Nei (TN93) as best fitted substitution model. Bootstrap-posterior values are indicated on the node of each branch. Branches in red indicate the mir-206 copies identified for rainbow trout.

A

Correlation	133a1a	133a1b	133a2	499aa +ab	499ab	499ba	499bb	*smyhc*	*fmyhc*	*sox6*
133a1a	1	0,21	0,11	0,2	0,12	0,02	0,17	-0,12	-0,02	0,26
133a1b		1	0,55***	-0,1	0,16	0,14	0,09	-0,2	0,55***	0,4**
133a2			1	-0,1	-0,05	0,27	0,21	0,02	0,26	0,13
499aa+ab				1	0,71***	0,11	0,6***	0,26	-0,17	-0,38*
499ab					1	0,13	0,41**	0,46**	0,21	-0,27
499ba						1	0,69***	0,15	-0,24	-0,5**
499bb							1	0,08	-0,31*	-0,51***
smyhc								1	0,19	-0,46**
fmyhc									1	0,45**
sox6										1

B

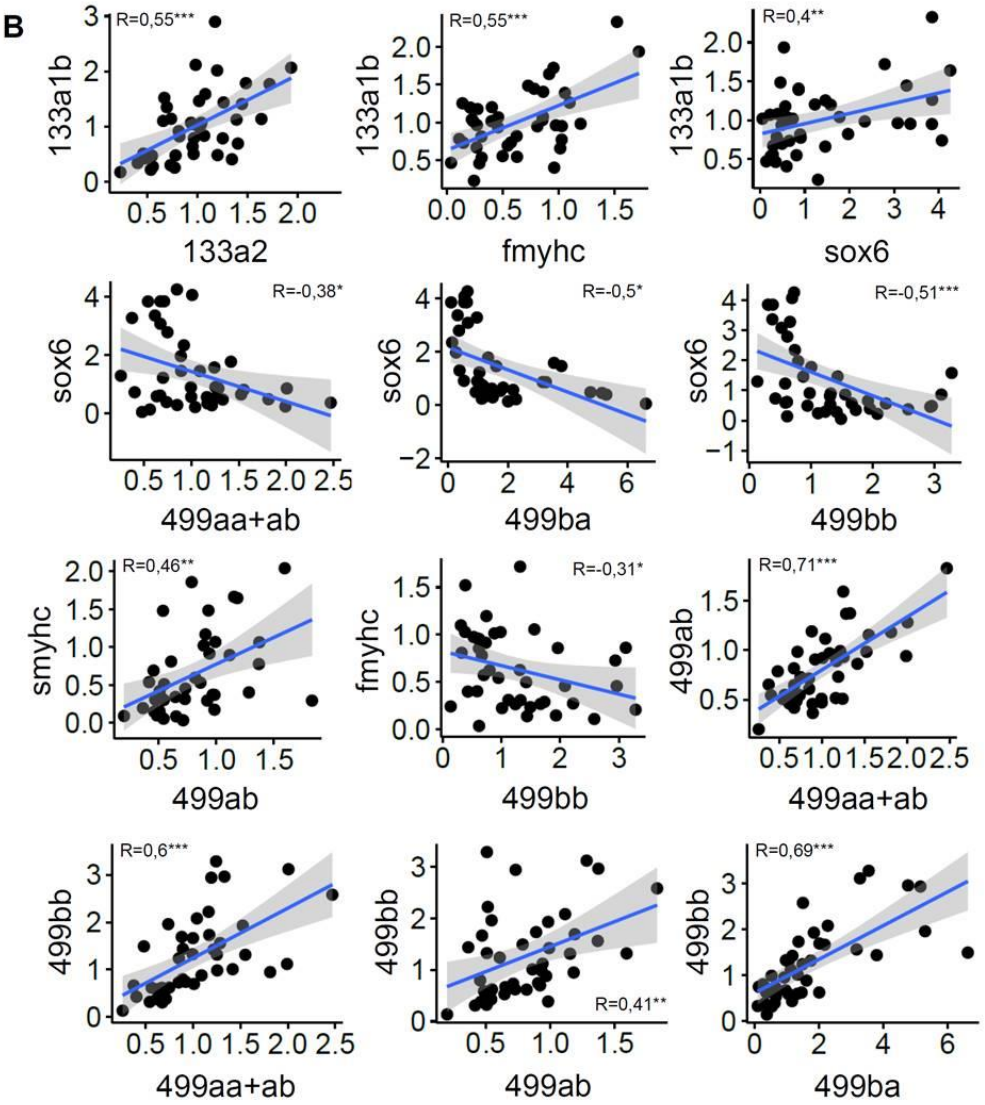

Supplementary Fig S3: Correlation of rainbow trout miRNAs and mRNAs expression. (A) Pearson's correlation (R) index between the expression of *omy-mir-133* and *omy-mir-499* paralogues, and *smyhc*, *fmyhc* and *sox6* mRNAs. (B) Plot char between gene expression values for *omy-mir-133a-1b* vs *omy-mir-133a-2*, *omy-mir-133a-1b* vs *fmyhc*, *omy-mir-133a-1b* vs *sox6*,

omy-mir-499aa+ab vs *sox6*, *omy-mir-499ba* vs *sox6*, *omy-mir-499bb* vs *sox6*, *omy-mir-499ab* vs *smyhc*, *omy-mir-499bb* vs *fmyhc*, *omy-mir-499aa+ab* vs *omy-mir-499ab*, *omy-mir-499aa+ab* vs *omy-mir-499bb*, *omy-mir-499ab* vs *omy-mir-499bb* and *omy-mir-499ba* vs *omy-mir-499bb*. Pearson correlation and p-value are indicated in the corners of the plot graphs. Significant differences between gene correlations are indicated with one ($P<0.05$), two ($P<0.01$) or three ($P<0.001$) asterisks.

8. CAPÍTULO III

Artigo em fase de escrita. Posterior submissão para Genome Biology and Evolution (fator de impacto: 3.94) ou American Journal of Physiology (fator de impacto: 3.08).

O capítulo III se refere ao trabalho e experimentos desenvolvidos para a comparação da expressão de parálogos linhagem-específicos (LSPs) entre pacus e tilápias do Nilo, submetidos a um modelo de jejum-realimentação, e também para a avaliação *in vitro* desses LSPs em mioblastos provenientes do músculo de contração rápida de pacus, submetidos a tratamentos com aminoácidos não-essenciais e leucina.

Lineage-specific paralogues regulating skeletal muscle growth in Ostariophysi superorder.

Bruno Oliveira Silva Duran[1], Daniel Garcia de la serrana[2], Edson Assunção Mareco[3], Robson Francisco Carvalho[1] and Maeli Dal-Pai-Silva[1*]

[1]São Paulo State University (UNESP), Institute of Biosciences, Department of Morphology, Botucatu, São Paulo, Brazil
[2]University of St. Andrews, Scottish Oceans Institute, School of Biology, St. Andrews, Fife, Scotland, United Kingdom
[3]University of West São Paulo (UNOESTE), Presidente Prudente, São Paulo, Brazil

* Corresponding author
E-mail: maeli@ibb.unesp.br

ABSTRACT

Whole genome duplication (WGD) events are considered a major feature of the evolution of eukaryotic genomes, providing raw materials in where natural selection can act to promote increasing complexity. Teleost fish have undergone a specific WGD (TSGD) in the base of the lineage, estimated at 333-225 million years ago. Around 15-21% of the TSGD-derived paralogues have been retained due to subfunctionalization and/or neofunctionalization processes. Recent studies have demonstrated differences in paralogues retention between the teleost superorders Ostariophysi and Acanthopterygii, many of them key components of the

myogenesis, protein synthesis and degradation. However, despite the progresses done in the identification of these lineage-specific paralogues (LSPs), their physiological roles remain unknown in the majority of cases. The pacu (*Piaractus mesopotamicus*) and the Nile tilapia (*Oreochromis niloticus*) belong to superorders Ostariophysi and Acanthopterygii, respectively. Both species are economically relevant for the Brazilian aquaculture and, therefore, objects of an intense research to improve their production. Skeletal muscle is the most abundant tissue in teleost fish, representing up to 65% of the total body mass for some species. Muscle growth is strongly dependent of the balance between protein synthesis and degradation, processes regulated by intrinsic and extrinsic signals. Among them, growth factors and amino acids have demonstrated to play an essential role in protein synthesis and muscle growth regulation. The fast muscle myoblast culture is arising as a very useful *in vitro* tool to study the regulation of muscle growth. The cell culture recapitulates all the steps from myogenesis: myoblast commitment, proliferation, fusion and myotube formation. Cell cultures can be manipulated to generate experimental conditions that would allow us to study muscle regulation, growth and development at different levels and under a variety of circumstances. Similarly, cell culture media can be modified to evaluate the role of nutrients or growth factors in the regulation of myogenesis. The myoblast cell culture has been successfully developed in Acanthopterygii and Protacanthopterygii species, what turns many of the assumptions derived from those models very difficult to extrapolate to Ostariophysi species. Therefore, the pacu myoblast culture is an excellent model to understand the regulation of myogenesis and muscle growth in Ostariophysi superorder. The aim of our work was to compare the expression of LSPs related to myogenesis, protein synthesis and protein degradation between Ostariophysi and Acanthopterygii. In order to mobilize these signaling pathways, we submitted pacus and Nile tilapias to a fasting-refeeding experiment, and also used pacu myoblast cell cultures to investigate the effects of amino acid treatments in LSPs expression. Our work contributed to better understand the evolutionary divergence of Ostariophysi and Acanthopterygii superorders and the regulation of skeletal muscle in fish, allowing the development of a theoretic framework that may help to improve muscle growth.

INTRODUCTION

Skeletal muscle in teleost fish represents around 65% of total body mass in several commercial species and it is the most abundant tissue, which allows underwater propulsion and represents the main protein reservoir in fish (Johnston, 2001; Sänger & Stoiber, 2001). There are

different populations of muscle fibres that can be classified accordingly to their contractile and metabolic properties, usually slow and fast fibres (Johnston *et al*., 2004), and fast muscle comprises the bulk of the fillet (up to 90% of the muscle mass), the main product of the aquaculture industry.

Postnatal skeletal muscle growth encompasses the main events of embryonic myogenesis and occurs through the activation of satellite cells, a group of myogenic precursor cells (MPCs) adjacent to the muscle fibres. Once activated, these satellite cells proliferate (myoblasts) and can fuse each other to form new fibres (hyperplasia) or can be incorporated by pre-existent fibres increasing their size (hypertrophy) (Rowlerson & Veggetti, 2001; Johnston, 2006; Johnston *et al*., 2011). Muscle growth is a multifactorial process that incorporates biotic and abiotic signals in its regulation, and the fibre size is the result of the balance between protein synthesis and degradation, whose signaling pathways are interrelated and modulate each other (Sandri, 2008; Vélez *et al*., 2014). Growth factors and amino acids have demonstrated to play an essential role in protein synthesis, indicating the integration of both endocrine and nutritional signals on these pathways regulating muscle growth.

In fish, the molecular networks have suffered an expansion of its number of components compared to vertebrates due to a whole genome duplication (WGD) event. The WGD are thought to provide raw materials in where natural selection can act to promote increasing complexity of organisms (Taylor *et al*., 2003). Around 333-225 million years ago, teleost fish have undergone a specific WGD in the common ancestor of the group (teleost-specific genome duplication - TSGD) (Jaillon *et al*., 2004). WGD are followed by diploidization and loss of duplicated genes. It has been estimated that around 15-21% of the paralogues originated during the TSGD have been retained through subfunctionalization and/or neofunctionalization mechanisms (Garcia de la serrana *et al*., 2014). During subfunctionalization each paralog acquires part of the original function of the ancestral gene, which many times culminates in a shared regulation of a biological process. In neofunctionalization the paralogues acquire a different function of the ancestral gene, which can confer a selective advantage (Maere & Van de Peer, 2010). Thus, the WGD increases the complexity of organisms and may contribute to high biological diversity.

Recent studies have demonstrated differences in paralogues retention between the teleost superorders Ostariophysi and Acanthopterygii. Garcia de la serrana *et al*. (2014) showed that 510 and 418 TSGD paralogues were differently retained in the Ostariophysi and Acanthopterygii superorders, indicating the existence of lineage-specific paralogues (LSPs). These LSPs may

have undergone different mechanisms of subfunctionalization and/or neofunctionalization during the evolution of the superorders. Many of them are key components of the myogenesis, protein synthesis and protein degradation pathways (Garcia de la serrana *et al*., 2014) and recent studies suggest that they might have different expression patterns (Mareco *et al*., 2015). However, despite the progresses done in the identification of these LSPs, their physiological roles remain mainly unknown.

Piaractus mesopotamicus and *Oreochromis niloticus* belong to Ostariophysi and Acanthopterygii superorders, respectively. *Piaractus mesopotamicus*, popularly known as pacu, is found in the wetland areas of the Brazilian Midwest region (Urbinati & Gonçalves, 2005). *Oreochromis niloticus*, popularly known as Nile tilapia, is one of the most commonly farmed fish in the world, due to its adaptability to different conditions and habitats (El-Sayed, 2006). The members of Characidae family (pacu, tambaqui and tambacu) correspond to the majority of native fish farmed, representing up to 33.5% of national production, while Nile tilapia alone represents 46.6% of fish production in the country (MPA, 2013).

The fish myoblast culture represents a very useful *in vitro* tool to understand the regulation of muscle growth and myogenesis (Bower & Johnston, 2010; Johnston *et al*., 2011; Garcia de la serrana & Johnston, 2013). Myoblast cell culture recapitulates the steps of myogenesis, with an early myoblast commitment, proliferation, fusion and maturation (Chargé & Rudnicki, 2004; Gabillard *et al*., 2010). The myoblast cell culture provides a controlled environment to study myogenesis regulation and examine the role of TSGD-paralogues in the different culture stages. Similarly, cell culture media can be modified to evaluate the role of nutrients, growth factors, drugs and temperature in the regulation of myogenesis (Johnston *et al*., 2011; Garcia de la serrana & Johnston, 2013).

Myoblast cell cultures have been successfully developed for Acanthopterygii and Protacanthopterygii species (Montserrat *et al*., 2007; Seiliez *et al*., 2008; Garcia de la serrana & Johnston, 2013). However, the same system has not been developed for Ostariophysi species. With differences in the LSPs retained for key components of the myogenesis, protein synthesis and degradation between superorders it is difficult to extrapolate conclusions at gene regulation level from Acanthopterygii and Protacanthopterygii myogenesis to Ostariophysi. The main Ostariophysi species studied is the zebrafish (*Danio rerio*), but due to its relatively small size it is almost impossible the isolation of enough myoblasts from the fast skeletal muscle, which strongly constrains any myoblast cell culture study (Froehlich *et al*., 2013). The pacu, as well as the Nile tilapia, exhibit indeterminate somatic growth with formation of new fibres for a

prolonged period of time and providing great increase of muscle mass in these animals (Rowlerson & Veggetti, 2001). The pacu can be used as a model to study myogenesis in Ostariophysi superorder, due to its relatively big size and fast growth that indicate a higher number of myoblasts in the muscle.

We hypothesized that distinct mechanisms of subfunctionalization and/or neofunctionalization occurred between the teleost superorders Ostariophysi and Acanthopterygii, which promoted a differential retention of LSPs. During this work we intended to compare the expression of LSPs related to myogenesis, protein synthesis and protein degradation between pacus and Nile tilapia, for a better understanding of the evolutionary divergence between Ostariophysi and Acanthopterygii superorders. This comparison allowed us to identify subfunctionalization and neofunctionalization events of the LSPs and to understand their roles during muscle growth in both lineages. For this proposal, we used pacus and Nile tilapias submitted to a fasting-refeeding model, commonly used to manipulate fish muscle growth. The fasting period is directly related to a higher protein degradation, whereas the refeeding triggers a more exacerbated protein synthesis (Bower et al., 2009). To provide further insight we also used pacu myoblast cell cultures, to evaluate the effects of non-essential amino acids and leucine treatments in LSPs expression.

MATERIAL AND METHODS

Fish and fasting-refeeding experiment

This work was approved by the Ethics Committee on Animal Use (CEUA) of Biosciences Institute, UNESP, Botucatu, São Paulo, Brazil. Juvenile pacus and Nile tilapias were obtained from the São Paulo Agency for Agribusiness Technology (APTA), Presidente Prudente, São Paulo, Brazil. In order to reduce potential external variables in pacus and Nile tilapia comparison, the fish were placed in similar 0.5 m^3 water tanks, equipped with the same water recirculation system. In addition, the animals were raised at the same temperature (28° C) and fed twice a day with the same commercial feed, appropriate for their developmental stages. In our study we used the fasting-refeeding model to evaluate protein degradation and protein synthesis processes in pacus and Nile tilapias. Fish were fasted for 4 days and then refed for 3 days. Fish were euthanized with an excess of benzocaine, at a concentration exceeding 250 mg/L, and body weight (g) was measured. Fast muscle samples were collected from the epaxial region before the fasting period (-4d), daily during fasting (-3d, -2d, -1d and 0d) and during refeeding (6h, 12h, 1d, 2d and 3d) (Figure 1).

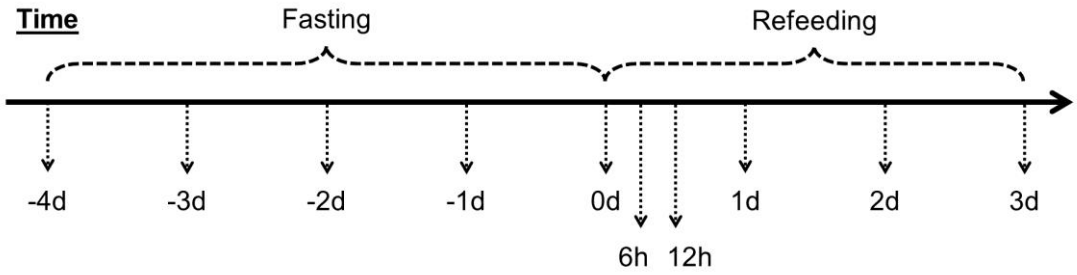

Figure 1. Fasting-refeeding experimental design. Muscle samples were collected at the indicated periods (d: days; h: hours).

Pacu myoblast cell culture

The protocol for the isolation and culture of pacu myoblasts were performed according to Bower & Johnston (2010). Fast muscle samples were collected from the epaxial region and mechanically dissociated with scalpels. The fragments were enzymatically digested with 0.2% collagenase type I (Sigma-Aldrich, USA) and with 0.1% trypsin (Sigma-Aldrich, USA), allowing the release of muscle cells. The suspension of cells was filtered in cell strainers (Corning, USA) to remove debris and resuspended in media with DMEM, 10% fetal bovine serum and 1% antibiotics (Sigma-Aldrich, USA). After cell counting in a Neubauer chamber, the cells were diluted at a concentration of 2×10^6 cells/mL and seeded in wells previously treated with poly-L-lysine e laminin (Sigma-Aldrich, USA), which have high affinity for the myoblasts. The myoblasts were incubated at 28ºC during 12 days. The media were changed every day and the morphology of myoblasts was monitored regularly.

Non-essential amino acids and leucine treatment

After 8 days of cell culture, during myotube formation, the myoblasts were incubated for 72 hours with free amino acid media (Earle's balance salt solution 1X, 9 mM $NaHCO_3$, 20 mM HEPES, Vitamin Mix 1X, 1% antibiotics and 4 g/L D-glucose - Sigma-Aldrich, USA). The media were prepared with deionized water sterilized through 0.22 µm filters. The myoblasts were then incubated for 24 hours in free amino acid media (-AA), media supplemented with non-essential amino acids (NEAA) (Sigma-Aldrich, USA) or media supplemented with non-essential amino acids and L-leucine (NEAA+LEU) (Sigma-Aldrich, USA). RNA extraction was performed 24 hours after the treatments. The results were obtained from three independent cell cultures.

LSPs identification

To select which LSPs we should evaluate in our study, we needed to identify genes retained as a single copy in Ostariophysi and two copies in Acanthopterygii, and genes retained as two copies in Ostariophysi and one copy in Acanthopterygii. A list was made with 248 genes related to myogenesis, protein synthesis and protein degradation pathways in skeletal muscle (data not shown), based on published articles in the field. Initially we downloaded the peptide sequences from *Danio rerio* and *Astyanax mexicanus*, both Ostariophysi, and *Gasterosteus aculeatus* and *Oreochromis niloticus*, both Acanthopterygii. The downloads were performed using the *BioMart* tool (http://www.ensembl.org/biomart/martview/a6a738c6a5bb5cfddc3a501898640dfe), available in *Ensembl Genome Browser 89* (http://www.ensembl.org/index.html). These files were visualized in the Notepad++ program and the peptide sequences of interesting genes relative to each species were annotated. The sequences were then compared to each other through the *BioEdit Sequence Alignment Editor* (Hall, 1999), which indicated genes retained differently between Ostariophysi and Acanthopterygii. In order to separate paralogue genes from isoforms of the same gene, we used the alignment program *MAFFT version 7* (http://mafft.cbrc.jp/alignment/server/). After this first selection, the peptide sequences of the species described above were also compared to the *Takifugu rubripes* and *Tetraodon nigroviridis* (Acanthopterygii) proteome in *Ensembl Genome Browser 89*, and the *Ictalurus punctatus* and *Piaractus mesopotamicus* (Ostariophysi) transcriptome in *BioEdit Sequence Alignment Editor*. The *Piaractus mesopotamicus* transcriptome was obtained in our laboratory (Mareco et al., 2015) and it is available in the *European Nucleotide Archive* - ENA (accession number PRJEB6656). After obtaining the peptide sequences of the LSPs genes, the *MEGA7* software (Kumar et al., 2016) was used to generate Neighbor-Joining or Maximum-Likelihood phylogenetic trees, and also estimate the best evolutionary model for each phylogenetic tree construction. Phylogenetic trees were visualized and edited using *FigTree v.1.4.2* software (http://tree.bio.ed.ac.uk/software/figtree/) (S1 File).

RNA extraction and reverse transcription

Total RNA was extracted using *TRIzol® Reagent* (Thermo Fisher Scientific, USA), according to the manufacturer's recommendations. RNA quantification was performed using the spectrophotometer *NanoVue™ Plus* (GE Healthcare, USA), which also allowed an estimative of

the RNA purity by measuring the absorbance at 260 nm (RNA quantity) and 280 nm (protein quantity). The RNA integrity was evaluated through electrophoresis in 1% agarose gel, confirmed by the presence of the bands of 28S and 18S ribosomal RNAs. In addition, the samples were submitted to the capillary electrophoresis system *2100 Bioanalyzer* (Agilent, USA), which provided a RNA integrity number (RIN) based on the 28S and 18S bands. The RNA sample is classified into a numerical system from 1 to 10, with 1 being the most degraded profile and 10 being the highest integrity profile. We only use samples with a RIN equal to or greater than 7.0. Extracted RNA was submitted to treatment with *DNase I Amplification Grade* (Thermo Fisher Scientific, USA) to eliminate any possible contaminating genomic DNA from the samples. RNA reverse transcription was performed using the *High Capacity cDNA archive kit* (Thermo Fisher Scientific, USA), following the manufacturer's guidelines. The products of reverse transcription were stored at -20ºC and used in the real time PCR.

Primer design and real time PCR

Initially the alignment program *MAFFT version 7* was used to identify regions with low similarity between the paralogues, where the forward and reverse primers needed to be designed to increase amplification specificity during qPCR reactions. Primers for pacus and Nile tilapias were designed using *Primer3 v.0.4.0* (Koressaar & Remm, 2007; Untergasser et al., 2012) (S1 Table). All primers were designed to amplify 50-200 bp products with annealing temperature of 60ºC. Any possible hairpin, self-dimer or cross-dimer structures formed by the primer pairs were assayed using *NetPrimer* software (Premier Biosoft, USA). The expression levels were detected by real time PCR using the *QuantStudio™ 12K Flex Real-Time PCR System* (Thermo Fisher Scientific, USA). Each cDNA sample was amplified using *GoTaq® qPCR Master Mix* (Promega, USA) and primers synthesized by Invitrogen (USA). The reactions were performed in duplicates, under the following conditions: 95ºC during 10 minutes, 40 cycles of denaturation at 95ºC during 15 seconds and annealing/extension at 60ºC during 1 minute. We analyzed of the Dissociation Curve (Melting Curve) at the end of each PCR reaction, which allowed the evaluation of the specificity of each primer set by the presence of a single fluorescence peak. The reaction efficiencies were calculated by the software *LinRegPCR* (Ramakers *et al*., 2003; Ruijter et al., 2009), and all obtained adequate values between 1.9 and 2. Relative quantification of expression was performed by the $2^{-\Delta\Delta Ct}$ method (Livak & Schmittgen, 2001), using the *DataAssist™ v3.01* software (Thermo Fisher Scientific, USA), which also allowed the selection of the best reference genes using the *geNorm* algorithm (Vandesompele et al., 2002). Relative

expression was normalized by the genes *ribosomal protein l13* (*rpl13*), *ribosomal protein l19* (*rpl19*) and *peptidylprolyl isomerase aa* (*ppiaa*), whose expression levels were constant between all samples.

Statistical analysis

Statistical analyses were performed using the parametric one-way ANOVA test, followed by Tukey's multiple comparisons test. Statistical significance was set at 5% ($p<0.05$) (GraphPad Prism 5 Software, USA).

RESULTS AND DISCUSSION

Fish and fasting-refeeding experiment

Body weights (g) of juvenile pacus and Nile tilapias were measured at the different sample collection periods, during fasting-refeeding experiment. The weights showed a decrease during fasting periods (-3d to 0d) and an increase after refeeding (6h to 3d) (Figure 2).

Groups	Pacu (g)	Nile tilapia (g)
-4d	12.60 ± 2.24	12.13 ± 1.64
-3d	10.70 ± 2.87	11.20 ± 1.52 [a]
-2d	11.92 ± 1.50	12.28 ± 1.83
-1d	10.37 ± 1.98	10.67 ± 1.37 [a]
0d	9.67 ± 1.84 [a]	10.93 ± 1.26 [a]
6h	12.02 ± 0.88	12.33 ± 1.22
12h	13.42 ± 1.60	13.55 ± 0.99
1d	13.47 ± 4.33	14.03 ± 1.19
2d	13.55 ± 3.29	13.98 ± 1.85
3d	14.68 ± 2.76 [b]	14.73 ± 2.29 [b]

Figure 2. Body weights of pacus and Nile tilapias. The body weights of juvenile pacus (*Piaractus mesopotamicus*) and Nile tilapias (*Oreochromis niloticus*) were measured immediately before the sample collection at the indicated periods: before the fasting period (-4d), during fasting (-3d, -2d, -1d and 0d) and during refeeding (6h, 12h, 1d, 2d and 3d) (d: days; h: hours). Data are presented as the mean ± SD (n=6). Different letters indicate significant differences between 3d group compared to other groups ($p<0.05$).

LSPs identification

From a list of 248 genes, we identified 7 LSPs related to myogenesis, 11 LSPs related to protein synthesis and 4 LSPs related to protein degradation pathways in skeletal muscle of pacus and Nile tilapias. Among them, 12 were Ostariophysi-specific genes (retained as two copies in Ostariophysi and one copy in Acanthopterygii, or present only in Ostariophysi), and 10 were Acanthopterygii-specific genes (retained as a single copy in Ostariophysi and two copies in Acanthopterygii, or present only in Acanthopterygii) (Figure 3).

Paralogue Ostariophysi-specific		
Symbol	**Name**	**Function**
igf2	*insulin-like growth factor 2*	Protein synthesis (Igf-Pik3-Akt pathway)
trim63	*tripartite motif containing 63, e3 ubiquitin protein ligase*	Protein degradation
fst	*follistatin*	Protein synthesis (inhibition of Myostatin pathway)
pja2	*praja ring finger 2, e3 ubiquitin protein ligase*	Protein degradation
cdc42bpa	*cdc42 binding protein kinase alpha (dmpk-like)*	Myogenesis (cytoskeleton reorganization and cell migration)
eif3j	*eukaryotic translation initiation factor 3 subunit J*	Protein synthesis (association with 40S ribosome)
rictor	*rptor independent companion of mtor complex 2*	Protein synthesis (subunit of Torc2)
grb2	*growth factor receptor bound protein 2*	Myogenesis (Ras-Mapk pathway)
igf2bp2	*insulin like growth factor 2 mRNA binding protein 2*	Protein synthesis (Igf-Pik3-Akt pathway)
pip4k2a	*phosphatidylinositol-5-phosphate 4-kinase type 2 alpha*	Protein synthesis (Igf-Pik3-Akt pathway)
raf1	*raf-1 proto-oncogene, serine/threonine kinase*	Myogenesis (Ras-Mapk pathway)
tgfb1	*transforming growth factor beta 1*	Myogenesis (Ras-Mapk pathway)
Paralogue Acanthopterygii-specific		
Symbol	**Name**	**Function**
igfbp4	*insulin-like growth factor binding protein 4*	Protein synthesis (Igf-Pik3-Akt pathway)
akt2	*v-akt murine thymoma viral oncogene homolog 2*	Protein synthesis (Igf-Pik3-Akt pathway)
rragc	*ras-related gtp binding c*	Protein synthesis (Lamtor-Rag complex)
chuk	*conserved helix-loop-helix ubiquitous kinase*	Protein degradation (NFκB pathway)
myod1	*myogenic differentiation 1*	Myogenesis (myogenic regulatory factor)
atf4	*activating transcription factor 4*	Protein degradation (endoplasmic reticulum stress)
igfbp3	*insulin like growth factor binding protein 3*	Protein synthesis (Igf-Pik3-Akt pathway)
pik3ca	*phosphatidylinositol-4,5-biphosphate 3-kinase catalytic subunit alpha*	Protein synthesis (Igf-Pik3-Akt pathway)
mef2d	*myocyte enhancer factor 2d*	Myogenesis
tgfb3	*transforming growth factor beta 3*	Myogenesis (Ras-Mapk pathway)

Figure 3. Lineage-specific paralogues (LSPs). The LSPs related to myogenesis, protein synthesis and protein degradation were identified for molecular analyses in skeletal muscle of pacus and Nile tilapias.

For each of these genes a phylogenetic tree was constructed between the species *Danio rerio*, *Astyanax mexicanus*, *Ictalurus punctatus* and *Piaractus mesopotamicus* (Ostariophysi), *Gasterosteus aculeatus*, *Takifugu rubripes*, *Tetraodon nigroviridis* and *Oreochromis niloticus* (Acanthopterygii) and *Homo sapiens* (Figure 4 and S1 File).

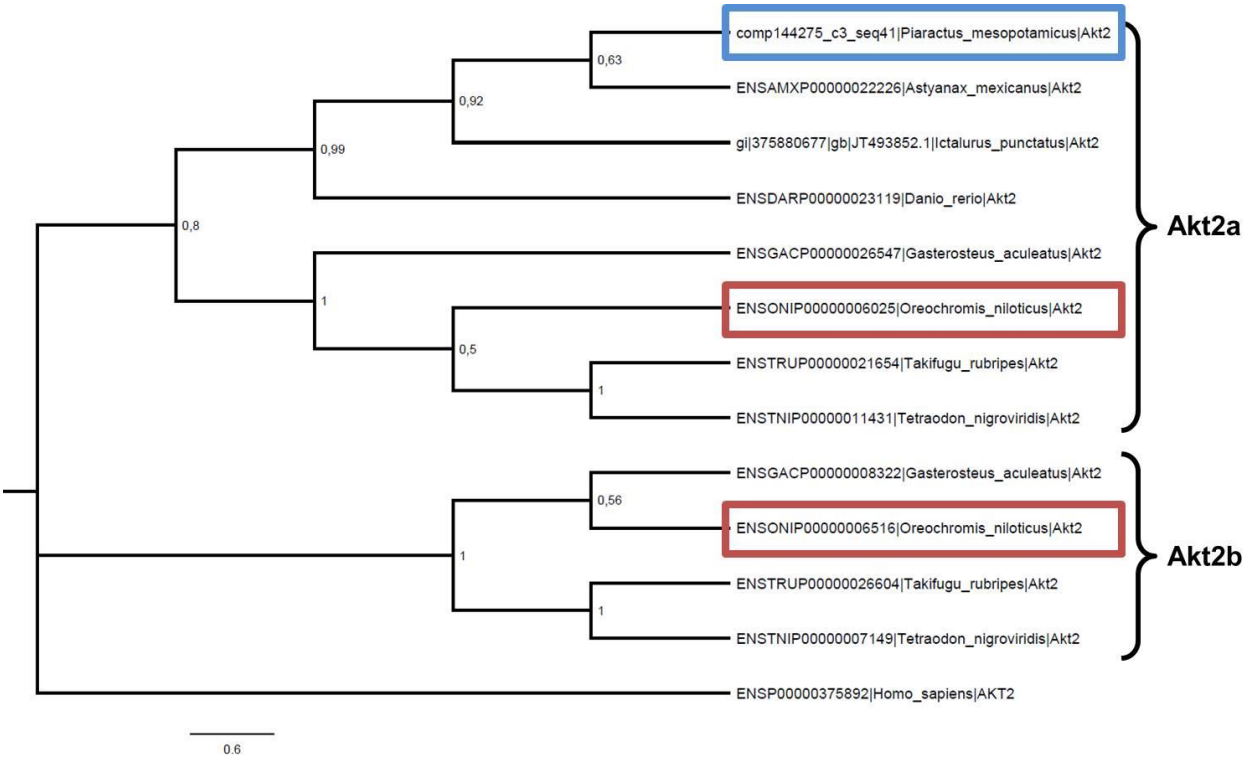

Figure 4. Teleost fish Akt2 phylogenetic analysis. Example of a phylogenetic tree showing relationships between Akt2 for different teleost fish species. Neighbor-Joining phylogenetic tree was constructed from a highly confidence alignment of 13 peptide sequences, and used Jones-Taylor-Thornton with Gamma distribution (JTT+G) as best fitted substitution model. Bootstrap-posterior values are indicated on the node of each branch. The species used in the tree are as follow: cave fish (*A. mexicanus*), zebrafish (*D. rerio*), stickleback (*G. aculeatus*), human (*H. sapiens*), channel catfish (*I. punctatus*), Nile tilapia (*O. niloticus*), pacu (*P. mesopotamicus*), green spotted pufferfish (*T. nigroviridis*) and fugu (*T. rubripes*). *Homo sapiens* was used as an out-group. The blue box indicates the Akt2 of pacu (Akt2a), and the red boxes indicate the Akt2 copies of Nile tilapia (Akt2a and Akt2b).

LSPs expression in fasting-refeeding experiment

Initially, despite the absence of paralogue copies, we evaluated the expression of *fbxo32* as a way to check whether the fasting-refeeding experiment was effective (Figure 5). Due to the large amount of data, both graphs (Figure 6) and heat maps (Figure 7) were constructed for the LSPs expression results.

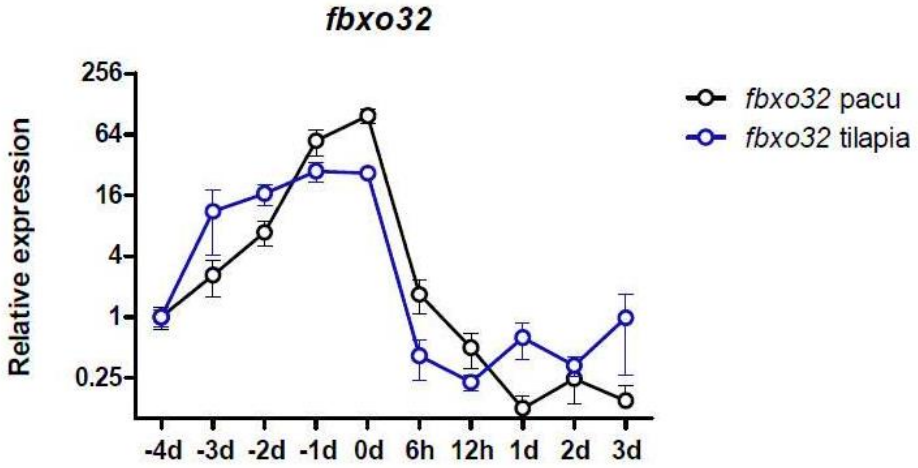

Figure 5. Relative expression of *fbxo32* in skeletal muscle of pacus and Nile tilapias. mRNA expression of *fbxo32* was assessed by real time PCR in skeletal muscle of pacus and Nile tilapias submitted to fasting-refeeding. The data are expressed as the fold change compared with -4d group and presented as the mean ± SEM (n=6).

Ostariophysi-specific paralogues (retained as two copies in Ostariophysi and one copy in Acanthopterygii)

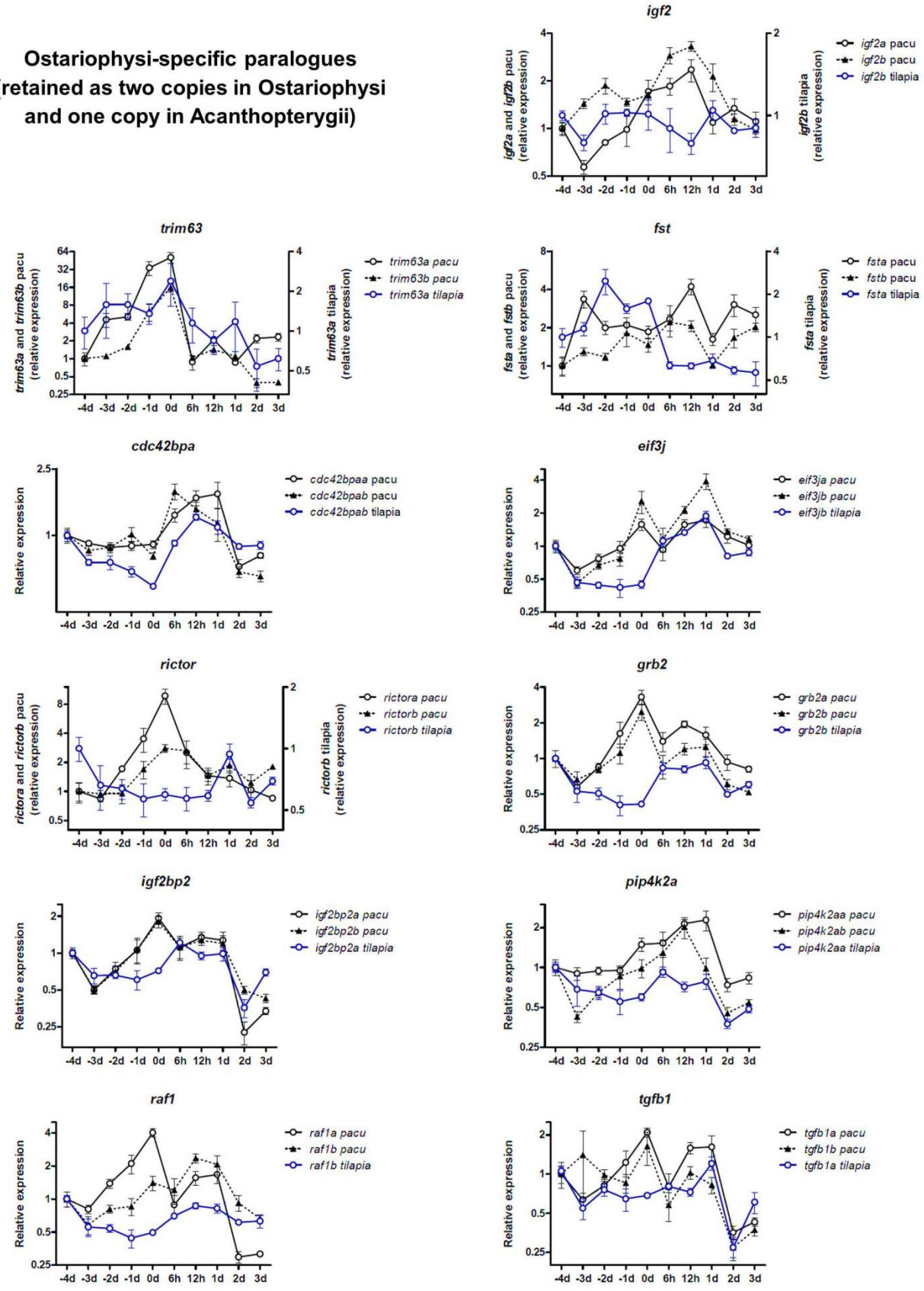

3513

3514

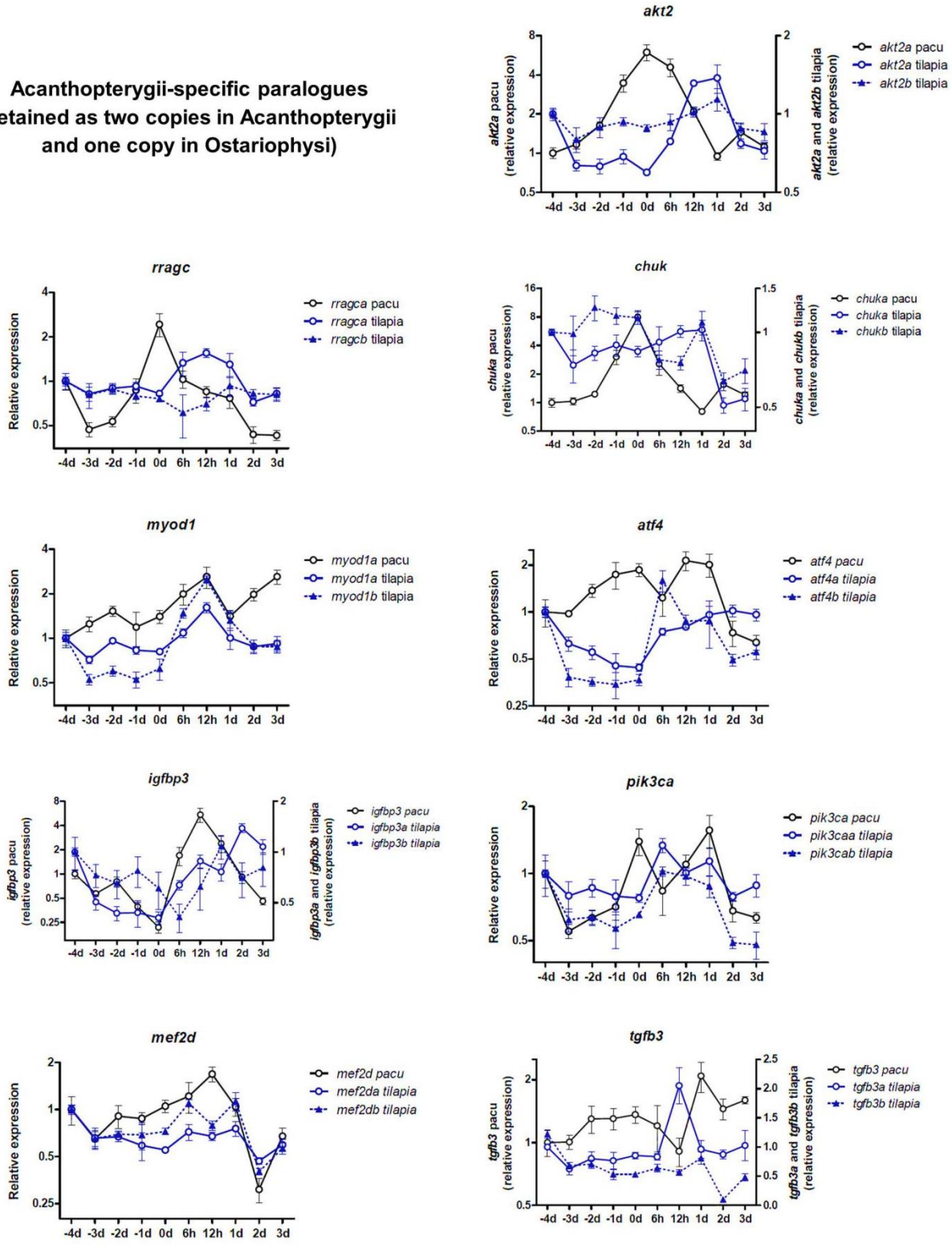

Figure 6. Relative expression of LSPs in skeletal muscle of pacus and Nile tilapias. mRNA expression of *igf2*, *trim63*, *fst*, *cdc42bpa*, *eif3j*, *rictor*, *grb2*, *igf2bp2*, *pip4k2a*, *raf1*, *tgfb1* (Ostariophysi-specific paralogues), *akt2*, *rragc*, *chuk*, *myod1*, *atf4*, *igfbp3*, *pik3ca*, *mef2d* and *tgfb3* (Acanthopterygii-specific paralogues) were assessed by real time PCR in skeletal muscle

of pacus and Nile tilapias submitted to fasting-refeeding. The data are expressed as the fold change compared with -4d group and presented as the mean ± SEM (n=6).

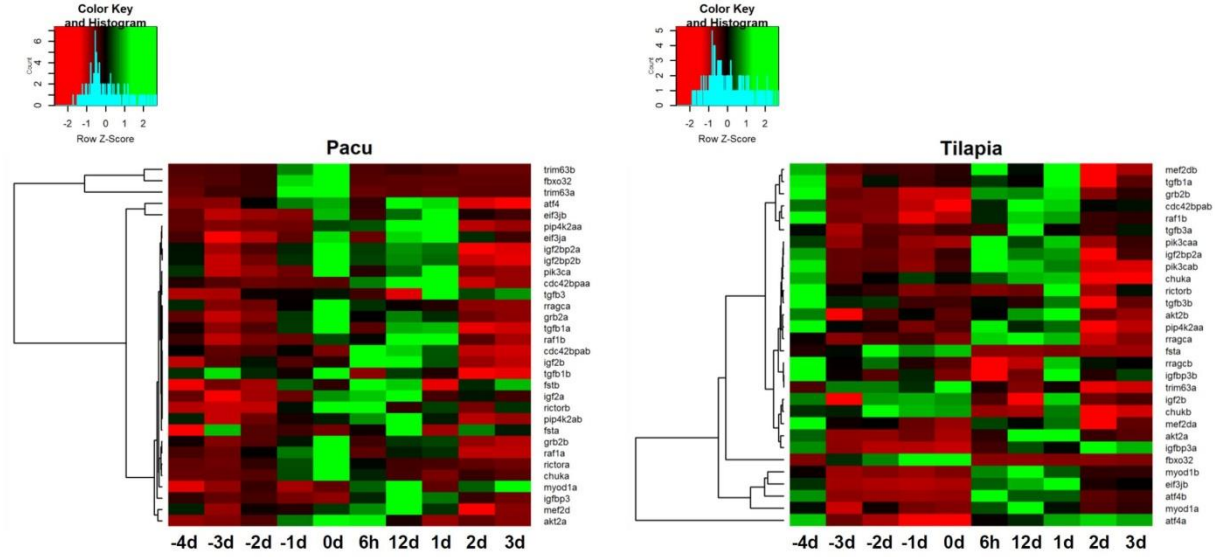

Figure 7. Heat maps of LSPs expression in skeletal muscle of pacus and Nile tilapias. The heat maps were constructed using the mean of Ct values normalized by the reference genes for each experimental group. The lines correspond to LSPs related to protein degradation, protein synthesis and myogenesis pathways. The columns correspond to the fasting-refeeding periods (d: days; h: hours). Changes in the colour indicate variation in LSPs expression levels according to fasting and refeeding treatments. The green colour indicates low levels of expression and the red colour indicates high levels of expression.

Expression of *fbxo32* showed that the fasting-refeeding experiment was effective. Fbxo32 is a class III ubiquitin ligase responsible for the polyubiquitination of protein substrates that need to be catabolized, regulating protein degradation and loss of skeletal muscle components (Bonaldo and Sandri, 2013). The *fbxo32* was highly expressed during fasting periods, in which occurs intense protein degradation, and showed low expression levels after refeeding.

Heat maps provided a broader view of LSPs expression, showing a different expression pattern between pacus and Nile tilapias. In pacus, most of paralogues increased their expression after 4 days of fasting (0d), and maintained high expression during 1 day of refeeding (6h, 12h and 1d). On the other hand, in Nile tilapias, paralogues decreased their expression immediately after 1 day of fasting (-3d), and increased again during 1 day of refeeding (6h, 12h and 1d). This indicates that these genes regulate skeletal muscle differently between the Ostariophysi and Acanthopterygii superorders, when submitted to periods of protein synthesis and degradation.

Line graphs also revealed a distinct LSPs behavior between pacus and Nile tilapias. The *fsta* in Nile tilapias was highly upregulated during protein degradation (-2d, -1d and 0d), whereas in pacus both *fsta* and *fstb* had high expression levels during protein synthesis (6h and 12h). These results were also observed for *igf2* expression. In addition to variations in the expression between species, some LSPs also showed different expression between their paralogue copies within the same species. Immediately after refeeding (6h and 12h), there was an upregulation of *rragca* and a downregulation of *rragcb* in Nile tilapias. Expression of *chuka* copy in Nile tilapia increased gradually up to 1 day after refeeding, in contrast with the *chukb* copy that showed a drop in its levels after 6 hours of refeeding. In pacus these differences between the paralogue copies were observed for *igf2* expression. Expression of *igf2a* had a sudden increase in 0d group, period of intense protein degradation, while *ifg2b* showed expression peaks after 6 and 12 hours of refeeding, during protein synthesis. These variations indicate the possible existence of LSPs subfunctionalization within the same species. While a paralogue could exert its functions more effectively during protein synthesis, its copy may play its role better during protein degradation, or the paralogue copies could act in the same signaling pathway but at different moments. LSPs involved with skeletal muscle myogenesis, such as *myod1*, *cdc42bpa* and *mef2d*, showed similar expression profile between pacus and Nile tilapias, with increased levels just after 6 hours of refeeding.

Our results revealed that the evolutionary process allowed a different molecular behavior between the Ostariophysi and Acanthopterygii superorders against to stimuli or situations of protein synthesis and degradation. It is difficult to explain what adaptive advantages this differential retention and distinct LSPs expression profiles have brought to each of the lineages, but these results show that the evolutionary history of Ostariophysi and Acanthopterygii culminated with divergent adaptations, that are reflected in molecular biology and, possibly, cytology and physiology of these animals.

Understanding how these LSPs act on the skeletal muscle of pacus and Nile tilapias is crucial for the handling of these fish, and shows that the knowledge obtained for one species does not always apply to all others. Our results are very promising and represent a major advance in research involving fish muscle growth.

As additional results, the expression of LSPs *pja2* and *igfbp4* were also evaluated. These genes are examples of LSPs that do not have a corresponding (orthologous gene) in the other lineage. The *pja2* gene is present only in the Ostariophysi superorder and the *igfbp4* gene is present only in the Acanthopterygii superorder (Figure 8). Since these LSPs can not be compared

between the species, their expression results have not been discussed, but it is important to note that *pja2* and *igfbp4* may be objects of future research aimed to understand their roles in fish skeletal muscle and their evolutionary histories in each of the lineages.

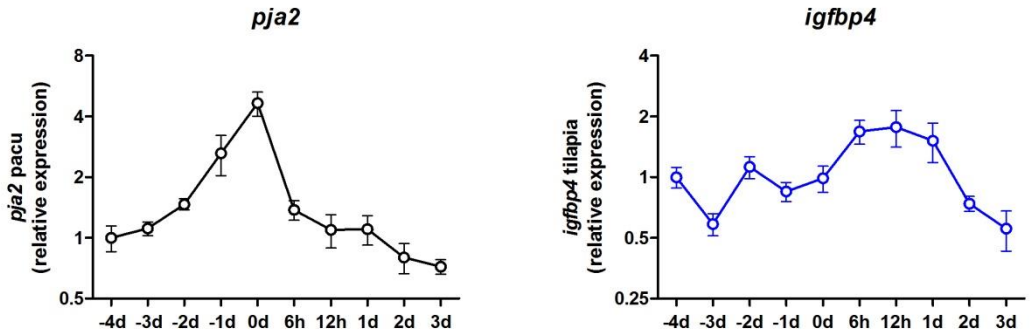

Figure 8. Relative expression of *pja2* and *igfbp4* in skeletal muscle of pacus and Nile tilapias respectively. mRNA expression of *pja2* and *igfbp4* were assessed by real time PCR in skeletal muscle of pacus and Nile tilapias submitted to fasting-refeeding. The data are expressed as the fold change compared with -4d group and presented as the mean ± SEM (n=6).

In addition, we performed pacu myoblast cell cultures to investigate the expression of LSPs in a more controlled environment, with fewer variables. We developed an *in vitro* fasting-refeeding model in which pacu myoblasts were submitted to media with no amino acids (-AA), with non-essential amino acids (NEAA) and with non-essential amino acids combined to leucine (NEAA+LEU). As for the LSPs expression in pacus and Nile tilapias, both heat map (Figure 9) and graphs (Figure 10) were constructed.

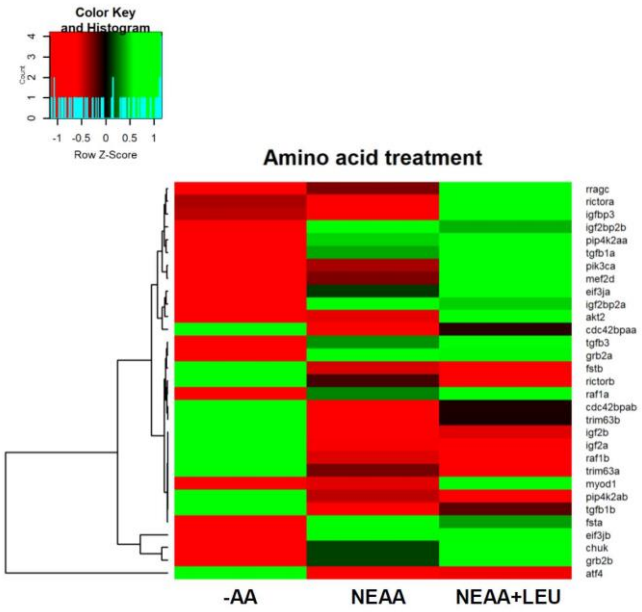

Figure 9. Heat maps of LSPs expression in pacu myoblast cell cultures treated with amino acids. The heat maps were constructed using the mean of Ct values normalized by the reference genes for each experimental group. The lines correspond to LSPs related to protein degradation, protein synthesis and myogenesis pathways. The columns correspond to the *in vitro* fasting-refeeding treatments: media with no amino acids (-AA), with non-essential amino acids (NEAA) and with non-essential amino acids combined to leucine (NEAA+LEU). Changes in the colour indicate variation in LSPs expression levels according to fasting and refeeding treatments. The green colour indicates low levels of expression and the red colour indicates high levels of expression.

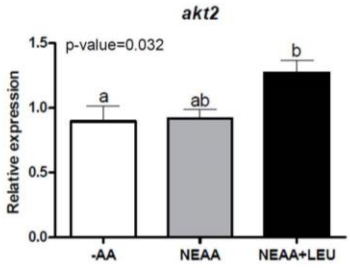
akt2
p-value=0.032
Relative expression
a
ab
b
-AA
NEAA
NEAA+LEU

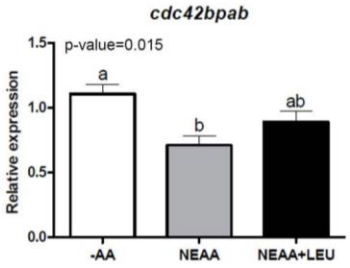
cdc42bpab
p-value=0.015
Relative expression
a
b
ab
-AA
NEAA
NEAA+LEU

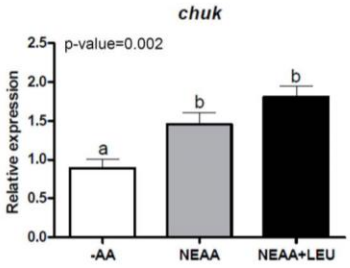
chuk
p-value=0.002
Relative expression
a
b
b
-AA
NEAA
NEAA+LEU

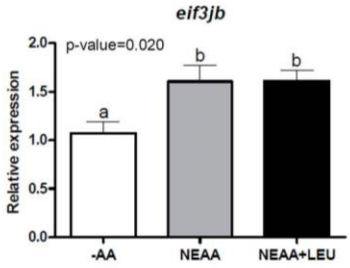
eif3jb
p-value=0.020
Relative expression
a
b
b
-AA
NEAA
NEAA+LEU

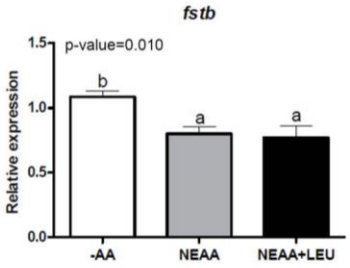
fstb
p-value=0.010
Relative expression
b
a
a
-AA
NEAA
NEAA+LEU

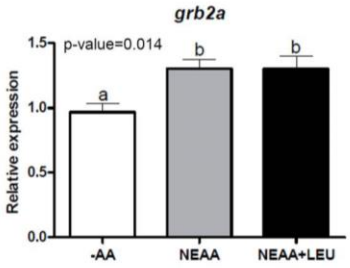
grb2a
p-value=0.014
Relative expression
a
b
b
-AA
NEAA
NEAA+LEU

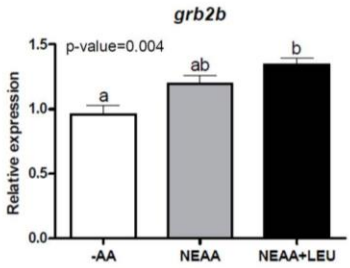
grb2b
p-value=0.004
Relative expression
a
ab
b
-AA
NEAA
NEAA+LEU

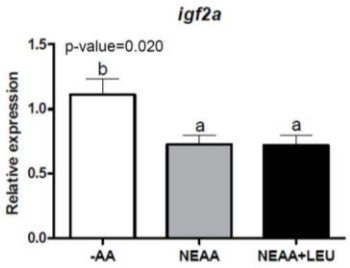
igf2a
p-value=0.020
Relative expression
b
a
a
-AA
NEAA
NEAA+LEU

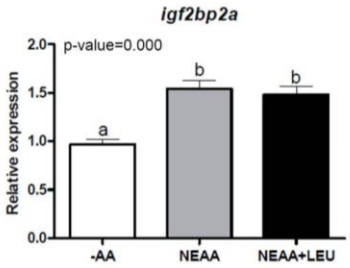
igf2bp2a
p-value=0.000
Relative expression
a
b
b
-AA
NEAA
NEAA+LEU

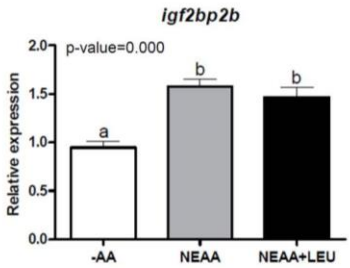
igf2bp2b
p-value=0.000
Relative expression
a
b
b
-AA
NEAA
NEAA+LEU

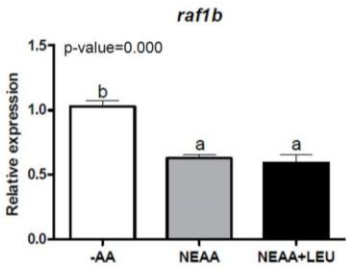
raf1b
p-value=0.000
Relative expression
b
a
a
-AA
NEAA
NEAA+LEU

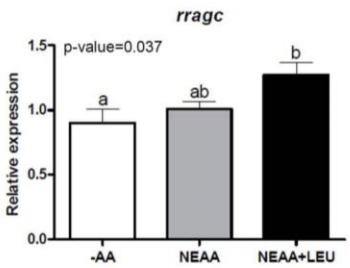
rragc
p-value=0.037
Relative expression
a
ab
b
-AA
NEAA
NEAA+LEU

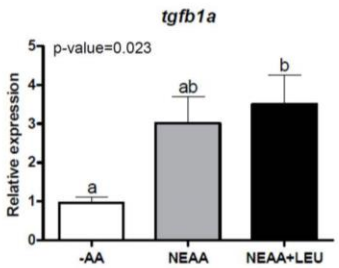
tgfb1a
p-value=0.023
Relative expression
a
ab
b
-AA
NEAA
NEAA+LEU

Figure 10. Relative expression of LSPs in pacu myoblast cell cultures treated with amino acids. mRNA expression of *akt2*, *cdc42bpab*, *chuk*, *eif3jb*, *fstb*, *grb2a*, *grb2b*, *igf2a*, *igf2bp2a*, *igf2bp2b*, *raf1b*, *rragc* and *tgfb1a* were assessed by real time PCR in pacu myoblast cell cultures submitted to *in vitro* fasting-refeeding: media with no amino acids (-AA), with non-essential amino acids (NEAA) and with non-essential amino acids combined to leucine (NEAA+LEU). The data are expressed as the fold change compared with -AA group and presented as the mean ± SEM (n=3 independent cell cultures). Only paralogues that had statistical differences between experimental groups are shown.

The heat map clustered the LSPs in two main groups: paralogues upregulated by amino acid treatment (with low expression in –AA group and high expression in NEAA and NEAA+LEU groups) and paralogues downregulated by amino acid treatment (with high expression in –AA group and low expression in NEAA and NEAA+LEU groups). Among those which had statistical differences between groups, *akt2*, *chuk*, *eif3jb*, *grb2a*, *grb2b*, *igf2bp2a*, *igf2bp2b*, *rragc* and *tgfb1a* were upregulated by amino acids.

These results shows that pacu myoblasts have some genes better responsive to amino acid treatments or situations of increased protein synthesis. Through this experiment, we obtained a set of genes that could have a more active role during protein synthesis and, possibly, during fish muscle growth. LSPs such as *grb2a*/*grb2b* and *igf2bp2a*/*igf2bp2b* represent possible markers of protein synthesis, since expression of both copies increased after incubation with amino acids, and show that sometimes the most interesting genes to be investigated are not those best known and studied, such as *igf2*. These amino acid-upregulated paralogues are excellent candidates to be better studied and evaluated in different conditions of myogenesis and muscle growth, and have the potential to be the focus of aquaculture researches.

REFERENCES

Bonaldo, P. and Sandri, M. Cellular and molecular mechanisms of muscle atrophy. *Disease Models and Mechanisms*. v. 6, p. 25-39, 2013.

Bower, N.I. and Johnston, I.A. Selection of reference genes for expression studies with fish myogenic cell cultures. *BMC Molecular Biology*. v. 10(80), p. 1-11, 2009.

Bower, N.I. and Johnston, I.A. Transcriptional regulation of the IGF signaling pathway by amino acids and insulin-like growth factors during myogenesis in atlantic salmon. *PLoS ONE*. v. 5(6), e11100, 2010.

Chargé, S.B.P. and Rudnicki, M.A. Cellular and molecular regulation of muscle regeneration. *Physiological Reviews*. v. 84(1), p. 209-238, 2004.

Duran, B.O.S., Fernandez, G.J., Mareco, E.A., Moraes, L.N., Salomão, R.A.S., Gutierrez de Paula, T., Santos, V.B., Carvalho, R.F. and Dal-Pai-Silva, M. Differential microRNA expression in fast- and slow-twitch skeletal muscle of Piaractus mesopotamicus during growth. *PLOS ONE*. v. 10(11): e0141967, 2015.

El-Sayed, A.F.M. *Tilapia culture*. Cambridge: CABI Publishing, 2006. 277p.

Froehlich, J.M., Galt, N.J., Charging, M.J., Meyer, B.M. and Biga, P.R. In vitro indeterminate teleost myogenesis appears to be dependent on Pax3. *In vitro Cellular & Developmental Biology – Animal*. v. 49(5), p. 371-385, 2013.

Gabillard, J.C., Sabin, N. and Paboeuf, G. In vitro characterization of proliferation and differentiation of trout satellite cells. *Cell and Tissue Research*. v. 342, p. 471-477, 2010.

Garcia de la serrana, D. and Johnston, I.A. Expression of heat shock protein (Hsp90) paralogues is regulated by amino acids in skeletal muscle of atlantic salmon. *PLoS ONE*. v. 8(9), e74295, 2013.

Garcia de la serrana, D., Mareco, E.A. and Johnston, I.A. Systematic variation in the pattern of gene paralog retention between the teleost superorders Ostariophysi and Acanthopterygii. *Genome Biology and Evolution*. v. 6(4), p. 981-987, 2014.

Jaillon, *et al*. Genome duplication in the teleost fish *Tetraodon nigroviridis* reveals the early vertebrate proto-karyotype. *Nature*. v. 431, p. 946-957, 2004.

Johnston, I.A. Genetic and environmental determinants of muscle growth patterns. In: Johnston, I.A. (Ed) *Muscle development and growth. Fish Physiology 18*. San Diego: Academic Press, 2001. 327p.

Johnston, I.A., Abercromby, M., Vieira, V.L.A., Sigursteindóttir, R.J., Kristjánsson, B.K., Sibthorpe, D. and Skúlason, S. Rapid evolution of muscle fibre number in post-glacial populations of Arctic charr *Salvelinus alpinus*. *The Journal of Experimental Biology*. v. 207, p. 4343-4360, 2004.

Johnston, I.A. Environment and plasticity of myogenesis in teleost fish. *The Journal of Experimental Biology*. v. 209, p. 2249-2264, 2006.

Johnston, I.A., Bower, N.I. and Macqueen, D.J. Growth and the regulation of myotomal muscle mass in teleost fish. *The Journal of Experimental Biology*. v. 214, p. 1617-1628, 2011.

Koressaar, T. and Remm, M. Enhancements and modifications of primer design program Primer3. *Bioinformatics*. v. 23(10), p. 1289-1291, 2007.

Livak, K.J. and Schmittgen, T.D. Analysis of relative gene expression data using real-time quantitative PCR and the $2^{-\Delta\Delta CT}$ method. *Methods*. v. 25(4), p. 402-408. 2001.

Maere, S. and Van de Peer, Y. Duplicate retention after small and largescale duplications. In: Dittmar, K. and Liberles, D. (Ed) *Evolution after gene duplication*. Hoboken: Wiley-Blackwell, 2010. 358p.

Mareco, E.A., Garcia de la serrana, D., Johnston, I.A. and Dal-Pai-Silva, M. Characterization of the transcriptome of fast and slow muscle myotomal fibres in the Pacu (*Piaractus mesopotamicus*). *BioMed Central Genomics*. 2015.

Montserrat, N., Sánchez-Gurmaches, J., Garcia de la serrana, D., Navarro, M.I. and Gutiérrez, J. IGF-I binding and receptor signal transduction in primary cell culture of muscle cells of gilthead sea bream: changes throughout in vitro development. Cell and Tissue Research. v. 330(3), p. 503-513, 2007.

MPA. Ministério da Pesca e Aquicultura. *Boletim estatístico da pesca e aquicultura – Brasil 2011*. 2013. 60p.

Nikki, J., Pirhonen, J., Jobling, M. and Karjalainen, J. Compensatory growth in juvenile rainbow trout, *Oncorhynchus mykiss* (Walbaum), held individually. Aquaculture. v. 235, p. 285-296, 2004.

Ramakers, C., Ruijter, J.M., Deprez, R.H.L and Moorman, A.F.M. Assumption-free analysis of quantitative real-time polymerase chain reaction (PCR) data. *Neuroscience Letters*. v. 339, p. 62-66, 2003.

Rowlerson, A. and Veggetti, A. Cellular mechanisms of post-embryonic muscle growth in aquaculture species. In: Johnston, I.A. (Ed) *Muscle development and growth. Fish Physiology 18*. San Diego: Academic Press, 2001. 327p.

RStudio Team. RStudio: integrated development for R. *RStudio*, Inc., Boston, MA, 2015.

Ruijter, J.M., Ramakers, C., Hoogaars, W.M.H., Karlen, Y., Bakker, O., van den Hoff, M.J.B. and Moorman, A.F.M. Amplification efficiency: linking baseline and bias in the analysis of quantitative PCR data. *Nucleic Acids Research*, v. 37(6), e45, 2009.

Sandri, M. Signaling in muscle atrophy and hypertrophy. *Physiology*. v. 23, p. 160-170, 2008.

Sänger, A.M. and Stoiber, W. Muscle fiber diversity and plasticity. In: Johnston, I.A. (Ed) *Muscle development and growth. Fish Physiology 18*. San Diego: Academic Press, 2001. 327p.

Seiliez, I., Gabillard, J.C., Skiba-Cassy, S., Garcia-Serrana, D., Gutiérrez, J., Kaushik, S., Panserat, S. and Tesseraud, S. An in vivo and in vitro assessment of TOR signaling cascade in rainbow trout (*Oncorhynchus mykiss*). *The American Journal of Physiology – Regulatory, Integrative and Comparative Physiology*. v. 295, p. R329-R335, 2008.

Taylor, J.S., Braash, I., Frickey, T., Meyer, A. and Van de Peer, Y. Genome duplication, a trait shared by 22000 species of ray-finned fish. *Genome Research*. v. 13, p. 382-390, 2003.

Untergasser, A., Cutcutache, I., Koressaar, T., Ye, J., Faircloth, B.C., Remm, M. and Rozen, S.G. Primer3 – new capabilities and interfaces. *Nucleic Acids Research*. v. 40(15), e115, 2012.

Urbinati, E.C. and Gonçalves, F.D. Pacu (*Piaractus mesopotamicus*). In: Baldisserotto, B and Gomes, L.C. (Ed) *Espécies nativas para piscicultura no Brasil*. Santa Maria: UFSM, 2005. 470p.

Vandesompele, J., Preter, K., Pattyn, F., Poppe, B., Van Roy, N., Paepe, A. and Speleman, F. Accurate normalization of real-time quantitative RT-PCR data by geometric averaging of multiple internal control genes. *Genome Biology*. v. 3(7), 0034, 2002.

Vélez, E.J., Lutfi, E., Jiménez-Almiburu, V., Riera-Codina, M., Capilla, E., Navarro, I. and Gutiérrez, J. IGF-I and amino acids effects through TOR signaling on proliferation and differentiation of gilthead sea bream cultured myocytes. *General and Comparative Endocrinology*. v. 205, p. 296-304, 2014.

3750 ***SUPPORTING INFORMATION***

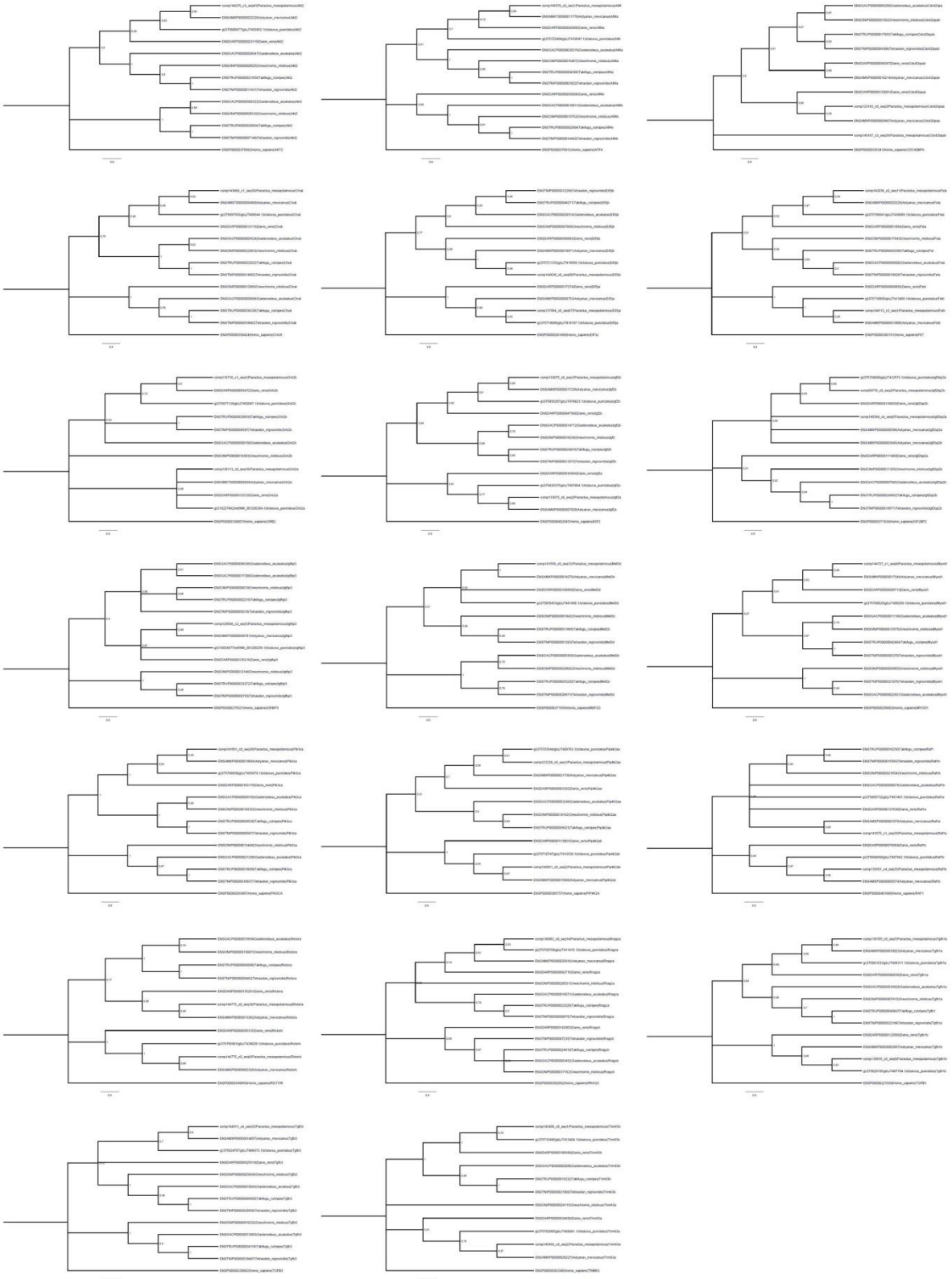

3751

3752

S1 File. Teleost fish LSPs phylogenetic analysis. Phylogenetic trees showing relationships between Akt2, Atf4, Cdc42bpa, Chuk, Eif3j, Fst, Grb2, Igf2, Igf2bp2, Igfbp3, Mef2d, Myod1, Pik3ca, Pip4k2a, Raf1, Rictor, Rragc, Tgfb1, Tgfb3 and Trim63a for different teleost fish species. Neighbor-Joining or Maximum-Likelihood phylogenetic trees were constructed from a highly confidence alignment of 13 peptide sequences, and used Jones-Taylor-Thornton with Gamma distribution (JTT+G) as best fitted substitution model. Bootstrap-posterior values are indicated on the node of each branch. The species used in the tree are as follow: cave fish (*A. mexicanus*), zebrafish (*D. rerio*), stickleback (*G. aculeatus*), human (*H. sapiens*), channel catfish (*I. punctatus*), Nile tilapia (*O. niloticus*), pacu (*P. mesopotamicus*), green spotted pufferfish (*T. nigroviridis*) and fugu (*T. rubripes*). *Homo sapiens* was used as an out-group.

S1 Table: Real time PCR primer sequences. Primers used for qPCR amplification of the LSPs *akt2*, *cdc42bpa*, *chuk*, *fst*, *igf2*, *igfbp4*, *myod1*, *pja2*, *rragc*, *trim63*, *atf4*, *eif3j*, *grb2*, *igf2bp2*, *igfbp3*, *mef2d*, *pik3ca*, *pip4k2a*, *raf1*, *rictor*, *tgfb1* and *tgfb3*. Primers were also designed for the reference genes *rpl13*, *rpl19*, *ppiaa* and *gapdh*, and also for the *fbxo32* to prove the efficacy of fasting-refeedng treatments. Accession code based on *European Nucleotide Archive* - ENA (accession number PRJEB6656) for pacu (Mareco et al., 2015) and *Ensembl Genome Browser 89* database (http://www.ensembl.org/index.html) for Nile tilapia.

Gene	Accession Code	Forward primer (5' to 3')	Reverse primer (5' to 3')
akt2a pacu	comp144275_c3_seq41	CCAATGCTGAGAGGGAAGAG	GTTGATGTCCATTGGCTCCT
akt2a tilapia	ENSONIP00000006025	AACCAATGGATGTTCTCAGC	GGACATAACCGCTTCCATCT
akt2b tilapia	ENSONIP00000006516	CTCCCCGAGTGACAGCAGTGG	CTGTTGCCTTCTCCTTCACC
cdc42bpaa pacu	comp123183_c0_seq3	GGCACTCTGACTTGTCCCTC	ACCTCTCTGATGGTGGGACT
cdc42bpab pacu	comp145167_c3_seq39	GATCTTCCAGTCGGGGTC	CTCCGTCTAACACCCCATCAC
cdc42bpab tilapia	ENSONIP00000001562	GTGAGCGGGAAGAGTTTGAG	TTTCTTCGGTGAGCAGGACT
chuka pacu	comp143689_c1_seq38	ATCGTTTGTGGGCACTCTTC	TACGCACTTTGCTTGTCCAC
chuka tilapia	ENSONIP00000022863	GCTGTTGGAGCCGATGGAGG	AGCAGAGGGGTTTCTTGGTT
chukb tilapia	ENSONIP00000012095	CGGCACAAACAAGCCATACT	TATCCTCAGCACCCAAAACC
fsta pacu	comp143036_c0_seq11	AATGTCCCGAGCCTTCCACT	CTCTGGCTCTGGCATTTCAC
fstb pacu	comp144113_c3_seq1	CACCACCATTCAGGAGCAG	GAAGAACGGGAGATGTCAGG
fsta tilapia	ENSONIP00000017943	GGATGCTGAAACACCACCTT	ATGTAGAGCACCTGGCACCT
igf2a pacu	comp133875_c0_seq2	AGAAGGCTCAAAGGCTCAGG	CTGTTGGGCACGGTCATC

igf2b pacu	comp133875_c0_seq1	CAACTTCCACAAGCCTCTCATCTC	CGTAGTCTTCTGTGGGATGC
igf2b tilapia	ENSONIP00000018238	CCCAGCAAAGATACGGACAT	CCTCTGGACCTTCATTCTGC
igfbp4 tilapia	ENSONIP00000011325	CCAGAGAGCGTTGGACAGATTG	GGCACTGTTTAGGGTGGAAATC
myod1a pacu	comp144727_c1_seq4	GTTCGTCGTCTTCCTCTTGC	ACCCGTGCTTTAACACCAAC
myod1a tilapia	ENSONIP00000013575	GACAGCAGCTCTTATTTCTC	GCTGCTGTTATCGGTGGAGAT
myod1b tilapia	ENSONIP00000009955	GCTCTGATGGCTTGGTGG	CAATGCTGGACAAACAGTCC
pja2 pacu	comp140246_c0_seq17	GCTTTGGCATAGCTCAGTCC	CTCTTGTCCCCTATGGTCGTC
rragca pacu	comp138962_c0_seq14	GCAACTGAGGGATGAGCTTC	CACCAGCGAGCTAATGATGA
rragca tilapia	ENSONIP00000020531	CCTTGTTTCTGGAGAGCAC	GAAGGTGGGGTCAAAGAAGTC
rragcb tilapia	ENSONIP00000017182	GAGGATAGCCCGACATCAGC	CCTTCTGTATGGAGGATTTGC
trim63a pacu	comp145456_c0_seq2	ATGTTGCTGTTGTCCATACTCTG	ATCACATCACCCAGGAGCA
trim63b pacu	comp142409_c0_seq1	GGCTCGGGTCTCTCCTCGG	CCAGGCGTTACGGAGACC
trim63a tilapia	ENSONIP00000024115	GTTGTCATCCTTCCGTGTCAG	TCTGAGAGGCGGTAGGTGTTC
atf4a pacu	comp145578_c0_seq1	GGAGCAAGAACCACCACAAT	GGGCAGTGAAGTGGACATCT
atf4a tilapia	ENSONIP00000016467	GTTGGAGCAGATGATGGCA	TCCAATGAAAGACTCCAGGTC
atf4b tilapia	ENSONIP00000010752	GGATGTGCTCAGTGACTTGG	CAGTGAGTCCAGGTCAAGGTC
eif3ja pacu	comp137884_c0_seq67	GAGGAATCAAAAGACAGCACAG	AAGCATCTTTCGCTAGTTCCA
eif3jb pacu	comp144636_c0_seq88	GAGTCCCAGGCTGATGTGC	GGGACACATGGCTTCAATTC
eif3jb tilapia	ENSONIP00000007868	ACAACAGGAGGCAATGGAAC	AGCTCCAAGTCTGCGTCTTC
grb2a pacu	comp138113_c0_seq16	CCCATCTTCCTGAGAGACATC	GTTAGGGTCCGAGTTGTCCA
grb2b pacu	comp116716_c1_seq1	CCCTGTTTGATTTTGACCCT	CGTAATTGCGTGGGAACATT
grb2b tilapia	ENSONIP00000010393	TATAGAGCAGGTCCCCCAGA	ACCAGTTGGGGTCAGAGTTG
igf2bp2a pacu	comp140394_c4_seq8	CCTGATGCTCCTGAGAGAATG	GCGGGGACTTTGATATGTGT
igf2bp2b pacu	comp59776_c0_seq2	GCTGCGGAGAAACCTATCAC	AACCTCCTCAGCAGTTTTGG
igf2bp2a tilapia	ENSONIP00000011355	CAGAAGGAAGCCAACGAGAC	TCCCTGTGTCCTCCTCAATC
igfbp3a pacu	comp129938_c2_seq1	TTCGTAGCCTGGCAGAGACT	GTTTCCGCATTCCAAACTGT
igfbp3a tilapia	ENSONIP00000008019	CGTTGGAACTGTGAAGGATG	GCTCTGGGTCTTCCTGTTCTC
igfbp3b tilapia	ENSONIP00000012146	GGGCTCATTTGTCAACATCA	CATTGACTGGCACTGTTGGT
mef2db pacu	comp141550_c0_seq12	CTTGCTGCTTTGTGAGGTGA	CCTCCTCTCTGTCTCCAACG
mef2da tilapia	ENSONIP00000024882	GACCAAAGTCCCCTTAATGATG	TTGACTGTCCGTAGCGTTTG
mef2db tilapia	ENSONIP00000001942	AAAGCCCGCTAAATGACCG	ATACTGGCACGGTGACTGG
pik3caa pacu	comp141601_c0_seq36	ACGAATGCCAAACCTTATGC	CGTATCCTCAGGGTGCTGTT
pik3caa tilapia	ENSONIP00000010535	TCTCAGGGCAGAGCAATCG	TGTCTCAACTGCTCGGTGTC
pik3cab tilapia	ENSONIP00000013444	CTCCCCTGTCAAGTTTCCTG	CTGTCAGTCAGGGGGTTGTC

pip4k2aa pacu	comp121239_c0_seq1	TTCGTGCTAATGTCTGTCCG	CGTTAGCCTGTTAGCCTGTCA
pip4k2ab pacu	comp140051_c0_seq2	CACAAGTGAGCACAAAGCG	GTCTCCCAGCAACAGCCTAA
pip4k2aa tilapia	ENSONIP00000018162	TGTCTTCTCTCACCGCCTTT	ATCTTCTGCCCATCGTTGAT
raf1a pacu	comp141875_c1_seq33	CTAAGCAATGGGCTAGGAATG	GAATGGTGCTGCTTGTTTTG
raf1b pacu	comp139101_c4_seq33	CCTCAGTAATGGGTTTGGCT	GAGGAGCGTCGTTGATAAGG
raf1b tilapia	ENSONIP00000021654	CTGCCTTTCTCCGACCATAG	TGCTGGTTTGGGAGGTAGAC
rictora pacu	comp144775_c0_seq10	GCGGAGTCTCCAGAGTAACG	CTTCACTGAGCACAGGGTC
rictorb pacu	comp144775_c0_seq9	CGCAACCGCTTTCTTATCTC	TTAGGGTCGCTGTTGAGCTT
rictora tilapia	ENSONIP00000013607	AAGAGGCTTCAGCAGCAGAG	AACCTGCGGGGAGTTAGTCT
tgfb1a pacu	comp136705_c0_seq7	TAGAGGATTGGAAGGGGGTC	CCAAAGGATACTTCGCCAAC
tgfb1b pacu	comp139916_c0_seq9	CTTGAGGTAAGCTGACTGTGGC	CAAAGACTTTCGCCTCCAAA
tgfb1a tilapia	ENSONIP00000007415	TGTGGACTTGGAGATGGTGA	TTCTGCTCCTCATCCTGCTT
tgfb3a pacu	comp144011_c4_seq32	AACAGTCGTCCTTGGTGTCC	GCAACTTGTCTTGGGCATTT
tgfb3a tilapia	ENSONIP00000025436	CCAGTCCGCCTCAAACAAC	GTTATCCTGTCCGCAACTCTG
tgfb3b tilapia	ENSONIP00000019232	CCCCTATCAAATCCAAGCG	TTGTCTTGACCGCAACTCTG
rpl13 pacu	comp141862_c0_seq1	ATCAACAGGAAAGTAGCCC	AGGATGAGTTTGGAGCGGTA
rpl13 tilapia	ENSONIP00000007470	GAATGGAATGATCCTGAACC	CAGAACGAACCTTGGTATGG
rpl19 pacu	comp145235_c0_seq2	GCAAACTGGTGAAGGATGGT	CTTGGACTCCCTGTAACGCC
rpl19 tilapia	ENSONIP00000020477	CCCAACGAGACCAATGAGAT	CGTGCCCTTTCTCTTACCAT
ppiaa pacu	comp145566_c0_seq1	ATTGTGGTTCGTGAAGTCGC	CCGCTGGGCAGAGTGATTAT
ppiaa tilapia	ENSONIP00000000799	CGGGTCCCAGTTCTTCATC	GCCGTAGGACTCCATCTTC
gapdh pacu	comp140533_c0_seq1	ACACACGACGACAAGACCAA	GTCCCTCTCGCTGAAAACTG
gapdh tilapia	ENSONIP00000016251	TGGTTTCCACTCCAAGAAGG	GTCTTCTGGGTGGCAGTGAT
fbxo32 pacu	comp145335_c1_seq5	TCTTTGGTGCTCCCCTTGTG	TAAAACCGAGGACGGCTGG
fbxo32 tilapia	ENSONIP00000009089	CCGAATGGAGAACATCCTG	GCAGAGTTTCTTCCACAGCA

3772

3773

3774

3775

3776

3777

3778

3779

3780

9. CONCLUSÕES

Considerando os resultados obtidos nos três capítulos, podemos concluir que as culturas celulares primárias de mioblastos de peixes representam um importante modelo *in vitro* para o estudo da miogênese e crescimento do músculo esquelético. As culturas celulares foram utilizadas para avaliação do desenvolvimento dos mioblastos em situações normais (experimentos referentes à miogênese de células musculares derivadas do músculo *fast* e *slow*), foram submetidas a diferentes tratamentos ou condições para avaliação do efeito isolado de moléculas (experimentos com ácido ascórbico, aminoácidos e eletroestimulação), ou foram utilizadas em estudos mais detalhados de resultados obtidos em experimentos *in vivo*, fornecendo um ambiente mais controlado e com menor número de variáveis (experimentos referentes aos estudos dos LSPs). Dessa forma, as culturas celulares possibilitaram a obtenção de novas informações e melhor compreensão dos mecanismos moleculares e celulares que regulam o tecido muscular dos peixes. Nosso trabalho permitiu a geração de conhecimento básico em biologia celular e molecular, fornece informações de referência para a pesquisa em outras espécies de peixes e pode contribuir para a elaboração de novas estratégias de criação e para a obtenção de melhorias na aquicultura.

10. APÊNDICE

Anexo 1: Aprovação do projeto de doutorado pela Comissão de Ética no Uso de Animais (CEUA) do Instituto de Biociências, UNESP, Botucatu, São Paulo, Brasil.

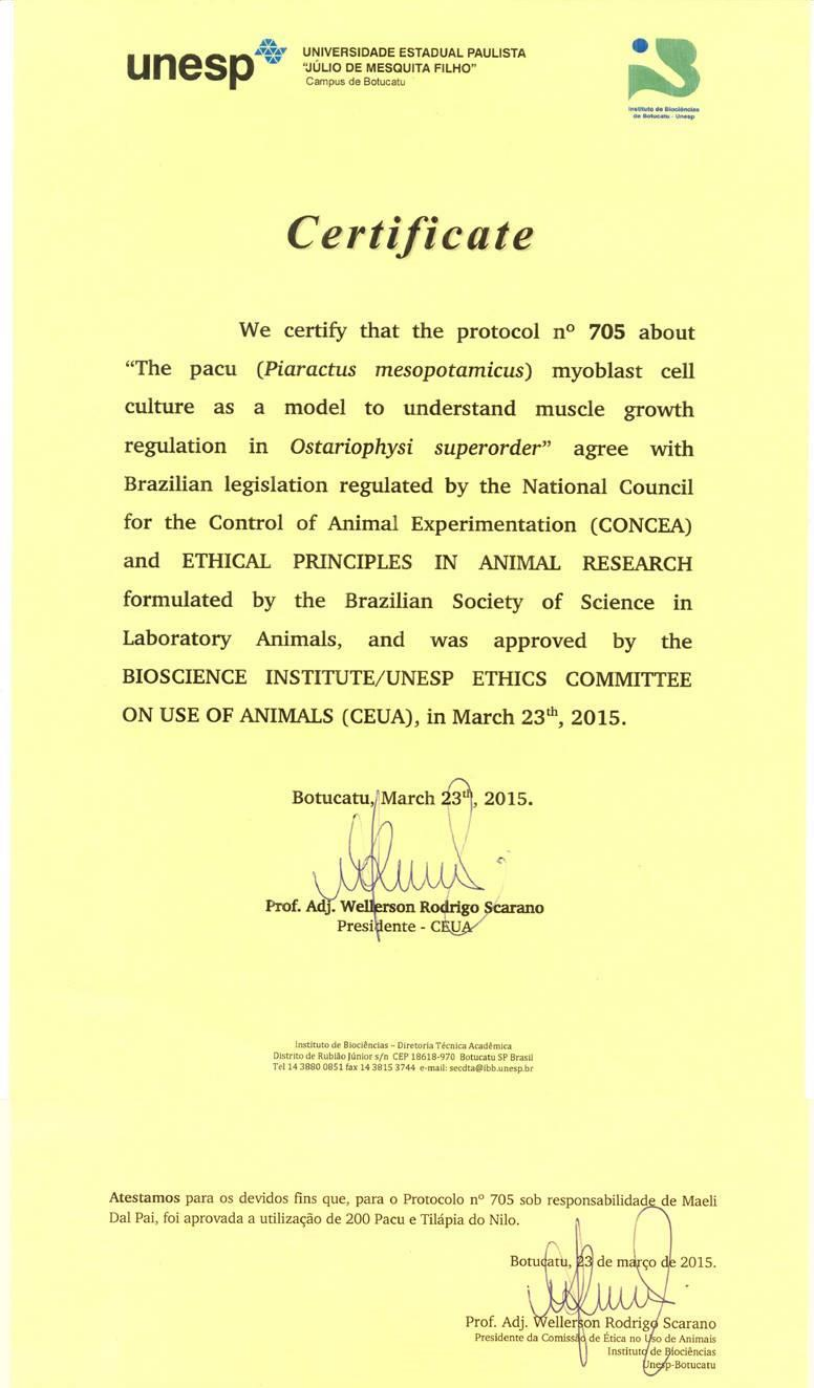

unesp UNIVERSIDADE ESTADUAL PAULISTA "JÚLIO DE MESQUITA FILHO" Campus de Botucatu

Certificate

We certify that the protocol nº **705** about "The pacu (*Piaractus mesopotamicus*) myoblast cell culture as a model to understand muscle growth regulation in *Ostariophysi superorder*" agree with Brazilian legislation regulated by the National Council for the Control of Animal Experimentation (CONCEA) and ETHICAL PRINCIPLES IN ANIMAL RESEARCH formulated by the Brazilian Society of Science in Laboratory Animals, and was approved by the BIOSCIENCE INSTITUTE/UNESP ETHICS COMMITTEE ON USE OF ANIMALS (CEUA), in March 23th, 2015.

Botucatu, March 23th, 2015.

Prof. Adj. Wellerson Rodrigo Scarano
Presidente - CEUA

Instituto de Biociências – Diretoria Técnica Acadêmica
Distrito de Rubião Júnior s/n CEP 18618-970 Botucatu SP Brasil
Tel 14 3880 0851 fax 14 3815 3744 e-mail: secdta@ibb.unesp.br

Atestamos para os devidos fins que, para o Protocolo nº 705 sob responsabilidade de Maeli Dal Pai, foi aprovada a utilização de 200 Pacu e Tilápia do Nilo.

Botucatu, 23 de março de 2015.

Prof. Adj. Wellerson Rodrigo Scarano
Presidente da Comissão de Ética no Uso de Animais
Instituto de Biociências
Unesp-Botucatu